THE UNIVERSITY OF MICHIGAN

COLLEGE OF ENGINEERING

Department of Civil Engineering

Technical Report

POST BUCKLING BEHAVIOR OF

TEE SHAPED ALUMINUM COLUMNS

Rafi Hariri

ORA Project 05154

This report was also a dissertation submitted by the author

in partial fulfillment of the requirements for the degree of Doctor

of Philosophy in The University of Michigan.

ACKNOWLEDGMENTS

TABLE OF CONTENTS

TABLE OF CONTENTS (Continued)

iv

TABLE OF CONTENTS (Continued)

LIST OF TABLES

LIST OF ILLUSTRATIONS

NOMENCLATURE

Abbreviations

$(B.S.)_\xi$, $(B.S.)_\eta$	Bending stiffness in the $\xi\zeta$ and $\eta\zeta$ planes
I. B. G.	Inelastic buckling gradient (relation 1.1)
F. R. M. S. L. $(\sigma_{r\ell})_f$	False reduced modulus stress in buckling to the left
F. R. M. S. R. $(\sigma_{rr})_f$	False reduced modulus stress in buckling to the right
R. M. L. $(E_{r\ell})$	Reduced modulus in buckling to the left
R. M. R. (E_{rr})	Reduced modulus in buckling to the right
R. M. S.	Reduced modulus stress
R. M. S. L. $(\sigma_{r\ell})$	Reduced modulus stress in buckling to the left
R. M. S. R. (σ_{rr})	Reduced modulus stress in buckling to the right
T. M. (E_t)	Tangent modulus
T. M. S. (σ_t)	Tangent modulus stress
Z. S. C. A.	Zero stress change axis
i. b. g.	$(I.B.G.)(\frac{L}{P_t})$ (relation 5.53)
r. m. s.	(R. M. S.)/critical stress

A	Cross sectional area
$[A]$	Matrix of the coefficients of the simultaneous linear equations (relation 4.70)
A_ℓ	Cross sectional area - left portion
A_r	Cross sectional area - right portion
A_1, A_2, A_3	Values of the integrals of relation 3.32
B	Ramberg-Osgood stress-strain relation constant (relation 4.65)
$\{B\}$	Vector, constants of the simultaneous linear equation (relation 4.70)
C	Torsional stiffness coefficient
$[C]$	Radius of curvature matrix (relation 5.36)
C_a	Average stiffness coefficient (relation 4.83)
C_w	Warping stiffness coefficient (relation 3.19)
D	Dimension of a square
D_1	Diameter of circle inscribed at juncture (Fig. 4.21)
E	Elastic modulus
E_{eff}	Effective elastic modulus
E_r	Reduced modulus
E_{rr}	Reduced modulus in buckling to the right
$E_{r\ell}$	Reduced modulus in buckling to the left
E_s	Secant modulus
E_t	Tangent modulus
$[E_{t_f}], [E_{t_w}]$	Matrix of the values of the tangent modulus at the flange and web networks

$E_{tx},\ E_{ty}$ $E_{bx},\ E_{by}$	Eccentricity of axial loading at the top and bottom faces, in the x and y directions (Fig. 3.3b)
$F_{x(e)},\ F_{x(i)}$ $F_{y(e)},\ F_{y(i)}$ $F_{z(e)},\ F_{z(i)}$	Components of the external and the internal forces along the x, y and z axes
$F_{\xi(e)},\ F_{\xi(i)}$ $F_{\eta(e)},\ F_{\eta(i)}$ $F_{\zeta(e)},\ F_{\zeta(i)}$	Components of the external and the internal forces along the ξ, η and ζ axes
G	Shear modulus
GE	See relation 4.8
G_s	Secant shear modulus
$[G_{s_f}],\ [G_{s_w}]$	Secant shear modulus matrix for the flange and the web
I_p	Polar moment of inertia
$I_x,\ I_y$	Moment of inertia with respect to x and y axes
J	Torsion constant (relation 2.39)
K	Coefficient of effective slenderness ratio
$(\dfrac{KL}{r})_r$	Effective reduced slenderness ratio
$(\dfrac{KL}{r})_{r\ell},\ (\dfrac{KL}{r})_{rr}$	Effective reduced slenderness ratios in buckling to the left or to the right (relation 2.37)
L	Column length
M_r	Moment at the reduced modulus load (relation 2.22)
$M_x,\ M_y$	Moment about the x and y axes

M_z	Moment about the z axis (torsional moment)
M_{xe}, M_{xi}, M_{xd} M_{ye}, M_{yi}, M_{yd} M_{ze}, M_{zi}, M_{zd}	External moment components due to eccentric loading, initial crookedness, and the lateral deflection, along the x, y and z axes
$M_{x(e)}$ $M_{y(e)}$ $M_{z(e)}$	External moment components along the x, y and z axes
$M_{\xi(e)}$, $M_{\xi(i)}$ $M_{\eta(e)}$, $M_{\eta(i)}$ $M_{\zeta(e)}$, $M_{\zeta(i)}$	External and internal moment components along the ξ, η and ζ axes
$M_{\zeta 1(e)}$, $M_{\zeta 2(e)}$	Components of the $M_{\zeta(e)}$
N	Normal vector
P, $\{P\}$	Axial load
P_{avg}	Average of the normal forces calculated at the longitudinal nodal points (relation 5.47)
P_c	Critical load
P_t	Tangent modulus load
P_u	Ultimate load
Q	Convergence optimizer (relation 5.46)
Q_1, Q_2	Components of Q (relation 5.50)
[R]	Curvature-deflection transformation matrix (relations 5.16, 5.17)
$\{S\}$	Average shear vector (relation 5.10)
[SR]	Matrix of the depth of strain regression (relation 5.37)

$\{U\}, \{U_o\}$	Lateral deflection and initial crookedness in the x direction
$\{V\}, \{V_o\}$	Lateral deflection and initial crookedness in the y direction
$\{a\}$	Coefficient of the difference equation (relation 4.61)
b	Overall breadth of the flange (Fig. 1.1)
$[b]$	Transformation matrix (xyz and $\xi\eta\zeta$ coordinate systems) (relation 3.1)
b_1, b_2, b_3, b_4	See Fig. 4.10
$[b]$ $[c]$	Matrices (relation 4.43)
c	Cycle of iteration for one cycle of increment
d	Overall depth of the section (Fig. 1.1)
dA	Element of area
dn	Element of length along the normal (Fig. 3.5)
d_n	See relation 4.72
ds	Element of length along the center line (Fig. 3.5)
e_{tx}, e_{ty}	Eccentricity of loading in the x and the y directions per unit length at the top face (relation 3.4)
e_x, e_y	Symmetrical end eccentricity in the x and y directions
f_1	Fillet radius (Fig. 6.4)
h	Dimension of the mesh (Fig. 4.8)
i, j, k, ℓ, m, n, p, q	Dummy variables

k	Edge condition coefficient (relation 2.42)
m	Number of the column segments (integer)
m_f, m_w	Number of flange and web network divisions in the x direction (integers) (Figs. 4.9, 5.7)
n_f, n_w	Number of flange and web network divisions in the y direction (integers) (Figs. 4.9, 5.7)
n	Cycle of increment
$[q_1]$	Transformation matrix (distributed load to concentrated load) (relation 5.8)
$[q_2]$	Transformation matrix (concentrated load to average shear) (relation 5.11)
$[q_3]$	Transformation matrix (average shear to moment) (relation 5.13)
r, r_x, r_y	Radius of gyration
$[r]$	$\frac{1}{L}[R]$
r_{ex}	Ratio of the eccentricity of loading in the x direction at the bottom to the same at the top
r_{ey}	Ratio of the eccentricity of loading in the y direction at the bottom to the same at the top
t	Thickness of flange (Fig. 1.1)
$\{u\}$, $\{u_o\}$	Lateral deflection and the initial crooked-ness in the x direction per unit length
$\{v\}$, $\{v_o\}$	Lateral deflection and the initial crooked-ness in the y direction per unit length
u, v, w	Displacement in the x, y and z directions (relations 4.4, 4.5)
w_o	Displacement of the point o in the z direction (relation 3.25)
w	Web thickness

$\{x\}$, $\{y\}$	Coordinates of the mesh
$\bar{x}$	Distance of the centroid of the cross section from the centroid of the flange (Fig. 3.3a)
x, y, z	Fixed coordinates (Fig. 3.1a)
x_o	Distance of the centroid from the outer surface (relation 1.1)
x_{ol}, x_{or}	Distance of the centroid from the outer left or right surfaces (Fig. 1.1)
x_l, x_r	Distance of the Z.S.C.A. from the left face of the flange in buckling to the left or to the right (Fig. 2.2)
z	Distance from the top of the column
Δ_1, Δ_2, Δ_3, Δ_4	Test-deflection readings (Fig. 6.10)
ΔA_f, ΔA_w $[\Delta A_f]$, $[\Delta A_w]$	Area of the mesh of the flange and the web
ΔP, $\{\Delta P\}$	Increment of the axial load
ΔP_{avg}	Increment of the average of the axial force evaluated at the longitudinal nodal sections
ΔP_l, ΔP_r	Increment of axial load of the left and the right portions
Δ_{ix}, Δ_{iy}	Initial crookedness at the mid-length of the column in the x and the y directions
Δ_x, Δ_y	Mid-length deflection in the x and the y directions
$\Delta\delta$, $[\Delta\delta]$	Increment of the lateral deflection
$\Delta\delta_o$	Increment of the lateral deflection at the mid-length
$\Delta\epsilon$	Increment of the strain
$\Delta\sigma$	Increment of the stress

$\Delta\phi$, $[-\Delta\phi]$	Increment of the curvature
$\Delta\phi_o$	Increment of the curvature at the mid-length
α, $\{\alpha\}$	Ratio of $(B.S.)_\eta$ to $(B.S.)_\xi$ (relations 3.37, 5.45)
α_1	Coefficient of juncture correction to torsion constant (relation 4.83)
α_1, α_2, α_3, α_4	See Fig. 4.11
β, $\{\beta\}$	Rotation (twist) of the cross section about the ζ axis
γ	Shear strain
γ_p	Plastic shear strain
γ_{xy}, γ_{xz}, γ_{yz}	Shear strain components
$[\delta]$	Matrix, deflection per unit length in the x and the y directions
$[\delta_o]$	Matrix, initial crookedness per unit length in the x and the y directions
δ_1	See Figs. 6.10 and 6.11
δ_{ix}, δ_{iy}	Initial crookedness at the mid-length per unit length in the x and the y directions
δ_x, δ_y	Lateral deflection at the mid-length per unit length in the x and the y directions
ϵ	Strain
ϵ_e	Elastic strain
$\{\epsilon_o\}$	Strain at the origin of the $\xi\eta\zeta$ coordinate
$[e_f(m \times n_f \times m_f)]$ $[\epsilon_w(m \times n_w \times m_w)]$	Strain matrices for the flange and the web
ϵ_p	Plastic strain

ϵ_t	Strain at the tangent modulus load
$\epsilon_{P.L.}$	Strain at the proportionality limit
$\epsilon_{xx}, \epsilon_{xy}, \ldots$	Strain components
η	Ratio of the tangent modulus to the elastic modulus (relation 2.26)
$\{\eta\}, \{\xi\}$	Coordinates of the centroid of the mesh
$\xi \ \eta \ \zeta$	Coordinate, fixed to the column cross section (Fig. 3.1b)
θ	Uniform twist per unit length
$\{\theta\}$	Concentrated angle change vector (relation 5.7)
λ	Length of the column segment
λ	See relation 4.71
ν	Poisson's ratio
$\{\xi\}, \{\eta\}$	Coordinates of the centroid of the mesh
$\overline{\xi}, \{\overline{\xi}\}$	See relations 3.35, 5.44
ρ	Distance of the element from the origin (Fig. 3.4)
$[\rho_f^2], [\rho_w^2]$	Matrix of ρ^2 for the networks of the flange and the web
σ	Stress
σ_c	Critical stress
σ_{c_ℓ}	Critical local buckling stress
σ_{c_t}	Critical torsional buckling stress
$[\sigma_f(m \times n_f \times m_f)]$ $[\sigma_w(m \times n_w \times m_w)]$	Stress matrices for the flange and the web

$\sigma_{P.L.}$	Stress at the proportionality limit
σ_e	Stress at the Euler load
σ_t	Tangent modulus stress
σ_{xx}, σ_{yy}, σ_{zz}	Components of σ
τ	Shear stress vector
τ_{xy}, τ_{yz}, τ_{xz}	Shear stress components
$[\tau_{xzf}]$, $[\tau_{yzf}]$	Matrices (shear stress components in the flange)
$[\tau_{xyw}]$, $[\tau_{yzw}]$	Matrices (shear stress components in the web)
$[-\phi]$	Curvature matrix (relation 5.5)
ψ	Warping function
$[\psi_f]$, $[\psi_w]$	Warping matrices for the flange and the web
ω	Relaxation factor
ω_b	Best value for ω

ABSTRACT

The post buckling behavior of a tee shaped column of aluminum alloy is the subject under study in this thesis. Attention is focused on the cases where the buckling is initiated in the plane of symmetry. The effects of initial curvature and eccentric loading in the plane of symmetry and in the directions towards or away from the flange receive consideration. In the case where the buckling starts in the direction away from the flange, the flange of the tee section would be subjected to increasing compressive stress and there would be corresponding decreases in the value of the tangent modulus while increasing areas of the web would be subjected to strain regression at the elastic rate. Thus, progressively the ratio of the bending stiffness about the axis of symmetry to that of the bending in the plane of symmetry will decrease and in some cases, depending on the ratio of the bending stiffness about the principal axes in the unloaded stage, before the load reaches the potential maximum, biaxial bending accompanied with torsion would commence. On the contrary, if buckling commences in the plane of symmetry and towards the flange, theoretically, the column will not buckle out of its plane of symmetry and planar bending will govern the behavior of the column.

A complete evaluation of tee-section column behavior is needed to provide an accurate estimate of the effects of initial column imperfections, eccentricity of loading, the preferred modes of

buckling and to afford a confirmation of the qualitative predictions made in the preceding paragraph. To achieve the foregoing aims an algorithm has been developed for use on a digital computer to provide by an incremental process a complete simulation of tee-section column behavior.

Bounds of behavior of a column, specifically a tee column, have been discussed and the differing inelastic buckling gradients and the reduced moduli in buckling towards or away from the flange have been explained and illustrated graphically. The problem of torsion of a cross section subjected to a varying strain in the inelastic range with possible presence of strain regression region has been treated.

A series of tests has been conducted to confirm the theoretical predictions. To carry out the experiments, a procedure of measuring the lateral displacements and the twist of the hinged-end columns in combined bending and torsion has been developed.

The results of the incremental analyses are presented in the form of tables and graphs. These results include the ultimate load carrying capacity of tee columns of various slenderness ratio with various amounts of initial crookedness in buckling towards or away from the flange, comparison of initial crookedness and the eccentric loading, comparison of the assumed half-sine curve deflection shape and the more exact deflection shape, some selected graphs of the load-deflection history and finally the results of the experiments in the form of a table and some graphs.

A thorough survey of literature covering all aspects of the
related studies was made and a complete bibliography of 107 refer-
ences is provided.

CHAPTER I

INTRODUCTION

1.1. STATEMENT OF THE PROBLEM

The behavior of a centrally loaded column of mono-symmetric cross section, specifically a "T" section, of aluminum alloy, which is stronger about the axis of symmetry and which has no eccentricity of loading, imperfections or residual stress, is the subject under study in this thesis. The effects of initial curvature will receive consideration.

The critical or buckling load in the inelastic range for a concentrically loaded metal column with no initial curvature and hinged at both ends is predicted by the tangent modulus theory.[1] In the limit as the increment above the tangent modulus load approaches zero, Shanley showed that bending would commence with no regression in compressive strain, but that for any finite amount of load above the tangent modulus load a strain regression would be initiated on the convex side and the strain at the concave side would start to increase.

By an incremental analysis, deflection of the column at a certain point, i.e., mid-length, and corresponding load values at different stages of deflection up to and beyond the maximum value of the load can be calculated and graphed. The slope of the load vs. deflection curve at the point of initiation of lateral deflection is called

the "Inelastic Buckling Gradient".[2] If torsional buckling is absent at

this point the value of Inelastic Buckling Gradient is given by[3]

$$\lim_{\Delta\delta\to0} \left|\frac{\Delta P}{\Delta\delta}\right| = \frac{P_t}{r^2} x_o \qquad (1.1)$$

where P_t is the tangent modulus load, r is the radius of gyration with

respect to axis of bending and x_o is the distance between the centroid

and the outer fiber of the convex side of the cross section measured on

a line perpendicular to the buckling axis.

If buckling is to occur about the y-axis, the moment of inertia

of the cross section about y-axis being less than that about x-axis, one

may calculate two different values of Inelastic Buckling Gradient,

depending on whether the column

would buckle to the left or to the

right (Fig. 1.1). In the case of no

initial imperfection or eccentric

loading, the most probable

direction of buckling would

perhaps be to the left, corre-

sponding to the smaller I. B. G.
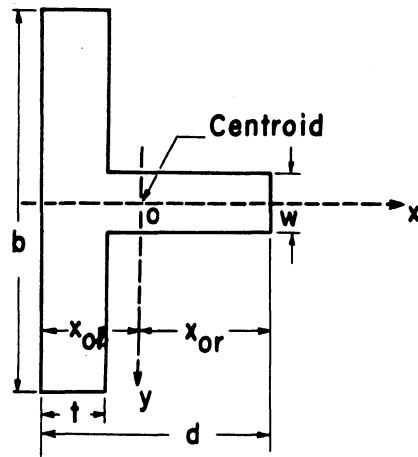
(inelastic buckling gradient).

Fig. 1.1. T-Section

If initial imperfection in the "T" section were such that it would

initiate buckling in one or the other direction or if it would be prevented

from deflecting in one direction, the column would presumably buckle

in the unsupported or initially curved direction. If buckling were

initiated in the direction with the larger I. B. G. , i. e. , to the right,

the behavior of the column would be quite different from the first case.
In the latter case the flange of the "T" section would be subjected to
increasing compressive stress corresponding to decreasing value of
tangent modulus and larger parts of the web would be subjected to strain
regression at the elastic rate. Thus, progressively, the ratio of
bending stiffness about the y-axis to that of the x-axis would increase
and in some cases, depending on the ratio of the bending stiffness with
respect to the x- and the y-axes in the unloaded stage before the load
reaches the potential maximum, biaxial bending accompanied with
torsion would commence. In other cases this happens in the unloading
stage as the elastically behaving portion of the web increases.

The internal torsional resistance of the section could be
presumed to be only due to St. Venant torsion (with the inelastic modi-
fication) and the warping torsional resistance can be neglected. If
buckling originates in the direction of the smaller I.B.G., i.e., to the
left, strain regression would start in the flange area and the web will
be under increasing compressive strain with corresponding decrease
in tangent modulus. In this case the ratio of bending stiffness about
the x-axis relative to the y-axis will increase and more resistance to
buckling out of the plane of the web will be introduced. Bending will
then continue in the plane of the web as it originated.

In this thesis the inelastic buckling behavior of "T" sections of
aluminum alloys will be studied quantitatively and compared with the
qualitative predictions made in the preceding paragraphs. Also,
quantitative study will be made on the effects of existence of initial

crookedness in the positive or negative directions of the x-axis in the plane of the web. The effects of eccentric loading in the plane of the web have also been studied and compared with the effect of initial imperfection. The study has been done for sections with different ratios of bending stiffness relative to the x- and the y-axes and with different material properties. Finally, a series of tests has been conducted to confirm the theoretically predicted behavior.

In order to evaluate the above buckling problem quantitatively, an algorithm has been developed for use on a high speed digital computer, that makes the manipulation of the incremental process possible. To carry out the experiment, a procedure of measuring the lateral displacements and the twist of the hinged-end columns in combined bending and torsion has been developed.

2.2. REVIEW OF THE PRIOR WORK

Musschenbroek[4] built the first testing machine and proposed the first empirical column formula for the ultimate load carrying capacity of the columns of rectangular cross section which states that ultimate load per unit area is proportional to $\left(\dfrac{D}{L}\right)^2$, where D is the depth and L is the length of the column. This happened almost twenty-five years before Euler started to develop his column theory in 1744.

Euler's equation for critical load of a column is one of the most famous equations in strength of materials and was published in 1759. The translation of essential portions of this publication by

J. A. Van den Broek (Am. J. Phys., Vol. 15, No. 4, July-August 1947, pp. 309-318) reveals Euler's ability to apply advanced mathematics to a practical problem. Euler's formula was in effect a generalization of Musschenbroek's special case for rectangular sections.

For many years Euler's formula was not generally applied to actual design, since tests of structures indicated that columns frequently failed below the Euler load. Euler's formula gives the average stress at which a slender (elastic) concentrically loaded and initially straight prismatic and homogeneous column will develop bifurcation of equilibrium.

Euler's formula gives a very high value for buckling load of short columns. In a period of over two hundred years between the introduction of Euler's formula and the presentation of Shanley's concept of column buckling, there have been a great many developments and modifications of the column theory. In 1889 Considère[5] conducted a series of 32 column tests and verified that for short columns the Euler formula gave too high a value for the buckling load. He suggested that if buckling occurs above the proportional limit the elastic modulus should be replaced in the Euler formula by an "E_{eff}" in order to evaluate the ultimate strength of the column. He also stated that the value of "E_{eff}" is between the modulus of elasticity (E) and the tangent modulus (E_t). During the same year Engesser,[6] independently of Considère, suggested that the column strength in the

inelastic range can be obtained by the substitution of the tangent modulus

in place of elastic modulus in the Euler formula.

In 1895 Jasinski[7] criticized the tangent modulus theory on the

grounds that it did not account for the non-reversible characteristic

of the stress-strain relation in the inelastic range. In 1910

Von Kármán[8] evaluated the effective or "reduced modulus" for the

rectangular and the idealized H-section columns. The reduced modulus

is also called the "double modulus" as it is a function of both the

elastic and the tangent modulus. The formula for the double modulus

as derived by Von Kármán for the rectangular section is

$$E_r = \frac{4E\,E_t}{\left(\sqrt{E} + \sqrt{E_t}\right)^2} \qquad (1.2)$$

The double modulus theory was considered to be the correct theory of

inelastic column behavior until 1946 when Shanley showed that it

presented a paradox.[9] In order to exceed the tangent modulus

(Euler-Engesser formula), it is necessary that the effective modulus

be greater than E_t, i.e., some portion of the cross section must be

subjected to a strain regression. This indicates that the column

begins to bend before reaching the double modulus load. Shanley

mathematically verified his conclusions[1] which are as follows:[11]

    1. The Engesser load (tangent modulus load) represents
the maximum load for which the column has only one
equilibrium configuration. Up to this load the idealized
column must remain straight; beyond this load it may
bend.

2. The double-modulus load represents the upper limit for the load that can theoretically be reached as the column continues to bend with increasing load. To develop the double-modulus load would require infinite lateral deflection at a constant value of the tangent modulus which is impossible.

3. For a given material, the maximum load that can be developed will generally be only slightly greater than the Engesser load because of the rapid decrease in E_t with increasing stress. Therefore, the Engesser load is considered as the practical upper limit for column strength.

Duberg and Wilder, III[12] applied Shanley's approach to an idealized H-section column with two point concentrations of area and with zero web area and they confirmed Shanley's concept of initiation of buckling at the tangent modulus load.

In 1950 Lin[13] studied slightly curved columns of rectangular cross section, including effects of strain reversal. In 1961 Johnston[14] analyzed the inelastic behavior of a concentrically loaded "model" consisting of two rigid end segments continuous with a short deformable central rectangular segment of aluminum alloy (Fig. 1.2).
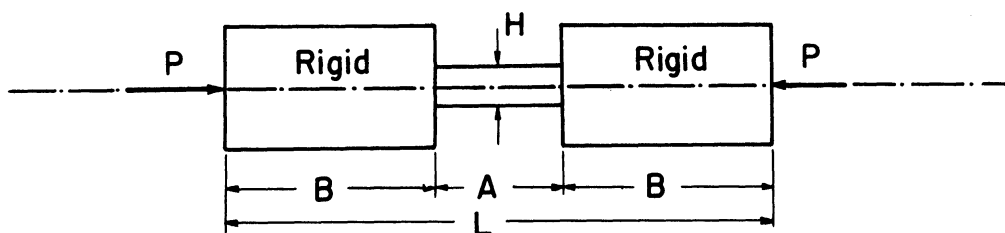
Fig. 1. 2. Johnston's Strut Model

In 1964 Augusti[15]

constructed a strut model made

of two rigid limbs connected by

a "central cell" and studied the

buckling and collapse of structural

elements in the inelastic range.

The cell consisted of two straight

filaments of vanishing thickness

in the plane of the paper (Fig. 1.3).
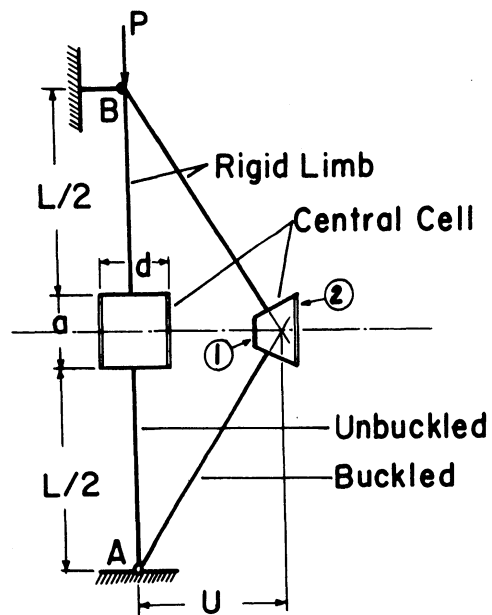
Fig. 1.3. Augusti's Inelastic
Strut Model

In 1966 Batterman and Johnston[16] presented the results of

their study on column behavior. This study had a broad scope and

included effects of the initial crookedness and residual stress on the

ultimate load carrying capacity of H-shaped columns of steel and

aluminum in bending about the weak and strong axes. Maximum load

was determined for different values of the slenderness ratio, yield

strength, residual stress and imperfection. In the above studies the

effect of torsion was not considered. The study of combined torsion

and flexure commenced in 1929 when Wagner[17] presented the first

theory of flexural-torsional buckling and also studied the effect of

eccentric loading. He assumed that the center of the twist coincides

with the shear center. Kappus[18] later stated that in general Wagner's

assumption was valid.

Ostenfeld[19] presented a correct theory for flexural-torsional buckling of tee, angle and channel sections accompanied by experimental results. In 1934 Wagner and Pretschner[20] presented some test results on angles and revised Wagner's earlier theory. In 1936 F. Bleich and H. Bleich derived the flexural-torsional buckling from energy considerations using variational principles;[21] later they revised their theory.[22] Lundquist and Fligg[23] and Niles[24] also studied and presented theories about torsional-flexural buckling. Goodier[25] simplified Wagner's theory and extended it to the case of a column subjected to bending about both principal axes, but he neglected the effect of the moment amplification caused by the deflection of the column. Timoshenko[26, 27] treated the torsional-flexural buckling of columns in the elastic region in 1945 and he also neglected the increase of the bending moment due to deflection of the column. Zickel[28] considered the influence of initial deflections and twist on biaxial bending of wide flange shapes. He assumed the initial twist to be finite in magnitude. The resulting equations were nonlinear and no general solutions were given for these equations. Hill and Clark[29] and Salvadori[30] made extensive studies of eccentrically loaded columns. Thürlimann[31] obtained an approximate solution for the case of small initial twist by modifying Zickel's equations. In 1966 Culver[32] developed a mathematical model for the biaxially loaded column with initial imperfection.

In 1950 B. G. Neal[33] presented the first solution for inelastic lateral torsional buckling of a rectangular beam. Galambos[34, 35]

presented a solution for inelastic lateral torsional buckling of wide

flange columns subjected to bending about the major principal axis

as a PhD dissertation at the Lehigh University. In 1962 Birnstiel[36]

treated H-columns loaded into the inelastic range in biaxial bending by

an incremental process and used a digital computer to evaluate the

ultimate load carrying capacity of these columns under eccentric

loading. He also recently completed a report on some experiments

of such nature.[37]

In 1964 Ringo[38] in his PhD dissertation developed an equi-

librium approach to the ultimate load on a biaxially loaded beam

column. In 1966 Rossow, Barney and Lee[39] introduced the effect

of initial curvature into the moment-curvature relationship and solved

the differential equation by double integration and then, using buckling

criterion, found interaction curves and suggested semiempirical

equations to approximate the interaction curves. In 1966 Lee, Fine

and Hastreiter[40] examined the problem of inelastic torsional

buckling strength of axially loaded H-columns.

References (41) through (45) give a comprehensive review of

the developments of the torsional, flexural or torsional-flexural

buckling behavior of the columns.

Inelastic range studies have always been carried out with the

assumption that the material yields at the proportionality limit, or

the inelastic range of the behavior has been approximated by straight

lines of stress-strain curve, except studies of column behavior by

Batterman and Johnston[16] where they assume a close mathematical
fit for the actual stress-strain relation. However, they neglect the
effect of the torsion.

1.3. INITIATION OF THE RESEARCH

In 1961 the author assisted Dr. Johnston[14] in his study of
"Buckling Behavior above the Tangent Modulus Load" where, with the
aid of a digital computer, he studied the behavior of structural
aluminum alloy struts of various lengths. The buckling model used
by Johnston in his study is shown on Fig. 1.2.

In Johnston's study of the "Inelastic Buckling Gradient", [3]
with which the author was closely associated, the most attention was
given to the definition and the evaluation of the I. B. G. with particular
reference to a tee section example. This study suggested an obvious
need for a more thorough evaluation of the actual column behavior
and obtaining a quantitative relation between column initial imper-
fection or eccentricity of loading and the preferred mode of buckling.

Later, the author assisted Batterman and Johnston[16] in their
study of "Behavior and Maximum Strength of Metal Columns". The
experience gained in this task helped considerably in completion of
this thesis.

CHAPTER II

BOUNDS OF BEHAVIOR OF A COLUMN
IN THE INELASTIC RANGE

GENERAL

The bounds of behavior of an ideal column in the inelastic

range will be discussed in this chapter. Included in these bounds is

the "inelastic buckling gradient". Duberg and Wilder[2] introduced

the I. B. G. for the symmetrical cross section and also determined

the complete load-deflection curve for an idealized H section column

using the Ramberg-Osgood[46] stress-strain relations. Later

Johnston[3] modified the I. B. G. for a monosymmetric section and

also considered the presence of the residual stress. In particular,

he noted the difference in the values of the I. B. G. for a T shaped

aluminum column when it buckles in the plane of symmetry towards

or away from the flange. Augusti[47] in his discussion of Johnston's

paper pointed out that the relation given for I. B. G. does not hold for

the case where buckling takes place in the elastic range and the

residual stress is not present. Augusti[15, 48] also introduced another

bound - the full yield line using his buckling model (Fig. 1.3). This

is useful when the yielding stress can be explicitly defined. However,

for a material which is continuously strain hardened the choice of a

yield point is not easy. Earlier in 1920, Osgood[49] noted the

difference in the reduced modulus loads for the different directions

of buckling of a "T" section and presented a graphical representation

of the variation of the reduced modulus in buckling towards or away

from the flange relative to the tangent modulus. In his study, Osgood

assumed that the area was concentrated along the center lines of the

web and the flange. When buckling is in the plane of symmetry, the

assumption of a line area for the flange would cause a considerable

error. In this study a detailed solution has been presented.

2.1. THE INELASTIC BUCKLING GRADIENT

i. Definition

The inelastic buckling gradient (I.B.G.)[3] is defined as the

initial slope at the tangent modulus buckling load of the curve obtained

by plotting column load as ordinate and maximum lateral column

deflection as abscissa. Derivation of I.B.G. for a material with a

continuously strain hardening characteristic in the neighborhood of

the stress corresponding to the tangent modulus load is a very simple

process. The value of I.B.G. depends on the shape of the cross

section as well as the elastic and inelastic properties of the column.

In all the following discussions and computations, the

Ramberg-Osgood[46] stress-strain curves can readily be adapted to

the procedure used in this study. However, it was desired to use

the actual stress-strain characteristic of the material and also

study the transition from elastic into inelastic region of behavior,

as Ramberg-Osgood curves do not have a truly straight line

representing the elastic range. The material properties used here are obtained by deriving a close mathematical fit for the stress-strain curves obtained from the experimental work (Chapter VI).

ii. Evaluation

The average critical stress of an initially straight and prismatic column of a homogeneous, isotropic and monotonically strain hardening material is given by

$$\sigma_c = \sigma_t = \frac{\pi^2 E_t}{(\frac{KL}{r})^2} \qquad (2.1)$$

where E_t = slope of the stress-strain curve at the critical stress

r = radius of gyration of the cross section with respect to axis about which buckling is to occur

K = the equivalent length factor, such that to make KL equal to the distance between two inflection points of the column deflection curve

σ_t = tangent modulus stress

The tangent modulus load, P_t, is

$$P_t = \sigma_t A \qquad (2.2)$$

where A is the area of the cross section. If buckling occurs in the elastic range the average critical stress is obtained by substituting the tangent modulus in equation (2.1) by the elastic modulus

$$\sigma_c = \sigma_e = \frac{\pi^2 E}{(\frac{KL}{r})^2} \qquad (2.3)$$

where σ_e is the Euler's critical buckling stress.

For a perfect hinged end condition, the equivalent length factor K = 1 and the shape of the deflection curve at the pending of buckling, when the resistance to bending along the column and across the cross section is uniform, is that of a half sine curve. An increment of deflected shape can be written in the following form

$$\Delta\delta = \Delta\delta_o \, \text{Sin} \, \frac{\pi z}{L} \tag{2.4}$$

where $\Delta\delta$ is the increment of the lateral deflection at a point having a distance z from the end of the column, and $\Delta\delta_o$ is the magnitude of the increment of the deflection at the mid-length.

Let us assume that the section of the column has only one axis of symmetry and the bending is to be initiated in the plane of symmetry of the column, i.e., the column is stronger in the direction of the other principal axis at this stage. Then, for an infinitesimal increase in the axial load above the buckling load, assuming deflection starts in the negative x-direction, the distribution of the stress at the mid-length section would be as shown in Fig. 2.1. The curvature of the column

Uniform strain across the cross section at the tangent modulus load
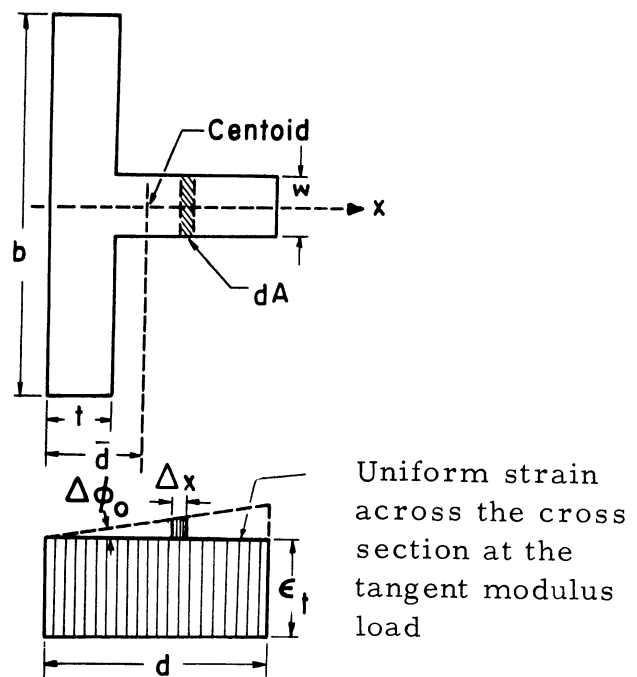
Fig. 2.1.   Strain Distribution at Initiation of Buckling

at a cross section which has a distance z from the end of the column will be

$$\Delta\phi = -\Delta\delta \frac{\pi^2}{L^2} \sin \frac{\pi z}{L} \tag{2.5}$$

At the mid-height, $z = \frac{L}{2}$, the curvature will be

$$\Delta\phi_0 = \Delta\phi_{z=\frac{L}{2}} = -\Delta\delta \frac{\pi^2}{L^2} \tag{2.6}$$

The strain increment of an element with a coordinate (x, y) will be

$$\Delta\phi = \Delta\delta (x + \overline{d}) \frac{\pi^2}{L^2} \tag{2.7}$$

For a small increment of strain, the following relation exists between change of strain and stress

$$\Delta\sigma = \Delta\epsilon E_t \tag{2.8}$$

Substituting for $\Delta\epsilon$ from (2.7) we get

$$\Delta\sigma = \Delta\delta (x - \overline{d}) E_t \frac{\pi^2}{L^2} \tag{2.9}$$

Now the increment of the axial load can be obtained by integrating $\Delta\sigma$ over the area of the cross section

$$\Delta P = \int_A \Delta\sigma \, dA \tag{2.10}$$

or

$$\Delta P = \int_A \Delta\delta (x + \overline{d}) E_t \frac{\pi^2}{L^2} \, dA$$

or $\tag{2.11}$

$$\Delta P = \Delta\delta E_t \frac{\pi^2}{L^2} \int_A (x + \overline{d}) \, dA$$

If the centroid of the cross section is chosen as the origin and

x, y are the principal axes, then

$$\int_A (x + \overline{d})\ dA = \overline{d}\ A \tag{2.12}$$

where $\overline{d}$ is the distance of the y-axis from the farthest left fiber.

Replacing for the value of the integral in the equation (2.11) from

(2.12)

$$\Delta P = \Delta\delta\ \frac{\pi^2 E_t}{L^2}\ A\ \overline{d} \tag{2.13}$$

according to (2.1) and (2.2), $\dfrac{\pi^2 E_t}{L^2}\ A = \dfrac{P_t}{r^2}$, so that

$$\frac{\Delta P}{\Delta\delta} = \frac{P_t}{r^2}\ \overline{d} \tag{2.14}$$

As $\Delta\delta$ tends to zero the left hand side of the equation (2.14) becomes

the slope of the load vs. deflection curve at the point of initiation of

bending

$$\lim_{\Delta\delta \to 0} \left|\frac{\Delta P}{\Delta\delta}\right| = \frac{P_t}{r^2}\ (\overline{d}) \tag{2.15}$$

Had we assumed that the deflection was initiated in the positive

direction of the x-axis in the above equation, d would have been

$(d - \overline{d})$ and the I. B. G. would have been

$$\lim_{\Delta\delta \to 0} \left|\frac{\Delta P}{\Delta\delta}\right| = \frac{P_t}{r^2}\ (d - \overline{d}) \tag{2.16}$$

This is the Johnston's modification of Duberg and Wilder's[2]

derivation of inelastic buckling gradient for a symmetrical cross

section.

In the equations (2. 15) and (2. 16), the value in parentheses
is the distance of the centroid from the outer fiber of the convex
side measured along a line parallel to the plane of bending.

It should be mentioned that if buckling begins in the elastic
range the deflection U will have the form of a half sine curve with
an indeterminate amplitude "U_o" such that

$$U = U_o \, \text{Sin} \, \frac{\pi z}{L} \tag{2.17}$$

As there is strain regression on the convex side, relation (2. 7)
will not be true. Consequently, the equations (2. 15) and (2. 16) will
not hold for the initiation of lateral buckling in the elastic range.
It is important to note that in the elastic range the slope of the load
vs. deflection curve at the point of incipient buckling is equal to
zero, i. e.,

$$\lim_{\Delta\delta \to 0} \left| \frac{\Delta P}{\Delta \delta} \right| = 0 \tag{2.18}$$

Buckling then takes place with no increase in the axial load. The
actual behavior of the column in this case can also be determined
by the incremental procedure.

As the curvature of the load-deflection curve of the column
is negative, the line tangent to the load-deflection curve at the
tangent-modulus load will provide an upper bound for the inelastic
column behavior.

2.2. TANGENT MODULUS

The tangent modulus stress and load can be obtained from equations (2.1) and (2.2) respectively. In the equation (2.1), σ_t (the tangent modulus stress) is expressed implicitly as E_t (tangent modulus) itself is a function of σ_t. Usually, as in the case of this problem, stress and the tangent modulus are expressed as functions of strain. Therefore, in order to evaluate the tangent modulus stress, for a specific equivalent slenderness ratio $(\frac{KL}{r})$, one must follow some iterative process to pick up the right value for strain whose corresponding values of the stress and the tangent modulus would satisfy the equation (2.1).

Formula (2.1) can be solved for $(\frac{KL}{r})$ and written in the following form

$$\frac{KL}{r} = \pi \sqrt{\frac{E_t}{\sigma_t}} \qquad (2.19)$$

If it is desired to have a graphical representation between the effective slenderness ratio and the tangent modulus stress, one may for numerous values of strain evaluate the corresponding stress and tangent modulus, and then by means of equation (2.19) determine the effective slenderness ratio, and thus avoid the iteration and reduce the length of the manipulation. Graphical representation of (2.19) along with other plots can be seen in Figures 2.6 through 2.10. A thorough explanation of these graphs will be given in the following pages. As the tangent modulus stress is the stress at which an ideal column with only infinitesimal imperfections from perfect

concentric loading starts to bend, the line ($P = \sigma_t A$) parallel to the

deflection axis is a lower bound for the ultimate load carrying

capacity of the column. Shanley states, "For a given material, the

maximum load that can be developed will generally be only slightly

greater than the Engesser (tangent modulus) load".[11] The incre-

mental procedure here will provide a comparison between the tangent

modulus load and the ultimate load for some chosen "T" columns.

2.3. REDUCED MODULUS (DOUBLE MODULUS)

i. Introduction and Definition

The reduced or double modulus load can be defined as the

load at which the inelastic buckling gradient becomes zero, if a

column is prevented from buckling above the tangent modulus load.

Therefore, it is an upper bound for the ultimate load carrying

capacity of the column; in fact, the double modulus load can never

be attained in a real column. In derivation of the reduced modulus

E_r or reduced modulus load P_r, the following assumptions are

made:

    i. On the convex side of the bent column where the

       strain regression is to occur, stress and strain

       are related by the elastic modulus "E", i.e.,

       unloading is elastic ($\Delta\sigma = E \Delta\epsilon$); this is proven

       experimentally.

    ii. On the concave side of the bent column, the incre-

       ments of the stress and the strain are related by

the tangent modulus ($\Delta\sigma = E_t \Delta\epsilon$) associated with

the compressive strain at which buckling starts.

One may make a gross mistake by using the tangent modulus

obtained at the tangent modulus load in the evaluation of the reduced

modulus. This means that the tangent modulus has been assumed to

remain constant beyond the tangent-modulus stress. The reduced

modulus stress, evaluated on such basis, is shown on Fig. 2.9

and may be termed "false reduced modulus" or "false reduced

modulus load". As it is seen in the graph, the error of such

assumption becomes larger and larger as one departs from the

linear portion of the stress-strain relation.

ii. Evaluation

The double modulus varies with the shape of the cross section.

Von Kármán[8] derived the formula (1.2) for the reduced modulus of

a rectangular cross section. In the case of the "T" section, the

double modulus depends not only on the dimensions of the section

but also on the buckling direction.[3]

Let us assume that buckling occurs in the positive x

direction and the curvature of the bending (in the plane of symmetry)

is ($-\phi$). During bending, since there is no change in the column

load, the algebraic sum of the change in the load of the unloading

segment (ΔP_r) and the loading segment (ΔP_ℓ) should be equal to

zero (Fig. 2.2)

$$\int_A \Delta\sigma \, dA = \Delta P_\ell + \Delta P_r = 0 \qquad (2.20)$$

or

$$\int_{A_\ell} (x_r - \overline{d} - x) \phi E_t dA_\ell + \int_{A_r} (x_r - \overline{d} - x) \phi E dA_r = 0 \qquad (2.21)$$

During bending, the internal resisting moment (M_r) is equal to the

integral of the moment of the elements of the load change $(\Delta P = \Delta\sigma dA)$

about the bending axis. As bending takes place about the "zero strain

change axis (Z.S.C.A.)", x_r, the moment should be taken about this

axis, i.e.,

$$M_r = \int_A \Delta\sigma \left[x - (x_r - \overline{d}) \right] dA$$

or $\qquad\qquad\qquad\qquad\qquad\qquad\qquad\qquad\qquad\qquad\qquad (2.22)$

$$M_r = \int_A \Delta\sigma (x - x_r) dA + \overline{d} \int_A \Delta\sigma dA$$

Strain distribution line after buckling

Uniform strain across the cross section of a column held straight prior to buckling

Uniform stress across the cross section of a column held straight prior to buckling

Stress distribution line after buckling
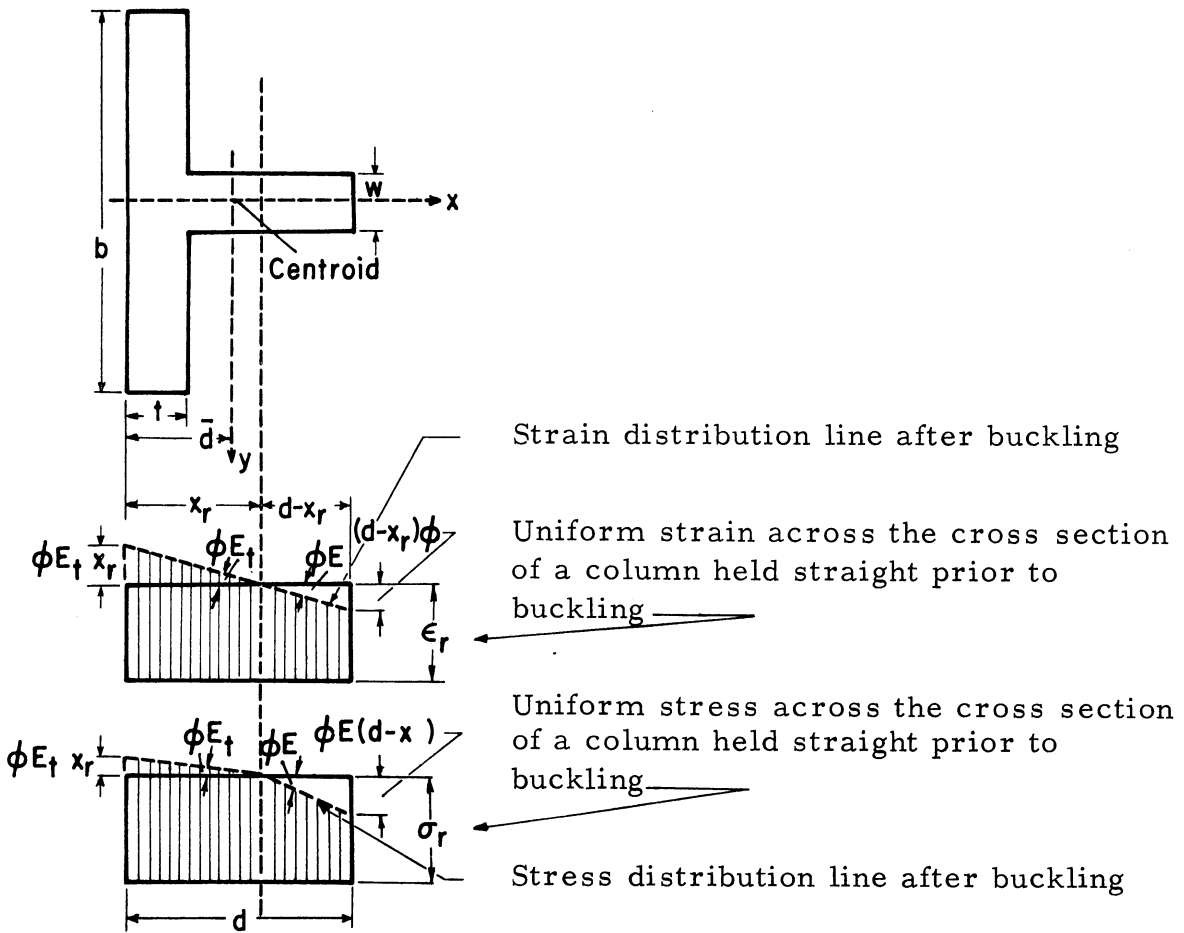
Fig. 2.2. Stress and Strain Distribution at
the Reduced Modulus Load

According to (2.20), the second integral is equal to zero, then

$$M_r = \int_A \Delta\sigma (x - x_r)\, dA \tag{2.23}$$

The right hand side of the equation (2.23) is the moment with respect to the y principal axis. Thus, it is shown that the internal resisting moment with respect to the Z.S.C.A. and the y principal axis are equal. Equation (2.22) can be written in the following form

$$M_r = \int_{A_\ell} [x - (x_r - \overline{d})]^2\, \phi\, E_t\, dA_\ell + \int_{A_r} [x - (x_r - \overline{d})]^2\, \phi\, E\, dA_r \tag{2.24}$$

Now consider the equation relating the moment to the curvature

$$M_r = E_r\, I_{yy} \tag{2.25}$$

by solving equation (2.21) for x_r and evaluating M_r from (2.24) one can obtain E_r from (2.25) in which I_{yy} is the moment of inertia with respect to the principal axis y. The reduced modulus obtained in this case, where buckling is to the right, will be named E_{rr}, and otherwise $E_{r\ell}$. In order to evaluate $E_{r\ell}$, E and E_t should be interchanged in the equations (2.21) and (2.24).

Now consider the evaluation of E_{rr}. Let

$$\eta = \frac{E_t}{E} \tag{2.26}$$

We will have three cases:

1. The Z.S.C.A. is in the web (Fig. 2.3a)

$$\Delta\sigma_1 = (x_r \phi) E_t \qquad\qquad \Delta P_1 = (x_r \phi) E_t b \frac{t}{2}$$

$$\Delta P_{21} = (x_r - t) \phi E_t b \frac{t}{2}$$

$$\Delta\sigma_2 = (x_r - t)\phi E_t$$

$$\Delta P_{22} = (x_r - t)\phi E_t w \frac{(x_r - t)}{2}$$

$$\Delta\sigma_3 = -(d - x_r)\phi E \qquad \Delta P_3 = -(d - x_r)\phi E_t w \frac{(d - x_r)}{2}$$

Line of uniform stress across the cross section of the column held straight prior to buckling
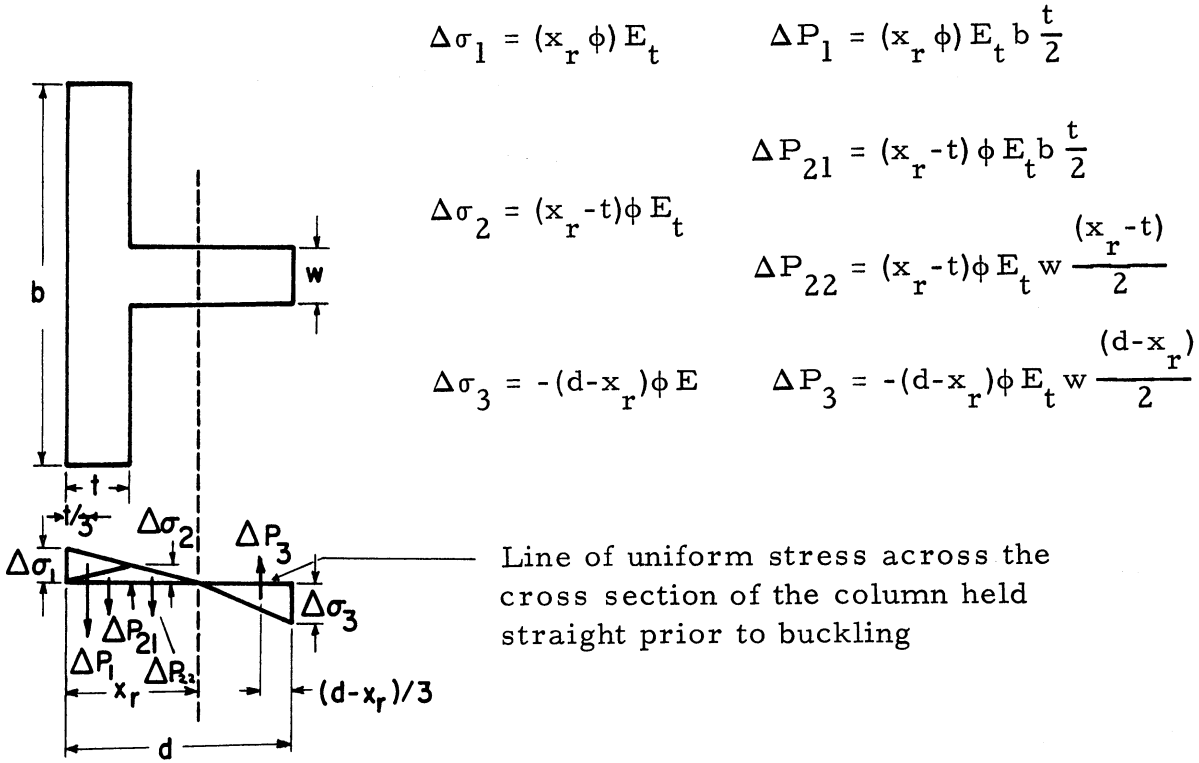
Fig. 2.3a. Stress Distribution - Z.S.C.A. in the web

then

$$\Delta P_1 + \Delta P_2 + \Delta P_{22} + \Delta P_3 = 0$$

or

$$E\phi \left\{ \eta \left[(2x_r - t) b \frac{t}{2} + (x_r - t)^2 \frac{w}{2} \right] - (d - x_r) \frac{w}{2} \right\} = 0 \qquad (2.27)$$

Equation (2.27) is a quadratic equation in terms of x_r and can be simplified and solved for x_r

$$x_r = \left\{ \left[d - \eta(\frac{b}{w} - 1) t \right] + \left[(d - \eta(\frac{b}{w} - 1) t)^2 - (d^2 + (\frac{b}{w} - 1) t^2 \eta)(1 - \eta) \right]^{\frac{1}{2}} \right\} / (1 - \eta)$$

$$(2.28)$$

M_r will be

$$M_r = \Delta P_1 (x_r - \frac{t}{3}) + \Delta P_2 \; (x_r - \frac{2t}{3}) + \Delta P_{22} \frac{2(x_r - t)}{3} + \Delta P_3 (d - x_r) \frac{2}{3}$$

or

$$M_r = E\phi \left\{ \eta \left[x_r \, bt \; \frac{(x_r - \frac{t}{3})}{2} + bt\,(x_r - t)\,(x_r - \frac{2t}{3}) + (x_r - t)^3 \, \frac{w}{3} \right] \right.$$

$$\left. + (d - x_r)^3 \, \frac{w}{3} \right\} \qquad (2.29)$$

2. The Z.S.C.A. is in the flange (Fig. 2.3b)

$$\Delta\sigma = x_r \phi E_t \qquad\qquad \Delta P_1 = x_r \phi E_t \, x_r \frac{b}{2}$$

$$\Delta\sigma_2 = (t - x_r) \phi E \qquad \Delta P_{21} = -(t-x_r)\phi E \; \frac{(t-x_r)}{2}$$

$$\Delta P_{22} = -(t-x_r)\phi E (d-t) \frac{w}{2}$$

$$\Delta\sigma_3 = (d - x_r)\phi E \qquad \Delta P_3 = -(d-x_r)\phi E \, w \, \frac{(d-t)}{2}$$

Stress distribution line
after buckling
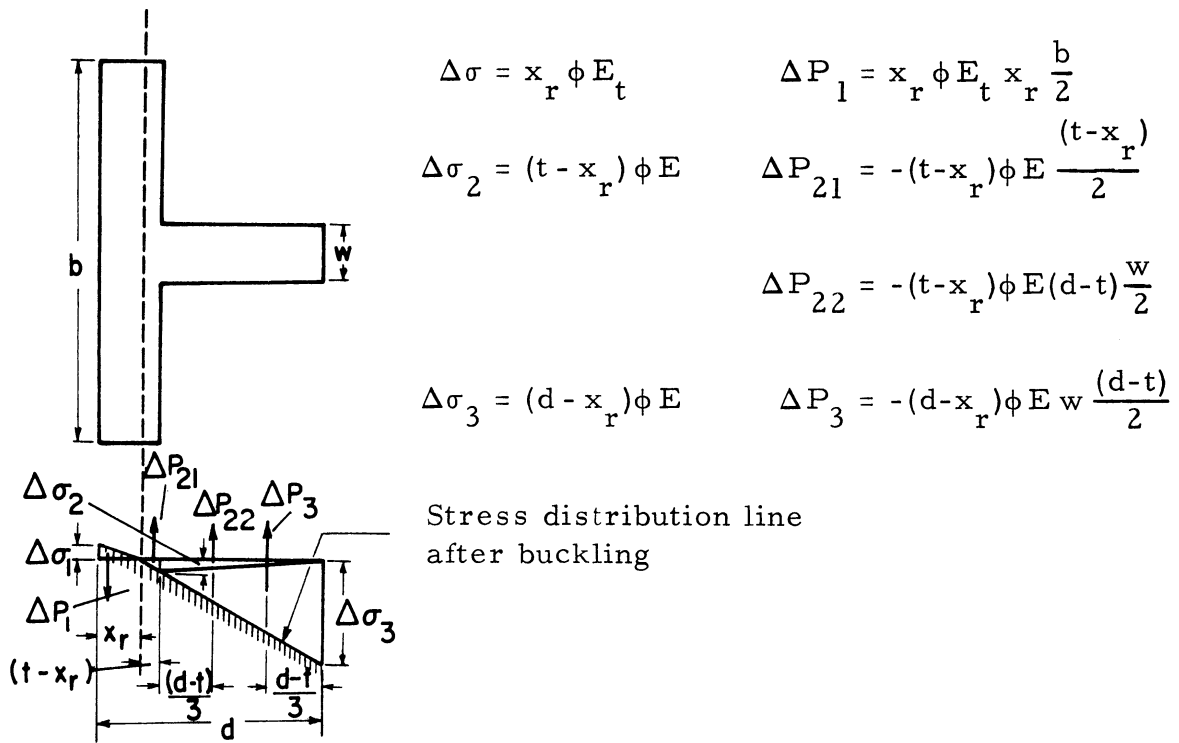
Fig. 2.3b. Stress Distribution - Z.S.C.A.
in the flange

$\Delta P = 0$ will give

$$x_r = \left\{ \left[t + w \, \frac{(d-t)}{b} \right] + \left[(t + w \, \frac{(d-t)}{b})^2 - (t^2 + w \, \frac{(d^2 - t^2)}{b})(1 - \eta) \right]^{\frac{1}{2}} \right\} / (1 - \eta)$$

$$(2.30)$$

and

$$M_r = E\phi \left\{ \eta \, x_r^3 \, \frac{b}{3} + (t - x_r)^3 \, \frac{b}{3} + (t - x_r)(d - t) \left[\frac{(d - t)}{3} + (t - x_r) \right] \frac{w}{2} \right.$$

$$\left. (d - x_r)(d - t) \left[\frac{2(d - t)}{3} + (t - x_r) \right] \frac{w}{2} \right\} \qquad (2.31)$$

3. The Z.S.C.A. coincides with inner surface of the flange (Fig. 2.3c).

This is the limiting point between cases (1) and (2).

$$\Delta\sigma_1 = t \, \phi \, E_t \qquad \Delta P_1 = t^2 b \phi \, \frac{E_t}{2}$$

$$\Delta\sigma_2 = (d - t) \phi E \qquad \Delta P_2 = -(d - t)^2 w \phi \, \frac{E}{2}$$

$\Delta P = 0$ gives:

$$\eta = \eta_1 = \frac{(d - t)^2 w}{t^2 b} \qquad (2.32)$$

Line of stress distribution
after buckling
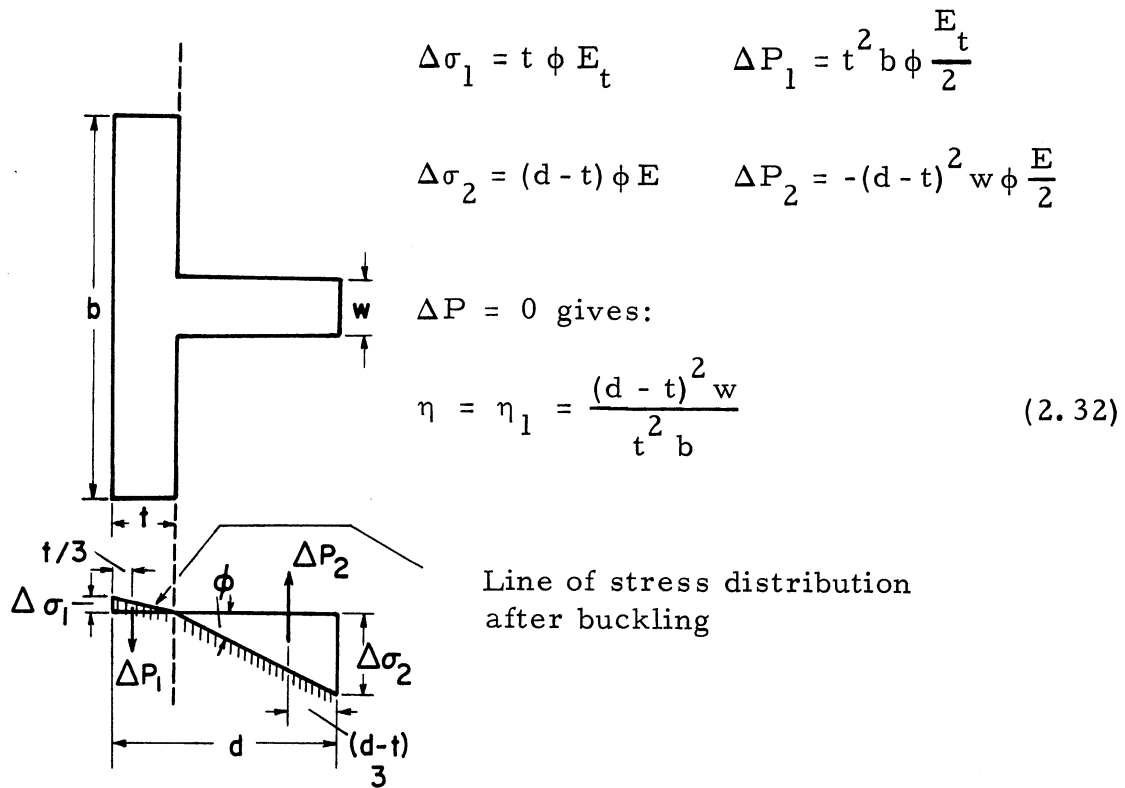
Fig. 2.3c. Stress Distribution - Z.S.C.A. at
the inner edge of the flange

For values of $\eta > \eta_1$ The Z.S.C.A. will be at the flange

and

for values of $\eta < \eta_1$ The Z.S.C.A. will be at the web

Considering equations (2.24) or (2.29) or (2.31) we can write

$$M_r = E \, I_{rr} \, \phi \qquad (2.34)$$

where I_{rr} is the weighted moment of inertia of the cross section with

respect to the Z.S.C.A. with the area on the elastic and inelastic

portions each having a weight equal to 1 and "η" respectively, where

"η" is defined in (2.26). Then using equation (2.25)

$$E_{rr} = \frac{EI_{rr}}{I_{yy}} \qquad (2.35)$$

The preceding equations and discussion of E_{rr} will hold for

$E_{r\ell}$ by interchanging x_r and x_ℓ (distance of the Z.S.C.A. from

the left face of the flange, in buckling to the left) and also E and E_t

(because the elastic and inelastic regions will interchange) in the

equations (2.24) through (2.33).

The reduced modulus stress is given by the following relation

$$\sigma_r = \frac{\pi^2 E_r}{(\frac{KL}{r})^2} \qquad (2.36)$$

which is the same as the expression for the tangent modulus stress

in which σ_t and E_t are replaced by σ_r and E_r. As for every value

of tangent modulus we have two different reduced moduli, E_{rr} and

$E_{r\ell}$. We will have two distinct values for double modulus stress,

one in buckling to the right, σ_{rr}, and the other in buckling to the

left, $\sigma_{r\ell}$. Each is an upper bound for the ultimate load carrying

capacity of the column in buckling towards the direction associated

with its derivation. Equation (2.36) is an implicit function, as both

σ_r and E_r are functions of strain. (Both stress and the tangent

modulus are expressed as functions of strain.) In order to evaluate

the σ_r for a given $(\frac{KL}{r})$, one has to apply some iterative process.

For a chosen value of strain, stress and the tangent modulus

and thereby the reduced modulus can be calculated. Having the

reduced modulus, one can obtain the corresponding effective slender-

ness ratio from

$$\left(\frac{KL}{r}\right)_r = \pi \sqrt{\frac{E_r}{\sigma}} \qquad (2.37)$$

This has been done for numerous values of strain, the graphs of

$(\frac{KL}{r})_{rr}$ (or $(\frac{KL}{r})_{r\ell}$) vs. σ and E_{rr} (or $E_{r\ell}$) are shown in

Figures 2.7 and 2.8. Also the variation of $\frac{E_r}{E}$ vs. $\frac{E_t}{E}$ in buckling

towards or away from the flange is shown in Fig. 2.9.

2.4. CRITICAL TORSIONAL BUCKLING

In order to have lateral buckling in the column, the dimensions

of the column should be such that the torsional buckling will not occur

prior to the lateral buckling.

In 1929 Wagner[50] explained the phenomenon of the elastic

torsional buckling in the following manner: Let the member be

subjected to a twist and z be the axis of rotation passing through

the center of twist of the cross section (Fig. 2.4). If rotation at z

is β and at $z + dz$ it is $(\beta + \frac{d\beta}{dz} dz)$, then the rotation of a fiber

which has a distance ρ from the

center of twist will be $\rho \frac{d\beta}{dz}$.

Wagner suggested that the com-

ponent of the normal stress $(\frac{P}{A})$,

when displaced due to rotation,

on the plane perpendicular to the

rotation axis, will induce a torque,

i. e.,
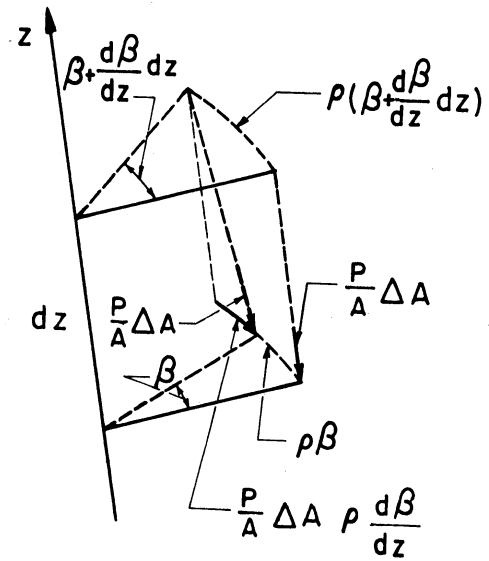
Fig. 2.4. Torsional Buckling

$$M_z = \int_A \frac{P}{A} \rho \frac{d\beta}{dz} \rho \ dA = \frac{P}{A} I_p \frac{d\beta}{dz} \qquad (2.38)$$

where I_p = polar moment of inertia with respect to the center of twist.

If the torsion is uniform, $\frac{d\beta}{dz} = \theta$, and the warping rigidity C_w is

negligible, then at the equilibrium position

$$M_z = C \theta \qquad (2.39)$$

where

C = torsional stiffness (G J)

G = shear modulus

and for a T section

$$J = \frac{1}{3}bt^3 + \frac{1}{3}w(d - t)^3 - 0.21t^4 - 0.105w^4 + \alpha_1 D_1^4$$

(For explanation refer to Fig. 4.21.) Combining equations (2.38) and

(2.39), one may find the critical torsional buckling stress

$$\sigma_{c_t} = \frac{C}{I_p} \qquad (2.40)$$

If the lateral buckling is to occur prior to the torsional buckling in

the inelastic range, the above explanation and the derivation of critical

torsional buckling stress will hold with one modification. Since in

the inelastic range the shear stress and strain are related to one

another by G_s (secant shear modulus - equation (4.68)) instead of

G for the elastic range, then the torsional stiffness coefficient in the

equation (2.40) will be

$$C = G_s J \qquad (2.41)$$

2.5. LOCAL BUCKLING

The local buckling phenomenon should be studied prior to the

choice of the dimensions of the cross section. The web of some of the

tee shape specimens chosen for the test buckled locally. In order to

study the local buckling in the flange or the web of the tee column,

one may treat it as a flat plate being compressed from opposite edges.

At a critical stress the plate may buckle out of its plane prior to the

commencement of the overally column buckling. Such buckling may

occur either in the elastic or the inelastic range.

In 1891 Bryan[51] presented a solution for the elastic buckling

strength of a long rectangular plate simply supported along all edges

and subjected to a longitudinal compressive load. Bleich[22]

suggested the following equation for the approximate local buckling

stress (in the elastic or inelastic range) of a flat plate segment of a

long column under uniform compressive load.[55, 56]

$$\sigma_{c_\ell} = k \ \frac{\pi^2 E \sqrt{\eta}}{12(1 - \nu^2)(\frac{b}{t})^2}$$

where $\quad \eta = \dfrac{E_t}{E}$

ν = Poisson's ratio

$\dfrac{b}{t}$ = width-thickness ratio

and k depends on the longitudinal boundary conditions. For one edge

fixed and the other free k = 1.277

(Fig. 2.5).

In recent years Stowell,[52]

Haaijer[53] and Thürlimann[54] have
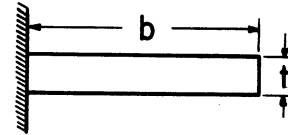
Fig. 2.5. Coefficient k
and the Edge Condition

studied the inelastic local buckling of steel plates in the strain-hardening

range. However, the problem of this thesis is more complex than for

a uniform compressive stress distribution, as the column cross

section will be subjected to a varying strain. This condition results

in a varying stress and differing tangent moduli for different elements.

The presence of strain regression will make the problem still more

complicated. For the practical purpose of this thesis equation (2.42)

will be used together with the assumption that one edge of the plate is

fixed and the other is free and that the maximum stress acting on the

cross section of the flange or the web is acting uniformly across and

along that segment of the column. The graph of uniform compressive

stress vs. the critical local buckling stress, based on equation (2.42),

for the different widths of the web (d = 1.5$''$, 2.5$''$, 3$''$) and the flange

(b = 4$''$) with the line $\sigma = \sigma_{c_\ell}$ (drawn to scale) is shown on Fig. 2.10.
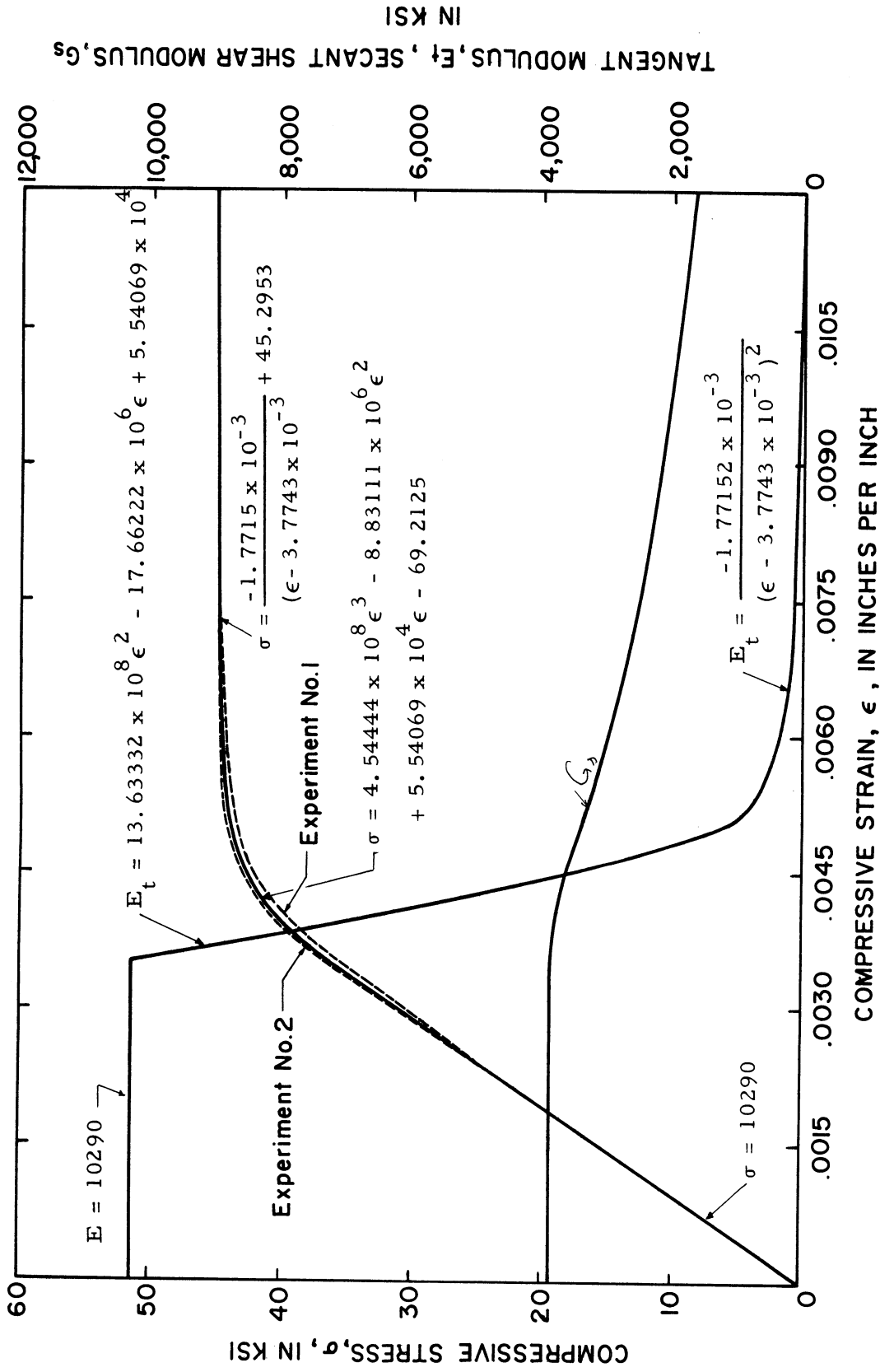
Fig. 2.6. Stress-Strain, Tangent Modulus Strain and Secant Shear Modulus Strain (#1) (Mathematical Fit and the Experiments)
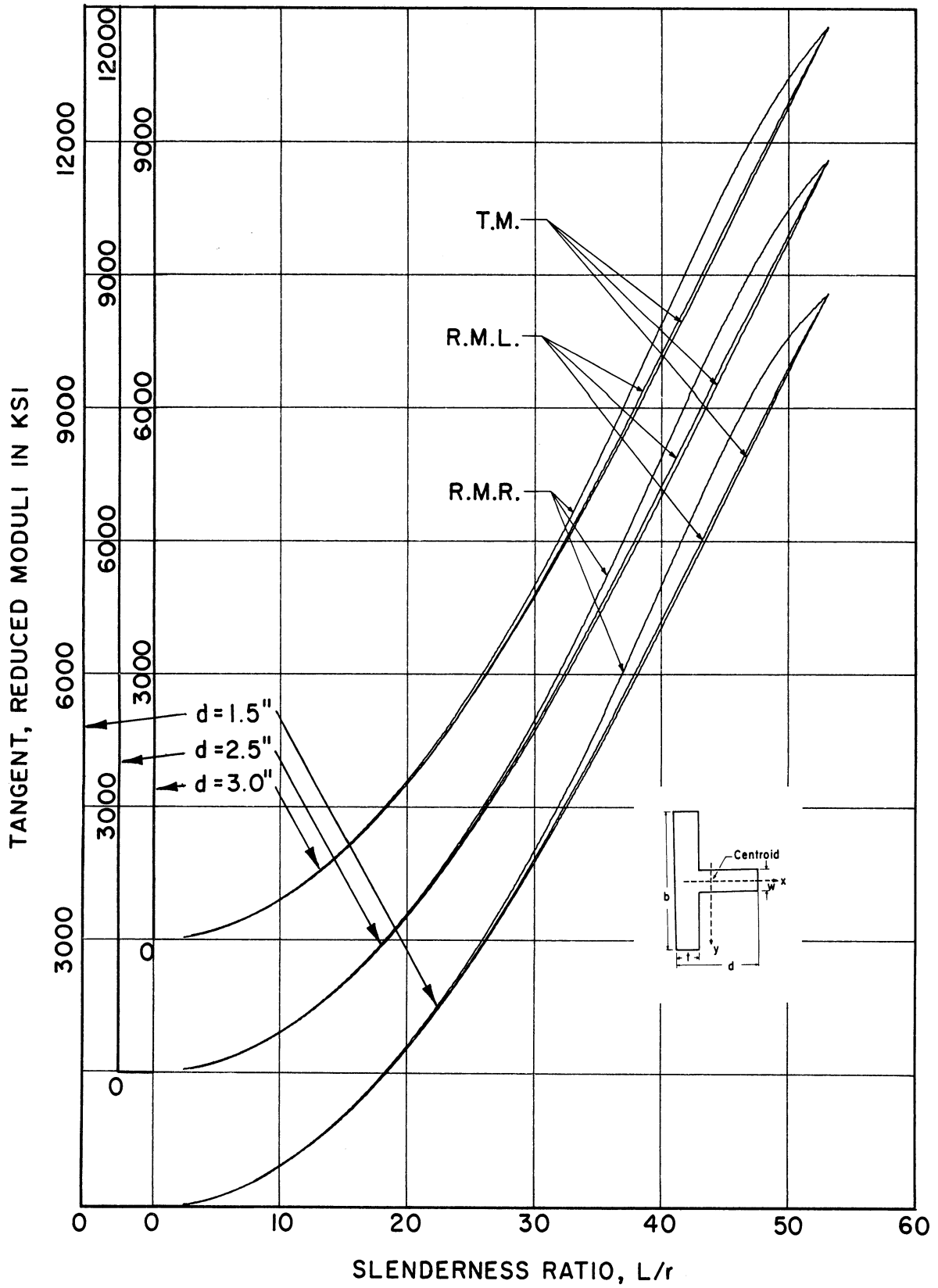
Fig. 2.7. Tangent and Reduced Moduli in Buckling to the Left and to the Right vs. Slenderness Ratio
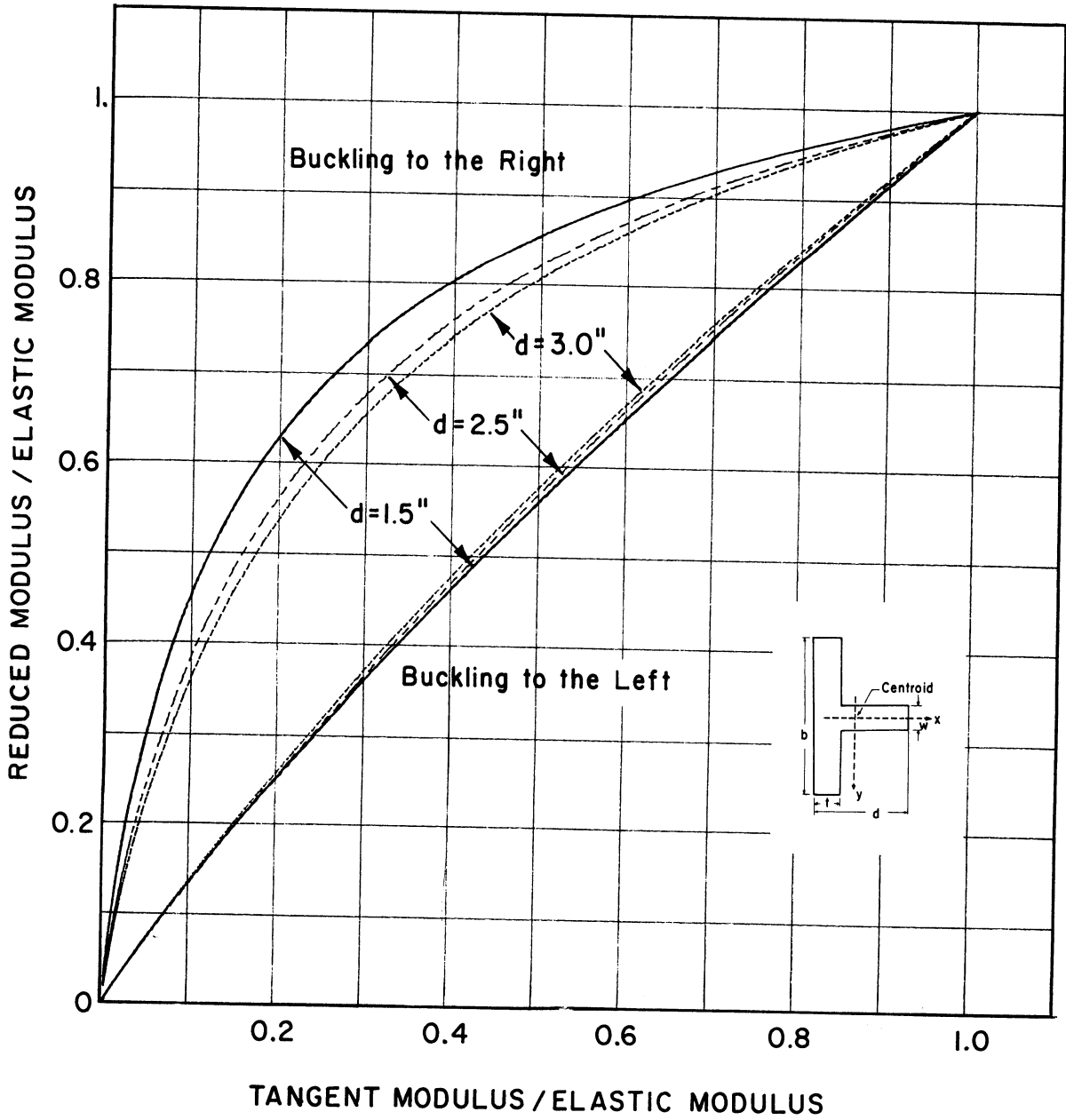
Fig. 2.8. Reduced Modulus in Buckling to the Left and to the Right
vs. Tangent Modulus
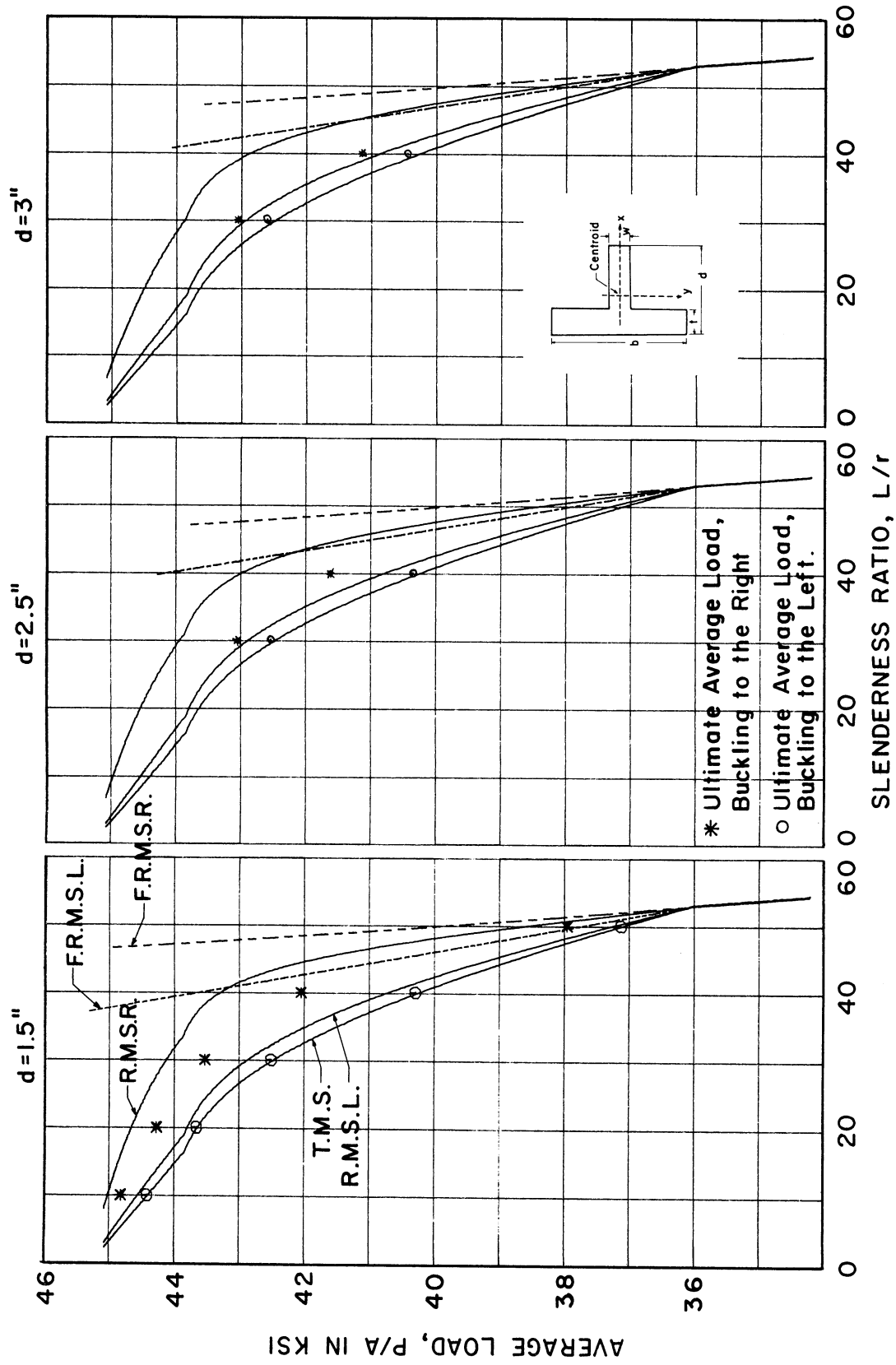
Fig. 2.9. Tangent, Reduced, False Reduced Modulus Stresses and Ultimate Average Stress vs. Slenderness Ratio
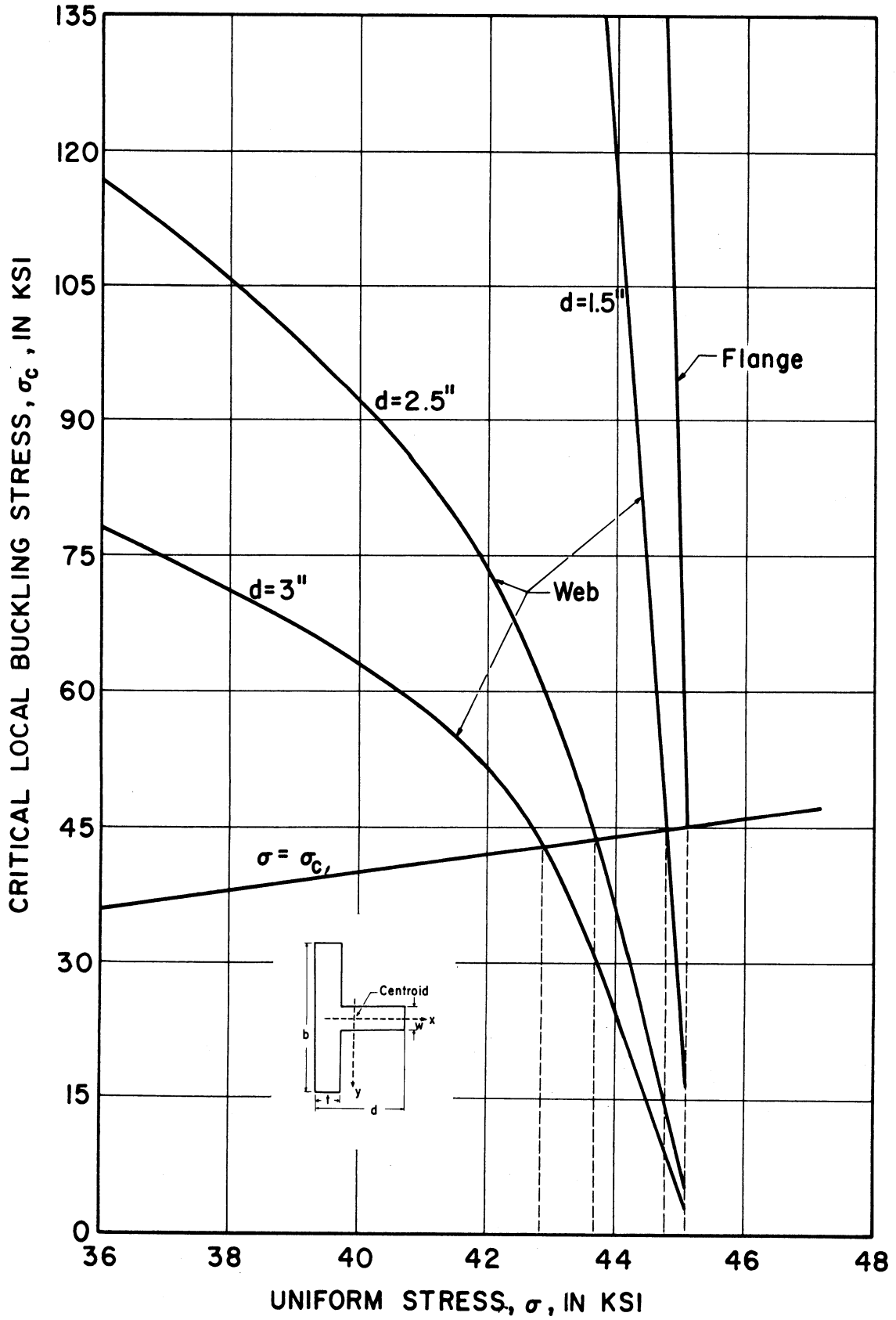
Fig. 2.10. Critical Local Buckling for Flange and Web vs.
Uniform Compressive Stress

CHAPTER III

THE EQUATIONS OF FLEXURAL-TORSIONAL BUCKLING

3.1. SELECTION OF THE COORDINATES

In order to best write the equations of flexural-torsional buckling of a column, it is essential to choose and define a proper coordinate system. In the case of a "T", the cross section is composed of two rectangular segments with a rather large width to thickness ratio. The following assumptions can be made which will result in considerable simplification of the method of solution of the problem with a negligible deviation from the exact solution:

i. Only St. Venant torsion is present and the contribution of warping restraint to the torsional resistance is negligible.

ii. At all stages of the deformation of the column, the center of twist remains at the point of intersection of the center lines of the web and the flange. At any cross section under consideration the movement of the twist center is determined by the manner of distribution of the normal stress, and also by the ratio of the width of the flange to the width of the web. However, the smallness of this movement justifies the above assumption.

In cases where it is desired to take the effect of the warping

or the effect of change of location of the center of twist into consid-

eration, one may adapt the pro-

cedures of this chapter with

modifications which will be

explained. For simplicity, the

origin of the xyz coordinate

system is chosen to coincide

with the center of twist of the

top face of the column. The

stationarsy xyz Cartesian

coordinate system is oriented

with respect to the unloaded

shape of the ideal column

(Fig. 3.1a), such that x- and

y-axes lie along the center

line of the web and the flange

respectively, and the positive

direction of the z-axis is

chosen from top to the bottom

of the column.
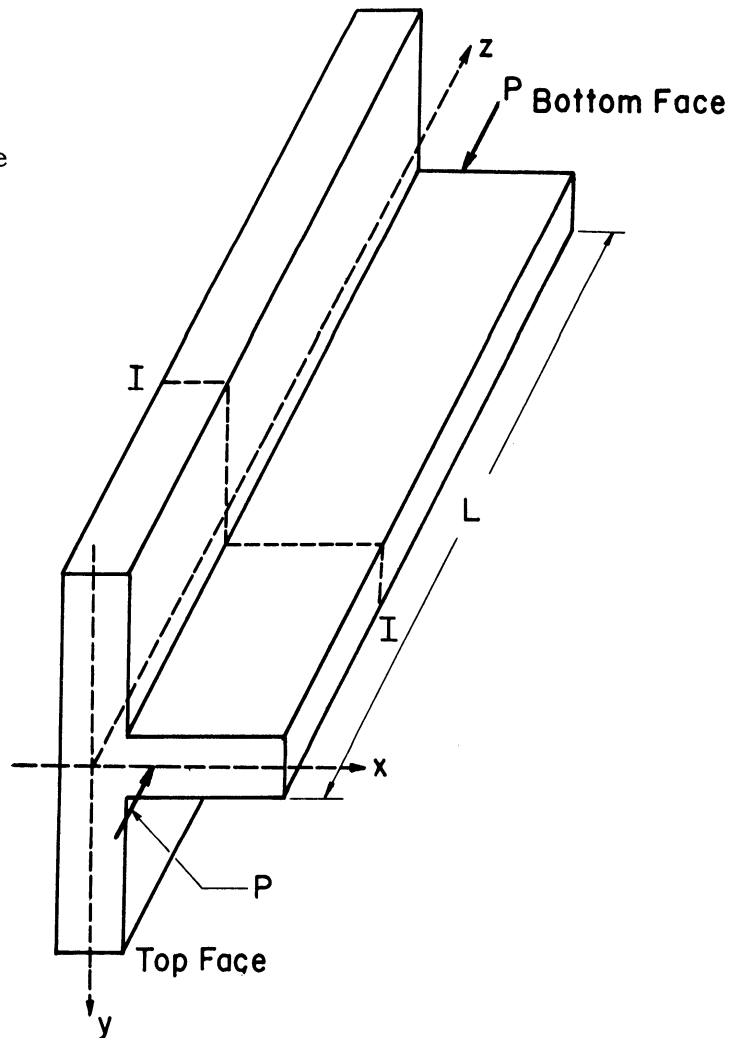
Fig. 3.1a. "Ideal" Column and the
Fixed Coordinates.

The ξ, η and ζ, mutually orthogonal coordinate axes, are

so chosen that ξ and η axes coincide with the center-line axes of the

flange and the web of the displaced cross section, respectively.

Thus, the $\xi\eta$ plane is taken to

be fixed to the cross section

under consideration. There-

fore, its lateral motion and

twist is the same as that of

the column at that cross

section. This makes the ζ

axis remain tangential to the

deflected longitudinal axis

passing through the center

of twist of the cross

section of the column
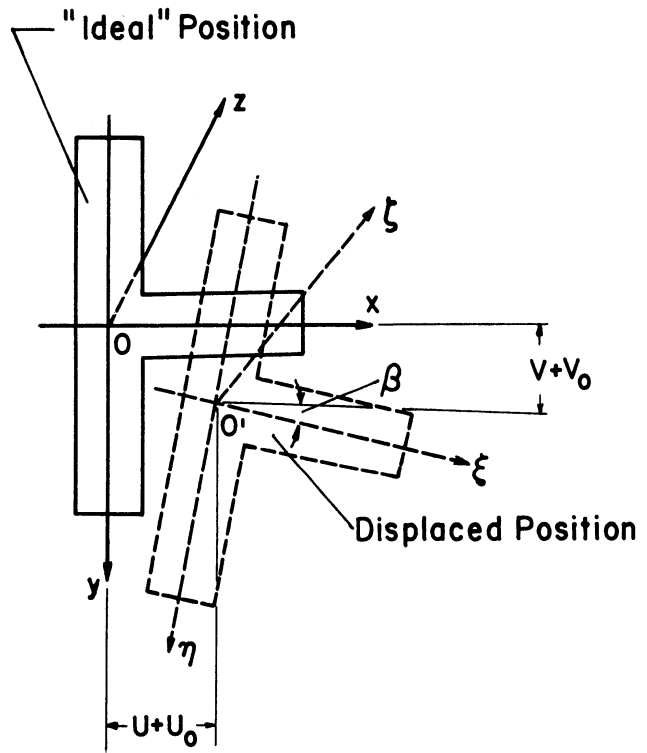
(Figs. 3.1b, c).

Fig. 3.1b. Cross Section I-I
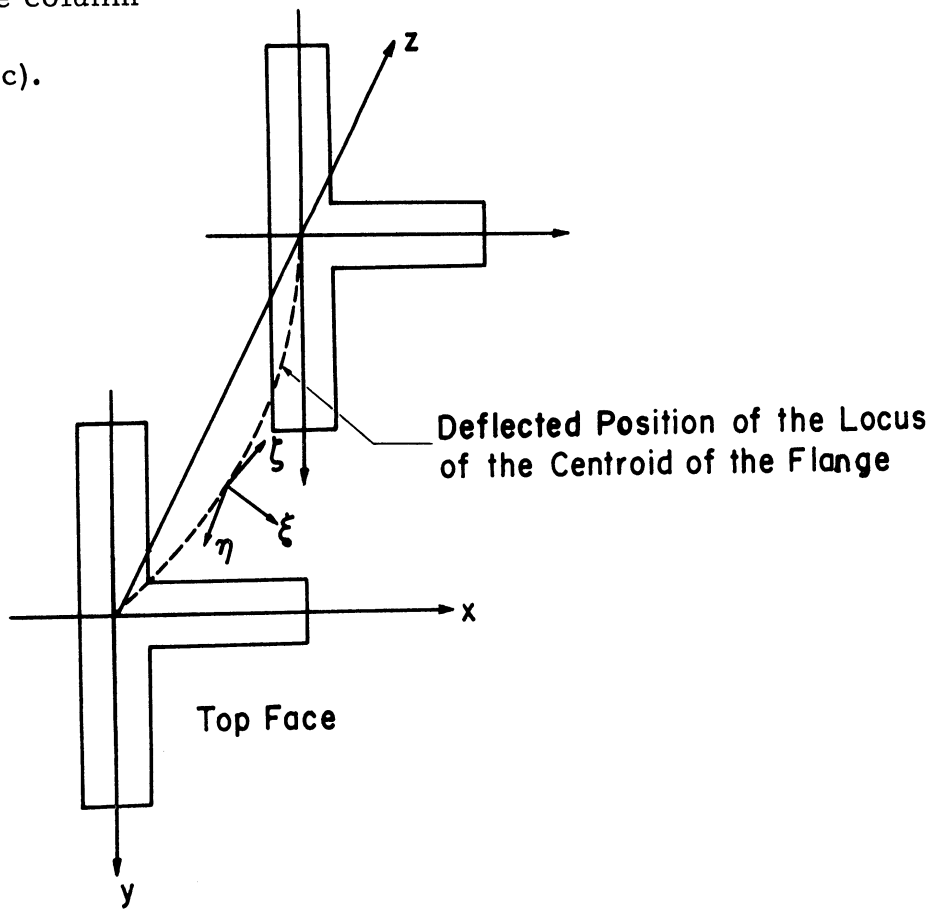
Fig. 3.1c. xyz and the $\xi\eta\zeta$ Coordinates

3.2. TRANSFORMATION OF COORDINATES

The x-, y- and z-axes are taken to be the initial reference axes and ξ, η and ζ are the moving axes. In general, $\xi\eta\zeta$ has a translation and a rotational motion relative to the xyz-axes. Neglecting the component of the translation of the $\xi\eta\zeta$ axes in the z direction (due to shortening of the column) we can designate the components of the displacement of the center of twist (the origin of the $\xi\eta\zeta$ axes) from its initial position in the x and y directions by U and V respectively (Figs. 3.2a, b, c).
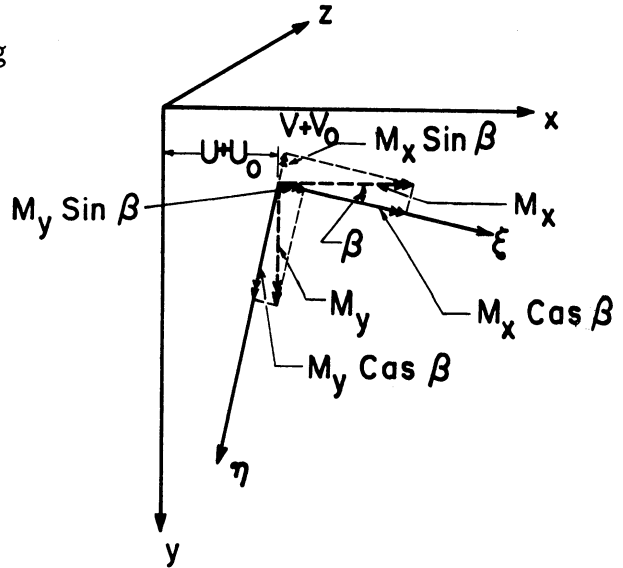
Fig. 3.2a. Transformation in the Cross Section Parallel to the xy Plane
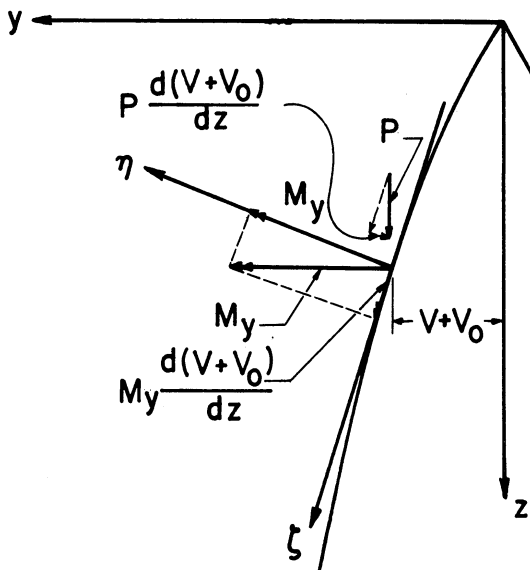
Fig. 3.2b. Transformation in the Cross Section Parallel to the yz Plane
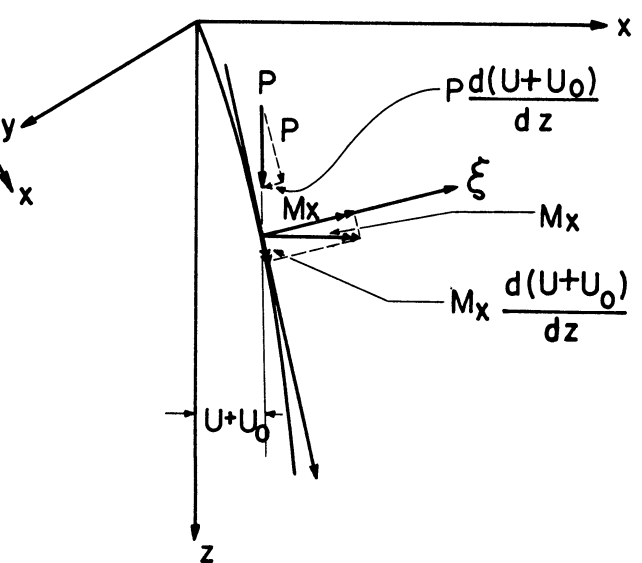
Fig. 3.2c. Transformation in the Cross Section Parallel to the zx Plane

The rotational part of the motion can be designated by the angle of rotation β, taken positive clockwise. The angle of rotation β is small ($\beta \ll 1$ radian) so we may approximate Sin_β by β and Cos_β by 1. Also we assume that $(U + U_o)'$ and $(V + V_o)'$ are small. Then we express the matrix $[b]$ in the following form

$$[b] = \begin{bmatrix} 1 & \beta & -(U + U_o)' \\ -\beta & 1 & -(V + V_o)' \\ (U + U_o)' & (V + V_o)' & 1 \end{bmatrix} \qquad (3.1)$$

where U and V are lateral deflections from the unloaded position in the x and y directions respectively and U_o and V_o are the initial crookedness. U, V, U_o and V_o all are functions of (z), the longitudinal axis.

ξ, η, ζ and x, y, z are related by $[b]$ in the following form

$$\left\{ \xi, \eta, \zeta \right\} = \left\{ x, y, z \right\} [b]^T \qquad (3.2)$$

3.3. BOUNDARY AND INITIAL CONDITIONS

i. Boundary Conditions

In the case of the concentric loading the boundary conditions at the ends of the column $z = 0$ and $z = L$ are

$U = V = 0$ No lateral displacement.

$U'' = V'' = 0$ No restraints against rotation about the

                     x- and y-axes are imposed.

$\beta = 0$ No restraint against twisting about the

                     longitudinal axis is imposed, so it will

twist from its original position due to torque resulting from the component of the moment about the y-axis along the ζ axis; but the position of the end section at z = 0 is assumed to be the reference position and therefore β is taken to be equal to zero. In the case of the symmetrical behavior with respect to the mid-height section of the column, i.e., symmetrical initial crookedness, the twist at the other end (z = L) will also be zero.

At the mid-height section, $z = \dfrac{L}{2}$

$U' = V' = 0$ Slope of the lateral deflection curve is zero - symmetrical case.

$\beta' = 0$ Twist is maximum; torque is zero.

In the case of eccentric loading the above conditions hold except when they are contrary to the following:

$U'' \neq 0$ at z = 0, L   When end eccentricity exists in the x direction.

$V'' \neq 0$ at z = 0, L   When end eccentricity exists in the y direction.

$\beta \neq 0$ at z = L   When eccentricity at two ends

$U', V', \beta' \neq 0$ at $z = \dfrac{L}{2}$ and/or initial imperfection are unsymmetrical.

The clockwise twist is assumed to be positive. The twist of the columns results from a positive torque in the upper portion (from $z = 0$ to where $\beta' = 0$) of the column and a negative torque in the lower portion (where $\beta' = 0$ to $z = L$).

ii. End Eccentricity

In the case of eccentric loading the curvature of the deflected shape at any end section in the plane parallel to the line of eccentricity will be different from zero and its value will be determined by the magnitude of the eccentricity, the axial load and also by the moment-curvature properties of the cross section. In a general case, eccentricity with respect to both x- and y-axes and at both ends of the column can be considered. If eccentricity of loading exists with respect to the y-axis, then the biplanar bending accompanied by torsion will commence with the start of loading. The moments about the x- and y-axes resulting from the eccentric loading alone at a cross section which has a distance z from the top can be written as (Figs. 3.3a, b, c)

$$M_{xe} = P\left[E_{ty} + \left(\frac{E_{by} - E_{ty}}{L}\right) z\right]$$

$$M_{ye} = -P\left[E_{tx} + \left(\frac{E_{bx} - E_{tx}}{L}\right) z\right]$$

(3.3)
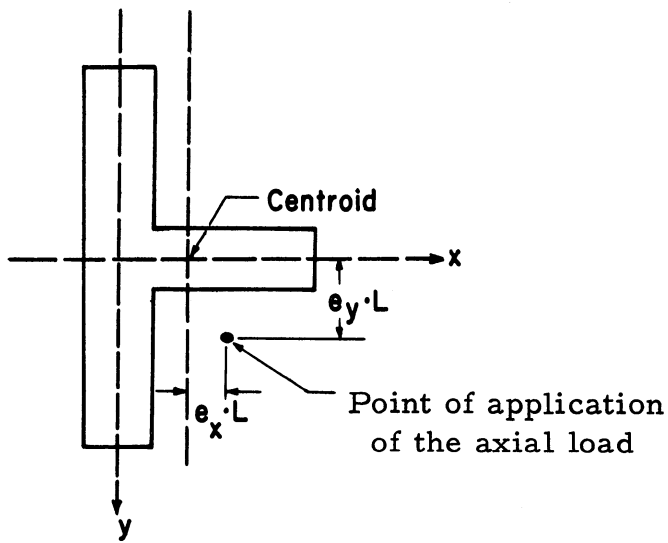
Fig. 3.3a. Eccentric Loading
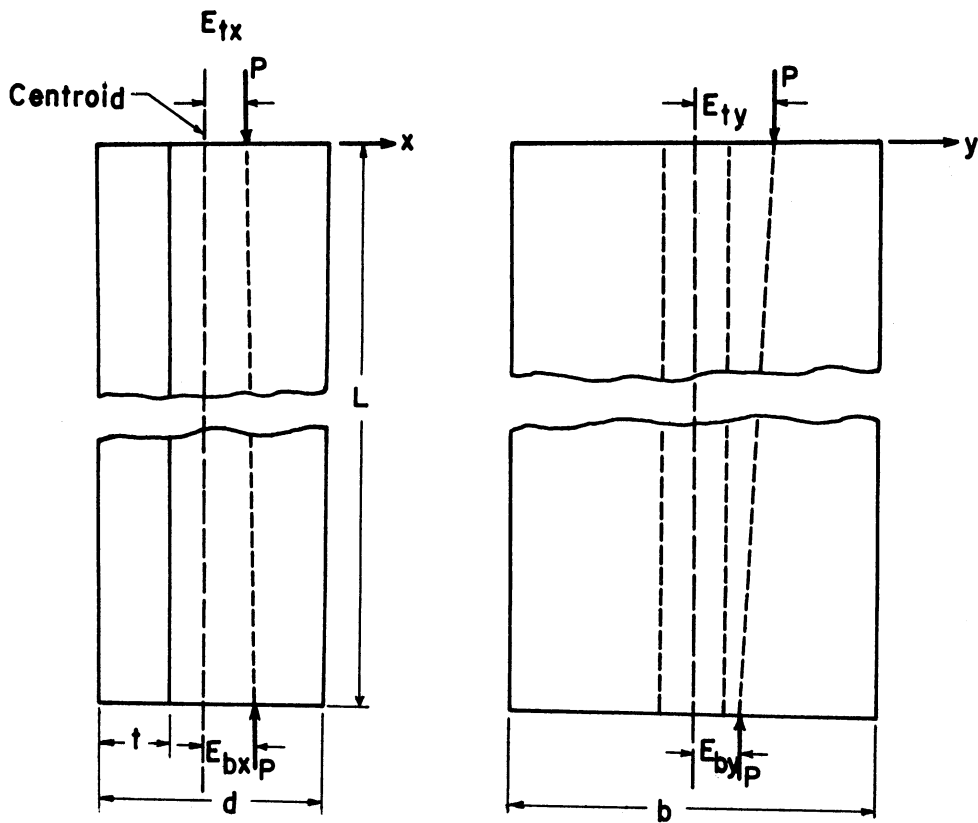
Fig. 3.3b, c.   Eccentricity of Loading
at the Top and the Bottom Faces

where E_{tx} and E_{ty} are the eccentricity in the x and y directions at

the top of the column and E_{bx} and E_{by} are the same values at the

bottom section of the column.   Let us assume

$$e_{tx} = \frac{E_{tx}}{L}$$

$$e_{ty} = \frac{E_{ty}}{L}$$

and $\qquad\qquad\qquad\qquad\qquad\qquad\qquad\qquad$ (3.4)

$$r_{ex} = \frac{E_{bx}}{E_{tx}}$$

$$r_{ey} = \frac{E_{by}}{E_{ty}}$$

Then the moment due to eccentricity will be

$$M_{xe} = P\, e_{ty}\, L\left[1 + (r_{ey} - 1)\frac{z}{L}\right]$$

$$\qquad\qquad\qquad\qquad\qquad\qquad\qquad\qquad (3.5)$$

$$M_{ye} = -P\, e_{tx}\, L\left[1 + (r_{ex} - 1)\frac{z}{L}\right]$$

iii. Initial Crookedness of the Column

Initial imperfection in the direction of one or both principal axes can be taken into consideration in this analysis. Initial imperfection can be either expressed in the form of a function or a vector which gives the value of the initial crookedness at the nodal points along the length of the column. These values can be obtained by measuring the actual initial crookedness at the required sections.

A sinusoidal or parabolic shape of crookedness can be expressed in the following forms:

sinusoidal shape:

$$U_o(z) = \Delta_{ix}\, Sin\left(\frac{\pi z}{L}\right) \qquad\qquad u_o(z) = \delta_{ix}\, Sin\frac{\pi z}{L}$$

$$\qquad\qquad\qquad\qquad or \qquad\qquad\qquad\qquad (3.6)$$

$$V_o(z) = \Delta_{iy}\, Sin\left(\frac{\pi z}{L}\right) \qquad\qquad v_o(z) = \delta_{iy}\, Sin\frac{\pi z}{L}$$

parabolic shape:

$$U_o(z) = \Delta_{ix} \frac{z(L-z)}{4L^2} \qquad u_o(z) = \delta_{ix} \frac{z}{4L} \left(1 - \frac{z}{L}\right)$$

or $\hspace{3cm}$ (3.7)

$$V_o(z) = \Delta_{iy} \frac{z(L-z)}{4L^2} \qquad v_o(z) = \delta_{iy} \frac{z}{4L} \left(1 - \frac{z}{L}\right)$$

Δ_{ix} and Δ_{iy} are the magnitude of initial crookedness at the mid-height section and

$$\delta_{ix} = \frac{\Delta_{ix}}{L}$$

$$\delta_{iy} = \frac{\Delta_{iy}}{L}$$

$$u_o = \frac{U_o}{L} \hspace{3cm} (3.8)$$

$$v_o = \frac{V_o}{L}$$

The moment due to initial crookedness alone at a section which has

a distance z from the top section will be

$$M_{xi}(z) = -P v_o(z) L$$

$$\hspace{6cm} (3.9)$$

$$M_{yi}(z) = P u_o(z) L$$

3.4. THE EQUATIONS OF FLEXURAL-TORSIONAL BUCKLING

i. Moment Curvature Relation

Positive moment or torque is represented by a vector pointing

in the positive direction of the xyz or $\xi\eta\zeta$ coordinate systems with

directions expressed in accordance with the right-hand rule at the

top face. In the elastic range of the behavior of the column, the

following relations hold between the moment and the flexure at all

the sections along the length of the column[57]

$$M_x = -EI_x V''(z)$$

$$M_y = EI_y U''(z)$$

(3.10)

Beyond the proportionality limit equations (3.10) no longer hold and

the introduction of a functional relationship between the moment and

the curvature is extremely difficult, if not impossible.

In planar bending the moment curvature relation will be a

function of the cross sectional shape, the average stress, the depth

of the strain regression, the direction of buckling, and the stress-

strain relation. In biplanar bending the difficulties in expressing

the moment-curvature relation will increase because the moment-

curvature relation in one principal plane will be an implicit function

of the same relation in the other principal plane. Interaction curves

can be prepared for any stress-strain relation and cross section

to give the relation between the moment and the curvature to be used

in manual calculation. However, in feeding these interaction curves

to the computer memory either they must be expressed as algebraic

functions (or a group of algebraic functions), or be given in the form

of a matrix.

In the first case one has to develop these functions for any

specific stress-strain relationship and the cross sectional shape.

In general, these functions cannot precisely represent the inter-

action curves, but some acceptable approximation can be made.

If the interaction curves are prepared in the form of a matrix, the number of the elements of the matrix grows larger as one tends to reduce the error of the solution. For an acceptable error the elements of the matrix will occupy a considerable number of locations of the computer memory and therefore make the other parts of the computer manipulation extremely difficult. An alternative solution is to choose the number of the elements of the matrix as few as possible and then use the interpolation procedure to obtain a closer answer. However, this process requires extra computation in addition to the preparation of interaction curves and the related matrix and the error of computation will be significant.

For the above mentioned reasons and because in incremental column analysis, the parameters of the moment-curvature relation, such as average normal strain, depth of strain regression, axial load and lateral deflection in x and y directions also have to be determined on an iterative basis, no attempt has been made to develop a separate and direct moment-curvature relation for the inelastic range of the column behavior. However, during every increment of the axial load and the lateral deflection of the column the moment and curvature relation has been evaluated. A detailed description of the iterative procedure is given in Chapter V.

ii. External Moment and Force Components

Moment Components:

The components of the moment due to deflection caused by the concentric load P can be written as

$$M_{xd}(z) = -P L v(z)$$

$$M_{yd}(z) = -P L \left[\frac{\overline{x}}{L} - u(z) \right]$$

(3.11)

The moment components due to the load eccentricity, initial imperfection and the lateral deflection from the unloaded position will be

$$M_{x(e)} = M_{xd} + M_{xi} + M_{xe}$$

$$M_{y(e)} = M_{yd} + M_{yi} + M_{ye}$$

$$M_{z(e)} = 0$$

(3.12)

or

$$M_{x(e)} = -P L \left[v(z) + v_o(z) - e_{ty} (1 + (r_{ey} - 1) \frac{z}{L}) \right]$$

$$M_{y(e)} = -P L \left[\frac{\overline{x}}{L} - u(z) - u_o(z) + e_{tx} (1 + (r_{ex} - 1) \frac{z}{L}) \right]$$

(3.13)

$$M_{z(e)} = 0$$

Using the transformation relation (3.2) we can write

$$M_{\xi(e)} = M_{x(e)} + \beta M_{y(e)}$$

$$M_{\eta(e)} = -\beta M_{x(e)} + M_{y(e)}$$

(3.14)

$$M_{\zeta 1(e)} = M_{x(e)} \left[U(z) + U_o(z) \right]' + M_{y(e)} \left[V(z) + V_o(z) \right]'$$

Torque applied externally on the cross section under consideration will have another component besides $M_{\zeta 1(e)}$. This component results from the torque produced by the components of the normal stress on the plane of the cross section (refer to equation (2.38)).
Hence,

$$M_{\zeta 2(e)} = -\frac{d\beta}{dz} \int_A \sigma \rho^2 dA$$

where ρ is the distance of the element from the center of the twist and σ is the normal stress acting on that element (Fig. 3.4). Therefore, torque exerted can be written as
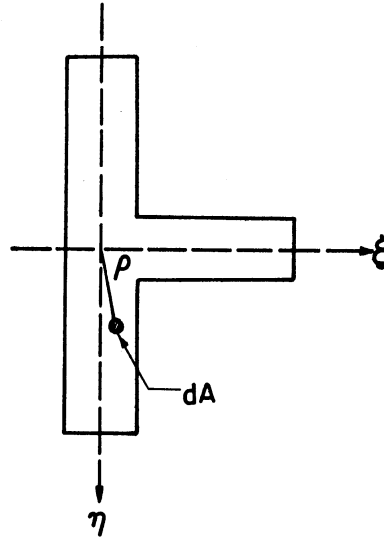
Fig. 3.4. Torque Component

$$M_{\zeta(e)} = M_x \left[U(z) + U_o(z) \right]' + M_y \left[V(z) + V_o(z) \right]' - \frac{d\beta}{dz} \int_A \sigma \rho^2 \, dA$$

(3.15)

Force Components:

The only force assumed to be acting is the axial load P so

$$F_{x(e)} = 0$$

$$F_{y(e)} = 0 \qquad\qquad (3.16)$$

$$F_{z(e)} = P$$

Using the transformation relations we get

$$F_{\xi(e)} = -P \left[U(z) + U_o(z) \right]'$$

$$F_{\eta(e)} = -P \left[V(z) + V_o(z) \right]' \qquad\qquad (3.17)$$

$$F_{\zeta(e)} = P$$

iii. Internal Resisting Moment and Force Components

Moment Components:

It is assumed that:

1. the effect of the shear stress in lateral displacement is negligible.

2. the slope of the deflected curve is small (U', $V' \ll 1$); therefore, the components of the axial force P on the ξ and η axes can be taken equal to zero

$$F_{\xi(e)} = F_{\eta(e)} = 0 \tag{3.18}$$

3. uniaxial stress-strain relation will not change due to the shear stress (Chapter IV).

4. strain at any element of the cross section is proportional to its distance from the center of curvature.

Having made the above assumptions we can write

$$M_{\xi(i)} = -\int_A \sigma(\xi, \eta)\, \eta\, dA$$

$$M_{\eta(i)} = \int_A \sigma(\xi, \eta)\, \xi\, dA \tag{3.19}$$

and the resisting torque[58]

$$M_{\zeta(i)} = C\beta' - C_w \beta'''$$

where C is the torsional stiffness and is discussed in Chapter IV. The torque resisted by bending resulting from non-uniform warping of adjacent cross sections ($C_w \beta'''$), where C_w is called warping rigidity, is assumed to be negligible in this case; therefore,

$$M_{\zeta(i)} = C\beta' \tag{3.20}$$

Force Components:

$$F_{\xi(i)} = 0$$

$$F_{\eta(i)} = 0 \qquad (3.21)$$

$$F_{\zeta(i)} = -\int_A \sigma(\xi, \eta)\, dA$$

3.5. EQUILIBRIUM CONDITIONS

The equilibrium conditions can be written as

$$F_{\xi(e)} + F_{\xi(i)} = 0$$

$$F_{\eta(e)} + F_{\eta(i)} = 0 \qquad (3.22)$$

$$F_{\zeta(e)} + F_{\zeta(i)} = 0$$

and

$$M_{\xi(e)} + M_{\zeta(i)} = 0$$

$$M_{\eta(e)} + M_{\eta(i)} = 0 \qquad (3.23)$$

$$M_{\zeta(e)} + M_{\zeta(i)} = 0$$

substituting for the values of F's and M's in the above equations

$$P - \int_A \sigma(\xi, \eta) \, dA = 0$$

$$PL \left\{ \left[[v(z) + v_0(z)] - e_{ty} \left[1 + (r_{ey} - 1) \frac{z}{L} \right] \right] \right.$$

$$\left. + \beta \left[[\frac{\bar{x}}{L} - u(z) - u_0(z)] + e_{tx} \left[1 + (r_{ex} - 1) \frac{z}{L} \right] \right] \right\} + \int_A \sigma(\xi, \eta) \, \eta \, dA = 0$$

$$PL \left\{ \beta \left[[v(z) + v_0(z)] - e_{ty} \left[1 + (r_{ey} - 1) \frac{z}{L} \right] \right] \right.$$

$$\left. - \left[[\frac{\bar{x}}{L} - u(z) - u_0(z)] + e_{tx} \left[1 + (r_{ex} - 1) \frac{z}{L} \right] \right] \right\} + \int_A \sigma(\xi, \eta) \, \xi \, dA = 0$$

$$PL^2 \left\{ \left[[v(z) + v_0(z)] - e_{ty} \left[1 + (r_{ey} - 1) \frac{z}{L} \right] \right] [u(z) + u_0(z)]' \right.$$

$$\left. + \left[[\frac{\bar{x}}{L} - u(z) - u_0(z)] + e_{tx} \left[1 + (r_{ex} - 1) \frac{z}{L} \right] \right] [v(z) + v_0(z)]' \right\}$$

$$+ \beta' \int_A \sigma(\xi, \eta) \, \rho^2 \, dA - C\beta' = 0 \qquad (3.24)$$

Equilibrium equations (3.24) should be satisfied for all the cross sections along the column. The above equilibrium equations are very general and take into account the biplanar bending accompanied by the twist with or without initial crookedness and end eccentricity of loading.

3.6. WARPING EFFECT

In case consideration of warping deformation is needed for a more refined solution, the elastic warping displacement at any point of a cross section, [*] having relatively thin walls, can be calculated from[36, 59]

---

[*]Does not apply near the longitudinal edges but this has a negligible effect for thin walled sections.

$$w = w_o - \beta' \int_0^s r_s \, ds - \int_0^n r_n \, dn \qquad (3.25)$$

where w_o denotes the displacement in the z direction of the point from which s is measured (Fig. 3.5). The integral $\int_0^s r_s \, ds$ represents twice the area swept by the radius ρ as we move along the middle line of the cross section from the origin of s, while the integral $\int_0^n r_n \, dn$ represents twice the area swept by the same radius as we move from the center line to the element along the normal line. The
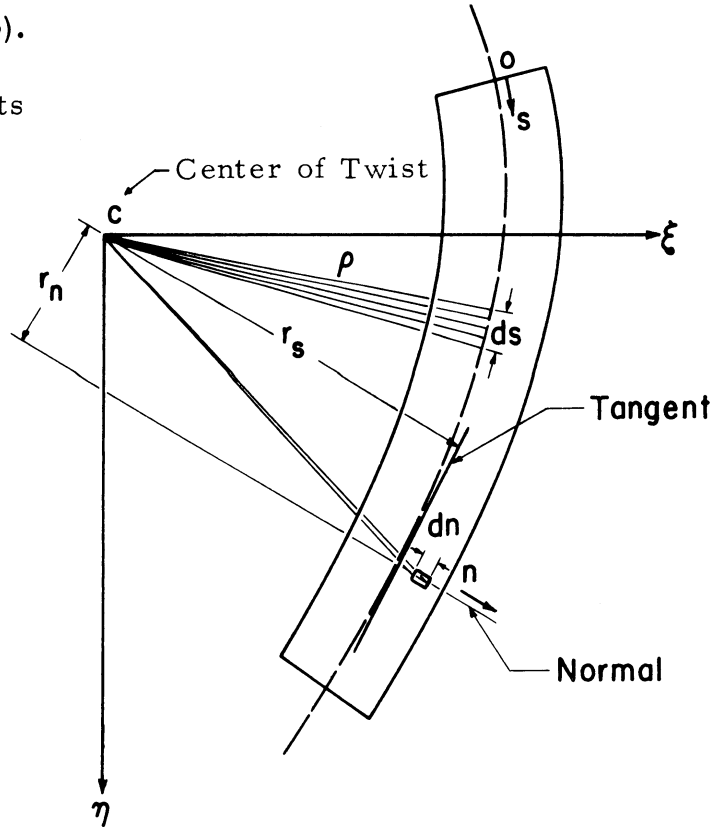
Fig. 3.5. Warping of the Cross Section

swept area should be taken positive if the radius ρ is rotating in the positive direction, i.e., from ξ to η. The contribution of the second integral is negligible for thin-walled cross sections.

In the inelastic region equation (3.25) cannot be used and a rigorous solution is needed to evaluate the warping. Warping of cross sections subjected to combined elastic and inelastic torsion is discussed in Chapter IV. However, in Chapter IV it is assumed that the center of twist coincides with the intersection of the center lines of the flange and the web. In order to modify this assumption

one should, by using the shear stress values obtained from rigorous

solution, determine the new center of twist. If the new center of

twist did not (with an acceptable approximation) coincide with the

assumed one, a new center of twist should be chosen and the evalu-

ation of warping displacement, strain, shear stress, and the center

of twist should be repeated until an acceptable solution is obtained.

After the instantaneous center of twist is located, the term "ρ"

in equation (3.15) should be redefined as the distance between the

element and the instantaneous center of twist. Also, the change of

strain due to the warping displacement should be taken into consid-

eration.

3.7. PLANAR BENDING

Equilibrium equations (3.24) can be simplified for the case

of planar bending. Cases studied in this thesis exclude the initial

imperfection or eccentricity of loading in the plane parallel to the

flange. Also, it is assumed that the column is initially stronger in

the flange direction than in the web direction. Previously it was

explained that in case buckling starts in the plane of symmetry of

the "T" section towards the flange, theoretically, planar bending will

govern the behavior of the column. But when buckling initiates in

the direction away from the flange (to the right) up to the stage where

bending stiffness of the column in the plane of the symmetry is

greater than the bending stiffness in the plane parallel to the flange,

the biplanar bending will not commence. Therefore, it is advantageous to express the simplified equilibrium conditions for the planar bending in the plane of symmetry. In this case

$$\beta = \beta' = v = v_o = v' = v_o' = e_{ty} = r_{ey} = 0$$

and   (3.26)

$$\sigma(\xi, \eta) \equiv \sigma(\xi)$$

Hence, the equilibrium equations will reduce to two equations as follows

$$P - \int_{-\frac{t}{2}}^{d-\frac{t}{2}} t(\xi)\ \sigma(\xi)\ d\xi = 0$$

(3.27)

$$PL\ [\frac{\bar{x}}{L} - u(z) - u_o(z)] + e_{tx}[1 + (r_{ex} - 1)\frac{z}{L}]\ - \int_{-\frac{t}{2}}^{d-\frac{t}{2}} t(\xi)\sigma(\xi)\,d\xi = 0$$

$t(\xi)$ is the dimension of the cross section in η direction

$$t(\xi) = b \qquad\qquad -\frac{t}{2} < \xi < \frac{t}{2}$$

(3.28)

$$t(\xi) = w \qquad\qquad \frac{t}{2} < \xi < d-\frac{t}{2}$$

Limiting Stage of Planar Bending

When the non-linear distribution of the stress exists on the cross section, the bending axis will no longer coincide with the principal axis parallel to the flange, or we may say that the "principal axis" about which the bending stiffness of the cross section (weighted moment of inertia) is to be minimum, will move parallel to its original position. If the bending axis is a line $\xi = \bar{\xi}$ then the bending stiffness in the plane of symmetry can be expressed as

$$(B.S.)_{\bar{\xi}} = \int_{-\frac{t}{2}}^{d-\frac{t}{2}} t(\xi) \, (\xi - \bar{\xi})^2 \, E_t(\xi) \, d\xi \qquad (3.29)$$

$\bar{\xi}$ has to be evaluated such that it would make $(B.S.)_{\bar{\xi}}$ a minimum,

i.e.,

$$\frac{d}{d\bar{\xi}} (B.S.)_{\bar{\xi}} = 0$$

$$(3.30)$$

$$\frac{d}{d\bar{\xi}} \int_{-\frac{t}{2}}^{d-\frac{t}{2}} t(\xi) \, (\xi - \bar{\xi})^2 \, E_t(\xi) \, d\xi = 0$$

$t(\xi)$ in the above equation is sectionally continuous (3.28).

If the stress and its derivative with respect to the strain in the inelastic range is a continuous function of strain, then $E(\xi)$ will also be sectionally continuous, separated by the border line of the elastic and inelastic zones. The integral equation (3.30) can be divided to the sectionally continuous domains and integrated and finally written in the following form

$$\frac{d}{d\bar{\xi}} \left[A_1 \bar{\xi}^2 + A_2 \bar{\xi} + A_3 \right] = 0 \qquad (3.31)$$

where

$$A_1 = \int_{-\frac{t}{2}}^{d-\frac{t}{2}} t(\xi) \, E(\xi) \, d\xi$$

$$A_2 = -2 \int \xi \, t(\xi) \, E(\xi) \, d\xi \qquad (3.32)$$

$$A_3 = \int_{-\frac{t}{2}}^{d-\frac{t}{2}} t(\xi) \, \xi^2 \, E(\xi) \, d\xi$$

Equation (3.31) is a continuous function with respect to $\bar{\xi}$; therefore, according to Leibnitz's rule[60]

$$\int_{-\frac{t}{2}}^{d-\frac{t}{2}} \frac{d}{d\bar{\xi}} \left[t(\xi) \, E_t(\xi) \, (\xi - \bar{\xi})^2 \right] \, d\xi = 0 \qquad (3.33)$$

or

$$\int_{-\frac{t}{2}}^{d-\frac{t}{2}} \left[t(\xi) \, E_t(\xi) \, (\xi - \bar{\xi}) \right] \, d\xi = 0 \qquad (3.34)$$

Solving (3.33) for $\bar{\xi}$ we get

$$\bar{\xi} = \frac{\displaystyle\int_{-\frac{t}{2}}^{d-\frac{t}{2}} t(\xi) \, E_t(\xi) \, \xi \, d\xi}{\displaystyle\int_{-\frac{t}{2}}^{d-\frac{t}{2}} t(\xi) \, E_t(\xi) \, d\xi} \qquad (3.35)$$

Now the bending stiffness in the plane of symmetry can be found by substituting the value of $\bar{\xi}$ from (3.35) in (3.29). While bending is taking place in the plane of symmetry, axis of symmetry remains as the axis about which the bending stiffness is maximum. Bending stiffness in bending out of the plane of symmetry can be expressed in the following form

$$(\text{B.S.})_\eta = \int_{\xi_1}^{\xi_2} \int_{\eta_1}^{\eta_2} E_t(\xi) \, \eta^2 \, d\eta \, d\xi$$

or

$$(B.S.)_\eta = \frac{b^3}{3} \int_{-\frac{t}{2}}^{\frac{t}{2}} E_t(\xi) \, d\xi + \frac{w^3}{3} \int_{\frac{t}{2}}^{d-\frac{t}{2}} E_t(\xi) \, d\xi \qquad (3.36)$$

Let α be the ratio of the bending stiffness in the plane parallel to

the flange $(B.S.)_\eta$ to the bending stiffness in the plane of symmetry

$(B.S.)_\xi$, i.e.,

$$\alpha = \frac{(B.S.)_\eta}{(B.S.)_\xi} \qquad (3.37)$$

As long as the value of α for all the cross sections along the column

remains greater than unity, biplanar bending will not commence.

CHAPTER IV

TORSIONAL STIFFNESS

4.1. INTRODUCTION

At the stage where the elastic limit is surpassed and a linear relation between stress and strain no longer exists, the presence of bending moment in the cross section will subject different elements of the cross section to a varying strain, and therefore their inelastic properties (i.e., tangent modulus, secant shear modulus, Poisson's ratio) will vary from one point to another. At some stage of loading when strain regression is present, an abrupt change in the material properties of the neighboring elements of the border line of the elastic (regression) and inelastic zones of the cross section exists. Evaluation of the torsional stiffness coefficient of a cross section under above condition is a complex problem. The behavior of a member in the above condition is similar to that of a composite member made of numerous elements with different "elastic" properties.

In inelastic column analysis, when torsion commences, one encounters such problems as the relation between the amount of torque applied and the rotation produced or the shear stress distribution.

The precise solution of this problem is very complex,

involving three dimensional analysis, as torsional moment as well

as flexural moment varies along the column. In practice a variety

of geometrically complicated composite sections are being used.

Composite sections are used in reinforced concrete and aircraft,

as well as some very specialized applications. Some problems on

the torsion of compound prismatic bars have been treated analytically

by Muskhelishvilli,[61] Cowan,[62] Mitra,[63] Gorgidze,[64]

Sherman,[65] Craven,[66] Takeyama,[67] and Suhareviki.[68] These

problems generally dealt with cross-sectional shapes that could

easily be conformally mapped. The torsion problem of a member

with constant elastic properties across the cross section and with

a nonclassical geometry of cross section may be solved by relaxation

methods, as used by Christopherson,[69] Southwell,[70] Shaw,[71, 72]

Allen,[73] Dobie,[74] and others. Ely and Zienkiewicz[75] applied

relaxation method to the solution of torsion of some composite bars

of special cross sections, made of two different materials (G_1, G_2).

In this chapter (starting from compatibility conditions and using the

relaxation method) a procedure will be introduced to solve the

torsion problem of composite members with application to the

torsion of a "T" shaped member in column analysis. The iteration

process is carried out by means of a MAD program written for the

7090 digital computer.

4.2. ASSUMPTIONS

To reduce the complexities and apply the solution to the problem of torsion of a "T" shaped column, certain assumptions have been made.

The structural shape has a uniform cross section and there is no restraint against longitudinal displacement of the elements of the cross section.

The torsional moment is assumed constant along any one segment of the member. (By segment is meant an arbitrary increment of column length chosen for the numerical solution.) As we increase the number of segments in column analysis, this assumption tends to become more accurate.

With the above assumptions only St. Venant torsion will be present and thus the magnitude of the rotation, β, along the member within the length of the segment of the column will be a linear function of the length of the segment.

4.3. DISPLACEMENT EQUATIONS

Assume a prismatic bar of length L fixed at one end to the xy plane and with origin of the coordinate system fixed at the center of twist of the bar with the z-axis coinciding with the longitudinal axis of the bar and torque M_z acting counterclockwise on the front face (Fig. 4.1).
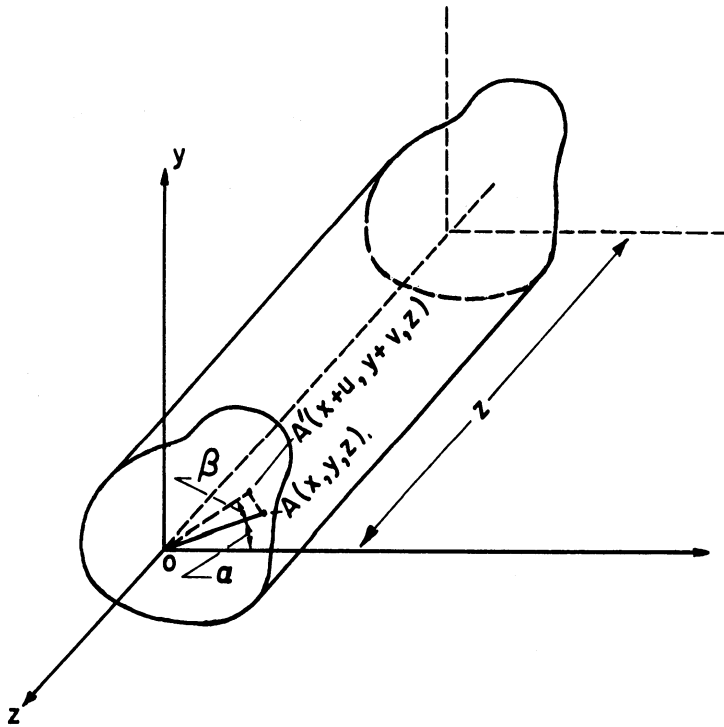
Fig. 4.1. A Prismatic Bar under Torsion

If θ is assumed to be the rotation per unit length (uniform torsion)

then

$$\beta = \theta z \qquad (4.1)$$

and point A(x, y, z) after application of torque will displace to

A'(x + u, y + v, z + w), then

$$u = \overline{OA}\left[\cos(\alpha + \beta) - \cos(\alpha)\right] = \overline{OA}\left[\cos\alpha\cos\beta - \sin\alpha\sin\beta - \cos\alpha\right]$$
$$(4.2)$$
$$v = \overline{OA}\left[\sin(\alpha + \beta) - \sin(\alpha)\right] = \overline{OA}\left[\sin\alpha\cos\beta + \cos\alpha\sin\beta - \sin\alpha\right]$$

assuming that $\beta \ll 1$ then $\sin\beta \simeq \beta$ and $\cos\beta \simeq 1$, and $\overline{OA}\sin\alpha = y$,

$\overline{OA}\cos\alpha = x$.

$$u = -y\beta$$
$$(4.3)$$
$$v = x\beta$$

or

$$u = -\theta yz$$

$$v = \theta xz$$

(4.4)

The displacement in the z direction, w, is assumed to be independent

of z and only a function of x and y and therefore can be written

$$w = \theta\psi(x, y)$$

(4.5)

ψ which defines the warping of the end surface is called the warping

function.

The above assumptions are used in St. Venant's semi-inverse

method to reduce the governing equilibrium equations to one differ-

ential equation. Thus, the objective will be to find the function

$\psi(x, y)$ so that the equilibrium equations and the boundary conditions

will be satisfied.

4.4. EQUILIBRIUM EQUATIONS

If in general terms we assume that the displacement vector

is u (i.e., $u_1 = u$, $u_2 = v$, $u_3 = w$) then strain vector in Cartesian

coordinates will be[76]

$$\epsilon_{ij} = \frac{1}{2}(u_{i,j} + u_{j,i} + u_{k,i}u_{k,j})$$

(4.6)

$$(i = 1, 2, 3; \ j = 1, 2, 3; \ k = 1, 2, 3)$$

neglecting the nonlinear term $u_{k,i}u_{k,j}$ equation (4.6) can be

written as

$$\epsilon_{ij} = \frac{1}{2}(u_{i,j} + u_{j,i})$$

(4.7)

which is a linear approximation and is known as Lagrange's equation

of compatibility of strains. Assuming that there exists a linear

relation between the strain and stress components in the Cartesian

coordinates and in the neighborhood of the state of the present stress

or strain, stress vector τ can be written

$$\tau_{ij} = (GE)_{ij} \, \epsilon_{ij} \qquad (4.8)$$

where $(GE)_{ij}$ is equal to E_s when $i = j$ and is equal to $2G_s$ when

$i \neq j$. The secant elastic modulus (E_s) and the secant shear modulus

(G_s) are defined in the following relations[11] (Figs. 4.2 and 4.3)
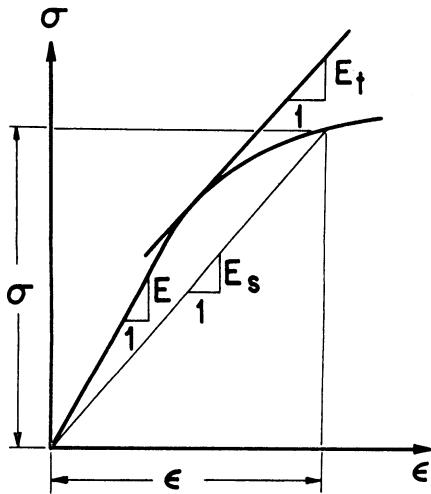
Fig. 4.2. Elastic,
Tangent and Secant Moduli
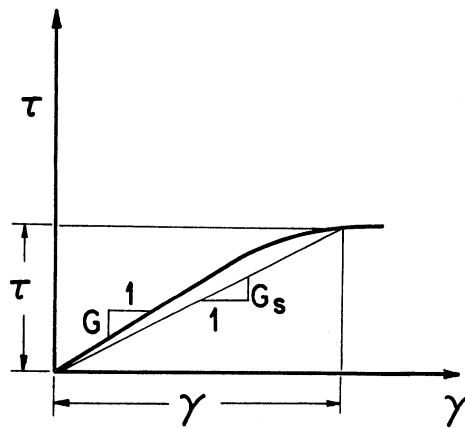
Fig. 4.3. Shear and Secant
Shear Moduli

$$E_s = \frac{\sigma}{\epsilon}$$

$$\qquad (4.9)$$

$$G_s = \frac{\tau}{\gamma}$$

where σ = axial stress

ϵ = total strain, including inelastic strain

τ = shear stress in pure shear

γ = shear strain in pure shear

and σ and ϵ are evaluated in the uniaxial stress. The equilibrium

equations can be written in the following form

$$\tau_{ji,j} + F_i = 0 \qquad (4.10)$$

Using equations (4.7), (4.8) and (4.10) along with displacement

equations (4.4) and (4.5) strain components in xyz coordinates will be

$$\epsilon_{xx} = \epsilon_{yy} = \epsilon_{zz} = 0$$

$$\gamma_{xy} \ (\text{or} \ 2\epsilon_{xy}) = \gamma_{yx} \ (\text{or} \ 2\epsilon_{yx}) = 0$$

$$\gamma_{yz} \ (\text{or} \ 2\epsilon_{yz}) = \gamma_{zy} = \theta(\frac{\partial \psi}{\partial y} + x) \qquad (4.11)$$

$$\gamma_{zx} \ (\text{or} \ 2\epsilon_{zx}) = \gamma_{xz} = \theta(\frac{\partial \psi}{\partial x} - y)$$

and stress components will be

$$\sigma_x \ (\text{or} \ \tau_{xx}) = \sigma_y \ (\text{or} \ \tau_{yy}) = \sigma_z \ (\text{or} \ \tau_{zz}) = 0$$

$$\tau_{xy} = \tau_{yx} = 0$$

$$\tau_{yz} = \tau_{zy} = G_s(x,y) \ \theta(\frac{\partial \psi}{\partial y} + x) \qquad (4.12)$$

$$\tau_{zx} = \tau_{xz} = G_s(x,y) \ \theta(\frac{\partial \psi}{\partial x} - y)$$

Equations (4.12) show that the secant shear modulus (G_s) is assumed

to be a function of x and y only and independent of z. As we reduce

the length of the element the correctness of this assumption will

improve. Using the equilibrium equations it will be shown that the

assumption G_s being independent of z is compatible with the

assumed displacement vector. Equilibrium equation (4.10) can be

written

$$\frac{\partial \sigma_x}{\partial x} + \frac{\partial \tau_{xy}}{\partial y} + \frac{\partial \tau_{xz}}{\partial z} + F_x = 0$$

$$\frac{\partial \tau_{yx}}{\partial x} + \frac{\partial \sigma_y}{\partial y} + \frac{\partial \tau_{yz}}{\partial z} + F_y = 0 \qquad\qquad (4.13)$$

$$\frac{\partial \tau_{zx}}{\partial x} + \frac{\partial \tau_{zy}}{\partial y} + \frac{\partial \sigma_z}{\partial z} + F_z = 0$$

There is no external force acting on the element; therefore,

$$F_x = F_y = F_z = 0$$

Using stress relations (4.12) the first two equations of (4.13) are

satisfied.

Had we assumed G_s to be a function of z then the first two

equations of (4.13) should have been written as

$$0 + 0 + \frac{\partial G_s(x, y, z)}{\partial z} \; \theta \; (\frac{\partial \psi}{\partial x} - y) \; + 0 = 0$$

$$\qquad\qquad (4.14)$$

$$0 + 0 + \frac{\partial G_s(x, y, z)}{\partial z} \; \theta \; (\frac{\partial \psi}{\partial y} + x) \; + 0 = 0$$

as

$$(\frac{\partial \psi}{\partial x} - y) \; = \; 0$$

and

$$(\frac{\partial \psi}{\partial y} + x) \; = \; 0$$

give a trivial solution of $\tau_{yz} = \tau_{zy} = \tau_{xz} = \tau_{zx} = 0$. Therefore,

$\dfrac{\partial G_s(x, y, z)}{\partial z}$ should be taken equal to zero $(G_s = G_s(x, y))$.

The third and governing equilibrium equation will be

$$\frac{\partial G_s(x,y)}{\partial y} \quad \theta\left(\frac{\partial \psi}{\partial y} + x\right) \quad + \quad G_s(x,y) \quad \theta \frac{\partial^2 \psi}{\partial y^2}$$

$$+ \quad \frac{\partial G_s(x,y)}{\partial x} \quad \theta\left(\frac{\partial \psi}{\partial x} - y\right) \quad + \quad G_s(x,y) \quad \theta \frac{\partial^2 \psi}{\partial x^2} = 0$$

or

$$G_s(x,y)[\nabla^2 \psi(x,y)] + \frac{\partial G_s(x,y)}{\partial x}\left(\frac{\partial \psi}{\partial x} - y\right) + \frac{\partial G_s(x,y)}{\partial y}\left(\frac{\partial \psi}{\partial y} + x\right) = 0$$

(4.15)

In the case of constant G_s across the cross section

$$\frac{\partial G_s(x,y)}{\partial x} = \frac{\partial G_s(x,y)}{\partial y} = 0$$

and equation (4.15) will reduce to the Laplace equation ($\nabla^2 \psi = 0$).

4.5. BOUNDARY CONDITIONS

The surface of the bar is free of external forces

($F_x = F_y = F_z = 0$); therefore, the normal component of the stress

at the boundary should be equal to zero. Unit vector N normal to

the boundary can be written as

$$\vec{N} = \frac{dy}{ds}\vec{i} - \frac{dx}{ds}\vec{j}$$

(4.16)

and the stress vector

$$\vec{\tau} = \tau_{xz}\vec{i} + \tau_{yz}\vec{j}$$

(4.17)

to satisfy the above condition

$$\vec{N} \cdot \vec{\tau} = 0$$

(4.18)

or

$$\tau_{xz}\frac{dy}{ds} - \tau_{yz}\frac{dx}{ds} = 0$$

(4.19)

Substituting for τ_{xy} and τ_{yz} from (4.12)

$$\theta G_s(x, y) \left[(\psi_{,x} - y) \frac{dy}{ds} - (\psi_{,y} + x) \frac{dx}{ds} \right] = 0$$

as $G_s(x, y) \neq 0$

$$(\psi_{,x} - y) \frac{dy}{ds} - (\psi_{,y} + x) \frac{dx}{ds} = 0 \quad \text{on} \quad S \qquad (4.20)$$

equation (4.20) should be satisfied on the lateral surface of the

element.

On the two boundary surfaces at the end of the element

defined by planes of $z = 0$ and $z = L$, stresses given by (4.12) should

produce a torque equivalent to the one applied externally and more-

over, the resultant force should be equivalent to zero. The first

condition requires that

$$M_z = \int_A (x \tau_{yz} - y \tau_{xz}) \, dA \qquad (4.21)$$

or

$$M_z = \theta \int_A \int_A G_s(x, y) (x^2 + y^2 + x \frac{\partial \psi}{\partial y} - y \frac{\partial \psi}{\partial y}) \, dx \, dy \qquad (4.22)$$

Equation (4.22) gives the relation between the applied torque (M_z)

and the rotation per unit length, θ. Even if we could express the

warping function ψ as an explicit function of x and y, the analytical

integration of the above equation would not be a simple problem, as

in general, G_s is not a continuous function of x and y. As we shall

see, the warping function ψ will also be discontinuous.

A third condition demands that

$$\int_A \tau_{xz} \, dA = 0$$

and (4.23)

$$\int_A \tau_{zy} \, dA = 0$$

substituting for τ_{zy} and τ_{zx} from (4.12)

$$\int \int_A \theta G_s(x, y) \left(\frac{\partial \psi}{\partial x} - y\right) dx \, dy = 0$$

(4.24)

$$\int \int_A G_s(x, y) \left(\frac{\partial \psi}{\partial y} + x\right) dx \, dy = 0$$

As θ is constant, it can be taken out of the integral sign and canceled; therefore, we should prove that

$$\int \int_A G_s(x, y) \left[\left(\frac{\partial \psi}{\partial y} + x\right)\right] dx \, dy = 0 \qquad (4.25)$$

and similarly the second equation can be proved. Multiplying both sides of equation (4.15) by "y" and integrating over the end section boundary A and adding it to equation (4.25),

$$\int \int_A G_s(x, y) (\psi_{,y} + x) dx \, dy + \int \int_A y[G_s(x, y) \nabla^2 \psi + G_s(x, y) (\psi_{,x} - y) + \cdots$$

$$+ G_s(x, y) (\psi_{,y} + x)] \, dx \, dy = 0 + \int \int_A (y \cdot 0) \, dx \, dy = 0$$

Left hand side can be written as

$$\int \int_A \left[y G_s(x, y)_{,x} (\psi_{,x} - y) + y G_s(x, y) \psi_{,xx} + G_s(x, y) (\psi_{,y} + x) + \cdots \right.$$

$$\left. y G_s(x, y)_{,y} (\psi_{,y} + x) + y G_s(x, y) \psi_{,yy} \right] dx \, dy = 0$$

or

$$\int\int_A \left[\frac{\partial}{\partial x} \left[y\, G_s(x, y)\, (\psi_{,x} - y)\right]\right] dx\, dy +$$

$$\int\int_A \left[\frac{\partial}{\partial y} \left[y\, G_s(x, y)\, (\psi_{,y} + x)\right]\right] dx\, dy = 0$$

The above equation can be written as[60] (Fig. 4.4)

$$\oint_S \left[y\, G_s(x, y)\, (\psi_{,x} - y)\right] dy - \oint_S \left[y\, G_s(x, y)\, (\psi_{,y} + x)\right] dx = 0$$

or

$$\oint_S \left[\left[y\, G_s(x, y)\, (\psi_{,x} - y)\right] \frac{dy}{ds} - \left[y\, G_s(x, y)\, (\psi_{,y} + x)\right] \frac{dx}{ds}\right] ds = 0$$

or

$$\oint_S y\, G_s(x, y) \left[(\psi_{,x} - y) \frac{dy}{ds} - (\psi_{,y} + x) \frac{dx}{ds}\right] ds = 0$$

or

$$\oint_S f\, ds = 0 \qquad\qquad (4.26)$$

where

$$f = f(x, y) = y\, G_s(x, y) \left[(\psi_{,x} - y) \frac{dy}{ds} - (\psi_{,y} + x) \frac{dx}{ds}\right] \qquad (4.27)$$
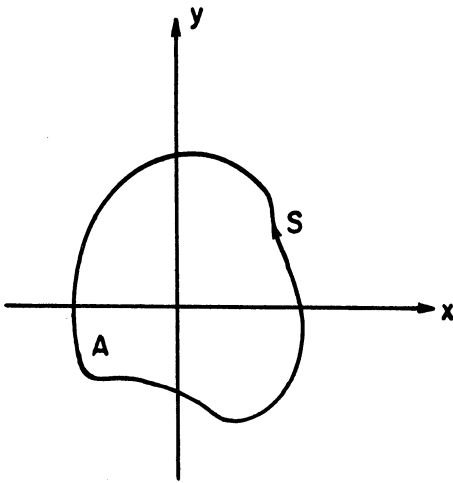
The term inside the bracket is the same as equation (4.20). If the lateral boundary condition is satisfied, this bracket will be equal to zero and consequently equation (4.25) will be satisfied.

Fig. 4.4. Cross Section and the Boundary

When discontinuity is present in the functions ψ and G_s, as in the case of the existence of strain regression, the boundary can be divided into two or more regions and the above procedure followed and integration taken in different regions separately. Finally, it will be concluded that the integration (4.26) should be taken over all boundaries of divided regions, for example, as in the case of the Fig. 4.5
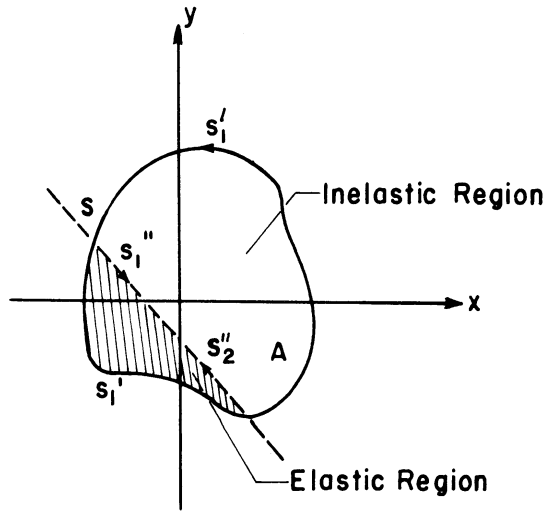
Fig. 4.5. Elastic and Inelastic Regions

$$\oint_{S_1} (f)_1 \, ds + \oint_{S_2} (f)_2 \, ds = 0 \qquad (4.28)$$

S_1 and S_2 can be divided into two parts

$$S_1 = S_1' + S_1'' \qquad\qquad S_2 = S_2' = S_2''$$

then equation (4.27) can be written as

$$\int_{S_1'} (f)_1 \, ds + \int_{S_1''} (f)_1 \, ds + \int_{S_2'} (f)_2 \, ds + \int_{S_2''} (f)_2 \, ds = 0$$

S_1' and S_2' form the outer boundary of the surface (A) and (4.2) is satisfied on the boundary

$$\int_{S_1'} (f) \, ds + \int_{S_2'} (f) \, ds = \oint_{S} (f) \, ds = 0$$

Now conditions (4.26) will become

$$\int_{S_1''} (f)_1 ds + \int_{S_2''} (f)_2 ds = 0$$

as $S_1'' = -S_2'' = S''$, then

$$\int_{S''} (f)_1 ds - \int_{S''} (f)_2 ds = 0 \qquad (4.29)$$

The subscript on (4.26) means equation (4.26) written for that region.

Equation (4.29) indicates that the components of the shear stress at the separating boundary when approaching from region (1) or (2) should be the same.

$$(\tau_{xz})_1 = (\tau_{xz})_2$$

$$(4.30)$$

$$(\tau_{yz})_1 = (\tau_{yz})_2$$

or, in other words, if equations (4.30) together with equations (4.20) are satisfied the boundary conditions (4.23) will also be satisfied.

4.6. DIFFERENCE EQUATIONS

In order to solve the problem of inelastic torsion one should find a warping function $\psi(x, y)$ that satisfies both the differential equation of equilibrium (4.15) and the boundary condition (4.20) with the supplemental relation (4.30).

Except for a few cases for which analytical solutions may be possible, solutions of the differential equations of equilibrium with complex boundary conditions are not presently available. Numerical

methods must be used to solve such a problem. The differential

equations of equilibrium are replaced by "finite difference equations".

The relaxation procedure for solution of finite difference equations

was initiated by Christopherson[69] and Southwell.[70] Shaw[71, 72]

has also applied the relaxation method to some torsion problems.

In this analysis a modification of the relaxation method will

be used to evaluate the warping function and consequently the torque-

rotation relations. Prior to forming the finite difference equation

for the differential equation (4.15) the following should be reviewed:

4.7. POLYNOMIAL FUNCTION

Suppose that y, a function of the independent variable x, is

required to have the values y_0, y_1, y_2,..., y_n when x has the

values 0, h, 2h, ..., nh. It can be proved that the function

$$y = a_0 + a_1 x + a_2 x^2 + \ldots + a_n x^n \qquad (4.31)$$

which is a polynomial in x of degree n, and in which the (n + 1)

quantities of a are constants, satisfies the imposed requirements,

and all the differentials of (4.31) are continuous and have finite

values in the considered range (x being finite). The nth differential

$d^n y/dx^n$ has the constant value of $n a_n$ and the higher differentials

are zero.

4.8. APPROXIMATE DIFFERENTIATION

In this procedure a range of three points will be applied in calculation of the differentials.

Therefore, the following relations will be given without proof (Fig. 4.6)
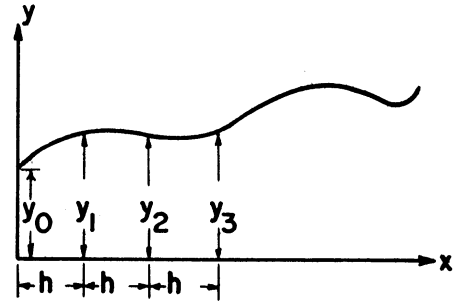
Fig. 4.6. Derivatives at 0, 1, and 2

$(n = 2, \text{ given: } y_0, y_1, y_2, h)$

$$
\begin{cases}
h \left(\dfrac{dy}{dx} \right)_0 = \dfrac{1}{2} (-3y_0 + 4y_1 - y_2) \\[2ex]
h \left(\dfrac{dy}{dx} \right)_1 = \dfrac{1}{2} (-y_0 + y_2) \\[2ex]
h \left(\dfrac{dy}{dx} \right)_2 = \dfrac{1}{2} (y_0 - 4y_1 + 3y_2) \\[2ex]
h^2 \left(\dfrac{d^2 y}{dx^2} \right)_{0,1,2} = (y_0 - 2y_1 + y_2)
\end{cases}
\qquad (4.32)
$$

4.9. FINITE-DIFFERENCE APPROXIMATION TO THE PARTIAL DIFFERENTIAL EQUATION OF EQUILIBRIUM

After a range of three points and a network of squares of side "h" has been considered, we shall formulate the finite-difference equation for the differential equation (4.15).

Let us assume that functions $G_s(x, y)$ and $\psi(x, y)$ and the first derivative of $G_s(x, y)$ and the first and second derivatives of $\psi(x, y)$ with respect to x and y are comtinuous in the neighborhood of point "o" (Fig. 4. 7) within a domain of radius "h". In order to treat the differential equation (4. 15) in a manner more suitable for this discussion it can be written in the following form
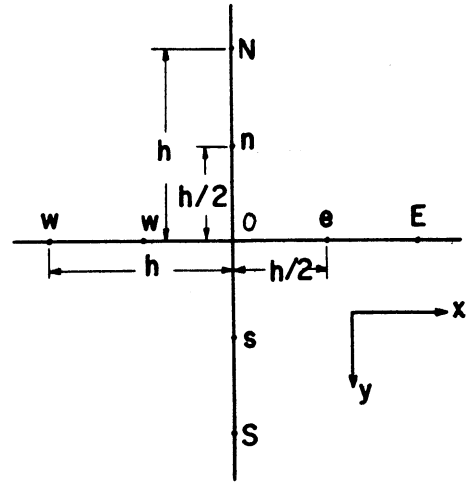
Fig. 4. 7. Point "o" and the Neighboring Domain

$$\frac{\partial}{\partial x}\left[G_s(x, y)(\psi_{,x} - y)\right] + \frac{\partial}{\partial y}\left[G_s(x, y)(\psi_{,y} + x)\right] = 0$$

or

$$\frac{\partial}{\partial x}\left[G_s(x, y)\psi_{,x}\right] + \frac{\partial}{\partial y}\left[G_s(x, y)\psi_{,y}\right] = \frac{\partial}{\partial x}\left[y\,G_s(x, y)\right] - \frac{\partial}{\partial y}\left[x\,G_s(x, y)\right]$$

or

$$\frac{\partial}{\partial x}\left[G_s(x, y)\psi_{,x}\right] + \frac{\partial}{\partial y}\left[G_s(x, y)\psi_{,y}\right] = \left[y\,G_{s,x} - x\,G_{s,y}\right]$$

or

$$\frac{\partial}{\partial x}\left[G_s(x, y)\psi_{,x}\right] + \frac{\partial}{\partial y}\left[G_s(x, y)\psi_{,y}\right] = g(x, y) \tag{4.33}$$

where

$$g(x, y) = y\,\frac{\partial G_s(x, y)}{\partial x} - x\,\frac{\partial G_s(x, y)}{\partial y} \tag{4.34}$$

Now consider point o of the mesh with four surrounding points

N, E, S, W and four mid-points n, e, s, w (Fig. 4.7), then using

equations (4.32), g(x,y) can be expressed for point o as follows

$$g(x,y)_o = \frac{1}{h}\left[y(o)\left[G_s(e) - G_s(w)\right] - x(o)\left[G_s(s) - G_s(n)\right]\right] = b(o)$$

(4.35)

having the values of G_s at the nodal points the right hand side of

the equation (4.33) can be evaluated for the mesh. These values

are constant for a chosen mesh and will tend to a more accurate

value as mesh size becomes smaller. To evaluate the left side of

(4.33)

$$\begin{cases} (\psi_{,x})_e = \dfrac{\psi(E) - \psi(o)}{h} \\[2mm] (\psi_{,x})_w = \dfrac{\psi(o) - \psi(W)}{h} \\[2mm] (\psi_{,y})_n = \dfrac{\psi(o) - \psi(N)}{h} \\[2mm] (\psi_{,y})_s = \dfrac{\psi(S) - \psi(o)}{h} \end{cases}$$

(4.36)

and

$$\left(\frac{\partial}{\partial x}(G_s\psi_{,x})\right)_o = \frac{(G_s\psi_{,x})_e - (G_s\psi_{,x})_w}{h}$$

$$= \frac{1}{h^2}\left[G_s(e)\left[\psi(E) - \psi(o)\right] - G_s(w)\left[\psi(o) - \psi(W)\right]\right]$$

$$= \frac{1}{h^2}\left[G_s(e)\psi(E) + G_s(w)\psi(W) - \left[G_s(e) + G_s(w)\right]\psi(o)\right]$$

similarly

(4.37)

$$\left(\frac{\partial}{\partial x}(G_s\psi_{,y})\right)_o = \frac{1}{h^2}\left[G_s(s)\psi(S) + G_s(n)\psi(N) - \left[G_s(s) + G_s(n)\right]\psi(o)\right]$$

and thus the finite-difference equation for the differential equation of the equilibrium can be written as

$$\frac{1}{h^2} \left[G_s(n)\,\psi(N) + G_s(e)\,\psi(E) + G_s(s)\,\psi(S) + G_s(w)\,\psi(W) - \left[G_s(n) + G_s(e) + G_s(s) + G_s(w) \right] \psi(o) \right] = b(o) \qquad (4.38)$$

where $b(o)$ is expressed in (4.35) and has a constant value at every nodal point. Solving (4.37) for $\psi(o)$ we will have

$$\psi(o) = \left[G_s(n)\,\psi(N) + G_s(e)\,\psi(E) + G_s(s)\,\psi(S) + G_s(w)\,\psi(W) - h^2 b(o) \right] /$$

$$\left[G_s(n) + G_s(e) + G_s(s) + G_s(w) \right]$$

or

$$\psi(o) = \left[G_s(n)\,\psi(N) + G_s(e)\,\psi(E) + G_s(s)\,\psi(S) + G_s(w)\,\psi(W) \right] / c(o) + d(o)$$

$$(4.39)$$

where $d(o) = -h^2 b(o)/c(o)$

$$(4.40)$$

$$c(o) = G_s(n) + G_s(e) + G_s(s) + G_s(w)$$

Now we write the difference equation for the point (i, j) (i^{th} row and j^{th} column) of the mesh (Fig. 4.8)
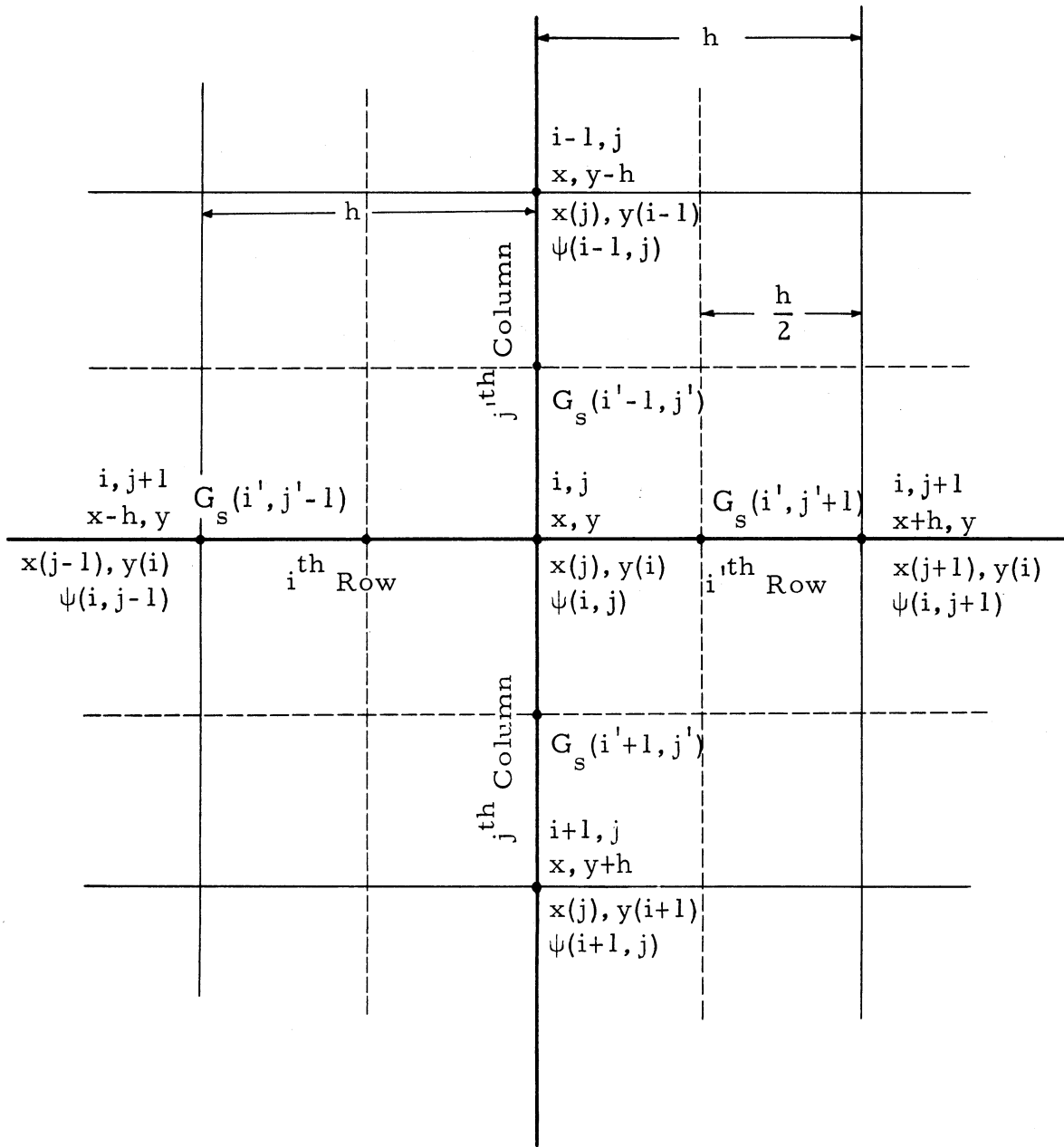
Fig. 4.8. Point (i,j) and the Neighboring Mesh

where

$$i' = 2i - 1$$

$$j' = 2j - 1$$

(4.41)

$$\psi(i,j) = \left[G_s(i'-1,j') \, \psi(i-1,j) + G_s(i'+1,j') \, \psi(i+1,j) + \right.$$

$$G_s(i',j'-1) \, \psi(i,j-1) + G_s(i',j'+1) \, \psi(i,j+1) \Big] / c(i,j)$$

$$- h^2 b(i,j)/c(i,j) \tag{4.42}$$

where

$$c(i,j) = G_s(i',j'-1) + G_s(i',j'+1) + G_s(i'+1,j') + G_s(i'-1,j')$$

and $\tag{4.43}$

$$b(i,j) = \frac{1}{h} \left[y(i)[G_s(i',j'+1) - G_s(i',j'-1)] - x(j)[G_s(i'+1,j') - G_s(i'-1,j')] \right]$$

If G_s is constant, equation (4.42) will reduce to the finite difference

equation of the Laplacian operator ∇^2

$$G_{s,x} = G_{s,y} = 0$$

$$G_s(i',j'-1) = G_s(i',j'+1) = G_s(i'+1,j') = G_s(i'-1,j') = c(i,j)/r$$

$$b(i,j) = 0$$

and equation (4.42) will become

$$\psi(i,j) = \left[\psi(i,j+1) + \psi(i,j-1) + \psi(i+1,j) + \psi(i-1,j) \right] / 4 \tag{4.44}$$

4.10. DIFFERENCE EQUATIONS FOR BOUNDARY CONDITIONS OF T SECTION

Choosing the xy coordinate system as shown below with the

origin in the centroid of the flange (assumed to be the center of the

twist) and x, y-axis parallel to the sides of the cross section,

boundary condition (4.20) will be simplified. On the sides parallel

to the x-axis, (Fig. 4.9), dy = 0, dS = dx and equation (4.20)

becomes

$$(\psi,_y + x) = 0 \qquad (4.45)$$
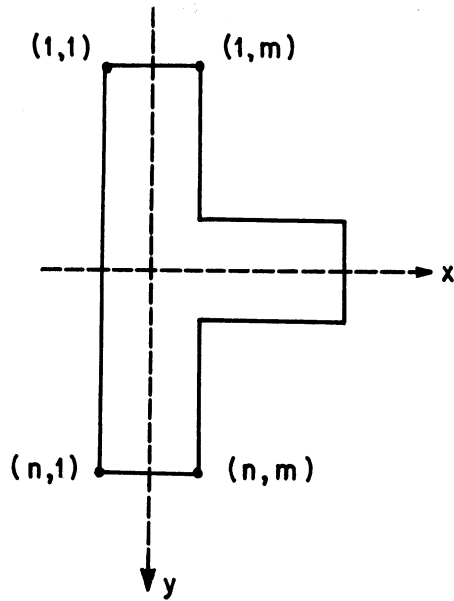
On the sides parallel to the y-axis,

dx = 0, dy = dS and equation (4.20)

becomes

$$(\psi,_x - y) = 0 \qquad (4.46)$$

Fig. 4.9. Boundary of
the T Cross Section

Applying equations (4.32) to the above boundary conditions we can

write

For sides parallel to x

on the negative side of y

$$\frac{1}{2h} \left[-3\psi(1,j) + 4\psi(2,j) - \psi(3,j) \right] + x(j) = 0$$

on the positive side of y $\qquad (4.47)$

$$\frac{1}{2h} \left[-3\psi(n,j) + 4\psi(n-1,j) - \psi(n-2,j) \right] - x(j) = 0$$

For sides parallel to y

on the left side

$$\frac{1}{2h} \left[-3\psi(i,1) + 4\psi(i,2) - \psi(i,3) \right] - y(i) = 0$$

on the right side $\qquad (4.48)$

$$\frac{1}{2h} \left[-3\psi(i,m) + 4\psi(i,m-1) - \psi(i,m-2) \right] + y(i) = 0$$

In order to treat the boundary nodal points in the process of iteration, the values of function ψ for the boundary points should be given in terms of the value of the ψ of the neighboring points; therefore, equations (4.47) and (4.48) should be solved for the boundary nodal points

Negative side of y parallel to x

$$\psi(1,j) = [4\psi(2,j) - \psi(3,j) + 2hx(j)]/3$$

Positive side of y parallel to x $\qquad j=1,2,\ldots,m \qquad$ (4.49)

$$\psi(n,j) = [4\psi(n-1,j) - \psi(n-2,j) - 2hx(j)]/3$$

Left side parallel to y

$$\psi(i,1) = [4\psi(i,2) - \psi(i,3) - 2hy(i)]/3$$

Right side parallel to y $\qquad i=1,2,\ldots,n \qquad$ (4.50)

$$\psi(i,m) = [4\psi(i,m-1) - \psi(i,m-2) + 2hy(i)]/3$$

Discontinuity

Equations (4.30) should be satisfied along the line of discontinuity. The basic assumption that has been made is that all elements of the cross section go through the same amount of unit rotation θ about the center of twist (centroid of the flange). Considering this assumption and using stress relations (4.12) for the elements along the discontinuity line, the following should hold

$$[G_s(x,y)(\psi_{,y} + x)]_1 = [G_s(x,y)(\psi_{,y} + x)]_2$$

$$\qquad (4.51)$$

$$[G_s(x,y)(\psi_{,x} - y)]_1 = [G_s(x,y)(\psi_{,x} - y)]_2$$

$[\ ]_1$ and $[\ ]_2$ mean the term evaluated in the regions (1) and (2)

respectively. In terms

of the difference

equation, assuming

that the nodal point

is on the border line

of the two regions,

equations (4.51) can

be written as follows

(Fig. 4.10)
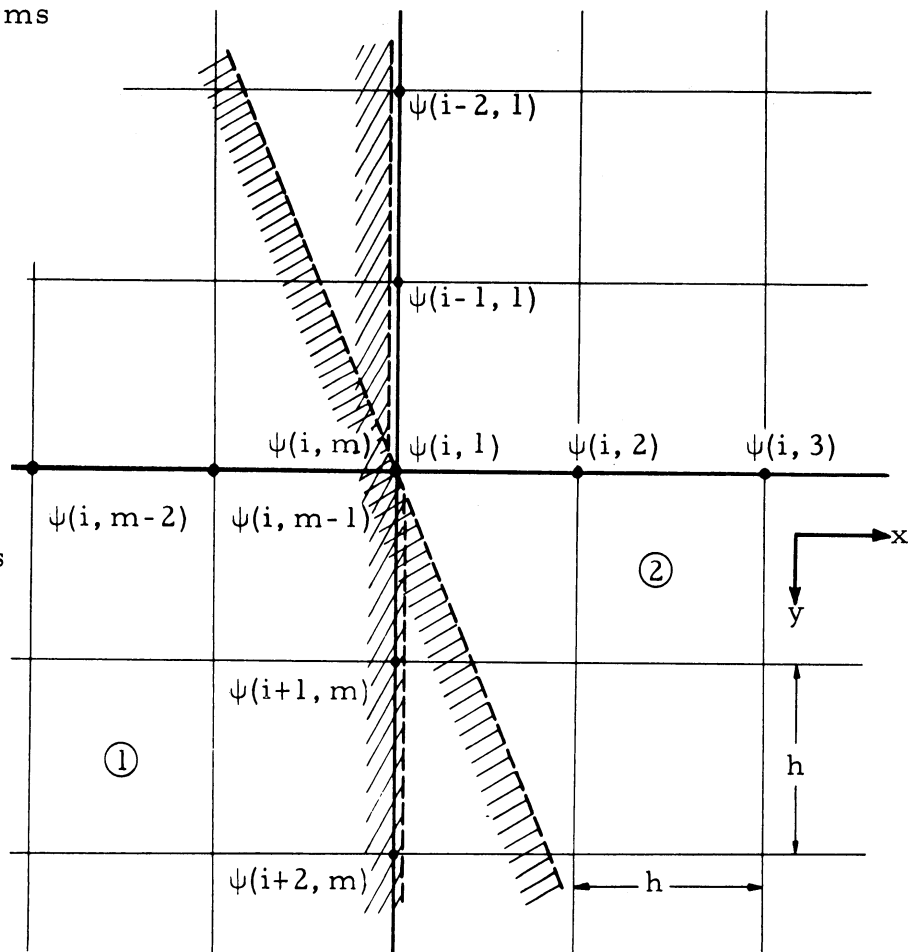
Fig. 4.10. Point on the Border Line of the Discontinuity

$$2h\left[G_s(i, m) - G_s(i, 1)\right]x(m) = G_s(i, 1)\left[-3\psi(i, 1) + 4\psi(i, 2) - \psi(i, 3)\right]$$

$$+ G_s(i, m)\left[-3\psi(i, m) + 4\psi(i, m-1) - \psi(i, m-2)\right]$$

$$2h\left[G_s(i, m) - G_s(i, 1)\right]y(i) = G_s(i, 1)\left[-3\psi(i, 1) + 4\psi(i-1, 1) - \psi(i-2, 1)\right]$$

$$+ G_s(i, m)\left[-3\psi(i, m) + 4\psi(i+1, m) - \psi(i+2, m)\right]$$

$$(4.52)$$

The above equations can be solved for $\psi(i, 1)$ and $\psi(i, m)$ so that in

the iteration process either one can be calculated in terms of the

other

$$\psi(i,1) = \left\{ \left[G_s(i,m)/G_s(i,1) + 1 \right] 2hx(m) + 4\psi(i,2) - \psi(i,3) \right.$$

$$\left. + \left[G_s(i,m)/G_s(i,1) \right] \left[-3\psi(i,m) + 4\psi(i,m-1) - \psi(i,m-2) \right] \right\} /3$$

$$\psi(i,m) = \left\{ \left[-1 + G_s(i,1)/G_s(i,m) \right] 2hy(i) + 4\psi(i+1,m) - \psi(i+2,m) \right.$$

$$\left. + \left[G_s(i,1)/G_s(i,m) \right] \left[-3\psi(i,1) + 4\psi(i-1,1) - \psi(i-2,1) \right] \right\} /3$$

$$(4.53)$$

Other forms of discontinuity can be treated in the same manner.

Points with Non-Equidistant Neighbors

In many cases a point near a boundary or the border line of two regions will not be surrounded by equidistant neighboring nodal points, or one may wish to make a change of net interval in a special region. Special formulas must be provided for such cases. Starting from the polynomial function (4.31) for a general case such as the one on the Fig. 4.11, equations (4.32) can be written as following
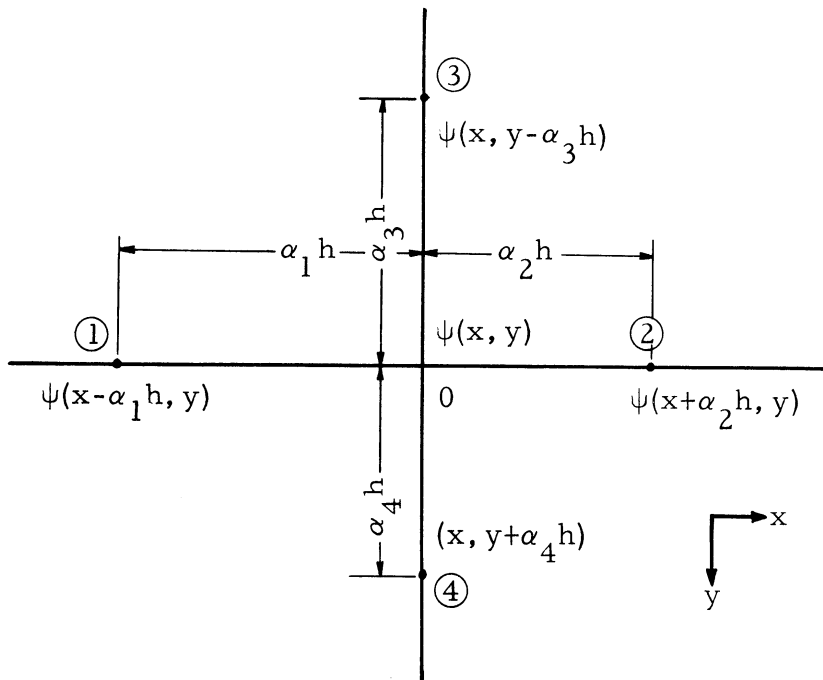
Fig. 4.11. Point with Non-Equidistant
Neighbors

$$\left(\frac{\partial \psi}{\partial x}\right)_0 = \frac{\alpha_1^2 \psi(2) + (\alpha_2^2 - \alpha_1^2)\psi(0) - \alpha_2^2 \psi(1)}{\alpha_1 \alpha_2 (\alpha_1 + \alpha_2) h}$$

$$= \frac{\alpha_1}{\alpha_2(\alpha_1 + \alpha_2)h}\psi(2) + \frac{\alpha_2 - \alpha_1}{\alpha_1 \alpha_2 h}\psi(1) - \frac{\alpha_2 \psi(0)}{\alpha_1(\alpha_1 + \alpha_2)h}$$

$$\left(\frac{\partial \psi}{\partial x}\right)_1 = \frac{-\alpha_1^2 \psi(2) + (\alpha_1 + \alpha_2)^2 \psi(0) - \alpha_2(2\alpha_1 + \alpha_2)\psi(1)}{\alpha_1 \alpha_2 (\alpha_1 + \alpha_2) h}$$

$$= \frac{-\alpha_1}{\alpha_2(\alpha_1 + \alpha_2)h}\psi(2) + \frac{\alpha_1 + \alpha_2}{\alpha_1 \alpha_2 h}\psi(0) - \frac{2\alpha_1 + \alpha_2}{\alpha_1(\alpha_1 + \alpha_2)h}\psi(1)$$

$$\text{(4.54)}$$

$$\left(\frac{\partial \psi}{\partial x}\right)_2 = \frac{\alpha_1(2\alpha_2 + \alpha_1)\psi(2) - (\alpha_1 + \alpha_2)^2 \psi(0) - \alpha_2^2 \psi(1)}{\alpha_1 \alpha_2 (\alpha_1 + \alpha_2) h}$$

$$= \frac{2\alpha_2 + \alpha_1}{\alpha_1(\alpha_1 + \alpha_2)h}\psi(2) - \frac{(\alpha_1 + \alpha_2)}{\alpha_1 \alpha_2 h}\psi(0) + \frac{\alpha_2}{\alpha_2(\alpha_1 + \alpha_2)h}\psi(1)$$

$$\left(\frac{\partial^2 \psi}{\partial x^2}\right)_{201} = 2\,\frac{\alpha_1 \psi(2) - (\alpha_1 + \alpha_2)\psi(0) + \alpha_2 \psi(1)}{\alpha_1 \alpha_2 (\alpha_1 + \alpha_2) h^2}$$

$$= \frac{2}{h^2}\left[\frac{1}{\alpha_2(\alpha_1 + \alpha_2)}\psi(2) - \frac{1}{\alpha_1 \alpha_2}\psi(0) + \frac{1}{\alpha_1(\alpha_1 + \alpha_2)}\psi(1)\right]$$

By changing the $\psi(1)$, $\psi(2)$, α_1, α_2 respectively to the $\psi(3)$, $\psi(4)$, α_3, α_4, the above relations will give the derivatives of ψ with respect to y. For $\alpha_1 = \alpha_2 = 1$ relations (4.54) reduce to those expressed

in (4.32). Using the above relations, governing difference equations and the boundary conditions for points with non-equidistant neighbors can be obtained; however,

in this study to simplify the manipulation, the straight lines of discontinuity have been approximated by a step-wise line (Fig. 4.12)
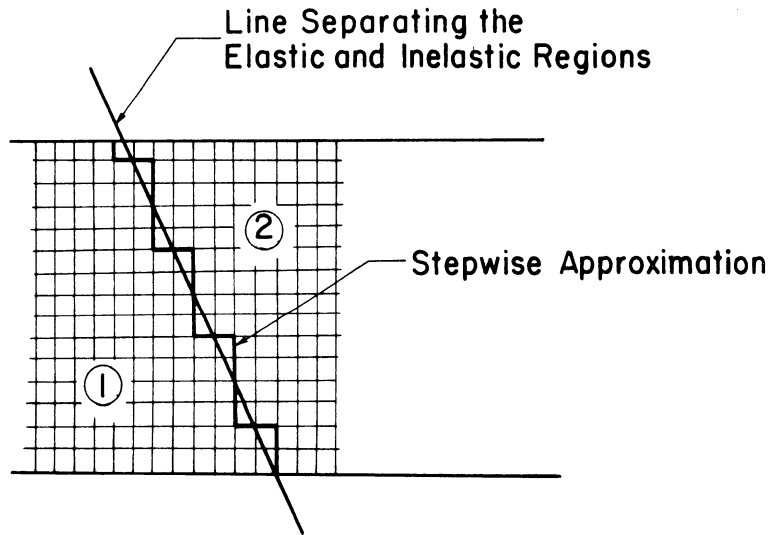
Fig. 4.12. Stepwise Approximation

4.11. CONVERGENCE OF THE ITERATION

Relations (4.32) and (4.54) can be obtained by applying Taylor's theorem and expanding the function $\psi(x, y)$ at the neighborhood of 0 (Fig. 4.13), as done by Young[78]
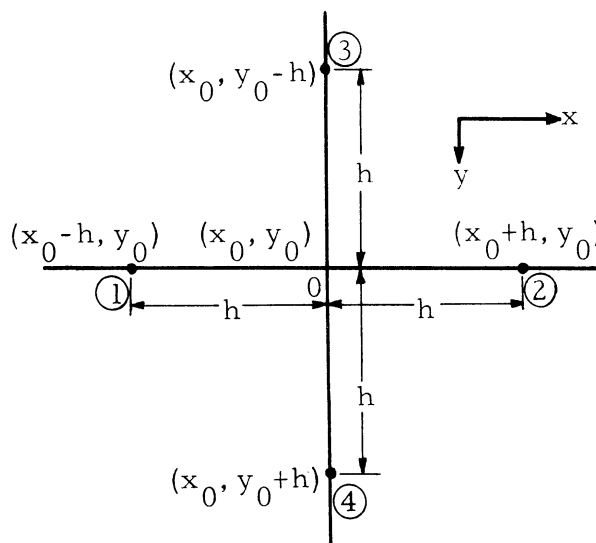
Fig. 4.13. Expansion of $\psi(x, y)$
in the Neighborhood of (x, y)

$$\psi(2) = \psi(0) + h(\psi_{,x})_0 + \frac{h^2}{2}(\psi_{,xx})_0 + \frac{h^3}{3}(\psi_{,xxx})_0 + \frac{h^4}{4}(\bar{\psi}_{,xxxx})_{0,2}$$

(4.55)

where

$$(\bar{\psi}_{,xxxx})_{0,2} = \psi_{,xxxx}(x_0 + \xi, y_0) \qquad 0 < \xi < h$$

(4.56)

similarly

$$\psi(1) = \psi(0) - h(\psi_{,x})_0 + \frac{h^2}{2}(\psi_{,xx})_0 - \frac{h^3}{3}(\psi_{,xxx})_0 + \frac{h^4}{4}(\bar{\psi}_{,xxxx})_{0,2}$$

(4.57)

Combining (4.55) and (4.57)

$$(\psi_{,xx})_0 = \frac{\psi(2) + \psi(1) - 2\psi(0)}{h^2} - \frac{h^4}{4}\left[(\psi_{,xxxx})_{0,2} + (\psi_{,xxxx})_{0,1}\right]$$

(4.58)

$$(\psi_{,x})_0 = \frac{\psi(2) - \psi(1)}{2h} - \frac{h^2}{12}\left[(\psi_{,xxx})_{0,2} + (\psi_{,xxxx})_{0,1}\right]$$

similarly the derivative with respect to y can be expressed

$$(\psi_{,yy})_0 = \frac{\psi(4) + \psi(3) - 2\psi(0)}{h^2} - \frac{h^4}{4}\left[(\psi_{,yyyy})_{0,4} + (\psi_{,yyyy})_{0,3}\right]$$

(4.59)

$$(\psi_{,y})_0 = \frac{\psi(4) - \psi(3)}{2h} - \frac{h^2}{12}\left[(\psi_{,yyy})_{0,4} + (\psi_{,yyy})_{0,3}\right]$$

Neglecting the higher order terms and substituting (4.58) and (4.59)

in (4.15), for each point (x, y) in the domain, we get

$$\left[G_s(x,y) + \frac{h}{2} G_s(x,y)_{,x} \right] \psi(x+h,y) + \left[G_s(x,y) - \frac{h}{2} G_s(x,y)_{,x} \right] \psi(x-h,y)$$

$$+ \left[G_s(x,y) + \frac{h}{2} G_s(x,y)_{,y} \right] \psi(x,y+h) + \left[G_s(x,y) - \frac{h}{2} G_s(x,y)_{,y} \right] \psi(x,y-h)$$

$$- 4 G_s(x,y)\psi(x,y) = h^2 \left[y\, G_s(x,y)_{,x} - x\, G_s(x,y)_{,y} \right] \tag{4.60}$$

(4.60) can be written in the following form

$$a_1 \psi(x-h,y) + a_2 \psi(x+h,y) + a_3 \psi(x,y-h) + a_4 \psi(x,y+h) - a_0 \psi(x,y) = t(x,y) \tag{4.61}$$

where a_i $(i=0,1,2,3,4)$ are functions of (x,y)

we observe that

$$a_0 = a_1 + a_2 + a_3 + a_4$$

If h is chosen such that

$$h < \min \left\{ \frac{2 G_s(x,y)}{\left| G_s(x,y)_{,x} \right|} \;,\; \frac{2 G_s(x,y)}{\left| G_s(x,y)_{,y} \right|} \right\} \tag{4.62}$$

the minimum being evaluated in the domain of the operation, then

all the a_i will be positive and convergence of the iteration process

will be guaranteed.[*]

4.12. SHEAR-STRESS-STRAIN RELATIONSHIP

In order to derive the shear stress relations (4.12) from

shear strain relations (4.11) the values of G_s used in equation

$$\tau = G_s \gamma \tag{4.63}$$

---

[*]For further details refer to reference (78)

should be defined and evaluated for the inelastic range. Suppose the relation between stress and strain is given by the Fig. 4.14. Total strain can be written as the summation of two strains, ϵ_e, elastic strain, and ϵ_p, plastic strain[11]

$$\epsilon = \epsilon_e + \epsilon_p \qquad (4.64)$$

or
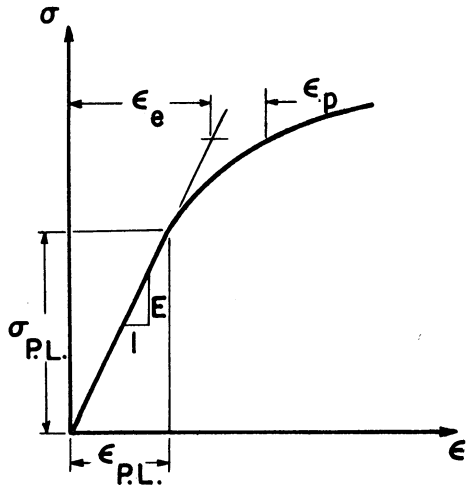
$$\epsilon = \frac{\sigma}{E} + \left(\frac{\sigma}{B}\right)^n \qquad (4.65)$$

Fig. 4.14. Total Strain vs. Stress

Now we plot the stress against the plastic strain. The relation between the plastic shear stress $(\tau)_p$ and strain $(\gamma)_p$ can be formed by dividing the stress ordinate of the Fig. 4.15 by two.
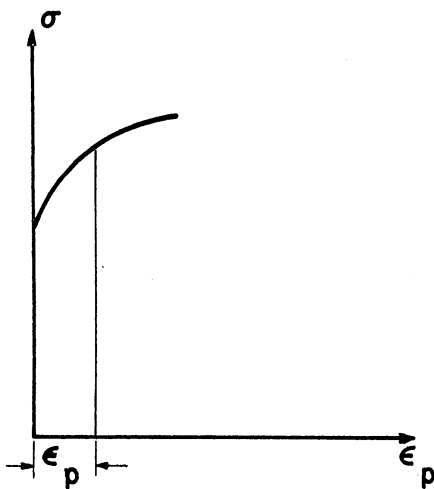
Fig. 4.15. Plastic Strain vs. Stress

The reason for this is: for pure compression along the z-axis

$\sigma_y = \sigma_x = 0$ and $\sigma_z = -\sigma$, then the principal shear stresses will be

$$\tau_{xy} = \frac{\sigma_x - \sigma_y}{2} = 0$$

$$\tau_{xz} = \frac{\sigma_x - \sigma_z}{2} = 0 \tag{4.66}$$

$$\tau_{yz} = \frac{\sigma_y - \sigma_z}{2} = \frac{\sigma}{2}$$

Since τ_{xz} and τ_{yz} are equal in pure compression the corresponding

inelastic strains ϵ_{xz} and ϵ_{yz} must also be equal, each being half of

the total inelastic strain ϵ_{ρ}. Therefore, to convert Fig. 4.14 to a

principal shear stress vs. the corresponding strain, stress ordinate

of Fig. 4.15 should be divided by two (Fig. 4.16). To form the

complete τ vs. γ diagram from

σ vs. ϵ diagram simply for

every value of plastic strain ϵ_{p_1}

should be calculated and then

corresponding point on (τ vs. γ)

diagram will be

$$(\tau_1 = \frac{\sigma_1}{2} \text{ vs. } (\gamma_e + \epsilon_{p_1})$$

(Figs. 4.17 and 4.18).
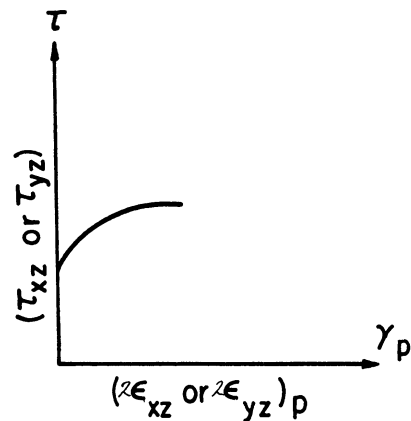
Fig. 4.16. Shear Stress vs.
Plastic Shear Strain
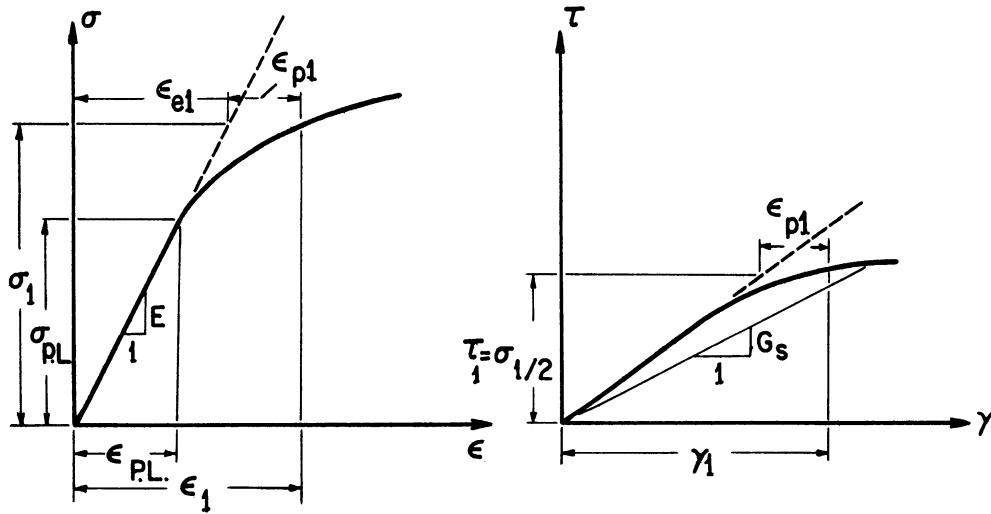
Figs. 4.17, 4.18. Conversion of Tensile Stress-Strain Diagram
to Shear Stress-Strain Diagram

The relation between modulus of elasticity E and shear modulus G

is given by the formula

$$G = \frac{E}{2(1 + \nu)}$$ (4.67)

in which ν is the Poisson's ratio.

4.13. EVALUATION OF G_s

For a given strain ϵ_1, the stress σ_1 can be calculated

graphically or mathematically. In case stress is given by an algebraic

formula in terms of strain,

$$\tau_1 = \frac{\sigma_1}{2}$$

and plastic strain $\qquad \epsilon_{p_1} = \epsilon_1 - \dfrac{\sigma_1}{E}$

shear strain $\qquad \gamma = \dfrac{\tau_1}{G} + \epsilon_{p_1}$

$$G_{s_1} = \frac{\tau_1}{\gamma_1} = \frac{\dfrac{\sigma_1}{2}}{\dfrac{\sigma_1}{2G} + \epsilon_1 - \dfrac{\sigma_1}{E}} = \frac{\dfrac{1}{2}}{\dfrac{2(1 + \nu)}{E} + \dfrac{\epsilon_1}{\sigma_1} - \dfrac{1}{E}}$$

or

$$G_{s_1} = \frac{E}{2\left(\nu + \dfrac{\epsilon_1 E}{\sigma_1}\right)}$$

or in general

$$G_{s} = \frac{E}{2\left(\nu + \dfrac{\epsilon}{\dfrac{\sigma}{E}}\right)} \qquad\qquad (4.68)$$

It can be seen from equation (4.68) that in the inelastic range the value of G_s varies as a function of ϵ (Fig. 4.19). In the elastic range, relation $\sigma = \epsilon E$ reduces the equation (4.68) to the relation (4.67) between G and E.
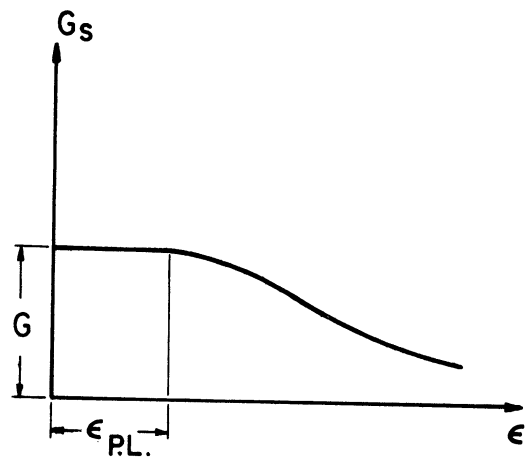
Fig. 4.19. Strain vs. Shear
Secant Modulus

It is obvious that in the case of combined compression and torsion, the value corresponding to the combined stress according to one of the failure criteria, such as VonMises criterion, should be considered; but in this problem the amount of torque and rotation and consequently the shear stress due to torsion are very small compared to the compressive stress. It is assumed that G_s is constant in the neighborhood of the considered strain. Moreover, the tensile (or compressive) stress-strain curve is used directly to compute $\tau = f(\gamma)$.

4.14. METHOD OF ITERATION

In any numerical solution of a differential equation, the continuum of points on the boundary and the interior region should be replaced by a discrete set of points. The value of the function is then considered only at these points rather than at every point of the governing region.

Liebmann[79] suggested an iterative procedure in the year 1918 and demonstrated the solution for the Laplace's equation. He divided the region into a square net and assigned approximate values to the function at the interior nodal points and known values at the nodal points of the boundary. Then traversing the region in an orderly manner repeatedly, and replacing the value of the function at each interior nodal point by the mean of the values of the four neighboring points, i.e.,

$$\psi(i,j) = \left[\psi(i,j-1) + \psi(i,j+1) + \psi(i+1,j) + \psi(i-1,j)\right]/4$$

(a special case of equation (4.42))

and using the newly calculated values immediately, he obtained a solution for the Laplace's equation.

Richardson[80] had suggested a similar method, earlier (1910), in which he did not replace the old values by the newly calculated ones until the whole cycle was completed. This method converges somewhat slower than the one suggested by Liebmann. In general, for each interior point $(\psi_{ij})_i$ and each boundary point $(\psi_{pq})_b$ we can form an equation, and hence will have a system of linear equations for the nodal points. The most popular method for solving the simultaneous linear equation is Gaussian elimination. A dense system of N equations for N unknowns can be solved with an order of $\dfrac{N^3}{3}$ multiplications, plus other arithmetic operations.

Elimination methods which are called direct methods are rarely applied to solution of elliptic difference equations because of the large storage space required to store matrix $a_{k\ell ij}$ in the relation

$$a_{k\ell ij}\,\psi_{ij} = b_{k\ell} \tag{4.69}$$

(repeat of the subscripts means summation on these subscripts)

For partial differential equations, N is usually chosen very large such that we can only store some multiple of N but not N^2 elements.

However, it is obvious that, disregarding the round-off errors, the elimination method will give the exact solution in a finite

number of steps. On the other hand, the indirect or iteration methods, both in operation and in storage, take full advantage of the numerous zero elements in the matrix [a]. Moreover, in contrast to the elimination method, iteration methods are self-correcting in the process of iteration and, therefore, minimize the round-off error.

The algorithm for an iterative method is very simple, but normally an exact solution can be achieved only with a very high number of iteration cycles.

The algorithm for the direct method is rather complicated. The above methods have been treated extensively by Householder[81] (1953) and Bodewig[82] (1956). If we write the two-dimensional matrix $[\psi_{ij}]$ in the form of a vector $\{\psi\}$ then equation (4.69) can be written as follows

$$[A]\{\psi\} = \{B\} \tag{4.70}$$

considering the difference equation (4.42) matrices $[A]$ and $\{B\}$ can be formed. $[A]$ is a matrix with no zero diagonal element and has diagonal dominance and also is not reducible. Then the method of successive displacements, sometimes called relaxation method, will converge in solving this problem.[83] This method was introduced by Seidel (1874), but is known as Gauss-Seidel method. Liebmann applied this method to the elliptic difference equations (1918).[79]

Overrelaxation

Overrelaxation is the change of any element of $[\psi]$ by ω times the exact amount of the change necessary to make that

element satisfy the equation written for it ($\omega > 1$). Young[84] and

Frankel[85] introduced this procedure and Friedman, [86]

Householder, [87] Arms, Gates and Zondek, [88] Keller, [89] and

others have studied and applied this theorem. They suggest and

prove that overrelaxation speeds the process of iteration considerably.

ω is called overrelaxation factor and the best value is[90]

$$\omega_b = 1 + \frac{\lambda}{(1 + \sqrt{1 - \lambda})^2} \qquad (4.71)$$

where λ is the limit value of d_n/d_{n-1} and

$$d_n = \max \ [\psi(i,j)]^n - [\psi(i,j)]^{n-1} \qquad (4.72)$$

n is the number of the iteration cycle. The theory indicates that

it is much better to overestimate than to underestimate ω to achieve

a better convergence rate.

The best method of choosing ω is to perform a number of

iterations with the iteration factor equal to 1, and estimate the

value of λ and thereby ω_b.

For solving the problem of torsional stiffness in the inelastic

range, i.e., the difference equation (4.42), the indirect method

with the advantages of overrelaxation procedure, explained above,

has been used and the difference equation (4.42) has been written

in the following form

$$\left[\psi(i,j)\right]^{n+1} = \omega\left[\; G_s(i'-1,j')\left[\psi(i-1,j)\right]^n + G_s(i'+1,j')\left[\psi(i+1,j)\right]^n\right.$$

$$+ G_s(i',j'-1)\left[\psi(i,j-1)\right]^n + G_s(i',j'+1)\left[\psi(i,j+1)\right]^n / c(i,j)$$

$$\left. - h^2 b(i,j)/c(i,j)\right] + (1 - \omega)\left[\psi(i,j)\right]^n \qquad (4.73)$$

4.15. TECHNIQUE

i. Choice of Mesh and Matrices

In order to use all the locations assigned to the variable $\psi(i,j)$ in carrying out the manipulation of the problem with the electrical digital computer, two different variable names have been assigned to the flange and the web, $\left[\psi_f\right]$ and $\left[\psi_w\right]$, respectively. $\left[\psi_f\right]$ has a dimension of $(n_f, m_f + 1)$ and the dimension of $\left[\psi_w\right]$ is $(n_w, m_w + 1)$ (Fig. 4.20). In order to preserve the continuity of $\left[\psi_f\right]$ and $\left[\psi_w\right]$ in the intersection the following relation is kept between them

$$\psi_w(i,0) = \psi_f(n+i, m_f - 1) \qquad i=1,2,\ldots,n_w$$

$$\psi_w(i,1) = \psi_f(n+i, m_f) \qquad i=2,3,\ldots,(n_w-1) \qquad (4.74)$$

$$\psi_w(i,2) = \psi_f(n+i, m_f + 1) \qquad i=1,2,\ldots,n_w$$
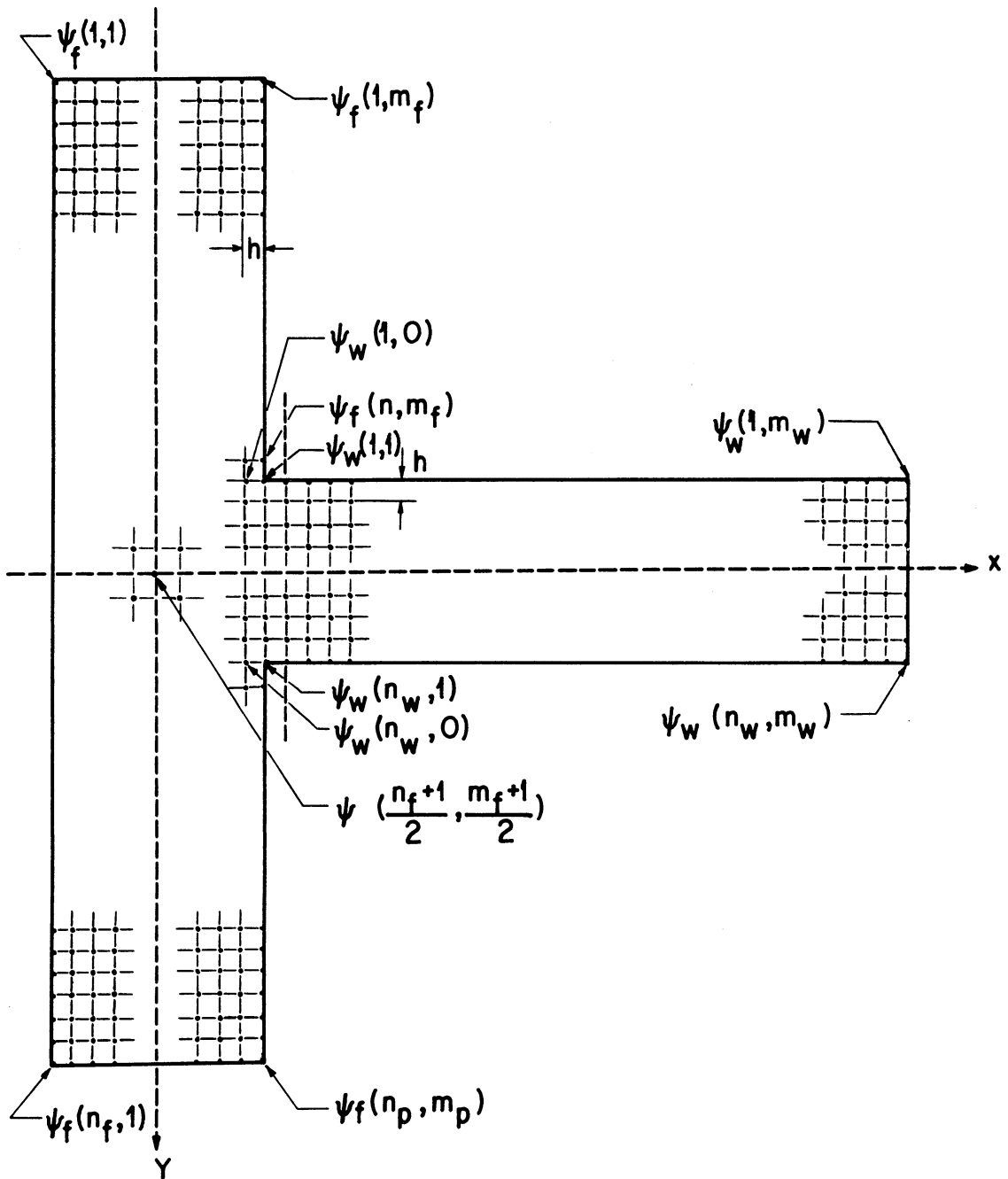
Fig. 4.20. Choice of a Network

The reason for excluding nodal points (1, 1) and $(n_{w, 1})$ of the web and

the corresponding nodal points of the flange in continuity relations is

the indeterminate nature of the values of ψ at these corner points

when approaching from x or y directions towards these points. Theoretically, the torsional stress at these corners is infinite. In this solution two extremely close points are assigned to the corner points, and therefore, and abrupt discontinuity exists between the values of ψ at these two points. In evaluation of torsional stiffness these corner points have been ignored.

For the same reason, two matrices have been designated for the values of secant shear modulus for the flange and the web, $\left[G_{s_f} (2n_f + 1, 2m_f + 1)\right]$ and $\left[G_{s_w} (2n_w + 1, 2m_w + 1)\right]$, respectively.

For simplicity in this analysis the dimensions of the T section have been chosen equal to some even multiples of the mesh size h, except for the length of the stem of the web, which can be taken any odd or even multiple of h. By doing so, existence of the non-equidistant points due to the geometry of the cross section have been avoided. Moreover, the center of the twist will coincide with a nodal point.

The dimensions of the cross section will be

$$t = (m_f - 1) h$$

$$b = (n_f - 1) h$$

$$w = (n_w - 1) h$$

$$d = (m_w - 1) h + t$$

$(m_f,\ n_f$ and n_w are odd integers)

ii. Evaluation of Matrices $[G_s]$ and $[\psi]$

In order to form the secant shear modulus matrices one has to evaluate the strain at that stage of bending and at the previous stage of bending for every nodal point, and determine whether the regression of strain has commenced at that point or not. In the former case the properties of the element, represented by that point, is chosen to be elastic, i.e., the secant shear modulus equal to G, and in the latter case with the strain at hand, inelastic secant shear modulus can be evaluated according to the previous discussion. Strain at the nodal points for two successive stages can be evaluated as follows

$$(\epsilon)^1 = (\epsilon_o)^1 - x(\phi_x)^1 - y(\phi_y)^1$$

$$(\epsilon)^2 = (\epsilon_o)^2 - x(\phi_x)^2 - y(\phi_y)^2$$

(4.76)

In the above equations x and y are the coordinates of the respective nodal point and ϵ_o is the strain of the origin of the xy-axes (center of twist) and $(-\phi_x)$ and $(-\phi_y)$ are the curvature in the x and y directions respectively. Superscripts 1 and 2 indicate the stage at which those values are given.

iii. Border Line of Discontinuity

Equating $(\epsilon)^1$ to $(\epsilon)^2$ the separating line of elastic and inelastic regions can be expressed

$$\left[(\phi_x)^2 - (\phi_x)^1\right] x - \left[(\phi_y)^2 - (\phi_y)^1\right] y = \left[(\epsilon_o)^2 - (\epsilon_o)^1\right]$$

(4.77)

This line will intersect the x- and y-axes at A and B respectively.

$$A \begin{cases} x = \dfrac{(\epsilon_o)^2 - (\epsilon_o)^1}{(\phi_x)^2 - (\phi_x)^1} \\ \\ y = 0 \end{cases} \qquad B \begin{cases} x = 0 \\ \\ y = \dfrac{(\epsilon_o)^2 - (\epsilon_o)^1}{(\phi_y)^2 - (\phi_y)^1} \end{cases} \qquad (4.78)$$

In case of the existence of the line of discontinuity, stepwise approximation of the border lines in the flange and the web can be made. Then some arbitrary values must be assigned to the elements of matrices $[\psi_f]$ and $[\psi_w]$ and the iteration to the extent of acceptable approximation carried out.

4.16. SHEAR STRESS AND TORQUE

After determining the values of the warping function, components of the shear stress can be found from the following relations

$$\left[\tau_{xz}(i,j)\right]_f = \theta G_{s_f}(i',j') \left[\frac{\psi_f(i,j+1) - \psi_f(i,j-1)}{2h} - y_f(i)\right]$$

$$(4.79)$$

$$\left[\tau_{yz}(i,j)\right]_f = \theta G_{s_f}(i',j') \left[\frac{\psi_f(i+1,j) - \psi_f(i-1,j)}{2h} + x_f(j)\right]$$

By changing the subscript f to w shear stress components for the web can be expressed in terms of $[\psi_w]$, $[G_{s_w}]$, $\{x_w\}$ and $\{y_w\}$. Then torque M_z can be evaluated using equation (4.22)

$$M_z = \sum_{i=1}^{n_f} \sum_{j=1}^{m_f} \left[x_f(j) \, \tau_{yzf}(i,j) - y_f(i) \, \tau_{xzf}(i,j) \right] \Delta A_f(i,j)$$

$$+ \sum_{k=1}^{n_w} \sum_{\ell=1}^{m_w} \left[x_w(\ell) \tau_{yzw}(k,\ell) - y_w(k) \tau_{xzw}(k,\ell) \right] \Delta A_w(k,\ell) \qquad (4.80)$$

where

$$\Delta A_f(i,j) = \Delta A_w(k,\ell) = h^2 \qquad \text{for the interior points}$$

$$= \frac{h^2}{2} \qquad \text{for the boundary points}$$

$$= \frac{h^2}{4} \qquad \text{for the corner points}$$

$$= \frac{3h^2}{4} \qquad \text{for the three corner point}$$

(line separating flange and web counted on boundary line)

4.17. TORSIONAL STIFFNESS COEFFICIENT

Thus, having evaluated M_z in terms of θ, stiffness coefficient can be evaluated from the relation

$$C = M_z / \theta \qquad (4.81)$$

4.18. CONCLUSIONS

The objective of this study was to determine an approximate acceptable value for the torsional stiffness coefficient under the conditions explained in this chapter, and to use this value in

the torsional behavior of the column under study. Going through this rigorous calculation for every iteration cycle of the deflection of the column is very much time consuming and rather impossible.

A study was made for a T section of the following dimensions

$$
\begin{aligned}
t &= 1 \text{ inch} \\
b &= 6 \text{ inches} \\
w &= 1 \text{ inch} \\
d &= 7 \text{ inches}
\end{aligned}
\tag{4.82}
$$

and twelve different cases of strain distribution and the stiffness coefficient for each case was evaluated, and then for the same cases the following computation was followed

$$
C_a = \frac{\displaystyle\sum_{i=1}^{n_f}\sum_{j=1}^{m_f} G_{s_f}(i,j)\, \Delta A_f(i,j)}{\displaystyle\sum_{k=1}^{n_f}\sum_{\ell=1}^{m_f} \Delta A_f(i,j)}\,(\tfrac{1}{3}bt^3 - 0.21t^4)
$$

$$
+ \frac{\displaystyle\sum_{k=1}^{n_w}\sum_{\ell=1}^{m_w} G_{s_w}(k,\ell)\, \Delta A_w(k,\ell)}{\displaystyle\sum_{k=1}^{n_w}\sum_{\ell=1}^{m_w} \Delta A_w(k,\ell)}\left[\tfrac{1}{3}(d-t)w^3 - 0.105w^4\right]
\tag{4.83}
$$

$$
+ \frac{\displaystyle\sum_{i=1}^{n_f}\sum_{j=1}^{m_f} G_{s_f}(i,j)\, \Delta A_f(i,j) + \sum_{k=1}^{n_w}\sum_{\ell=1}^{m_w} G_{s_w}(k,\ell)\, \Delta A_w(k,\ell)}{\displaystyle\sum_{i=1}^{n_f}\sum_{j=1}^{m_f} \Delta A_f(i,j) + \sum_{k=1}^{n_w}\sum_{\ell=1}^{m_w} \Delta A_w(k,\ell)}\,\alpha_1 D_1^4
$$

For this example h was taken

0.1 inch and α_1 = 0.105

(reference (91), figure 7)

and D_1 = 1.25 inch (Fig. 4.21).
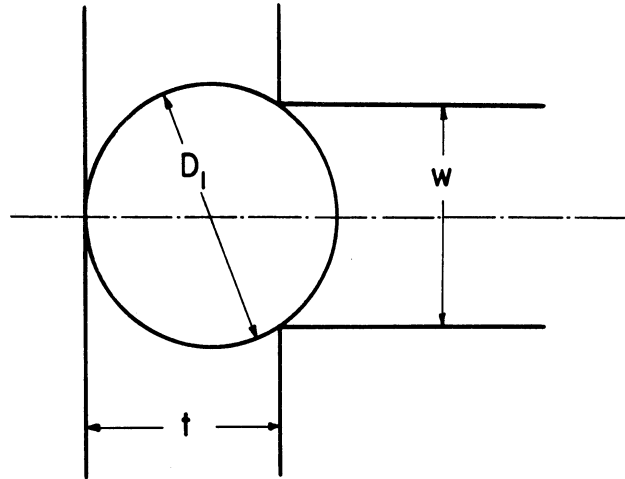
Fig. 4.21. Junction of Flange and Web

The range of variation for these twelve cases was found to be

$$0.92C_a < C < 1.54C_a \qquad (4.84)$$

(4.83) indicates that assumption of C_a as the stiffness coefficient

is more a conservative assumption and does not deviate "too much"

from the exact solution. To formulate a closer solution more cases

have to be considered and solved.

In the study of the column problem, equation (4.83) has been

used as an approximate value for the torsional stiffness of the

"T" section.

CHAPTER V

INCREMENTAL ANALYSIS OF "T" COLUMN BEHAVIOR

5. 1. INTRODUCTION

The procedure presented herein is the one used to determine the load deflection history and thereby the ultimate load carrying capacity of the column. This procedure is based on Newmark's numerical method[92] and uses Batterman and Johnston's method of expressing strains in terms of the radius of the curvature.[16]

In order to evaluate the integrals in the equilibrium, torsional stiffness, and the bending stiffness equations over the area of the cross section of the column, the cross section was divided into a grid network in a manner similar to Birnstiel's method.[36] Integrals were taken over each mesh area (assuming that the value of the integrant is constant over the mesh area and is equal to the same value for its centroid), and then summed over the cross sectional area. The effect of initial crookedness in the plane of symmetry and in either direction of the x-axis has been taken into consideration. Eccentric loading in the plane of symmetry has been studied and compared with the initial crookedness. Different ratios of bending stiffness with respect to two principal axes at the unloaded state have been studied. Comparison has been made between the assumed

sinusoidal deflected shape and the more exact deflected shape. Also, different stress-strain relations have been used to find the load-deflection history of the column. The results of the above studies will be illustrated graphically.

The steps followed in this analysis and also the MAD[93] language computer programs, written for the IBM 7090 to carry out the numerical manipulation, will be explained in this chapter.

5.2. STRESS-STRAIN RELATION

For the purpose of comparison of the analytical and the experimental results it was necessary to use experimentally determined elastic and inelastic properties of the material in the incremental analysis. This necessitated that the stress-strain relation be prepared in a manner that could easily be fed into the computer memory. The ideal case was to find a mathematical fit, as close as possible, to the experimental results.

The best fit curve consisted of three parts, beginning with a straight line portion and ending with a segment of a hyperbola, connected together with a portion of a parabola of third degree. These three segments were chosen such that the slopes of the two segments at the point of their intersection were the same. The method of least squares[94] was used to choose the separating points of the above three segments and the numerical calculations were done by the digital computer. The graphical representation of the algebraic fit for the stress-strain relation along with the

elastic (tangent) modulus and the secant shear modulus, evaluated

on the basis of discussion in Chapter IV, is shown on Fig. 2.6.

The equations of the best fit curve are:

Straight line segment $\epsilon \leqslant 0.0035$ $\qquad$ $\sigma = 10290 \times \epsilon$

$$E = \frac{\sigma}{\epsilon} = 10290$$

Parabola segment $0.0035 \leqslant \epsilon \leqslant 0.0050$ $\qquad$ $\sigma = 4.54444 \times 10^8 \epsilon^3$

$$- 8.83111 \times 10^6 \epsilon^2$$

$$+ 5.54069 \times 10^4 \epsilon$$

$$- 69.2125$$

$$E_t = \frac{d\sigma}{d\epsilon} = 13.63332 \times 10^8 \epsilon^2$$

$$- 17.66222 \times 10^6 \epsilon$$

$$+ 5.54069 \times 10^4 \tag{5.1}$$

Hyperbola segment $\epsilon \geqslant 0.0050$ $\qquad$ $\sigma = \left[-1.77152 \times 10^{-3} \right/$

$$\left(\epsilon - 3.7743 \times 10^{-3} \right) \Big]$$

$$+ 45.2953$$

$$E_t = \frac{d\sigma}{d\epsilon} = \left[-1.77152 \times 10^{-3} \right.$$

$$\left. \left(\epsilon - 3.7743 \times 10^{-3} \right)^2 \right]$$

Also two alternative stress-strain relations are used in the numerical

evaluations. The stress-strain curve used by Batterman and

Johnston[16] is called stress-strain curve #2 (Fig. 5.1). The stress-

strain curve used by Johnston[14] in the strut model study is called

stress-strain curve #3 (Fig. 5.2).
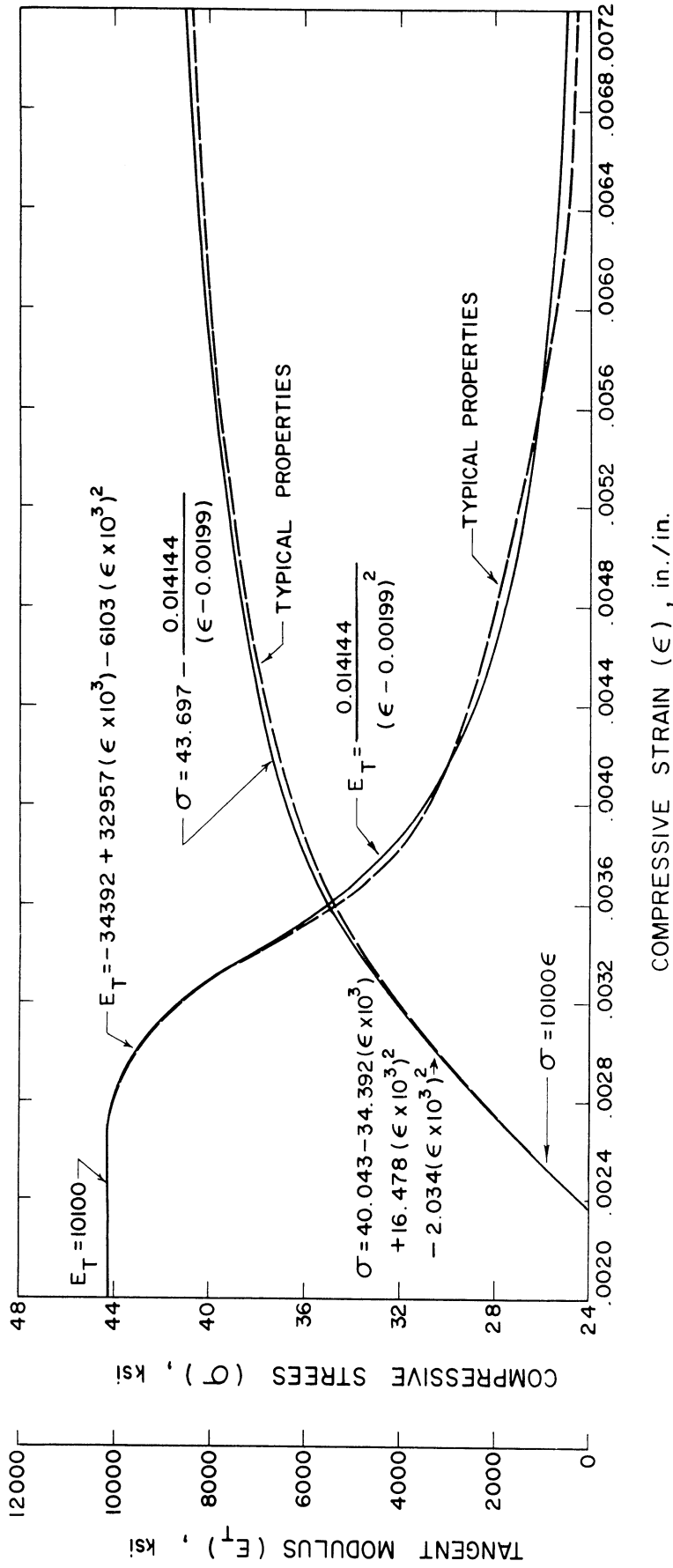
Fig. 5.1. Stress-Strain and Tangent-Modulus Strain Relation #2
(used in Batterman-Johnston column analysis)
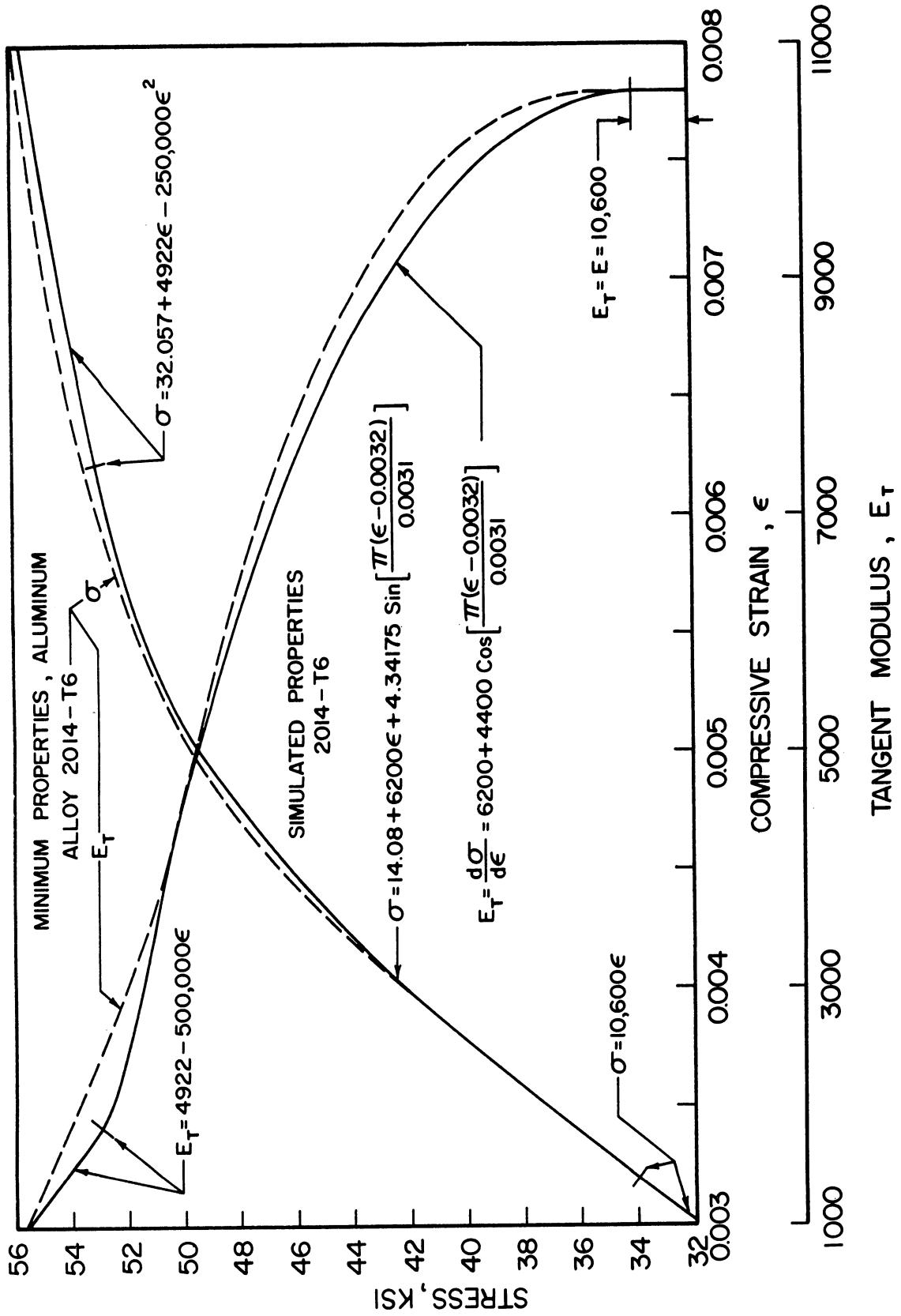
Fig. 5.2. Stress-Strain and Tangent Modulus-Strain Relation #3

5.3. BASIC RELATIONS USED IN THE INCREMENTAL PROCEDURE

i. Division of the Column Length

The column is divided into m equal segments of length λ

$$\lambda = \frac{L}{m} \tag{5.2}$$

The nodal points along the column are numbered consecutively starting with 0 from the top (left) and ending with m at the bottom (right).

In this chapter the longitudinal view of the column will be designated by an axis passing through the centroid of the flange (twist center) of the initially straight column (Fig. 5.3).
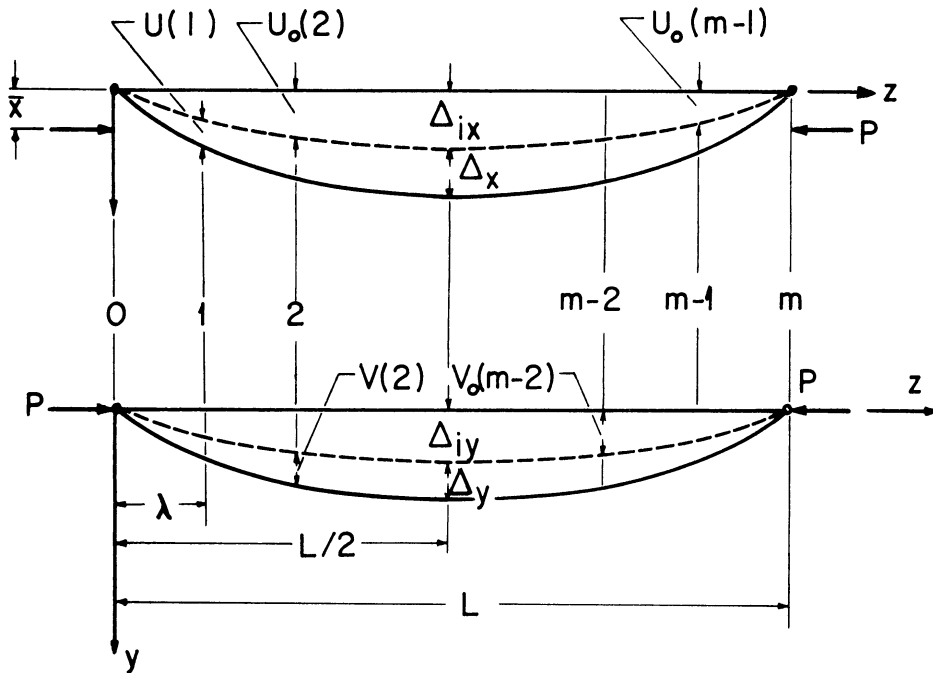
Fig. 5.3. Initial and Deflected Positions of the Column

If it is desired to have the mid-height section as a nodal point, m should be chosen an even number. All behavior characteristics of every nodal point, such as deflection, curvature, depth of strain

regression, and others which will be explained, can be distinguished

by the values of the subscripts of every variable, i.e., $\left[-\phi(\ell q)\right]_n$

represents the curvature at the ℓth nodal point ($\ell = 0, 1, \ldots, m$) along

the qth axis (q = 1 is x-axis, q = 2 is y-axis), after n cycle of

incrementing the fixed increment. The fixed increment in this analysis

is chosen to be the increment of the deflection of the mid-height of the

column in the x direction, i.e.,

$$\left[\Delta\delta\left(\frac{m}{2},1\right)\right]_1 = \left[\Delta\delta\left(\frac{m}{2},1\right)\right]_2 = \ldots\ldots = \left[\Delta\delta\left(\frac{m}{2},1\right)\right]_n \qquad (5.3)$$

ii. Curvature-Deflection Relation

Consider the vector $\left\{U\right\}$ with (m + 1) elements. The

element U_ℓ of the above vector represents the deflection of the column

in a longitudinal plane of the column under consideration. If $\left\{-\phi\right\}$

is the curvature vector of the deflection $\left\{U\right\}$ (Fig. 5.4), then,

using the Newmark's procedure, one may find the matrix $[R]$ such

that

$$\left\{U\right\} = [R]\left\{\phi\right\} \qquad (5.4)$$
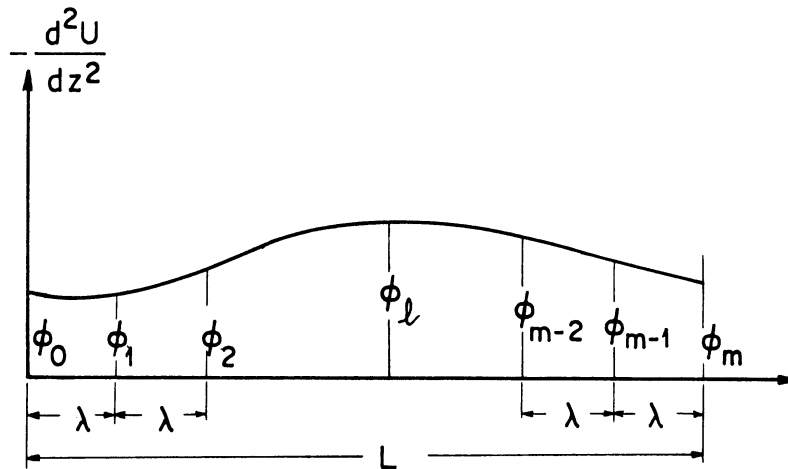
Fig. 5.4. Curvature Distribution along the Column

where $\{U\}$ and $\{\phi\}$ are

$$\{U\} = \begin{Bmatrix} U_0 \\ U_1 \\ U_2 \\ . \\ . \\ . \\ U_{m-1} \\ U_m \end{Bmatrix} \qquad\qquad \{\phi\} = \begin{Bmatrix} \phi_0 \\ \phi_1 \\ \phi_2 \\ . \\ . \\ . \\ \phi_{m-1} \\ \phi_m \end{Bmatrix} \qquad (5.5)$$

Matrix $[R]$ is the product of three matrices $[q_1]$, $[q_2]$ and $[q_3]$.

Matrix $[q_1]$ converts the distributed values of the curvature, $\{-\phi\}$,

into the concentrated angle changes, $\{\theta\}$, according to the following

relation (Fig. 5.5)

$$\{\theta\} = [q_1]\{\phi\} \qquad\qquad (5.6)$$
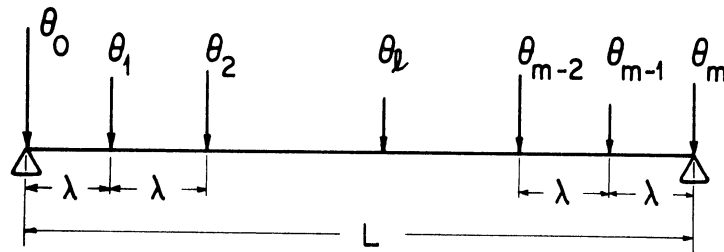
Fig. 5.5. Concentrated Angle Changes

where

$$\{\theta\} = \begin{Bmatrix} \theta_0 \\ \theta_1 \\ \theta_2 \\ \cdot \\ \cdot \\ \cdot \\ \theta_{m-1} \\ \theta_m \end{Bmatrix} \tag{5.7}$$

and

$$[q_1(m+1, m+1)] = \frac{L}{12m} \begin{bmatrix} 3.5 & 3. & -.5 & 0 & 0 & . & . & 0 & 0 & 0 \\ 1 & 10 & 1 & 0 & 0 & . & . & 0 & 0 & 0 \\ 0 & 1 & 10 & 1 & 0 & . & . & 0 & 0 & 0 \\ \cdot & \cdot & \cdot & \cdot & \cdot & \cdot & \cdot & \cdot & \cdot & \cdot \\ \cdot & \cdot & \cdot & \cdot & \cdot & \cdot & \cdot & \cdot & \cdot & \cdot \\ \cdot & \cdot & \cdot & \cdot & \cdot & \cdot & \cdot & \cdot & \cdot & \cdot \\ \cdot & \cdot & \cdot & \cdot & \cdot & \cdot & \cdot & \cdot & \cdot & \cdot \\ 0 & 0 & 0 & . & . & 0 & 1 & 10 & 1 & 0 \\ 0 & 0 & 0 & . & . & 0 & 0 & 1 & 10 & 1 \\ 0 & 0 & 0 & . & . & 0 & 0 & -.5 & 3. & 3.5 \end{bmatrix} \tag{5.8}$$

The moment vector in the conjugate beam loaded with the angle

changes will be equivalent to the displacement vector $\{U\}$. Matrix

$[q_2]$ relates the concentrated angle change (load), i.e., $\{\theta\}$, to the

average slope of the deflection curve (shear in the conjugate beam),

$\{S\}$, in the following equation[95]

$$\{S\} = [q_2] \{\theta\} \tag{5.9}$$

where

$$\{S\} = \begin{Bmatrix} S_1 \\ S_2 \\ \cdot \\ \cdot \\ \cdot \\ S_{m-2} \\ S_{m-1} \end{Bmatrix} \qquad (5.10)$$

and

$$[q_2(m-1, m+1)] = \frac{1}{m} \begin{bmatrix} 0 & m-1 & m-2 & m-3 & . & . & 2 & 1 & 0 \\ 0 & -1 & m-2 & m-3 & . & . & 2 & 1 & 0 \\ 0 & -1 & -2 & m-3 & . & . & 2 & 1 & 0 \\ . & . & . & . & . & . & . & . & . \\ . & . & . & . & . & . & . & . & . \\ 0 & -1 & -2 & . & . & . & -(m-2) & 1 & 0 \\ 0 & -1 & -2 & . & . & . & -(m-2) & -(m-1) & 0 \end{bmatrix}$$

$$(5.11)$$

Matrix $[q_3]$ transforms the average slope (shear) into the deflection

(moment in the conjugate beam) in the following form (Fig. 5.6)

$$\{U\} = [q_3] \{S\} \qquad (5.12)$$
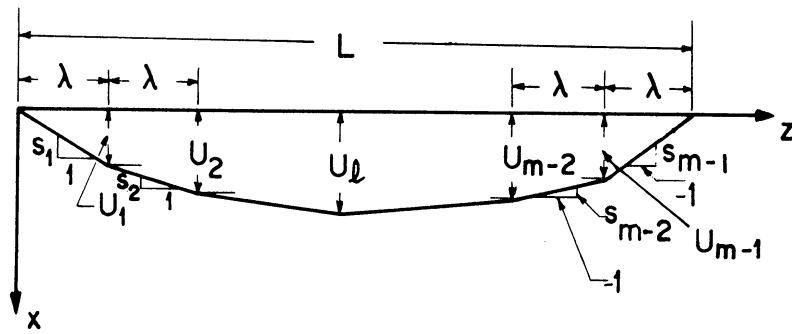
Fig. 5.6. Average Shear and Deflection

where

$$\left[q_3(m+1, m-1)\right] = \frac{L}{m} \begin{bmatrix} 0 & 0 & . & . & . & 0 & 0 \\ 1 & 0 & . & . & . & 0 & 0 \\ 1 & 1 & . & . & . & 0 & 0 \\ . & . & . & . & . & . & . \\ . & . & . & . & . & . & . \\ . & . & . & . & . & . & . \\ 1 & 1 & . & . & . & 1 & 0 \\ 1 & 1 & . & . & . & 1 & 1 \end{bmatrix} \qquad (5.13)$$

Combining (5.6), (5.9) and (5.12) we get

$$\left\{ U \right\} = \left[q_3 \right] \left[q_2 \right] \left[q_1 \right] \left\{ \phi \right\} \qquad (5.14)$$

Matrix $[R]$ can be found by comparing (5.4) and (5.14)

$$[R] = \left[q_3 \right] \left[q_2 \right] \left[q_1 \right] \qquad (5.15)$$

One can find $[R]$ by replacing for $\left[q_1 \right]$, $\left[q_2 \right]$ and $\left[q_3 \right]$ and performing the operation

(5.16)

$$[R] = \frac{L^2}{m^3}$$

$$R_{ij} = 0 \qquad \text{for} \quad i = 0, m$$

$$= \frac{(m - i) L^2}{12m^3} \qquad \begin{array}{l} \text{for} \quad j = 0 \\ \text{(except for } i = 0, m) \end{array}$$

$$= \frac{i L^2}{12m^3} \qquad \begin{array}{l} \text{for} \quad j = m \\ \text{(except for } i = 0, m) \end{array}$$

$$= \frac{[12i(m - i) - m] L^2}{12m^3} \qquad \text{for} \quad i = j$$

$$= \frac{j(m - i) L^2}{m^3} \qquad \text{for} \quad i > j$$

$$= \frac{i(m - j) L^2}{m^3} \qquad \text{for} \quad i < j$$

(5.17)

The above relations show that, except for the boundary elements,

the matrix $[R]$ is a symmetrical matrix

$$R_{ij} = R_{ji}$$

Matrix $[R]$ relates the curvature to the deflection as well as it

relates the increment of the curvature to the increment of the

deflection. This follows from distributive property of the matrices,[96]

as we can write

$$\left\{\phi\right\}_{n+1} = \left\{\phi\right\}_n + \left\{\Delta\phi\right\}_{n+1} \tag{5.18}$$

Using the relation (5.4)

$$\left\{U\right\}_{n+1} = [R]\left\{\phi\right\}_{n+1} = [R]\left\{\phi\right\}_n + [R]\left\{\Delta\phi\right\}_{n+1} = \left\{U\right\}_n + \left\{\Delta U\right\}_{n+1}$$

(5.19)

where

$$\left\{\Delta U\right\}_{n+1} = [R]\left\{\Delta\phi\right\}_{n+1} \tag{5.20}$$

Here, in every cycle of increment the algebraic increments of the curvature and the deflection are considered and related to one another. Because in the general case we shall have to evaluate the deflection in two directions, $\delta_{\ell 1}$ and $\delta_{\ell 2}$ will represent the deflection per unit length of the column at ℓ^{th} nodal point along the column in the x and y directions respectively. $\Delta\delta_{\ell 1}$ and $\Delta\delta_{\ell 2}$ will represent the increments of the above values. Using the matrix $[R]$ we can write

$$\Delta\delta_{\ell q} = \sum_{k=0}^{m} r_{\ell k} \Delta\phi_{kq} \qquad (q=1,2; \ell=0,1,\ldots,m) \qquad (5.21)$$

where $\Delta\phi_{kq}$ is the increment of the curvature of deflection in the qth $(q=1,2)$ direction at the ℓth nodal point along the column, and

$$r_{\ell k} = R_{\ell k}/L \qquad (5.22)$$

Relation (5.15) (or (5.17)) shows that elements of the first and the last rows of the matrix $[R]$ are zero, then

$$\det [R] = 0 \qquad (5.23)$$

and therefore $[R]$ is a singular matrix and its inversion is not possible. This means that in the general case for which the curvatures of the end sections are non-zero, with the ends prevented from deflecting, one cannot obtain the curvature vector $\{-\phi\}$ from the displacement vector $\{U\}$. In the case of concentric loading of the pinned-end column the end section curvatures are zero and therefore the first and the last elements of the deflection and curvature vectors and also the first and the last rows and columns of the matrix $[R]$ can be dropped so as to eliminate the singularity of the matrix $[R]$.

In this incremental procedure the vector $\{\Delta\phi\}$ was assumed, then,

using $[R]$, the increment of the displacement vector, $\{\Delta U\}$, was

evaluated by (5.20) and thus the need for the inversion of $[R]$ was

avoided. The advantage was taken of the matrix properties in the

process of modification of the assumed $\{\Delta\phi\}$ for a better value and

normalization of the $\{\Delta U\}$, i.e., both the modified $\{\Delta\phi\}$ and the

corresponding $\{\Delta U\}$ were multiplied by a scalar value to make the

deflection at the mid-height section equal to the assigned value, as

$$\{\Delta U\} = [R]\{\Delta\phi\}$$

$$a\{\Delta U\} = a[R]\{\Delta\phi\} \qquad (5.24)$$

$$\{a\Delta U\} = [R]\{a\Delta\phi\}$$

where a is a scalar factor. Part of the incremental analysis is

devoted to the assumption of a sinusoidal curve for the deflected

shape of the column. In this case we can write

$$U(z) = U_o \, \text{Sin} \, \frac{\pi z}{L} \qquad (5.25)$$

where U_o is the mid-height deflection, then

$$[-\phi(z)] = U(z) = -\frac{\pi^2}{L^2} U_o$$

and $\qquad\qquad\qquad\qquad\qquad\qquad\qquad\qquad\qquad\qquad (5.26)$

$$U_{z=\frac{L}{2}} = \frac{L^2}{\pi^2} \phi_{z=\frac{L}{2}}$$

Thus the matrix $[R]$ will have only one element, i.e.,

$$[R] = [\frac{L^2}{\pi^2}] \qquad (5.27)$$

iii. Equilibrium at the Nodal Points along the Column

In order to evaluate the values of the integrals in equations

(3.24) or (3.27) for planar bending, the distribution of stress over

the area of the cross section must be known. In general, the stress

cannot be expressed in the form of a single function in terms of ξ and

η. Thus, the integration cannot be carried out algebraically. Numer-

ical evaluation of the integrals required the division of the area of the

cross section into a grid network (Fig. 5.7). Then the values of the

integrant at the centroid

of every mesh and

thereby the values

of the integral over

its area were deter-

mined and summed

over the cross

sectional area.

Two different variable

names were chosen

to express the coor-

dinates of the mesh

centroids to differen-

tiate between a mesh

of the flange and of

the web.
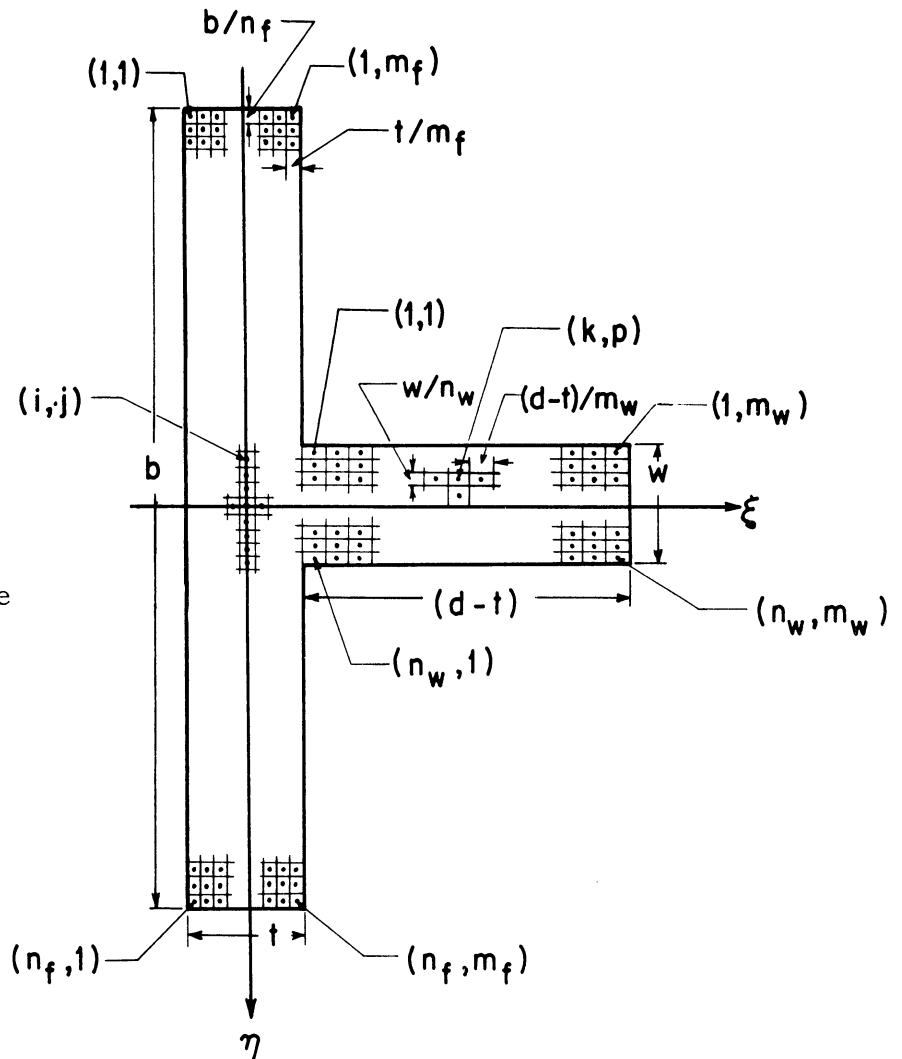
Fig. 5.7. Cross Section Divided into Grid Networks

Coordinates of the point (i, j) of the flange are

$$\xi_f = \xi_{fj} = -\frac{t}{2} + (j - \frac{1}{2})\frac{t}{m_f}$$

$$\eta_f = \eta_{fi} = -\frac{b}{2} + (i - \frac{1}{2})\frac{b}{n_f}$$

(5.28)

Coordinates of the point (k, p) of the web are

$$\xi_w = \xi_{wp} = \frac{t}{2} + (p - \frac{1}{2})(\frac{d - t}{m_w})$$

$$\eta_w = \eta_{wk} = -\frac{w}{2} + (k - \frac{1}{2})\frac{w}{n_w}$$

(5.29)

Now the integrals of the equations (3.24) at the ℓth nodal point along

the column can be written in a summation form

$$\int_A \sigma(\xi, \eta)\, dA = \sum_{i=1}^{n_f} \sum_{j=1}^{m_f} \sigma_{f\ell ij}\, \Delta A_{fij} + \sum_{k=1}^{n_w} \sum_{p=1}^{m_w} \sigma_{w\ell kp}$$

$$\int_A \sigma(\xi, \eta)\, \eta\, dA = \sum_{i=1}^{n_f} \sum_{j=1}^{m_f} \sigma_{f\ell ij}\, \eta_{fi}\, \Delta A_{fij} + \sum_{k=1}^{n_w} \sum_{p=1}^{m_w} \sigma_{w\ell kp}\, \eta_{wk}\, \Delta A_{wkp}$$

$$\int_A \sigma(\xi, \eta)\, \xi\, dA = \sum_{i=1}^{n_f} \sum_{j=1}^{m_f} \sigma_{f\ell ij}\, \xi_{fj}\, \Delta A_{fij} + \sum_{k=1}^{n_w} \sum_{p=1}^{m_w} \sigma_{w\ell kp}\, \xi_{wp}\, \Delta A_{wkp}$$

(5.30)

$$\int_A \sigma(\xi, \eta)\, \rho^2\, dA = \sum_{i=1}^{n_f} \sum_{j=1}^{m_f} \sigma_{f\ell ij}\, (\xi_{fj}^2 + \eta_{fi}^2)\, \Delta A_{fij} +$$

$$\sum_{k=1}^{n_w} \sum_{p=1}^{m_w} \sigma_{w\ell kp}\, (\xi_{wp}^2 + \eta_{wk}^2)\, \Delta A_{wkp}$$

where

$$\Delta A_{fij} = \frac{bt}{n_f m_f} = \Delta A_f$$

$$(5.31)$$

$$\Delta A_{wkp} = \frac{(d-t)w}{n_w m_w} = \Delta A_w$$

The area of the mesh is constant for the flange or for the web.

Therefore, ΔA_{fij} and ΔA_{wkp} can be factored out of the summation.

Using the above relations for ℓ^{th} nodal point along the column the

equilibrium conditions (3.24) can be written in the following form

$$P_\ell - \left[\Delta A_f \sum_{i=1}^{n_f} \sum_{j=1}^{m_f} \sigma_{f\ell ij} + \Delta A_w \sum_{k=1}^{n_w} \sum_{p=1}^{m_w} \sigma_{w\ell kp} \right] = 0 \qquad (5.31a)$$

$$P_\ell L \left\{ \left[(\delta_{\ell 2} + \delta_{o\ell 2}) - e_{t2} \left[1 + (r_{e2} - 1) \frac{\ell}{m} \right] \right] + \right.$$

$$\left. \beta_\ell \left[(\frac{\overline{x}}{L} - \delta_{\ell 1} - \delta_{o\ell 1}) + e_{t1} \left[1 + (r_{e1} - 1) \frac{\ell}{m} \right] \right] \right\}$$

$$+ \Delta A_f \sum_{i=1}^{n_f} \sum_{j=1}^{m_f} \sigma_{f\ell ij} \, \eta_{fi} + \Delta A_w \sum_{k=1}^{n_w} \sum_{p=1}^{m_w} \sigma_{w\ell kp} \, \eta_{wk} = 0$$

$$(5.31b)$$

$$P_\ell L \left\{ \beta_\ell \left[(\delta_{\ell 2} + \delta_{o\ell 2}) - e_{t2} \left[1 + (r_{e2} - 1) \frac{\ell}{m} \right] \right] - \right.$$

$$\left. \left[(\frac{\overline{x}}{L} - \delta_{\ell 1} - \delta_{o\ell 1}) + e_{t1} \left[1 + (r_{e1} - 1) \frac{\ell}{m} \right] \right] \right\}$$

$$+ \Delta A_f \sum_{i=1}^{n_f} \sum_{j=1}^{m_f} \sigma_{f\ell ij} \, \xi_{fj} + \Delta A_w \sum_{k=1}^{n_w} \sum_{p=1}^{m_w} \sigma_{w\ell kp} \, \xi_{wp} = 0$$

$$(5.31c)$$

$$P_\ell L^2 \left\{ \left[(\delta_{\ell 2} + \delta_{o\ell 2}) - e_{t2}\left[1 + (r_{e2} - 1)\frac{\ell}{m}\right] \right] (\delta'_{\ell 1} + \delta'_{o\ell 1}) \right.$$

$$\left. + \left[(\frac{\bar{x}}{L} - \delta_{\ell 1} - \delta_{o\ell 1}) + e_{t1}\left[1 + (r_{e1} - 1)\frac{\ell}{m}\right] \right] (\delta'_{\ell 2} + \delta'_{o\ell 2}) \right\}$$

$$+ \beta'_\ell \left[\Delta A_f \sum_{i=1}^{n_f} \sum_{j=1}^{m_f} \sigma_{f\ell ij} \rho_{fij}^2 + \Delta A_w \sum_{k=1}^{n_w} \sum_{p=1}^{m_w} \sigma_{w\ell kp} \rho_{wkp}^2 \right.$$

$$- \left\{ \frac{\frac{1}{3}bt^3 - 0.21t^4}{n_f m_f} \sum_{i=1}^{n_f} \sum_{j=1}^{m_f} G_{s_{f\ell ij}} \right.$$

$$+ \frac{\frac{1}{3}(d-t)^3 - 0.105w^4}{n_w m_w} \sum_{k=1}^{n_w} \sum_{p=1}^{m_w} G_{s_{w\ell kp}} + \frac{\alpha_1 D_1^4}{n_f m_f + n_w m_w}$$

$$\left. \left. \left\{ \sum_{i=1}^{n_f} \sum_{j=1}^{m_f} G_{s_{f\ell ij}} + \sum_{k=1}^{n_w} \sum_{p=1}^{m_w} G_{s_{w\ell kp}} \right\} \right\} \right] = 0 \qquad (5.32d)$$

where

$$\rho_{fij}^2 = \xi_{fij}^2 + \eta_{fij}^2$$

$$\rho_{wkp}^2 = \xi_{wkp}^2 + \eta_{wkp}^2$$

$$(5.33)$$

The last term, in brackets, of the equation (5.32d) is the torsional stiffness of cross section of the column at the ℓth nodal point evaluated according to the equation (4.83).

iv. Evaluation of the Stress at the Centroid of the Mesh

Stress is given as a function of strain; therefore, the strain at the centroid of the mesh should be known so that the stress at that

point could be evaluated. Having made the assumption that the plane sections remain plane, in order to express the strain across any cross section along the column, it is necessary to know the strain at one point of the cross section, i.e., at the origin of the $\xi\eta\zeta$ axes, and the curvature of the deflected shape of the column in two non-parallel longitudinal planes at the same cross section. In general, in order to express the orientation of the strain distribution plane relative to the unstrained position, it is required to know the strain at three points which are not on a straight line. Let $\epsilon_{o\ell}$ be the strain at the centroid of the flange at the ℓth cross section. Strain ϵ at point (ξ, η) of this cross section will be

$$\epsilon_{\ell}(\xi, \eta) = \epsilon_{o\ell} - (\phi_{\ell 1} + \beta_{\ell}\phi_{\ell 2})\xi - (-\beta_{\ell}\phi_{\ell 1} + \phi_{\ell 2})\eta \qquad (5.34)$$

For the mesh of the flange and the web

$$\epsilon_{f\ell ij} = \epsilon_{o\ell} - (\phi_{\ell 1} + \beta_{\ell}\phi_{\ell 2})\xi_{fj} - (-\beta_{\ell}\phi_{\ell 1} + \phi_{\ell 2})\eta_{\ell i}$$

$$\epsilon_{w\ell kp} = \epsilon_{o\ell} - (\phi_{\ell 1} + \beta_{\ell}\phi_{\ell 2})\xi_{wp} - (-\beta_{\ell}\phi_{\ell 1} + \phi_{\ell 2})\eta_{\ell k} \qquad (5.35)$$

where $(-\phi_{\ell 1})$ and $(-\phi_{\ell 2})$ are the curvature of the deflected column in the xz and yz planes at the ℓth section, respectively. The strain at the origin is expressed in the following form

$$\epsilon_{o\ell} = \phi_{\ell 1} C_{\ell 1} = \phi_{\ell 2} C_{\ell 2} \qquad (\ell = 1, 2, \ldots, m) \qquad (5.36)$$

The magnitude of $C_{\ell q}$ is the same as the corresponding curvature of the deflected shape. Figure 5.8 gives the strain distribution at the ℓth cross section along the column and at the two consecutive incremental steps, n and (n + 1).
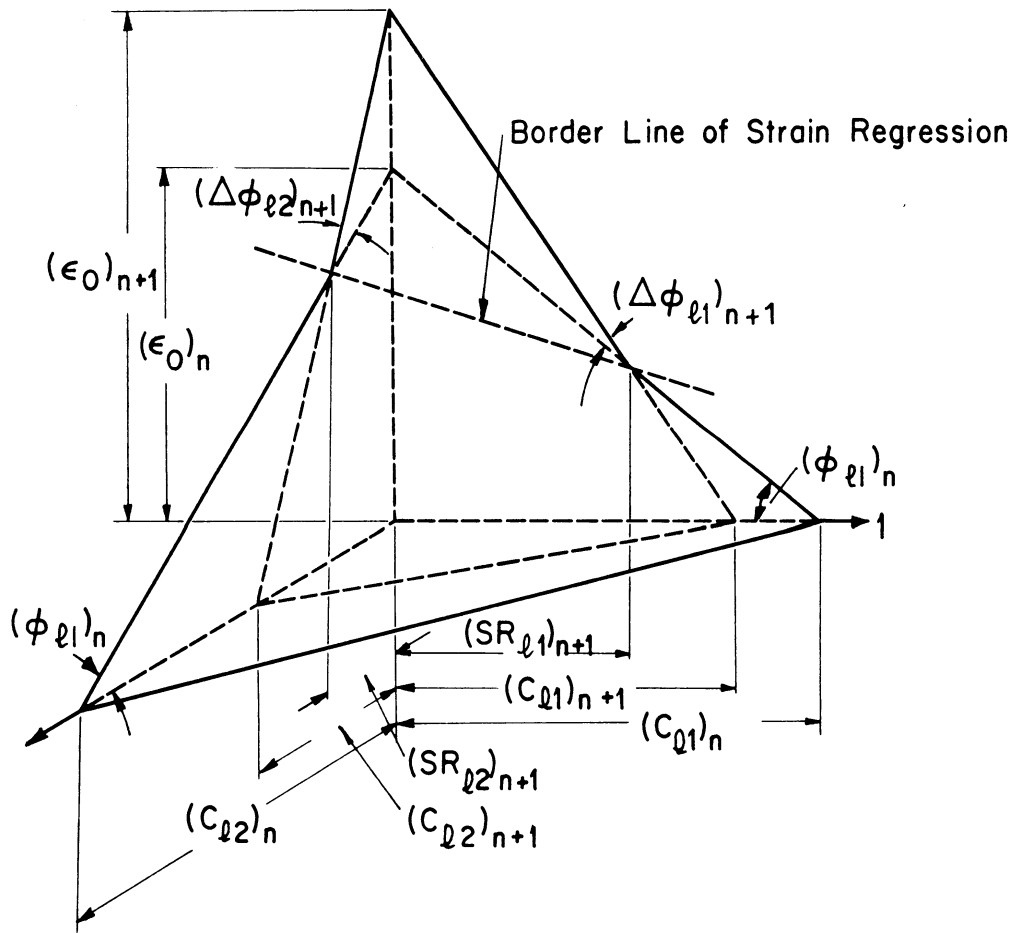
Fig. 5.8. Strain Distribution at the ℓth Cross Section

The depth of strain regression SR at the $(n + 1)^{th}$ incremental step, ℓ^{th} section and on the qth axis will be

$$[SR_{\ell q}]_{n+1} = \frac{[\phi_{\ell q} C_{\ell q}]_{n+1} - [\phi_{\ell q} C_{\ell q}]_n}{[\Delta \phi_{\ell q}]_{n+1}} \qquad (q=1, 2; \ell=1, 2, \ldots, m)$$

$$(5.37)$$

Stress at the Strain Regression Region

Having evaluated the strain at the centroid of the mesh, if strain regression has occurred, i.e.,

$$(\epsilon_{\ell ij})_{n+1} < (\epsilon_{\ell ij})_n \qquad (5.38)$$

then the stress will be

$$(\sigma_{\ell ij})_{n+1} = (\sigma_{\ell ij})_{max} - E\left[(\epsilon_{\ell ij})_{max} - (\epsilon_{\ell ij})_{n+1}\right] \qquad (5.39)$$

where $(\epsilon_{\ell ij})_{max}$ and $(\sigma_{\ell ij})_{max}$

are the maximum strain

recorded at the mesh (ℓij).

If strain reversal is present

(the fiber is in tension)

(Fig. 5.9), the stress will

correspond to the effective

strain (ϵ_{eff}), in the stress-

strain diagram, where
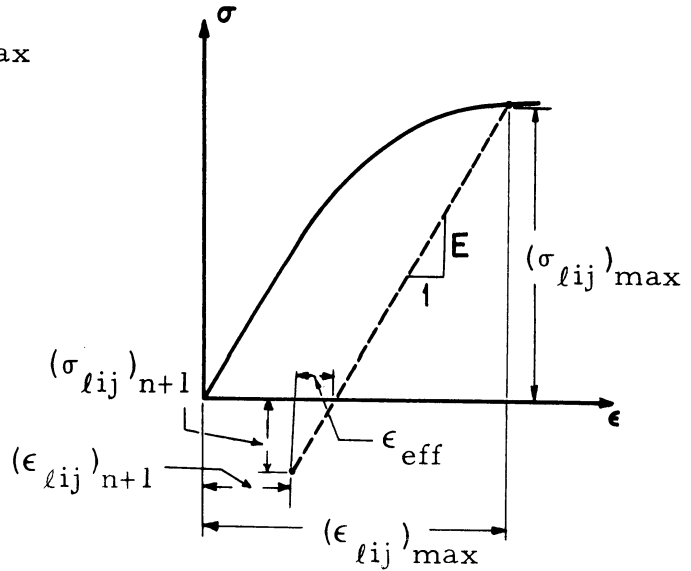
Fig. 5.9. Strain Regression - Stress Reversal

$$(\epsilon_{eff}) = (\epsilon_{\ell ij})_{n+1} - \left[(\epsilon_{\ell ij})_{max} - \frac{(\sigma_{\ell ij})_{max}}{E}\right] \qquad (5.40)$$

v. Planar Bending

In the stage where the biplanar bending accompanied with

torsion has not yet commenced, one should take advantage of the

simplifications which can be made in the preceding relations. In

planar bending (bending in the plane of symmetry)

$$\phi_{\ell 2} = \Delta\phi_{\ell 2} = U_{\ell 2} = \Delta U_{\ell 2} = \beta_\ell = 0 \qquad (\ell=1, 2, \ldots, m)$$

then

$$\epsilon_{f\ell 1j} = \epsilon_{f\ell 2j} = \cdots = \epsilon_{f\ell n_f j} \quad \text{and} \quad \epsilon_{w\ell 1p} = \epsilon_{w\ell 2p} = \cdots = \epsilon_{w\ell n_w p}$$

and   (5.41)

$$\sigma_{f\ell 1j} = \sigma_{f\ell 2j} = \cdots = \sigma_{f\ell n_f j} \quad \text{and} \quad \sigma_{w\ell 1p} = \sigma_{w\ell 2p} = \cdots = \sigma_{w\ell n_w p}$$

The equilibrium equations will reduce to

$$P_\ell - n_f \Delta A_f \sum_{j=1}^{m_f} \sigma_{f\ell 1j} + n_w \Delta A_w \sum_{p=1}^{m_w} \sigma_{w\ell 1p} = 0 \qquad (5.42a)$$

$$-P_\ell L \left(\frac{\overline{x}}{L} - \delta_{\ell 1} - \delta_{o\ell 1} \right) + e_{t1} \left[1 + (r_{e1} - 1) \frac{\ell}{m} \right]$$

$$+ n_f \Delta A_f \sum_{j=1}^{m_f} \sigma_{f\ell 1j} \, \xi_{fj} + n_w \Delta A_w \sum_{p=1}^{m_w} \sigma_{w\ell 1p} \, \xi_{wp} = 0 \qquad (5.42b)$$

and the strain at the centroid of the mesh will be

$$\epsilon_{f\ell ij} = \epsilon_{o\ell} - \phi_{\ell 1} \, \xi_{fj} \qquad (i=1, 2, \ldots, n_f)$$

(5.43)

$$\epsilon_{w\ell kp} = \epsilon_{o\ell} - \phi_{\ell 1} \, \xi_{wp} \qquad (k=1, 2, \ldots, n_w)$$

For the evaluation of the limiting point of the planar bending

equation (3.35) can be written in the following form

$$\overline{\xi}_\ell = \frac{n_f \Delta A_f \displaystyle\sum_{j=1}^{m_f} E_{t_{f\ell j}} \xi_{fj} + n_w \Delta A_w \displaystyle\sum_{p=1}^{m_w} E_{t_{w\ell p}} \xi_{wp}}{n_f \Delta A_f \displaystyle\sum_{j=1}^{m_f} E_{t_{f\ell j}} + n_w \Delta A_w \displaystyle\sum_{p=1}^{m_w} E_{t_{w\ell p}}} \qquad (5.44)$$

where

$$E_{t_{f\ell j}} = \text{the tangent modulus at the point } \xi_{ij} \text{ of the flange}$$
$$\text{at the } \ell^{th} \text{ section of the column}$$

$$E_{t_{w\ell p}} = \text{the tangent modulus at the point } \xi_{wp} \text{ of the web}$$
$$\text{at the } \ell^{th} \text{ section of the column}$$

The ratio of the stiffness α at the ℓth cross section of the column will be

$$\alpha_\ell = \frac{\dfrac{b^3 t}{3m_f} \displaystyle\sum_{j=1}^{m_f} E_{t_{f\ell j}} + \dfrac{w^3(d-t)}{3m_w} \displaystyle\sum_{p=1}^{m_w} E_{t_{w\ell p}}}{\dfrac{bt}{mf} \displaystyle\sum_{j=1}^{m_f} (\xi_{fj} - \overline{\xi}_\ell)^2 E_{t_{f\ell j}} + \dfrac{w(d-t)}{m_w} \displaystyle\sum_{p=1}^{m_w} (\xi_{wp} - \overline{\xi}_\ell)^2 E_{t_{w\ell p}}}$$

$$(5.45)$$

5.4. TECHNIQUE OF THE INCREMENTAL ANALYSIS

The technique of the incremental analysis may be summarized as follows:

Given:

    i.   the dimensions of the cross section b, d, t, w

    ii. the length of the column, L, or the slenderness ratio,

        $\dfrac{L}{r}$

    iii. the number of divisions of the grid, n_f, m_f, n_w, m_w

    iv. the number of the segments the column is to be divided

        into, m

    v.   the increment of the deflection Δx (at $z = \dfrac{L}{2}$, positive

        or negative)

vi. initial crookedness δ_{ix}, δ_{iy}; eccentricity of loading,

e_x, e_y (per unit length)

vii. relation between strain and stress, strain and tangent

modulus, and strain and secant shear modulus

viii. acceptable error in the evaluation of the axial load in

the longitudinal sections, satisfying the moment

equilibrium equations and the calculation of the twist

at the longitudinal sections.

Desired:

Equilibrium position after each increment of the

deflection together with all the related characteristics

such as deflection and curvature in the x and y directions,

twist along the column, axial load, moment about the

x- and y-axes, stress distribution across the column

and at the longitudinal nodal points, and the border line

of strain regression.

The following are some important points to be noted in the

process of convergence to an equilibrium position after each incre-

ment:

i. The estimated change of curvature vector in the nth

increment $\left(-\Delta\phi\right)_n$ was revised for a better estimate

according to the following relation

$$\left[(\Delta\phi_\ell)_n\right]_{(c+\frac{1}{2})} = (\Delta\phi_\ell)_n \ \frac{(\Delta P_{avg})_n + Q}{(\Delta P_\ell)_n + Q} \tag{5.46}$$

where c = the number of the cycle of iteration

$$(\Delta P_\ell)_n = (P_\ell)_n - (P_{avg})_{n-1}$$

$$(\Delta P_{avg})_n = (P_{avg})_n - (P_{avg})_{n-1} \qquad (5.47)$$

$$(P_{avg})_n = \frac{1}{m+1} \sum_{\ell=0}^{m} (P_\ell)_n$$

Having revised $[\{\Delta\phi\}_n]_c$ to $[\{\Delta\phi\}_n]_{c+\frac{1}{2}}$, using

matrix $[R]$ corresponding increment of deflection

$[\{\Delta U\}_n]_{c+\frac{1}{2}}$ can be obtained. Normalization of the

curvature and the deflection vectors may be done

according to (5.24),

$$[\{\Delta\phi\}_n]_{c+1} = a [\{\Delta\phi\}_n]_{c+\frac{1}{2}}$$

$$\qquad (5.48)$$

$$[\{\Delta U\}_n]_{c+1} = a [\{\Delta U\}_n]_{c+\frac{1}{2}}$$

where

$$a = \frac{(\Delta_x)_{inc}}{[(\Delta U(\frac{m}{2}))_n]_{c+\frac{1}{2}}} \qquad (5.49)$$

and $(\Delta_x)_{inc}$ = mid-length deflection increment

The term Q in the equation (5.46) is used to optimize

the convergence rate.[16] The value of Q should be

chosen such that the numerator and the denominator of

the fraction in the equation (5.46) would always be

positive. In the unloading stage where (ΔP_{avg})

and (or) (ΔP_ℓ) are negative, the fraction may become
negative and consequently the revised values in the
cycles of iteration will oscillate between a negative
and a positive value without achieving convergence.
For the same reason Q was assumed to be the sum
of two values

$$Q = Q_1 + Q_2 \tag{5.50}$$

where

Q_1 = largest value of $\left\{ \Delta P \right\}$

Q_2 = a positive value which should be

reduced if the convergence rate is

slow and visa versa

In the loading stage where (ΔP_{avg}) is positive if the
magnitude of (ΔP_ℓ) is smaller than the (ΔP_{avg})
a greater curvature change and otherwise a smaller
curvature change should be assumed. In the unloading
stage where (ΔP_{avg}) is negative, the curvature
revision scheme should be inverse of the above
procedure. The fraction in the equation (5.37) follows
the above scheme.

ii. The change of curvature vector $\left\{ -\Delta\phi \right\}$ should be
controlled such that if its magnitude becomes smaller
than a specific value the direction (sign) of that value
will be changed. This will prevent the underflow of
the values of the change of curvature vector $\left\{ -\Delta\phi \right\}$.

The change of direction of the increment of the curvature occurs in the unloading stage and at the sections close to the end of the column in the case of eccentric loading.

The steps followed to obtain the desired results are summarized in the computer program flow chart in Appendix A.

5.5. RESULTS

The cross sectional dimensions of the tee columns which were analyzed incrementally by means of the 7090 digital computer are as follows (Fig. 5.7)

$$b = 4. \text{ inch}$$

$$t = .279 \text{ inch}$$

$$w = .218 \text{ inch}$$

$$d = 1.5, 2.5, 3. \text{ inch}$$

(5.51)

Other section properties were

	d = 1.5 inch	d = 2.5 inch	d = 3. inch	
Area, $inch^2$	1.382	1.600	1.709	
I_x, $inch^4$	1.489	1.490	1.490	
I_y, $inch^4$	.161	.734	1.245	
r_x, inch	1.038	.965	.934	(5.52)
r_y, inch	.342	.677	.853	
$\alpha = \dfrac{I_x}{I_y}$	9.248	2.030	1.197	
$\bar{d}$, inch	.283	.518	.660	

Load-deflection history of columns of various combinations of slender-

ness ratio, initial crookedness, eccentrically or concentrically loaded

(Fig. 5.10) (with three different stress-strain relations) was deter-

mined. Combinations which were studied are summarized in Table 5.1.
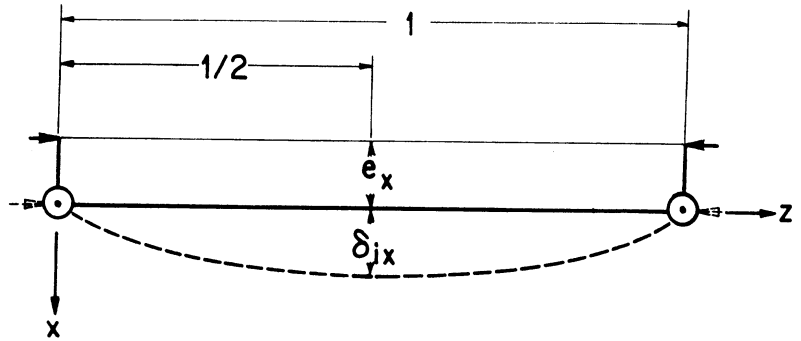
Fig. 5.10. Eccentric Loading-Initial Crookedness

Table 5. 1

Combinations Analyzed Incrementally

by Digital Computer

Stress-Strain Relations	d	KL/r	Initial Crookedness*	Eccentric Loading**
#1	1. 5"	10 20 30 40 50 60 80 100 120 160 200	*	**
	2. 5" and 3. "	30 40	*	—
#2 and #3	1. 5"	40	*	—

*concentric loading - initial crookedness assumed to be a half-sine

curve (equation 3. 6); δ_{iy} = 0, δ_{ix} = ($\pm$0. 0, $\pm$0. 0001, $\pm$0. 0005,

$\pm$0. 001, $\pm$0. 002, $\pm$0. 004).

**no initial crookedness - e_{tx} = e_x, r_{ex} = 1, e_{ty} = 0 (equation 3. 4,

Fig. 5. 10), e_x = ($\pm$0. 001, $\pm$0. 002).

In the following pages the summary of the results of the incremental analysis will be shown graphically and tabulated. Some selected graphs of the load-deflection history will also be presented. For all the graphs the stress-strain relation used is #1 and $d = 1.5''$ unless otherwise is indicated.

The lines indicated by (i. b. g.) in the graphs are the tangent lines to the dimensionless load-deflection curves, i. e.,

$$(\text{i. b. g.}) = \lim_{\Delta\delta \to 0} \left| \frac{\Delta P/P_t}{\Delta\delta/L} \right| = \frac{L}{P_t} \lim_{\Delta\delta \to 0} \left| \frac{\Delta P}{\Delta\delta} \right|$$

$$= (\text{I. B. G.})\left(\frac{L}{P_t}\right) \tag{5.53}$$
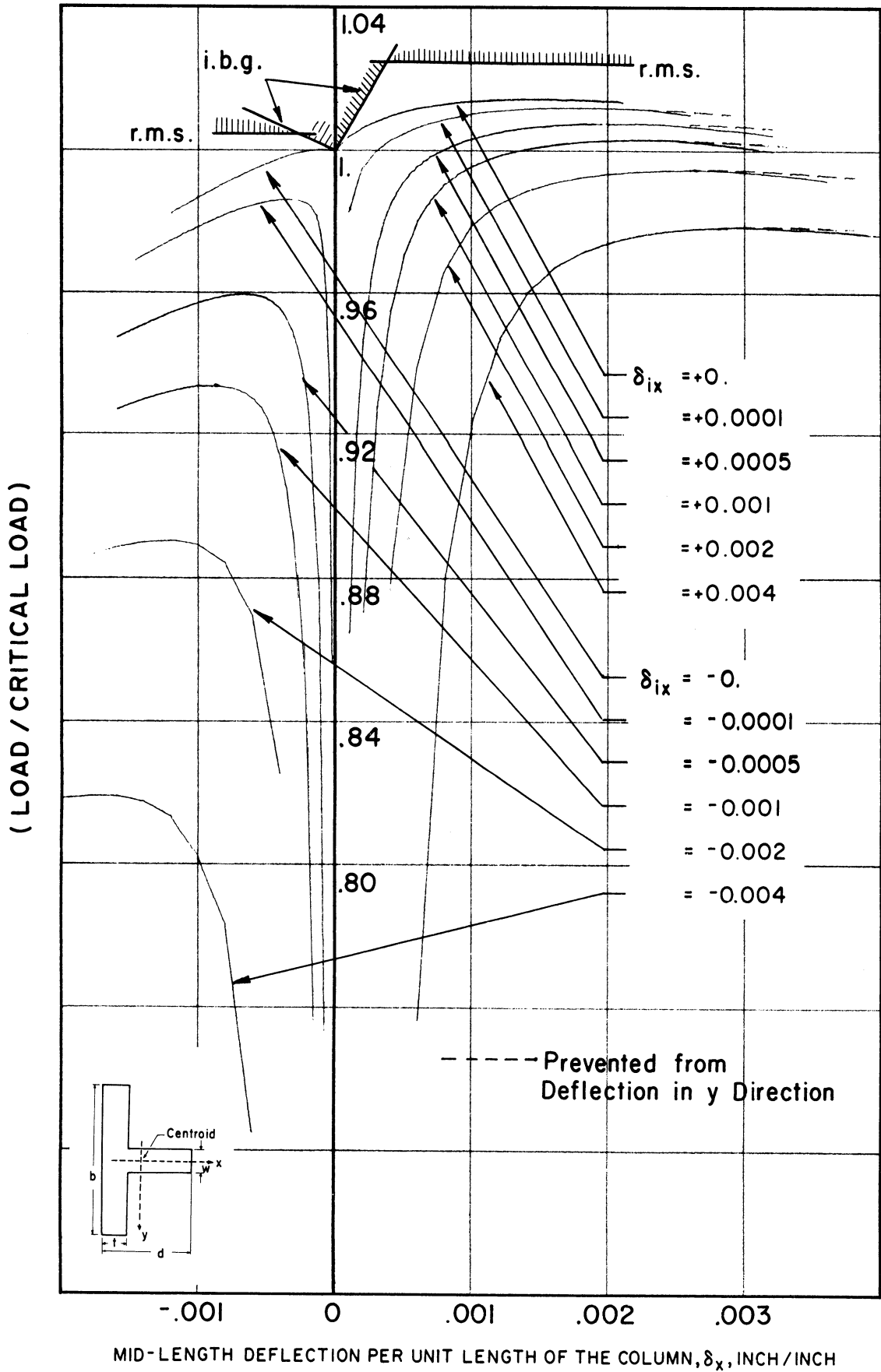
Fig. 5.11. Dimensionless Load vs. Mid-length Deflection
(initial crookedness; L/r = 20)

MID-LENGTH DEFLECTION PER UNIT LENGTH OF THE COLUMN,δ_x,INCH/INCH
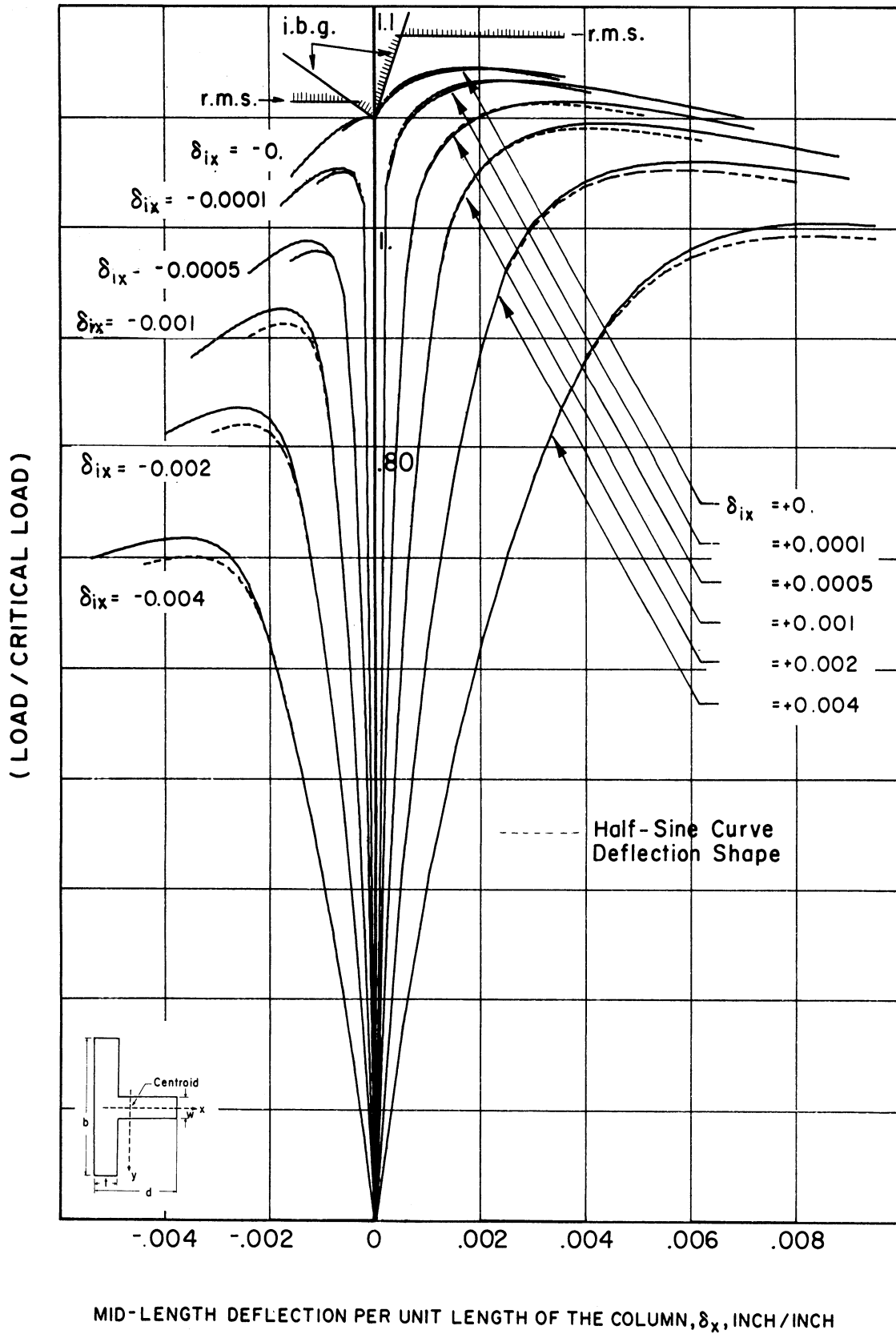
Fig. 5.19. Dimensionless Load vs. Mid-length Deflection (initial crookedness; d = 1.5''; L/r = 40; stress-strain relation #3; half-sine curve deflection-shape comparison)
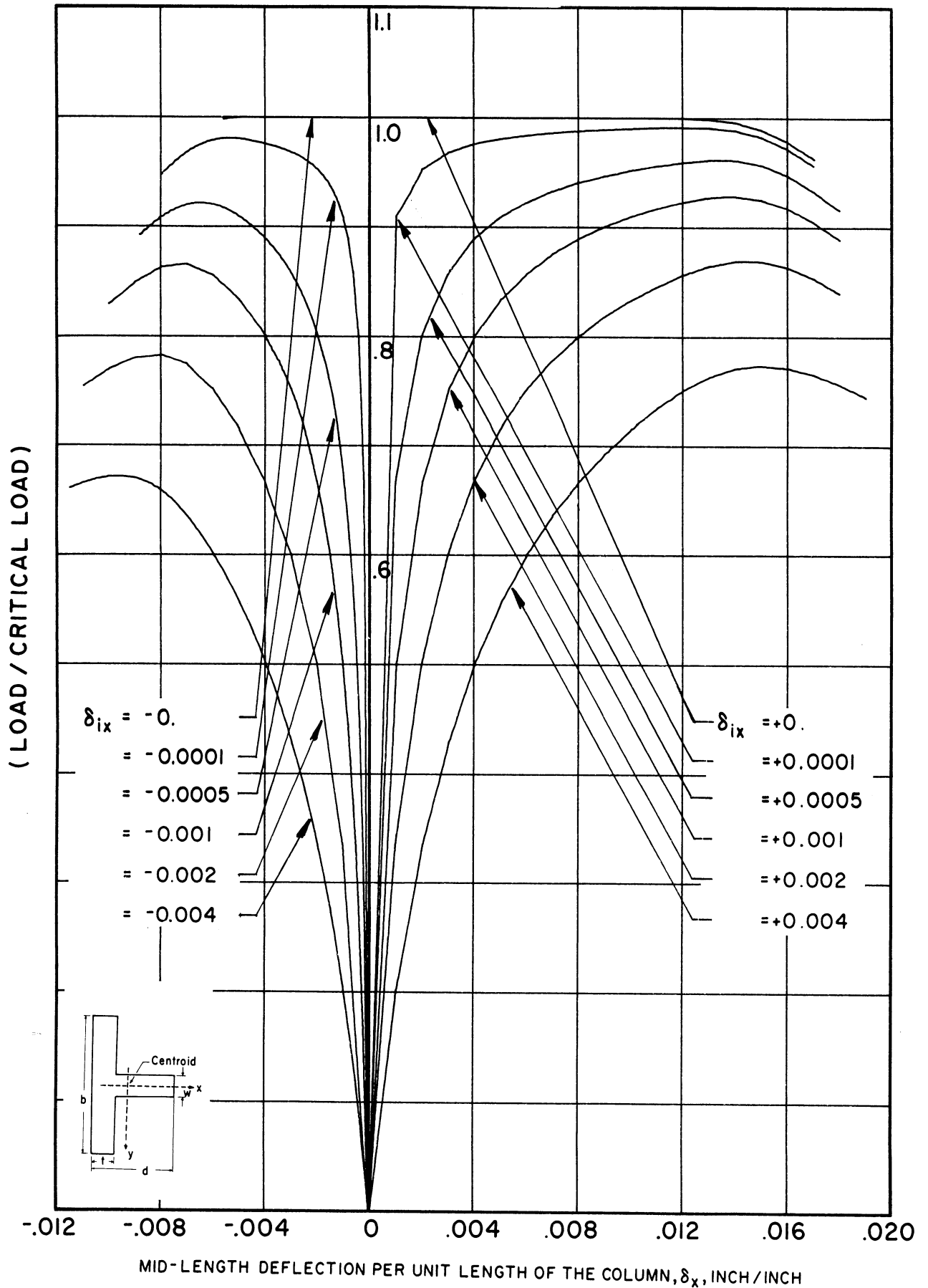
Fig. 5.13. Dimensionless Load vs. Mid-length Deflection
(initial crookedness; L/r = 80)
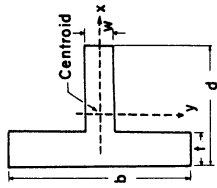
Table 5.2

Ultimate Average Stress

Buckling towards or away from the flange

(initial crookedness; d = 1.5"; stress-strain relation #1)

	Buckling to the Left										Buckling to the Right								
	Initial Crookedness, δ_{ix}						False Reduced Modulus Stress, $(\sigma_r)_f$	Reduced Modulus Stress, σ_r	I.B.G. $(\frac{L}{A})$	Critical Stress, σ_c	I.B.G. $(\frac{L}{A})$	Reduced Modulus Stress, σ_r	False Reduced Modulus Stress, $(\sigma_r)_f$	Initial Crookedness, δ_{ix}					
KL/r	-.0040	-.0020	-.0010	-.0005	-.0001	-.0000								+.0000	+.0001	+.0005	+.0010	+.0020	+.0040
10	40.914	42.409	43.233	43.678	44.128	44.422	64.327	44.560	367.10	44.403	1577.50	45.020	283.469	44.766	44.722	44.626	44.578	44.398	44.085
20	35.762	38.870	40.748	41.864	43.036	43.661	56.152	43.800	721.60	43.645	3101.10	44.650	150.123	44.270	44.170	43.975	43.776	43.414	42.705
30	30.305	35.690	37.548	39.278	41.272	42.510	49.764	42.870	1053.40	42.472	4526.70	44.120	89.162	43.530	43.306	42.911	42.524	41.796	40.420
40	24.883	29.623	33.290	35.754	38.438	40.290	43.551	40.720	1330.80	40.247	5719.10	43.300	57.640	42.046	41.615	40.884	40.089	38.695	36.408
50	20.020	24.158	27.668	30.449	34.460	37.120	37.742	37.290	1534.40	37.120	6593.60	38.680	39.912	37.952	37.175	35.560	34.246	32.360	29.095
60	16.055	19.237	21.910	23.966	26.764	28.112	28.112	28.112	0000.00	28.112	0000.00	28.112	28.112	28.112	27.759	26.802	25.806	24.037	21.082
80	10.597	12.380	13.690	14.558	15.501	15.813	15.813	15.813	0000.00	15.813	0000.00	15.813	15.813	15.813	15.680	15.210	14.690	13.740	12.223
100	7.409	8.433	9.134	9.567	9.993	10.120	10.120	10.120	0000.00	10.120	0000.00	10.120	10.120	10.120	10.045	9.775	9.468	8.933	8.048
120	5.429	6.068	6.473	6.730	6.958	7.028	7.028	7.028	0000.00	7.028	0000.00	7.028	7.028	7.028	6.981	6.810	6.622	6.285	5.721
160	3.255	3.548	3.719	3.831	3.926	3.953	3.953	3.953	0000.00	3.953	0000.00	3.953	3.953	3.953	3.931	3.854	3.762	3.602	3.341
200	2.163	2.322	2.411	2.468	2.517	2.530	2.530	2.530	0000.00	2.530	0000.00	2.530	2.530	2.530	2.517	2.477	2.429	2.339	2.192

Table 5.3

(Ultimate Load/Critical Load)

Buckling towards or away from the flange

(initial crookedness; d = 1.5"; stress-strain relation #1)

	Buckling to the Left									Buckling to the Right								
	Initial Crookedness, δ_{ix}						False Reduced Modulus Load/P_c	Reduced Modulus Load/P_c	I.B.G. $\left(\frac{L}{d}\right)\left(\frac{P_t}{}\right)$	I.B.G. $\left(\frac{L}{d}\right)\left(\frac{P_t}{}\right)$	Reduced Modulus Load/P_c	False Reduced Modulus Load/P_c	Initial Crookedness, δ_{ix}					
KL/r	-.0040	-.0020	-.0010	-.0005	-.0001	-.0000							+.0000	+.0001	+.0005	+.0010	+.0020	+.0040
10	.921	.955	.974	.984	.994	1.000	1.449	1.004	8.267	35.526	1.014	6.384	1.008	1.007	1.005	1.004	1.000	.993
20	.819	.891	.934	.959	.986	1.000	1.287	1.004	16.534	71.052	1.023	3.440	1.014	1.012	1.008	1.003	.995	.978
30	.714	.817	.884	.925	.972	1.001	1.172	1.009	24.801	106.580	1.039	2.099	1.025	1.020	1.010	1.001	.984	.952
40	.618	.736	.827	.888	.955	1.001	1.082	1.012	33.066	142.099	1.076	1.432	1.045	1.034	1.016	.996	.961	.905
50	.539	.651	.745	.820	.928	1.000	1.017	1.005	41.335	177.630	1.042	1.075	1.022	1.001	.958	.923	.872	.784
60	.571	.684	.779	.853	.952	1.000	1.000	1.000	00.000	000.000	1.000	1.000	1.000	.987	.953	.918	.855	.750
80	.670	.783	.866	.921	.980	1.000	1.000	1.000	00.000	000.000	1.000	1.000	1.000	.992	.962	.929	.869	.773
100	.732	.833	.903	.945	.987	1.000	1.000	1.000	00.000	000.000	1.000	1.000	1.000	.993	.966	.936	.883	.795
120	.772	.863	.921	.958	.990	1.000	1.000	1.000	00.000	000.000	1.000	1.000	1.000	.993	.969	.942	.894	.814
160	.823	.898	.941	.969	.993	1.000	1.000	1.000	00.000	000.000	1.000	1.000	1.000	.994	.975	.952	.911	.845
200	.855	.918	.953	.975	.995	1.000	1.000	1.000	00.000	000.000	1.000	1.000	1.000	.995	.979	.960	.925	.866

MID-LENGTH DEFLECTION AND TWIST PER UNIT LENGTH; δ_x, δ_y INCH/INCH; β/L RAD/INCH

Fig. 5.14. Dimensionless Load vs. Mid-length Deflections and Twist
(initial crookedness; d = 2.5"; L/r = 30)

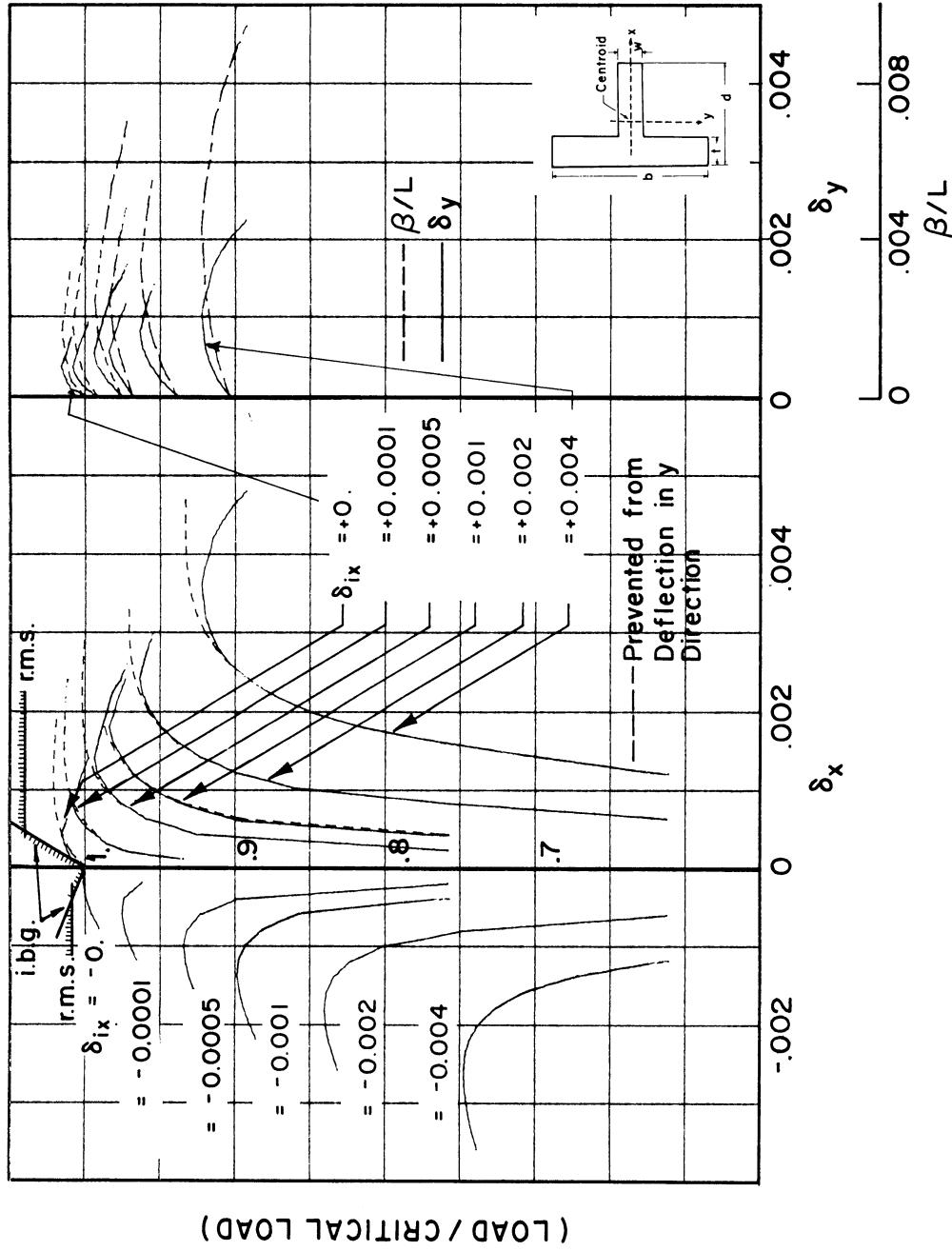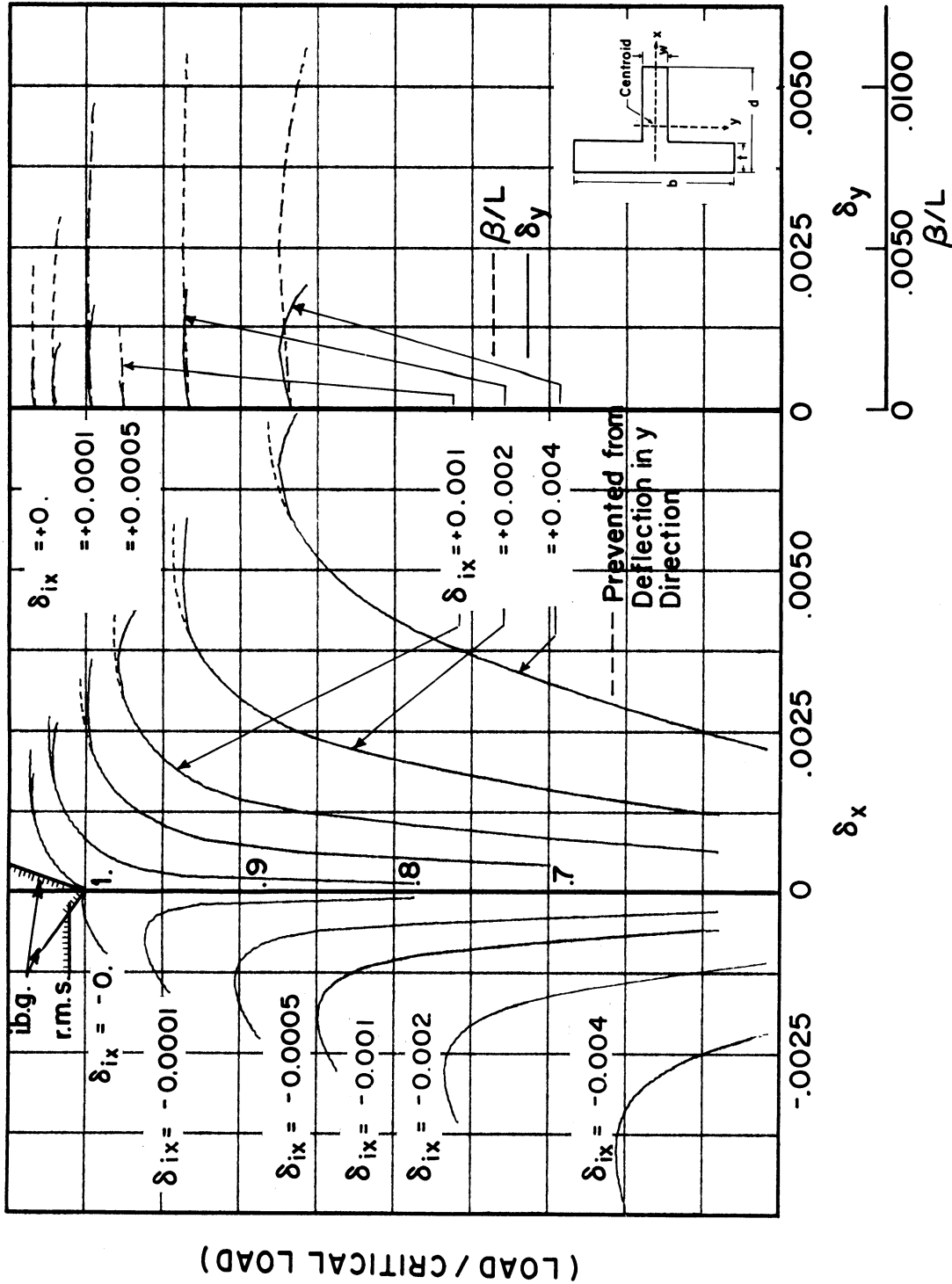MID-LENGTH DEFLECTION AND TWIST PER UNIT LENGTH; δ_x, δ_y INCH/INCH; β/L RAD/INCH

Fig. 5.15. Dimensionless Load vs. Mid-length Deflections and Twist
(initial crookedness; d = 2.5"; L/r = 40)

-144-
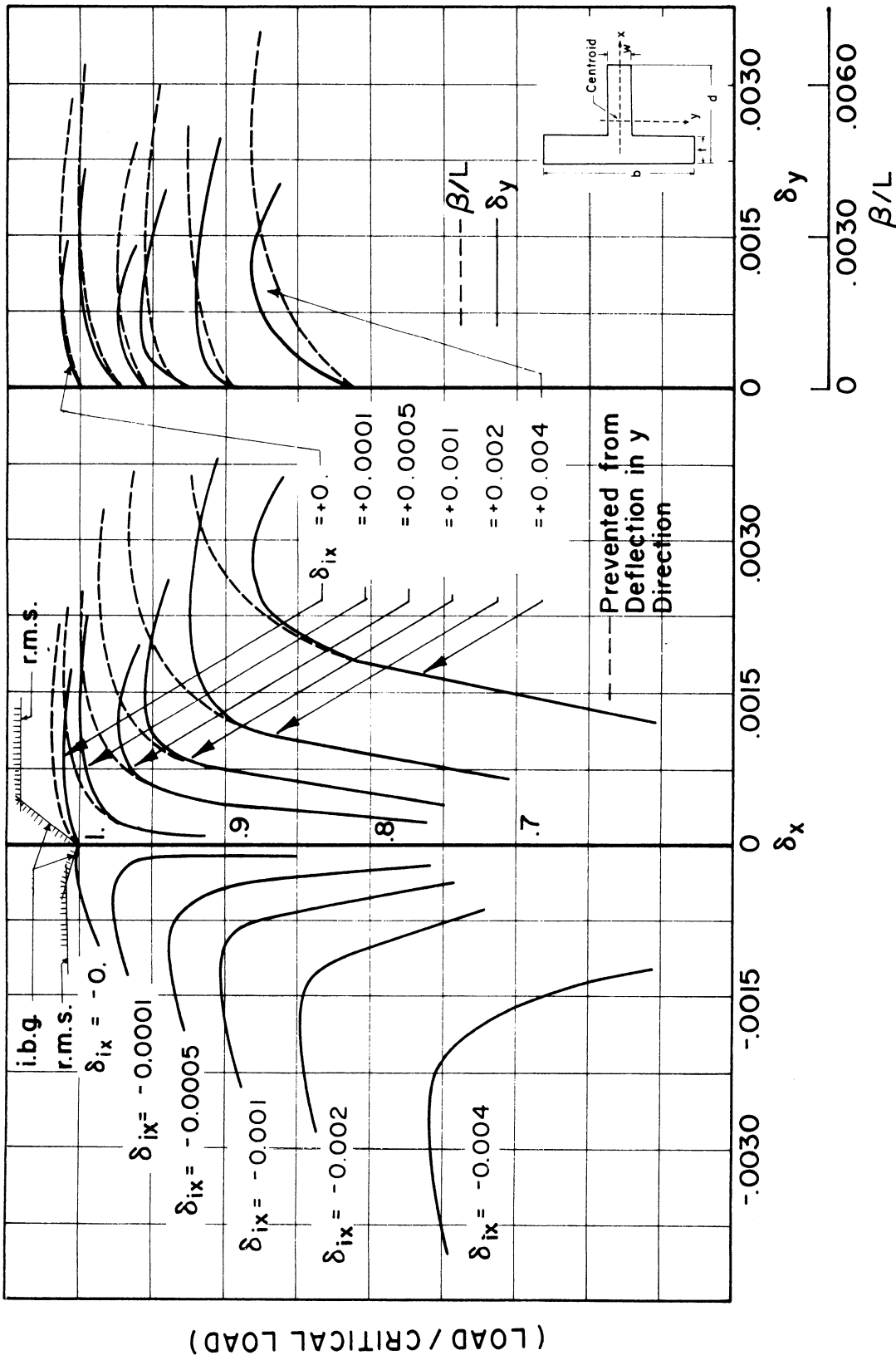
MID-LENGTH DEFLECTION AND TWIST PER UNIT LENGTH; δ_x, δ_y INCH/INCH; β/L RAD/INCH

Fig. 5.16. Dimensionles Load vs. Mid-length Deflections and Twist (initial crookedness; d = 3.$^{\prime\prime}$; L/r = 30)
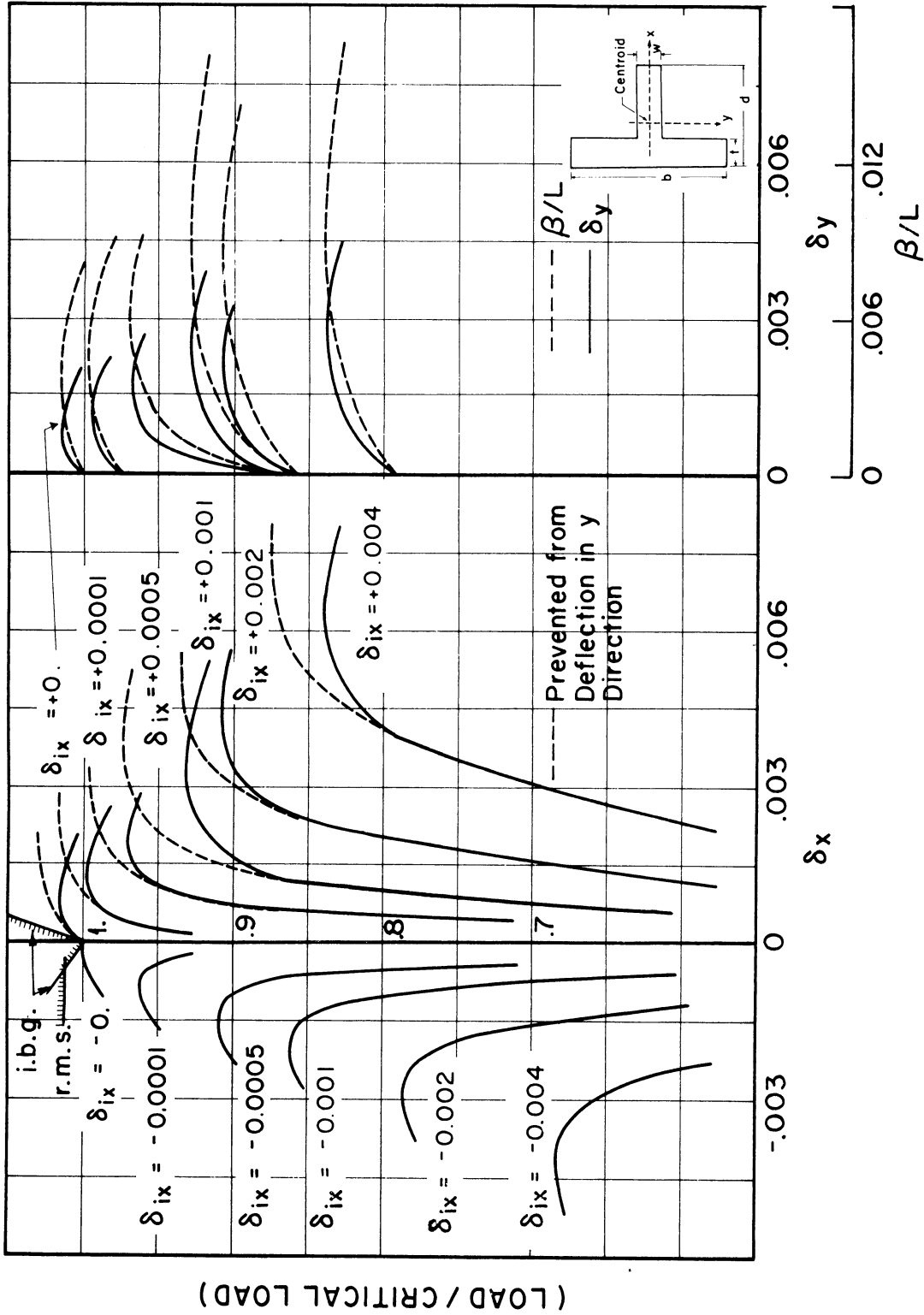
Fig. 5.17. Dimensionless Load vs. Mid-length Deflections and Twist (initial crookedness; $d = 3.''$; $L/r = 40$)

Table 5.4

Ultimate Average Stress
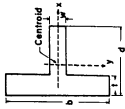
Buckling towards or away from the flange

(initial crookedness; d = 2.5", 3"; stress-strain relation #1)

d	KL/r	Buckling to the Left — Initial Crookedness, δ_{ix}						False Modulus Reduced Stress, $(\sigma_r)_f$	Reduced Modulus Stress, σ_r	I.B.C.G. $\left(\frac{L}{r}\right)\left(\sqrt{\frac{A}{}}\right)$	Critical Stress, σ_r	I.B.C.G. $\left(\frac{L}{r}\right)\left(\sqrt{\frac{A}{}}\right)$	Reduced Modulus Stress, σ_r	False Modulus Reduced Stress, $(\sigma_r)_f$	Buckling to the Right — Initial Crookedness, δ_{ix}					
		-.0040	-.0020	-.0010	-.0005	-.0001	-.0000								+.0000	+.0001	+.0005	+.0010	+.0020	+.0040
2.5"	30	31.746	35.688	38.163	39.680	41.432	42.521	49.764	42.870	974.9	42.472	3732.6	44.120	89.162	43.128	42.811	42.200	41.782	40.920	39.180
2.5"	40	26.385	30.875	34.179	36.341	38.688	40.310	43.551	40.720	1231.7	40.247	4718.2	43.300	57.640	41.655	41.120	40.195	39.400	37.720	35.220
3"	30	32.258	36.040	38.356	39.830	41.497	42.531	49.764	82.870	986.2	42.472	3496.7	44.120	89.162	43.021	42.450	41.200	40.600	39.231	37.500
3"	40	26.910	31.272	34.487	36.543	38.779	40.323	43.551	40.720	1246.0	40.247	4418.0	43.300	57.640	41.120	40.250	39.120	37.350	36.500	33.550

Table 5.5

(Ultimate Load/Critical Load)

Buckling towards or away from the flange

(initial crookedness; d = 2.5", 3"; stress-strain relation #1)

| d	KL/r	Buckling to the Left — Initial Crookedness, δ_{ix}						False Modulus Reduced Load/P_f	Reduced Modulus Load/P_f	I.B.C.G. $\left(\frac{L}{r}\right)\left(\sqrt{\frac{P_f}{}}\right)$	I.B.C.G. $\left(\frac{L}{r}\right)\left(\sqrt{\frac{P_f}{}}\right)$	Reduced Modulus Load/P_f	False Modulus Reduced Load/P_f	Buckling to the Right — Initial Crookedness, δ_{ix}					
		-.0040	-.0020	-.0010	-.0005	-.0001	-.0000							+.0000	+.0001	+.0005	+.0010	+.0020	+.0040
2.5"	30	.747	.840	.899	.934	.976	1.001	1.172	1.009	22.953	87.884	1.039	2.099	1.015	1.008	.994	.984	.963	.922
2.5"	40	.656	.767	.849	.903	.961	1.002	1.082	1.012	30.604	117.176	1.076	1.432	1.035	1.022	.999	.979	.937	.875
3"	30	.760	.849	.903	.938	.977	1.001	1.172	1.009	23.219	82.330	1.039	2.099	1.013	.999	.970	.956	.924	.883
3"	40	.669	.777	.857	.908	.964	1.002	1.082	1.012	30.958	109.771	1.076	1.432	1.022	1.000	.972	.928	.907	.834
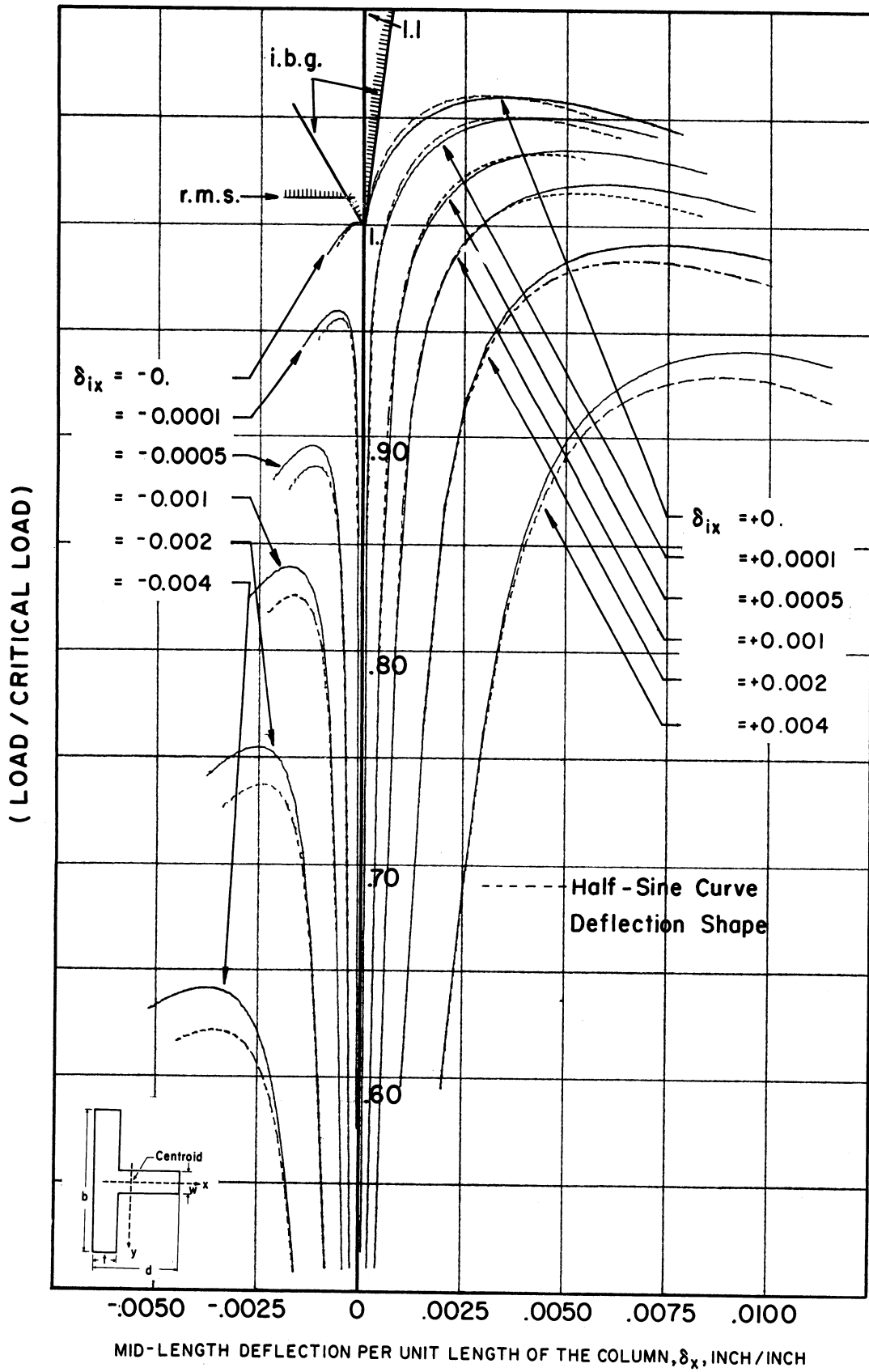
Fig. 5.18. Dimensionless Load vs. Mid-length Deflection
(initial crookedness; d = 1.5"; L/r = 40; stress-strain relation #2;
half-sine curve deflection-shape comparison)

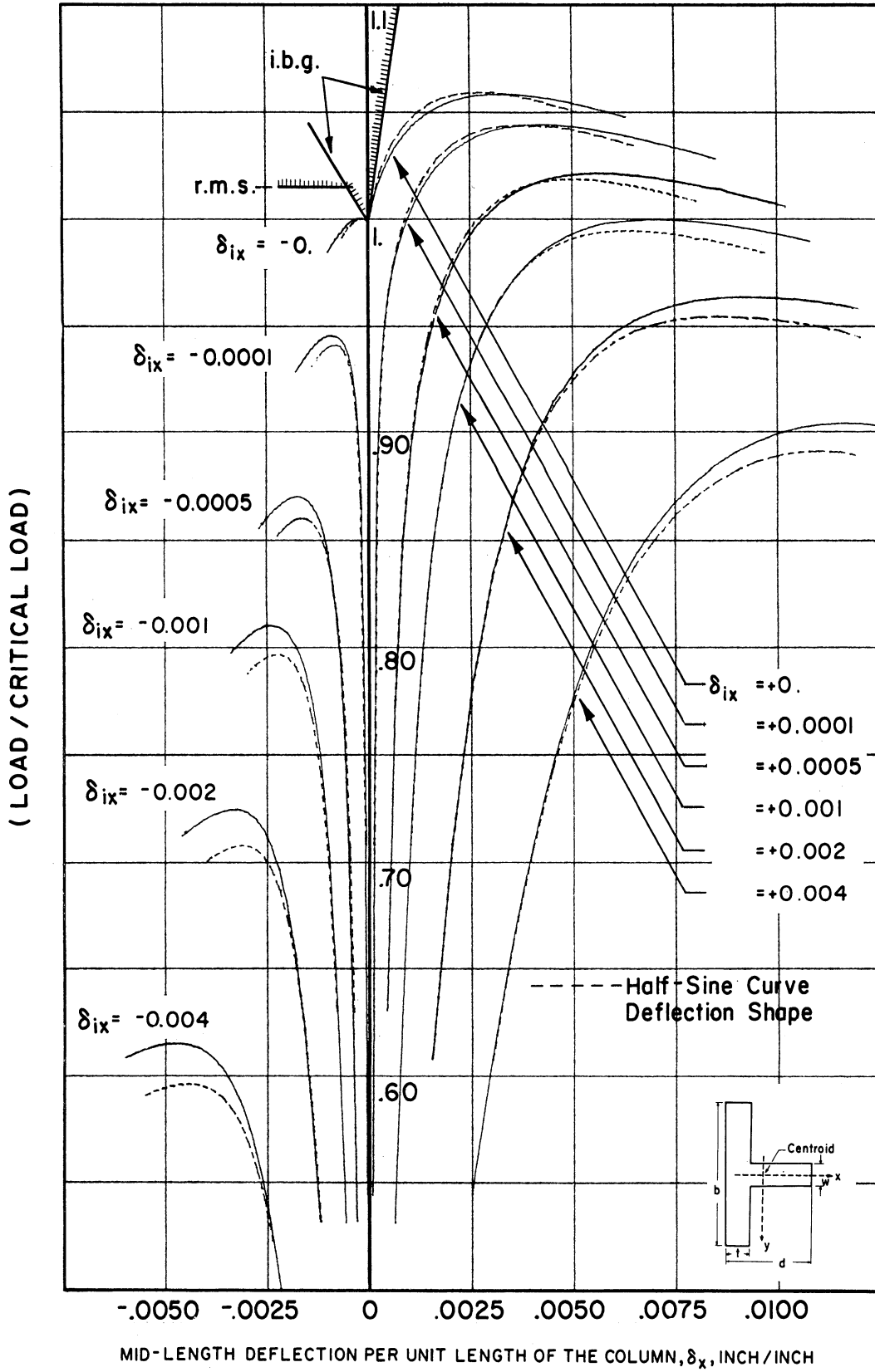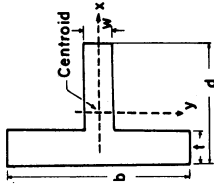Fig. 5.12. Dimensionless Load vs. Mid-length Deflection
(initial crookedness; L/r = 40;
half-sine curve deflection-shape comparison)

Table 5.6

Ultimate Average Stress

Buckling towards or away from the flange
Comparison with the half-sine deflection shape assumption
(d = 1.5"; stress-strain relations #1, #2, #3)

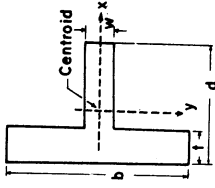| Stress-Strain Relation	KL/r	Deflection Shape	Buckling to the Left — Initial Crookedness, δ_{ix}: -.0040	-.0020	-.0010	-.0005	-.0001	-.0000	False Reduced Modulus Stress, $(\sigma_r)_f$	Reduced Modulus Stress, σ_r	I.B.G. $\left(\frac{L}{A}\right)$	Critical Stress, σ_t	I.B.G. $\left(\frac{L}{A}\right)$	Reduced Modulus Stress, σ_r	False Reduced Modulus Stress, $(\sigma_r)_f$	Buckling to the Right — Initial Crookedness, δ_{ix}: +.0000	+.0001	+.0005	+.0010	+.0020	+.0040
#1	30	**	30.305	34.690	37.548	39.278	41.272	42.510	49.746	42.870	1053.4	42.472	4526.7	44.120	89.162	43.530	43.306	42.911	42.524	41.796	40.420
#1	30	*	29.603	34.139	37.176	39.028	41.159	42.515								43.550	43.294	42.862	42.436	41.632	40.141
#1	40	**	24.883	29.623	33.290	35.754	38.438	40.290	43.551	40.720	1330.8	40.247	5719.1	43.300	57.640	42.046	41.615	40.884	40.089	38.695	36.408
#1	40	*	24.188	28.977	32.739	35.376	38.120	40.295								42.073	41.609	40.796	39.910	38.368	35.949
#2	40	**	22.304	26.245	29.184	31.132	33.364	34.807	38.425	35.210	1149.6	34.766	4940.2	38.470	55.020	36.838	36.529	35.994	35.446	34.460	32.733
#2	40	*	21.614	25.637	28.715	30.807	33.241	34.811								36.866	36.530	35.931	35.308	34.196	32.335
#3	40	**	28.278	33.325	37.260	40.019	43.486	46.002	48.878	46.620	1518.8	45.931	6526.7	50.700	60.850	48.676	47.022	46.973	45.971	44.306	41.568
#3	40	*	27.415	32.570	36.648	38.959	43.281	46.002								48.714	48.003	46.846	45.726	43.895	40.979

* Deflection shape is assumed to be a half sine curve

** Column divided into six equal segments

Table 5.7

(Ultimate Load/Critical Load)

Buckling towards or away from the flange
Comparison with the half-sine deflection shape assumption
(d = 1.5"; stress-strain relations #1, #2, #3)

Stress-Strain Relation	KL/r	Deflection Shape	Buckling to the Left — Initial Crookedness, δ_{ix} −.0040	−.0020	−.0010	−.0005	−.0001	−.0000	False Reduced Modulus Load/P_t	Reduced Modulus Load/P_t	I.B.G. $(\frac{P_t}{L})_t$	I.B.G. $(\frac{P_t}{L})_t$	Reduced Modulus Load/P_t	False Reduced Modulus Load/P_t	Buckling to the Right — Initial Crookedness, δ_{ix} +.0000	+.0001	+.0005	+.0010	+.0020	+.0040
#1	30	**	0.714	0.817	0.884	0.925	0.972	1.001	1.171	1.009	24.801	106.580	1.039	2.099	1.025	1.020	1.010	1.001	0.984	0.952
#1	30	*	0.697	0.804	0.875	0.919	0.969	1.001							1.025	1.019	1.010	0.999	0.980	0.945
#1	40	**	0.618	0.736	0.827	0.888	0.955	1.001	1.082	1.012	33.066	142.099	1.076	1.432	1.045	1.034	1.016	0.996	0.961	0.905
#1	40	*	0.601	0.720	0.813	0.879	0.947	1.001							1.045	1.034	1.014	0.992	0.953	0.893
#2	40	**	0.642	0.755	0.839	0.895	0.960	1.001	1.105	1.013	33.066	142.099	1.107	1.158	1.060	1.051	1.035	1.020	0.991	0.941
#2	40	*	0.622	0.737	0.826	0.886	0.956	1.001							1.060	1.051	1.033	1.016	0.984	0.930
#3	40	**	0.616	0.726	0.811	0.875	0.947	1.001	1.064	1.015	33.066	142.099	1.104	1.325	1.060	1.046	1.023	1.001	0.965	0.905
#3	40	*	0.597	0.709	0.798	0.848	0.942	1.001							1.061	1.045	1.020	0.996	0.956	0.892

* Deflection shape is assumed to be a half sine curve

** Column divided into six equal segments
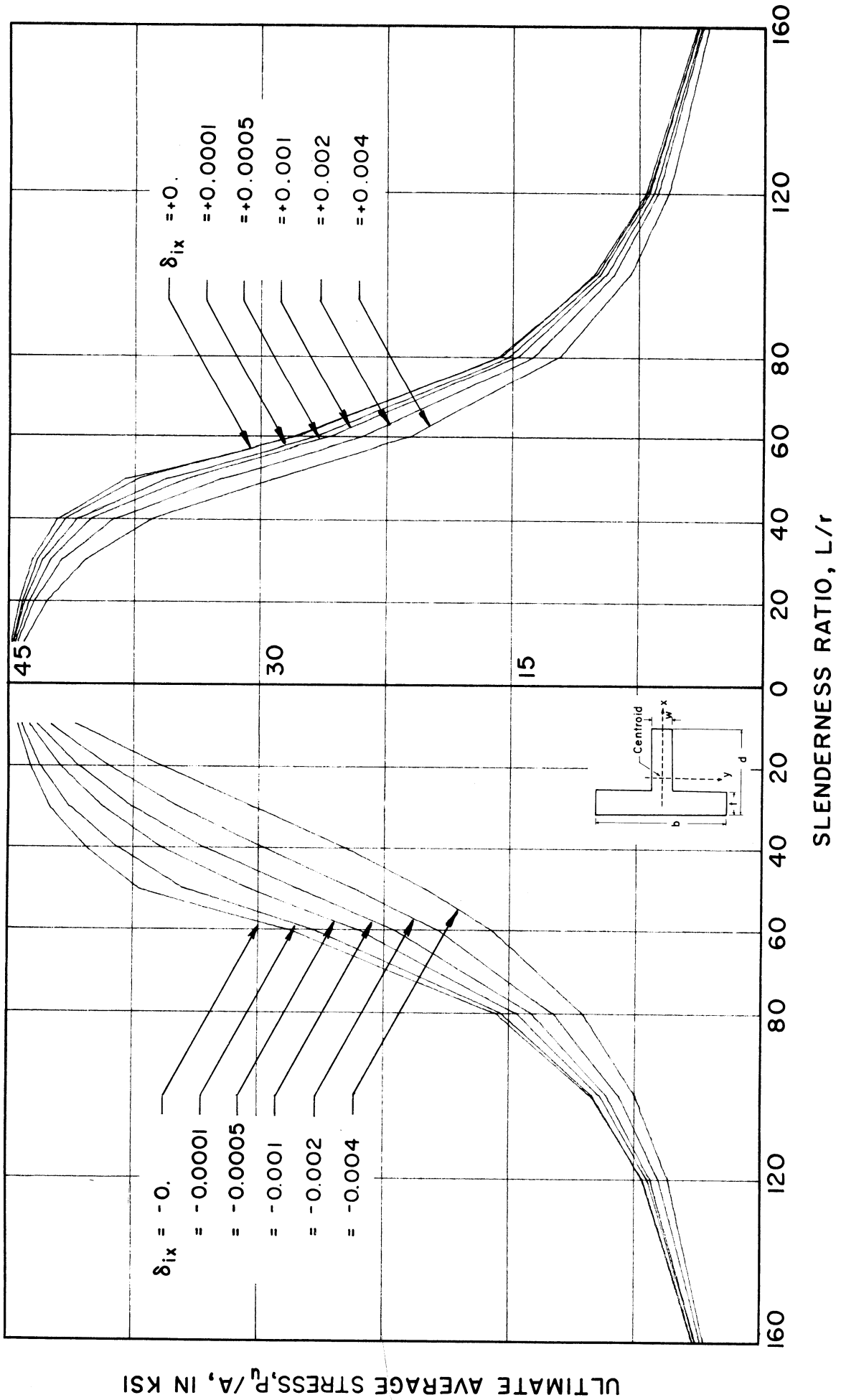
Fig. 5.20. Ultimate Average Stress vs. Slenderness Ratio
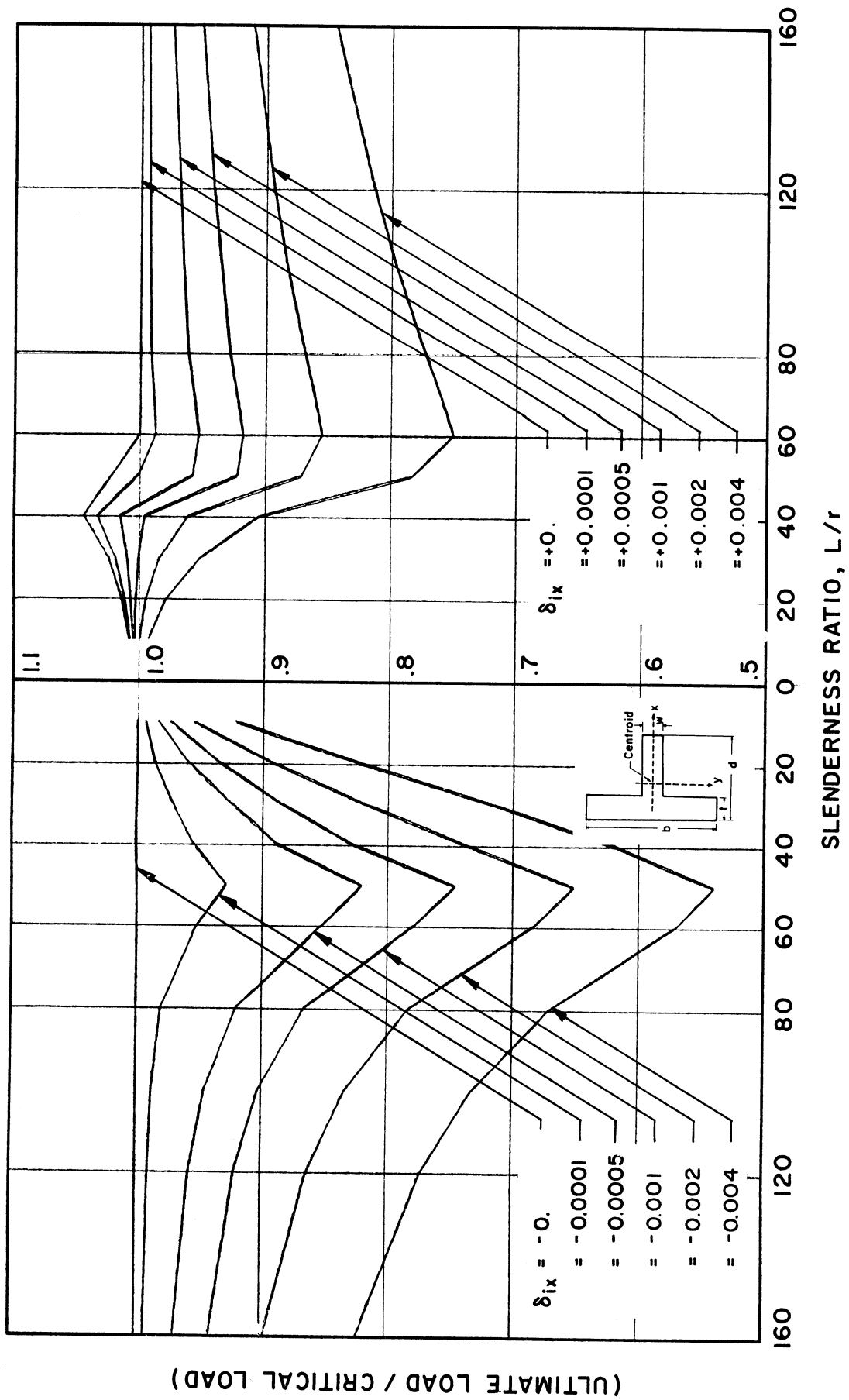
Fig. 5.21. (Ultimate Load/Critical Load) vs. Slenderness Ratio
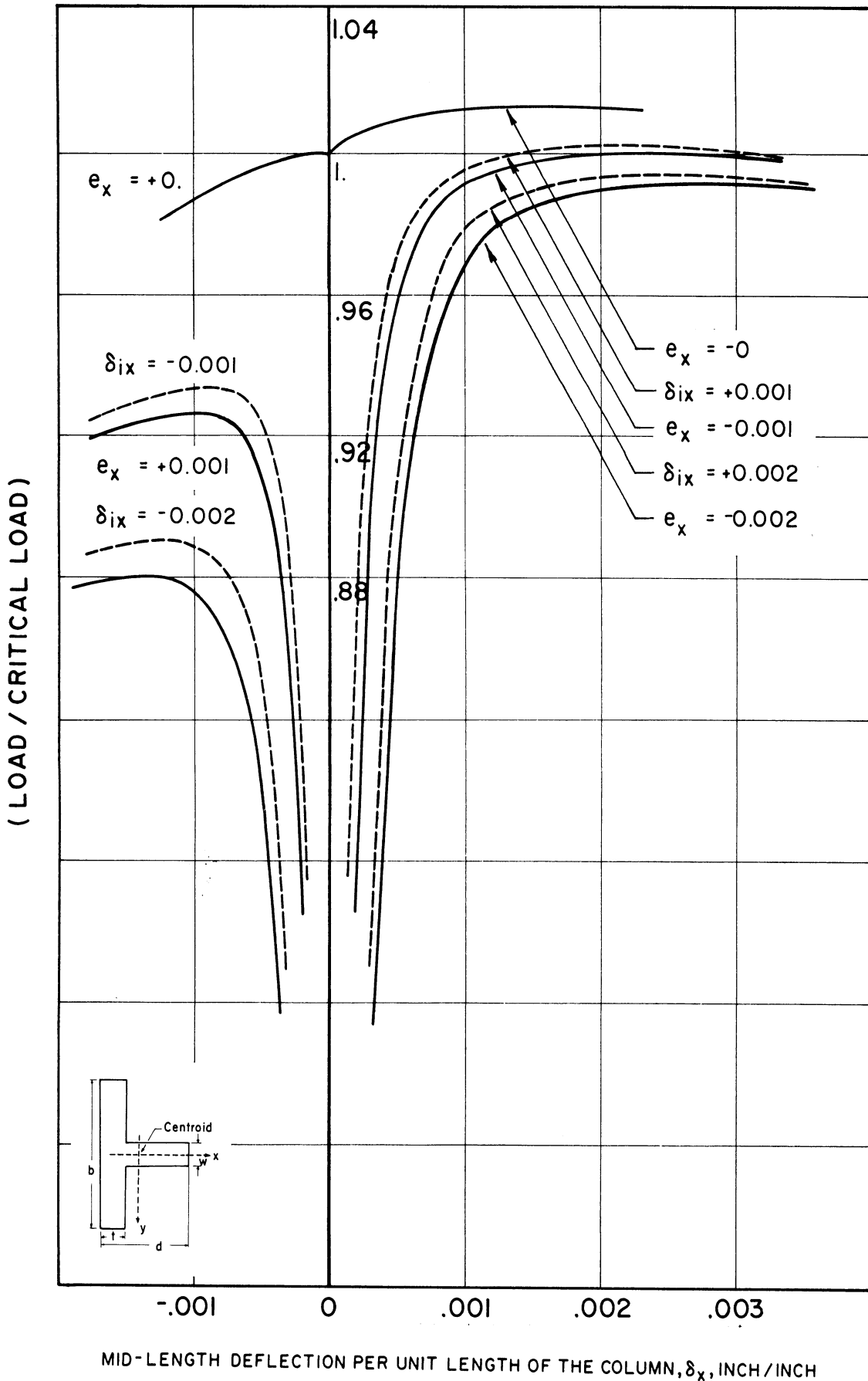
Fig. 5.22. Dimensionless Load vs. Mid-length Deflection
(eccentric loading - initial crookedness comparison; L/r = 20)
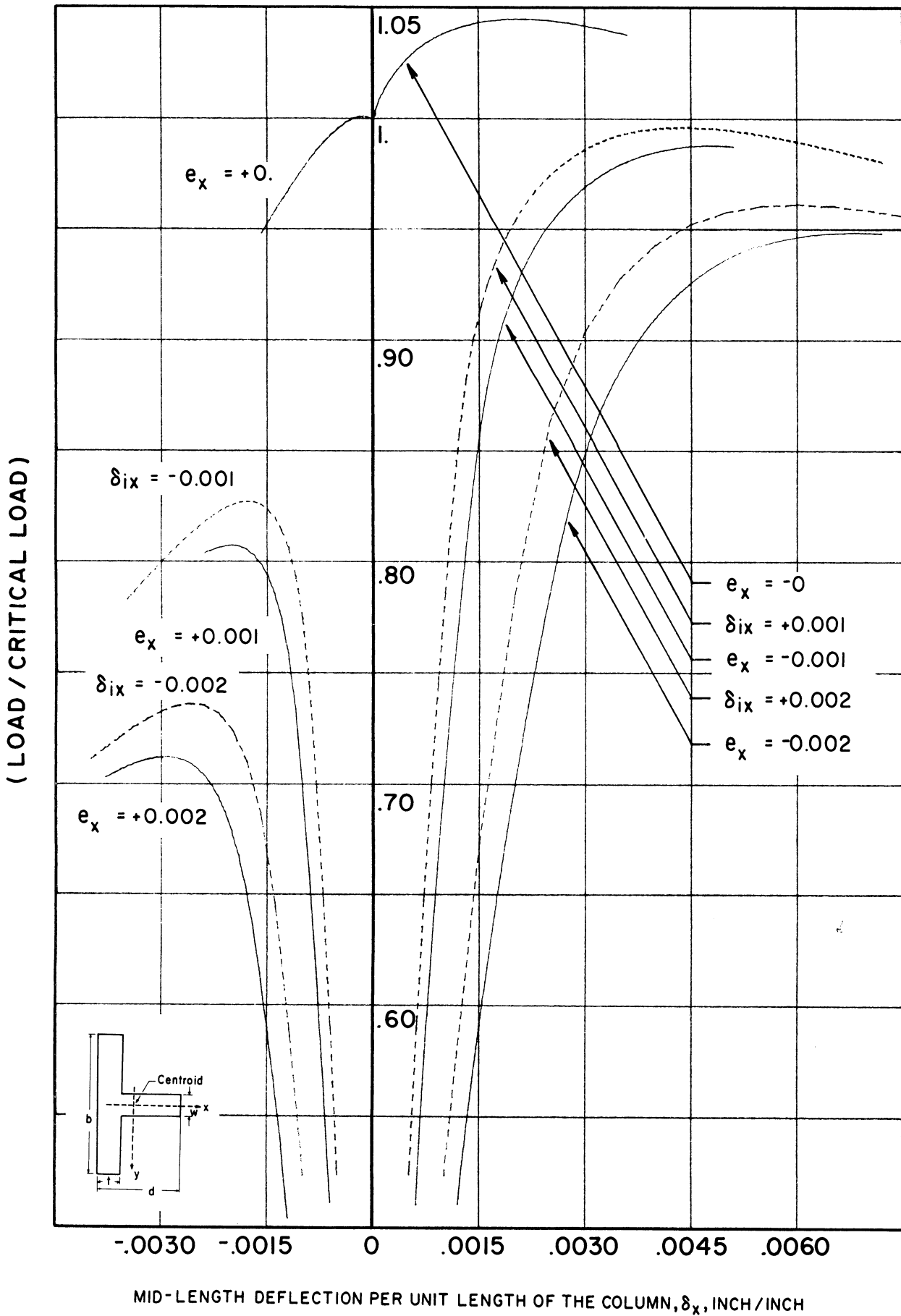
Fig. 5. 23. Dimensionless Load vs. Mid-length Deflection
(eccentric loading - initial crookedness comparison; L/r = 40)

MID-LENGTH DEFLECTION PER UNIT LENGTH OF THE COLUMN, δ_x, INCH/INCH
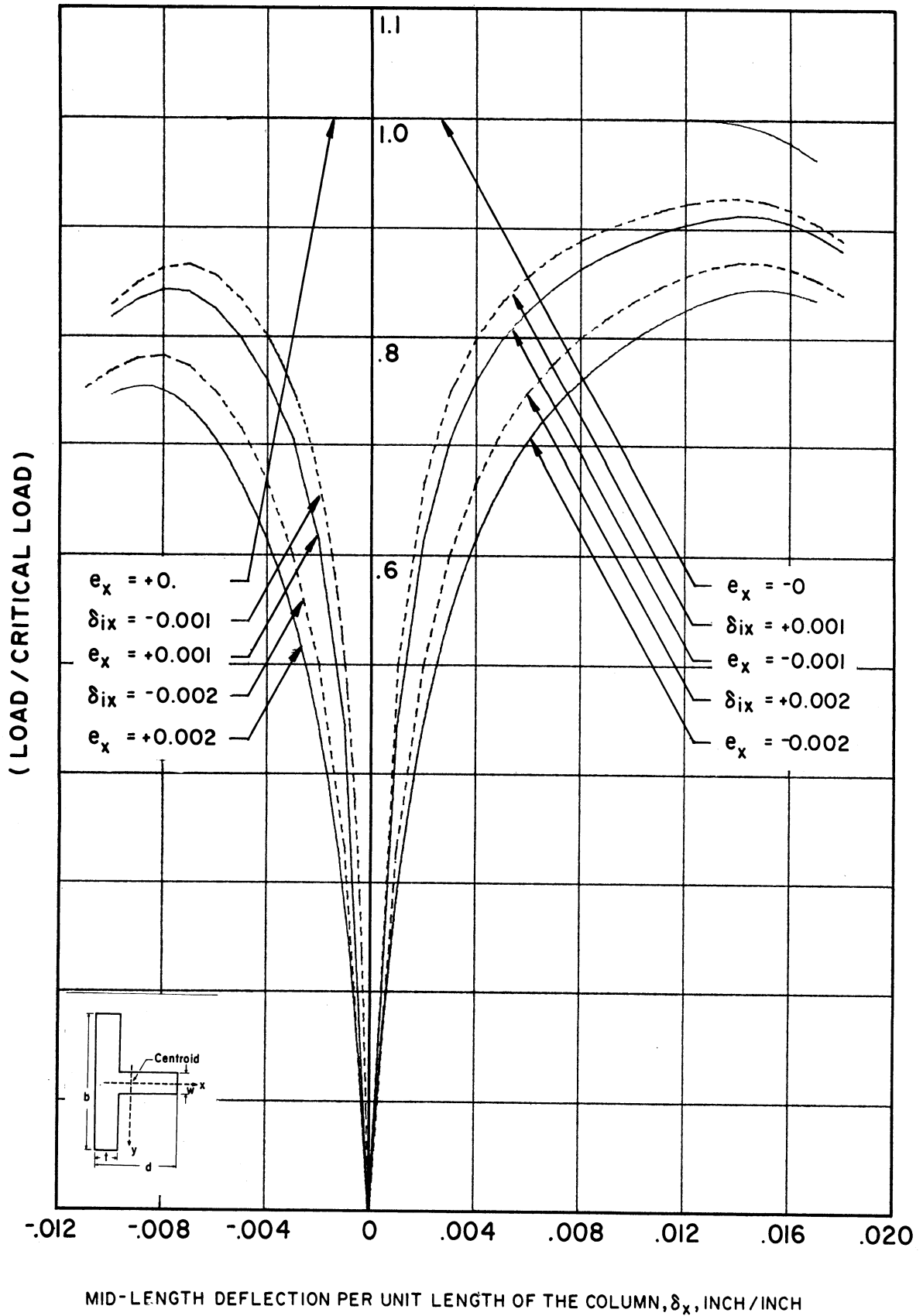
Fig. 5.24. Dimensionless Load vs. Mid-length Deflection
(eccentric loading - initial crookedness comparison; $L/r = 80$)

Table 5.8

Ultimate Average Stress

Buckling towards or away from the flange

Comparison of end eccentricity and initial crookedness

(d = 1.5"; stress-strain relation #1)

| KL/r	Buckling to the Left Crookedness $\delta_{ix} = -.002$	Eccentricity $e_x = +.002$	Crookedness $\delta_{ix} = -.001$	Eccentricity $e_x = +.001$	Buckling to the Right Eccentricity $e_x = -.001$	Crookedness $\delta_{ix} = +.001$	Eccentricity $e_x = -.002$	Crookedness $\delta_{ix} = +.002$
10	42.409	42.181	43.233	43.031	44.597	44.578	44.444	44.398
20	38.870	38.415	40.748	40.435	43.695	43.776	43.298	43.414
30	34.690	33.944	37.548	37.034	42.378	42.524	41.545	41.796
40	29.623	28.660	33.290	32.495	39.764	40.089	38.172	38.695
50	24.158	23.218	27.668	26.809	33.650	34.246	31.605	32.360
60	19.237	18.481	21.910	21.221	25.355	25.806	23.312	24.037
80	12.380	11.938	13.690	13.338	14.438	14.690	13.361	13.740
100	8.433	8.167	9.134	8.936	9.329	9.468	8.705	8.933
120	6.068	5.900	6.473	6.370	6.527	6.622	6.141	6.285
160	3.548	3.474	3.719	3.681	3.725	3.762	3.539	3.602
200	2.322	2.282	2.411	2.389	2.406	2.429	2.304	2.339

Table 5.9

(Ultimate Load/Critical Load)

Buckling towards or away from the flange

Comparison of end eccentricity and initial crookedness

(d = 1.5"; stress-strain relation #1)
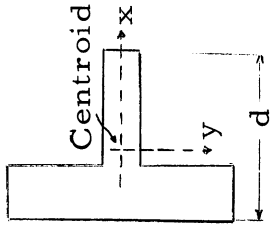
KL/r	Buckling to the Left				Buckling to the Right			
	Crookedness $\delta_{ix} = -.002$	Eccentricity $e_x = +.002$	Crookedness $\delta_{ix} = -.001$	Eccentricity $e_x = +.001$	Eccentricity $e_x = -.001$	Crookedness $\delta_{ix} = +.001$	Eccentricity $e_x = -.002$	Crookedness $\delta_{ix} = +.002$
10	.955	.950	.974	.969	1.004	1.004	1.001	1.000
20	.891	.880	.934	.926	1.001	1.003	.992	.995
30	.817	.799	.884	.872	.998	1.001	.978	.984
40	.736	.712	.827	.807	.988	.996	.948	.961
50	.651	.625	.745	.722	.907	.923	.851	.872
60	.684	.657	.779	.755	.902	.918	.829	.855
80	.783	.755	.866	.843	.913	.929	.845	.869
100	.833	.807	.903	.883	.922	.936	.860	.883
120	.863	.839	.921	.906	.929	.942	.874	.894
160	.898	.879	.941	.931	.942	.952	.895	.911
200	.918	.902	.953	.944	.951	.960	.911	.925

Fig. 5.25. Ultimate Average Stress vs. Slenderness Ratio (eccentric loading - initial crookedness comparison)
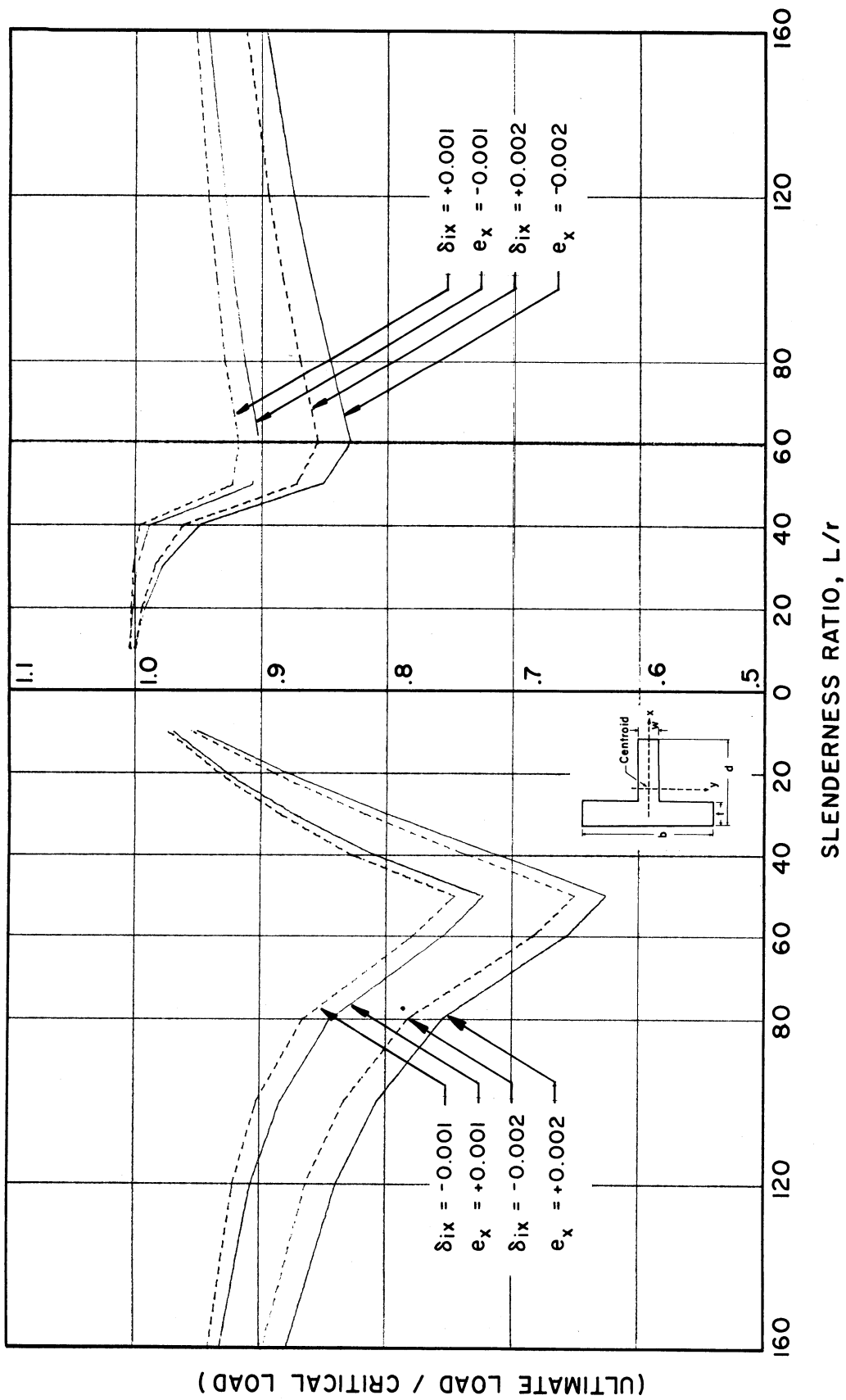
Fig. 5.26. (Ultimate Load/Critical Load) vs. Slenderness Ratio (eccentric loading - initial crookedness comparison)

CHAPTER VI

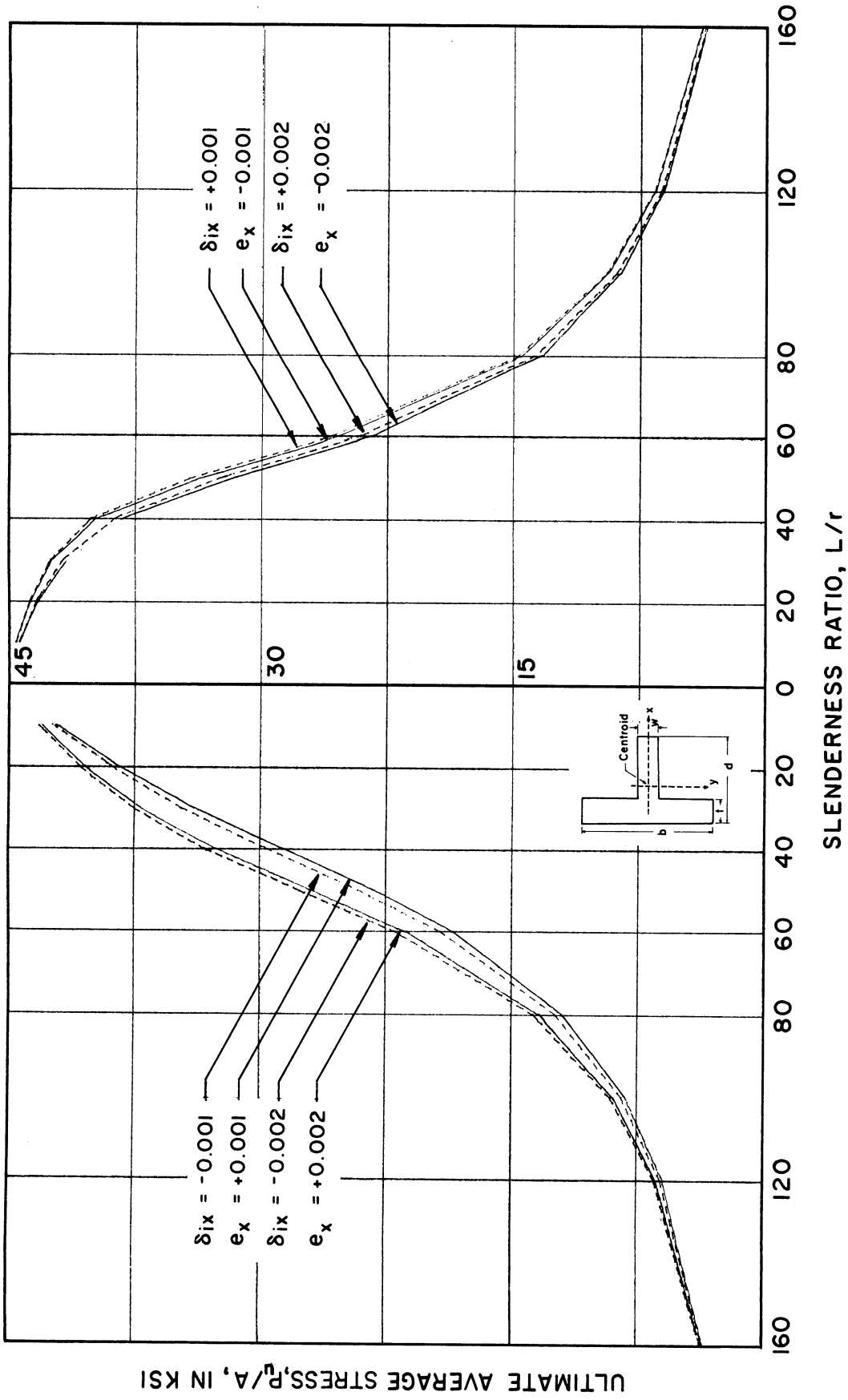## TESTING

6.1. INTRODUCTION

Previous Experiments

In a historical note on column construction, Hoff[41, 42] points

out that the columns which were hewn out of solid rocks and erected

almost five thousand years ago in Egypt, and twenty-five hundred

years ago in Persapolis still stand, while the scientific and mathe-

matical approach to the study of column problem started with Euler's

formula in 1744. Although Musschenbroek built the first testing

machine about 25 years prior to that date, his experimental research

on columns did not receive attention until it was discovered that

Euler's formula failed to give an answer to the column buckling in

the inelastic range. In 1889 Considère conducted a series of 32 column

tests that were important in relation to the tangent modulus theory.

Of large number of column tests which have been carried out,

a few will be cited, as follows:

In the 1920's several series of tests on rolled built-up columns

were conducted at the University of Wisconsin.[97] In these experi-

ments the effects of crookedness, eccentricity and imperfections of

rolling were studied and the results were compared with the "ideal"

column analysis. In these tests planar bending about the strong axis

was considered. These tests led to the development of design

specification formulas in railing engineering practice.

Massonnet and Campus[98] performed 95 tests on columns in

Belgium and developed some design formulas for columns under

oblique compression, and made a comparison with European column

specifications. In these tests they studied symmetric or unsymmetric

eccentrical loadings.

In 1956 Baker, Horne and Heyman[99] published results of

the tests performed on small models of three-dimensional frame-

works in which the columns were subjected to biaxial bending in

Cambridge.

In 1958 Mason, Fisher and Winter[100] performed tests on

24 welded hat-shaped sections, loaded eccentrically and bent about

the weak axis parallel to the flange.

Estuar and Tall[101] in 1964 reported on a test procedure on

pinned end columns. In January 1966, Lay, Aglietti and Galambos[102]

suggested some testing techniques for restrained beam-columns.

In May 1966 Yarimci, Yaura and Lu[103] published a report on

techniques for testing structures permitted to sway. The above

mentioned techniques were considerably helpful in developing the

testing procedure for the measurement of the lateral displacements

and the twist of the column explained in this chapter.

Recently Birnstiel, Leu, Tesoro and Tomasetti[37] concluded

a report on the experiments of the H-columns under biaxial bending,

in order to compare the results with the values determined from the

interaction formula published in the "Column Research Council Guide to Design Criteria for Metal Compression Members," and found the formula generally very conservative. In this experiment 16 H-columns of high strength low-alloy V65 steel were used. Twelve of these experiments were loaded with substantially alike eccentricities at both ends with respect to both axes of the column and not alike eccentricity of the two ends on the rest of the experiments. In the process of the experiment, load vs. deflection in two directions and the rotation were recorded. As in the general case of the behavior of the column, biaxial bending combined with torsion will deduce.

6.2. OBJECTIVE OF THE EXPERIMENT

In order to study the applicability of the analytical results and compare the results obtained from incremental analysis with those obtained experimentally, it was necessary to perform a series of tests on the behavior of "T" shaped aluminum alloy columns. However, the author experienced a great deal of technical difficulties, and some of the experiments in the early stages yielded surprising and unexpected results. However, the experiences gained and the guidance obtained cannot be overlooked.

In the first series of tests it was attempted to support the column at the mid-height at either the flange or the web side and in the direction parallel to the web and normal to the column axis in order to study the load vs. deflection history of the column after

initiation of buckling in the positive

or negative x direction (Fig. 6. 1).

Surprisingly, considerably

higher ultimate load carrying

capacity than the one anticipated

by theory was obtained in the

case where the column was

prevented from deflection

towards the negative direction

of the x-axis. The reasons

for this are threefold:
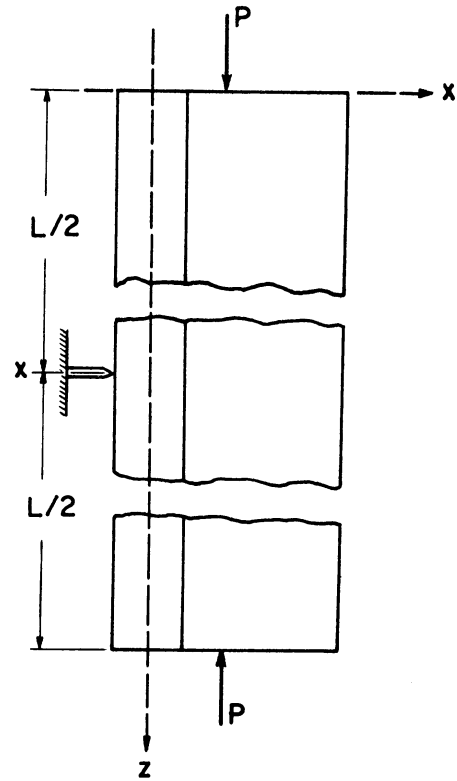
Fig. 6. 1. Column Supported
Laterally

i. The existence of the mid-height support changed the

effective length and the mode of behavior of the column.

ii. The existence of the eccentricity of loading at the ends,

no matter how small, in the positive direction of x was

producing horizontal force in the lateral support and this,

in turn, was changing the mode of deflection.

iii. The existence of even negligible initial imperfection or

crookedness in the plane parallel to the web and towards

the negative direction of x had the same effect as end

eccentricity.

However, in this series of tests, because of the above reasons and also over-estimation of the critical local buckling load, the failure occurred in local buckling of the flange. To eliminate the local buckling, the widths of the original test specimens were reduced. Also, the scheme of the experiment was changed, lateral support was omitted, and by intentionally giving end eccentricity along the x-axis and in one direction or the other the column was forced to deflect in the arbitrarily chosen direction.

6.3. MATERIAL PROPERTIES

The material properties of the columns used in the experiments were determined by compression tests on two specimens of the complete rolled aluminum alloy H-section which was then split longitudinally to form the T sections used as column specimens. The length of the first specimen was chosen to be 12 inches but occurrence of local buckling at 45.7 ksi determined the last point obtained for the curve of the stress-strain relation. The second specimen was cut shorter to an 8 inch length and was braced to delay the local buckling, but it buckled locally a step sooner than the first specimen as the rods which were used to brace the specimen might have exerted lateral pressure and changed the mode of local buckling towards outside (Fig. 6.2). However, the range of the stress-strain relation which was obtained was far more than enough for use in relating the test results to analytical studies, as that limit of stress was beyond that of the loading stage of the chosen column tests.

M-M "Precision Strain Gages" (made by MicroMeasurements, Inc., Romulus, Michigan) were used as electrical strain gages and the TINIUS OLSEN 400000 pounds Mechanical Testing Machine in the Civil Engineering Department Laboratory of The University of Michigan (Fig. 6.3) was used as a loading device.

The rate of machine head movement was chosen to be about 0.025 inch per minute in the elastic range and 0.05 inch in the inelastic region. The graph of stress-strain for the above tests and the approximated algebraic fit for them are given in Fig. 2.6. The average Poisson's ratio was 0.325.
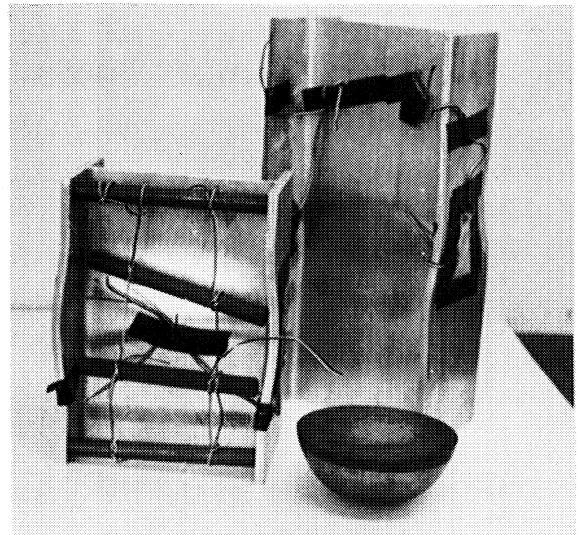
Fig. 6.2. Specimens of the Material Properties Test
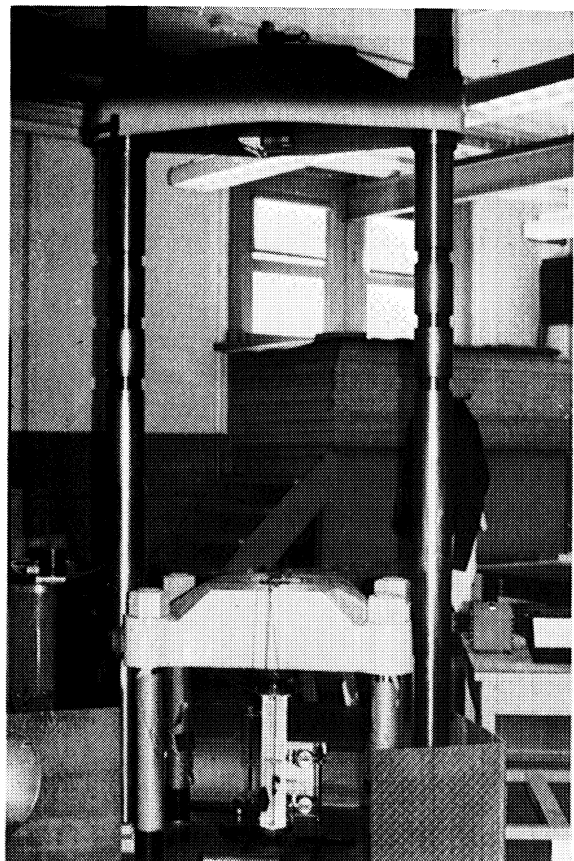
Fig. 6.3. Tinius Olsen Mechanical Testing Machine

6.4. COLUMN DIMENSIONS

Columns are compression members of considerable length compared to their cross sectional dimensions. Tee column test specimens of various lengths were prepared by cutting and milling from a 6 x 4 6061-T6 aluminum alloy H-section. Before cutting to length, the web of the H-section was cut along the line parallel to longitudinal axis. The end cut surfaces were milled to give a smooth surface with a rather precise right angle to the adjoint surfaces. Very negligible effect, if any, of the relief of the residual stress was observed as the specimens did not tend to become crooked or change their initial form after cutting. The cross sectional dimensions of each specimen were measured at a few points along the length by means of micrometer and vernier calipers with accuracy of 0.001 inch. The result of the measurements of the web thickness is somewhat differed from the one given in the Alcoa Structural Handbook.[104]

The dimensions of the cross section were (Fig. 6.4)
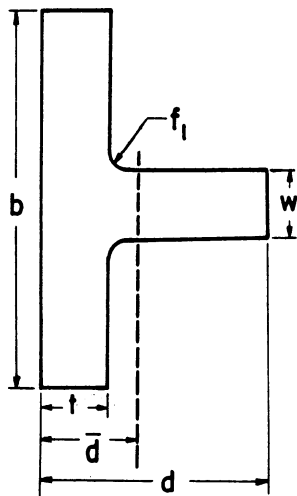
Fig. 6.4. Cross Section
Dimensions

f_1 = 0.230 inch (0.250 in the
    handbook)

t = 0.279 inch

w = 0.218 inch (0.230 in the
    handbook)

b = 4. inch

d = 2.5 inch (first series);
    1.5 inch (second series)

L = length of the specimens,
    chosen such that the
    slenderness ratio would
    be multiples of 10

(6.1)

Other section properties were calculated as follows:

For H section used as stress-strain test specimen:

Area = 3.464

For T section:

d = 1.5 inch

Area = 1.404 inch^2

I_x = 1.489 inch^4

I_y = 0.161 inch^4

r_x = 1.038 inch

r_y = 0.342 inch

$\overline{d}$ = 0.284 inch

d = 2.5 inch

Area = 1.622 square inch

I_x = 1.490 inch^4

I_y = 0.734 inch^4

r_x = 0.965 inch

r_y = 0.677 inch

$\overline{d}$ = 0.519 inch

(6.2)

6. 5. END CONDITION

Although a pinned-end column does not exist in actual structures and a column with absolutely no restraints at the end is a highly idealized member, study of its behavior is essential to the column design. In practice the end condition of columns lies between the two limiting points of full restraint and no restraint at all. Providing full end restraint in testing is perhaps even more difficult than furnishing restraint-free end condition. In the case of a column with full end restraint, especially short columns, where ultimate load is achieved in the inelastic range of the stress-strain relation due to St. Venant's effect, in the distribution of stress at the sections close to the end, a non-uniform flow will exist and the effectiveness of the end restraint will gradually reduce. Moreover, the presence of mixed problems will prevent us from studying the sole problem of overall buckling of the column.

Establishment of a complete restraint-free end condition is also difficult. However, the end resistance to rotation can be minimized to a negligible extent by means of techniques such as were used in these experiments. In the case of a pinned-end column the critical and governing state of stress will exist in the mid-height section with no end effects. For these reasons and because the basic problem of overall buckling was under study, the pinned-end condition was selected for the experiments and the analytical study. Of course, consideration of effective length for different end conditions, the effect of residual stress, transverse

load, symmetrical and unsymmetrical eccentric loading, and planar

or biplanar bending for varied slenderness ratios and cross sections

with different ratios of moment of inertia in the x and y directions is

also a feature of this study.

6. 6. END FIXTURES

A few variations of end fixtures have been used in testing of

the pinned-end columns. In 1887 Bauschinger used the conical end

fixtures[105] (Fig. 6. 5a) which allowed free rotation of column ends

and also ensured concentric loading. Later Von Kármán, in his

column tests, used a knife-edged bar bearing on a plane surface as

an end fixture[27] (Fig. 6. 5b).
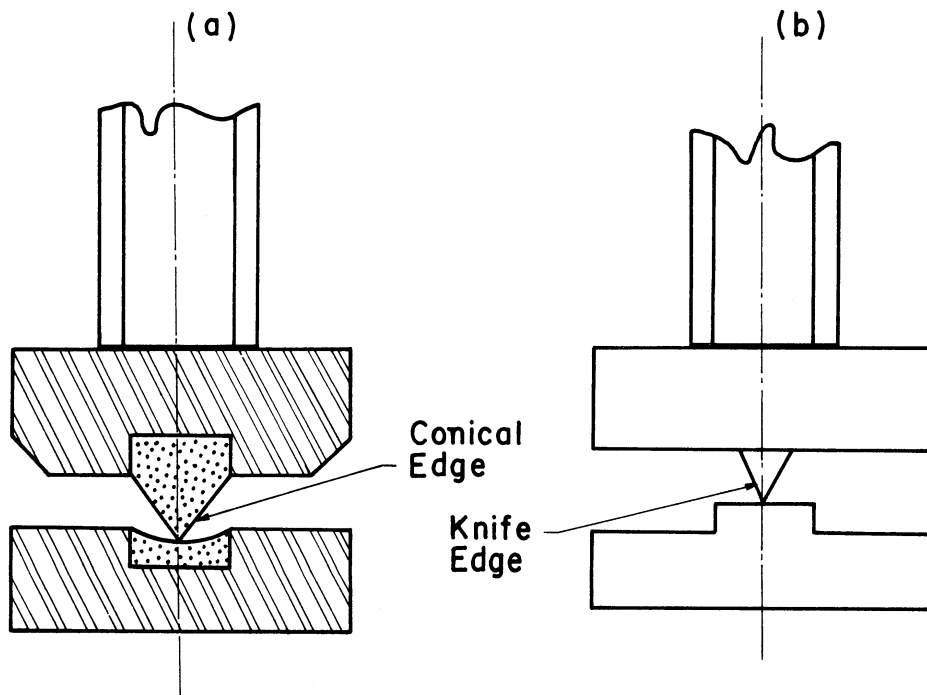
Fig. 6. 5a. End Fixture
used by Bauschinger

Fig. 6. 5b. End Fixture
used by Von Kármán

In this experiment a segment of a sphere with attachments, shown in Fig. 6.6, was utilized to provide a hinge action for each end of the column. Each end fixture consisted of four parts:

1. A segment of sphere of radius $2\frac{1}{4}''$ and height $2''$ (part #1), made of hardened crucible steel. The maximum load carrying capacity of the sphere was calculated from the equation[106]

$$P_{max} = C\, d^2 \qquad (6.3)$$

in which d is in inches and P is in kips. For $d = 4.5''$ and $C = 5$ kips/inch^2

$$P_{max} \simeq 100 \text{ kips} \qquad (6.4)$$

which provides a safety factor of almost 1.5 for this experiment in the highest loading case.

2. A circular plate of radius $5\frac{1}{2}''$ and thickness $\frac{5}{16}''$ made of hardened steel of sufficient shear resistance, set between the flat surface of the sphere and the end of the column to give smooth distribution of load and prevent local yielding (part #2).

3. A circular ring, to attach parts (#1) and (#2), and together with part (#4), prevent the column from slipping and help set the column in the desired position, as the three small screws could move the segment of the sphere with respect to the rest of the set-up some fraction of an inch (part #3). This part is also made of hardened steel.

4. A circular lead plate (part #4) of radius $5\frac{1}{2}''$ poured with the cross section of the column cut on it such that the centroid of the cut segment is at the desired position with respect to the center of the plate which coincides with both centers of the parts (#1) and (#2).

5. A circular hardened steel plate (part #5) of radius $7''$ and $1''$ thickness set between the part (#1) and the testing machine to distribute the load at the top and bottom of the machine on a larger area than the surface of contact of the sphere and thus prevent the local yielding of the headings of the machine.

Details of the end fixtures are shown in Fig. 6.6.
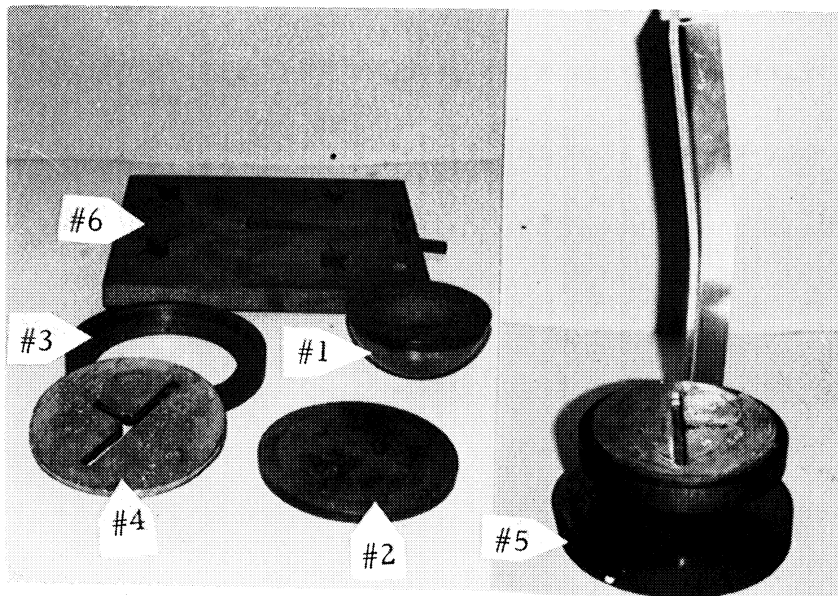
Fig. 6.6. Different Parts of the End Fixture

Part (#6) in Fig. 6.6 is a device which was used to determine the centroid of the cross section.

6.7. ATTACHMENT OF STRAIN GAGES

In the tests for obtaining the material properties, M-M Precision Strain Gages were used in order to have rather accurate strain readings in the inelastic range. For the column tests SR-4, A-8, strain gages were used. Strain gages were carefully attached. The surface of the contact was cleaned with a range of medium to soft emery paper. Then the surface was cleaned with carbon tetrachloride and finally with acetone. Duco cement, specially made for strain gage attachment, was used as adhesive and moderate pressure applied until the cement dried enough so that the edges of the gage would not draw away from the specimen. Protective measures were taken to secure the gages. Enough time was given for the cement to harden before testing the specimen.

The purpose of attaching the strain gages to the column was mainly to check the concentricity, or in some cases the correctness of intended eccentricity, in the initial steps of loading.

6.8. MEASUREMENT OF THE LATERAL DISPLACEMENTS AND THE TWIST

As the spherical end fixtures are free to rotate and displace their contact points with respect to fixed surfaces of the headings of the testing machine (Fig. 6.7), measurement of the displacements and the twist of a point along the column relative to the end points requires special attention and technique.

The method used in this experiment to measure the mid-height displacement and the twist, relative to the end section, is as follows:

Near each end of the column four pulleys were attached, two on two ends of the flange, one at the end of
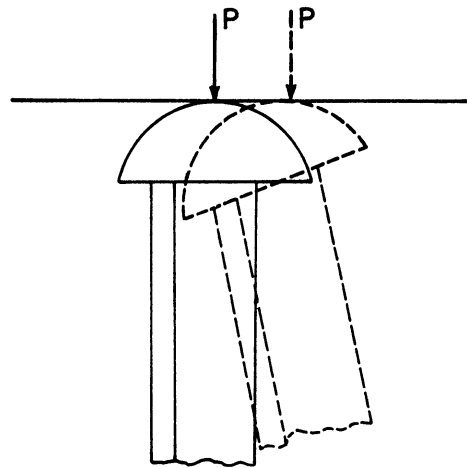
Fig. 6.7. End Fixture Movement

the web and the last one on the face of the flange. The centers of these pulleys had a certain measured distance ($\frac{3''}{4}$) from the end of the column (Fig. 6.8). The pulleys were adjusted such that the piano strings passing over them were exactly at the center of the cross section.
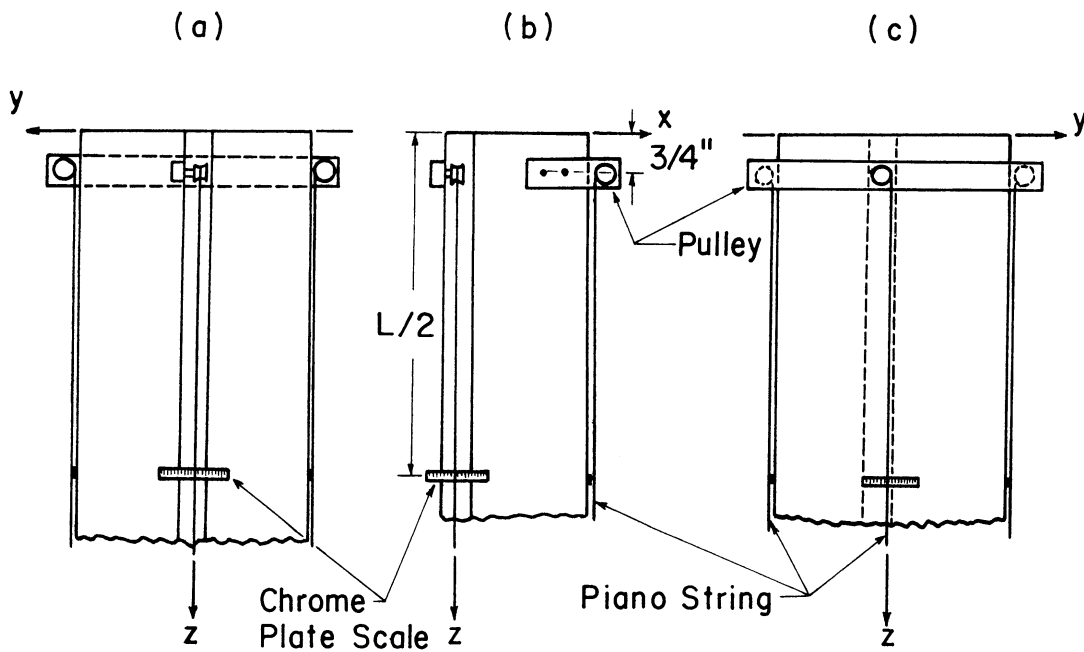
Fig. 6.8. Displacement and Twist Measurement Attachments

At the mid-height section 4 ferro
type chrome plates (blades),
with a scale divided to $(1/100'')$
and each with their axis perpen-
dicular to the respective piano
string, were attached to the
column with epoxy glue (Fig. 6.9).
The grooves of the pulleys were
very narrow in order to prevent
the string from sliding from its
original position. The wires
were fastened at the lower end

Fig. 6.9. Attached Pulleys and
Chrome Blades

and by means of some weight
attached to the other end of the wire, after passing over the upper

pulley, the wires were kept taut. The pulleys were lubricated to

eliminate the friction between the wire and the surface of the groove.

At the first step (400 lbs. of load to keep the column in position) and

at every step of reading the position of wire on the chrome plate

scale was recorded (such that the wire and its image on the chrome

plate and the reading edge were on a straight line). A magnifying

glass was used to read with a better accuracy. The mid-height

deflection and twist can be obtained from the above readings by the

aid of the following explanation:

Let us assume that the centroid of the flange is the center of the twist. xyz coordinate is fixed to the end of the column with its origin (o) at the center of twist, and x- and y-axes respectively, the axes of symmetry for the web and the flange (Fig. 6.10). $\xi\eta\zeta$ coordinate is fixed to the mid section of the column with its origin (o') at the center of twist and, ξ and η axes respectively, the axes of symmetry for the web and the flange at the mid-height section. When there are no displacements or twist, and no initial imperfection, xyz will coincide with $\xi\eta\zeta$. At some deformed stage, the mid-height section will have, in general, lateral deflection (U, V) and the twist (β).
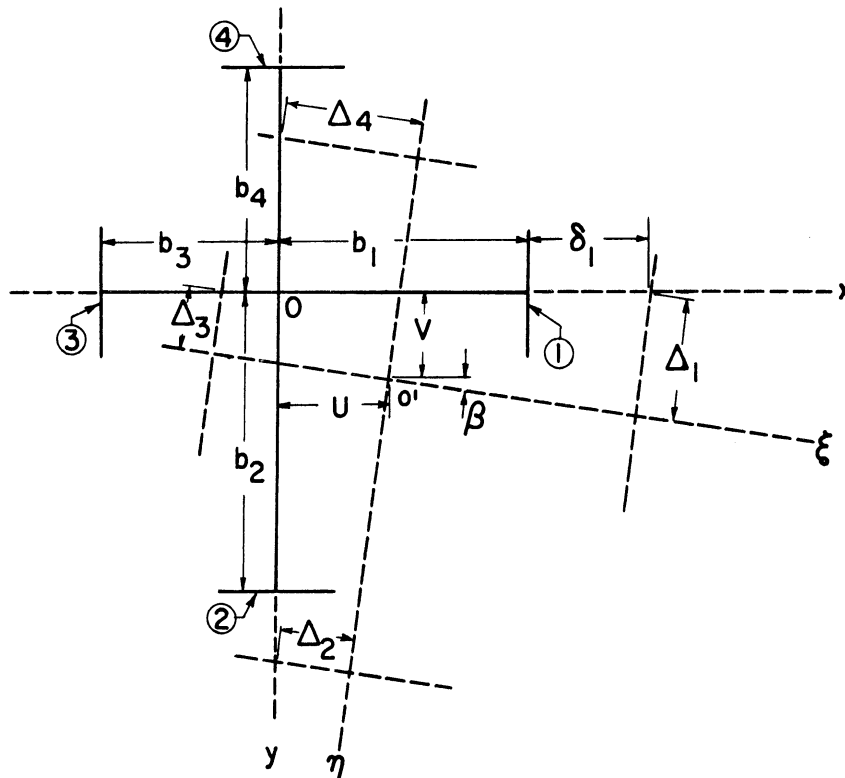
Fig. 6.10. Translated and Twisted Mid-length Section

Readings on chrome plate scales (minus the original readings) will give the values of Δ_1, Δ_2, Δ_3, Δ_4, which is the distance between the reflection of the initial position of the string on the plate and the present one. (The distance Δ is smaller than the distance between the wire and the chrome plate and the chrome plate will not interfere with the reading for small twist.) The following gives the relation between the readings and the displacements and the twist

$$\Delta_1 \cos_\beta = V + b_1 \sin_\beta$$

$$-\Delta_2 \cos_\beta = U - b_2 \sin_\beta$$

$$-\Delta_3 \cos_\beta = V - b_3 \sin_\beta \tag{6.5}$$

$$\Delta_4 \cos_\beta = U + b_4 \sin_\beta$$

Solving (6. 5) for

the twist

$$\tan_\beta = \frac{\Delta_1 + \Delta_3}{b_1 + b_3} = \frac{\Delta_2 + \Delta_4}{b_2 + b_4} \tag{6.6}$$

and the lateral displacements

$$U = \frac{1}{2} \left[(\Delta_4 - \Delta_2) \cos_\beta + (b_4 - b_2) \sin_\beta \right]$$

$$V = \frac{1}{2} \left[(\Delta_1 - \Delta_3) \cos_\beta + (b_1 - b_3) \sin_\beta \right] \tag{6.7}$$

Assuming β to be very small, then

$$\tan_\beta \approx \sin_\beta \approx \beta \quad \text{and} \quad \cos_\beta \approx 1$$

$$\beta = \frac{\Delta_1 + \Delta_3}{b_1 + b_3} = \frac{\Delta_2 + \Delta_4}{b_2 + b_4} \quad \text{(radian)}$$

$$U = \frac{1}{2}\left[(\Delta_4 - \Delta_2) + \frac{b_4 - b_2}{b_4 + b_2}(\Delta_4 + \Delta_2)\right] \tag{6.8}$$

$$V = \frac{1}{2}\left[(\Delta_1 - \Delta_3) + \frac{b_1 - b_3}{b_1 + b_3}(\Delta_1 + \Delta_3)\right]$$

In this experiment

$$b_2 = b_4 = \frac{b}{2}$$

$$b_1 = (d - \frac{t}{2})$$

$$b_3 = \frac{t}{2}$$

and

$$\beta = \frac{\Delta_2 + \Delta_4}{b} = \frac{\Delta_1 + \Delta_3}{d}$$

$$U = \frac{1}{2}\left[(\Delta_4 - \Delta_2)\right] \tag{6.9}$$

$$V = \frac{1}{2}\left[(\Delta_1 - \Delta_3) + (\frac{d - t}{d})(\Delta_1 + \Delta_3)\right]$$

Δ's are positive if the wire moves to the right (increasing the figures on the chrome plate scale) and negative otherwise. Accuracy of the data can be checked by the first equation of (6.9).

In reading the Δ's a slight error is encountered which can be corrected. Instead of Δ_1 ... in the above equations the value of

Δ'_1 ... should be used.

The following relation

exists between Δ' and
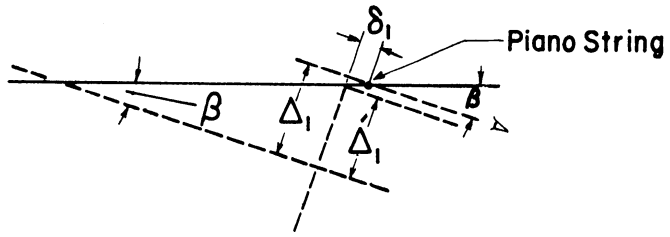
Δ (Fig. 6.11)

Fig. 6.11. Reading Error

$$\Delta' = \Delta_1 - \delta_1 \operatorname{Sin}_\beta$$

where δ_1 is the distance between the wire and the plate. As both β

and δ_1 are small, and as δ_1 decreases with increasing β, the above

error may be neglected, as it is done in this experiment. Thus, the

lateral deflections and the twist relative to the location of the center

of the pulleys were determined. By a simple parabolic-interpolation,

the deflections and the twist with respect to the end section were

calculated. Mechanical deflection gages were also used in the first

few steps to verify the other readings. They were also used in the

cases not involving the twist, i.e., $d = 1.5''$.

6.9. LOADING AND ADJUSTMENT

Loading the specimen concentrically, or with a certain eccen-

tricity, was the objective. To achieve this goal, the centroid of the

cross section used in the experiment cut to $\frac{1''}{4}$ length was determined

by means of the device shown on Fig. 6.4 (#6). Part #4 was poured

of lead such that its center would coincide or would have the desired

eccentricity with respect to the centroid of the cross section and to

hold the column in the end fixture. By loading in the elastic range

and checking the strains and deflections, by means of three small

screws of part #3, the necessary adjustments were made to set the

column in the desired position. This was a very long and delicate

job and required some amount of patience. The rate of head move-

ment of the testing machine was chosen to be 0.025 inch per minute.

Except for some scattered reading in two or three experiments,

the author was unable to take the desired data for the unloading part

of the experiment, as load dropped suddenly in all cases - in some

cases because of local buckling, in others because the unloading

time was extremely small.

Paris[107] in his study of plastic dynamic buckling of columns

took also the behavior of the testing machine into consideration. He

noted that the machine was set to a slow rate of head movement and

left on throughout the test. As the unloading time was extremely

small, therefore, little additional axial deformation could be

attributed to the turning of the screws of the testing machine. Paris

stated that comparatively large additional deformation noted in the

unloading stage was due to the release of strains within the testing

machine itself.

6.10. PROTECTIVE MEASURES

Although part #3 (the ring) of the end fixture would somewhat

prevent the column from sliding and skipping out, in the case of

extensive end rotation, the danger of end fixture and the column

being thrown out exists. In this

experiment protective measures

were taken, and protective plates

were set around the testing

machine (Fig. 6.3) and the top

end fixtures were loosely attached

to the machine by means of wire.

Wire was also wrapped around

the poles of the testing machine

to prevent the parts from flying

out (Fig. 6.12).
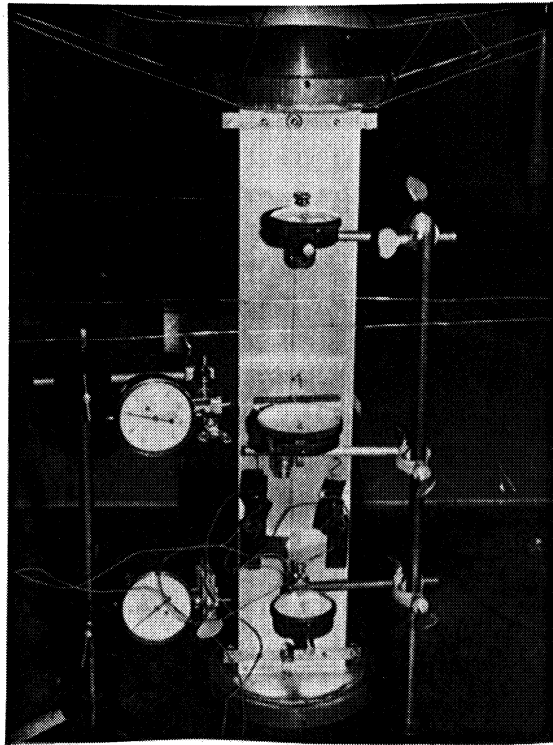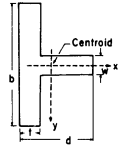
Fig. 6.12. Column under Test

6.11. SUMMARY AND RESULTS

The main objective of conducting the experiments was to

verify the analytical solution to the problem of asymmetrical behavior

of the "T" shaped column of aluminum alloy. Also, the material

properties were to be determined in order to be used in analytical

solution. The material properties (the stress-strain relation, the

Poisson's ratio) obtained from the experiment and its mathematical

fit, the elastic (tangent) and shear (secant shear) moduli evaluated

from the mathematical fit and according to discussion on torsional

stiffness (equation (4.68)) are shown on Fig. 2.6. Fourteen columns

were tested, eight with d = 2.5" and the rest with d = 1.5". The ultimate load carrying capacity of the tested columns and the corresponding values obtained by incremental procedure (computer results) are tabulated below:

Table 6.1

Table of Comparison of Experimental Results
with Analytical Results

d	KL/r	Eccentricity	Analytical	Experiment	$\frac{Anal.-Exp.}{Anal.}$	Remarks
1.5"	30	+.002	33.944	34.585	-1.88%	No torsion or local buckling
		+0.	42.511	42.870	-0.84%	No torsion or local buckling
		-0.	43.542	*		
		-.002	41.545	40.710	+2.01%	No torsion or local buckling
	40	+.002	28.660	29.362	-2.45%	No torsion or local buckling
		+.0	40.290	40.512	-0.55%	No torsion or local buckling
		-.0	42.047	*		
		-.002	38.172	37.405	+2.01%	No torsion or local buckling
2.5"	30	+.002	35.006	36.120	-3.18%	Web buckled locally after the ultimate load
		+.0	42.521	41.800	+1.70%	Failure due to local buckling of web
		-.0	43.128	*		
		-.002	40.140	38.950	+2.96%	Web buckled locally prior to the ultimate load
	50	+.002	23.851	24.520	-2.80%	Web buckled locally after the ultimate load
	60	-.002	23.338	24.084	+3.20%	No torsion was induced
	20	+0.	43.664	44.800	-2.60%	Failure due to local buckling in web
		+0.	43.664	42.600	+2.44%	Failure due to local buckling in web
		-0.	43.883	*		Were supported laterally
	40	+0.	40.310	43.150	-7.05%	Considerable difference between the experiment and the analytical result due to the lateral support. Failure due to local buckling in web
		-0.	41.682	*		

*Buckling did not follow this direction

Table 6.1 also gives the percentage difference between the computed and the tested values with respect to the computed values.

It can be noticed that test results are lower than the computed values in the case of negative eccentricity (buckling towards the web) and higher than the computed values otherwise. Also, it is noticeable that in the cases of concentric loading the columns deflected to the flange side (negative x direction) and as it is seen from Figs. 6.13 and 6.14 deflection started below their respective tangent modulus load and test ultimate loads were higher than the computed values. Although some discrepancies between the test and analytical results were observed (Figs. 6.13, 6.14, 6.15), the tests as well as the incremental procedure show that in buckling behavior of a tee column a considerable difference exists in the ultimate load carrying capacity of the T shaped aluminum alloy column when it buckles in the plane of symmetry towards or away from the flange.
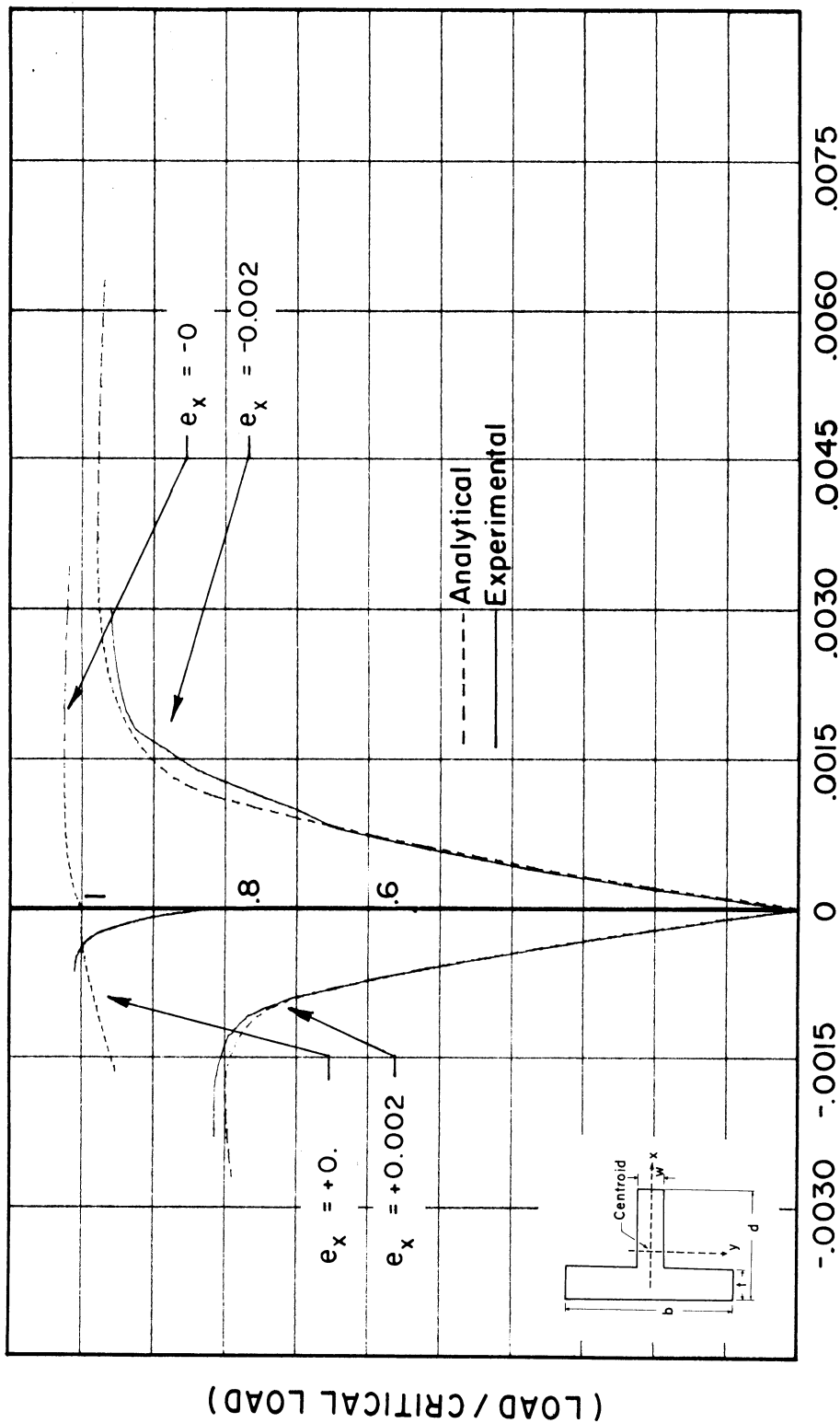
Fig. 6.13. Average Stress vs. Mid-length Deflection Curves
Test and Analytical Results (d = 1.5"; L/r = 30)
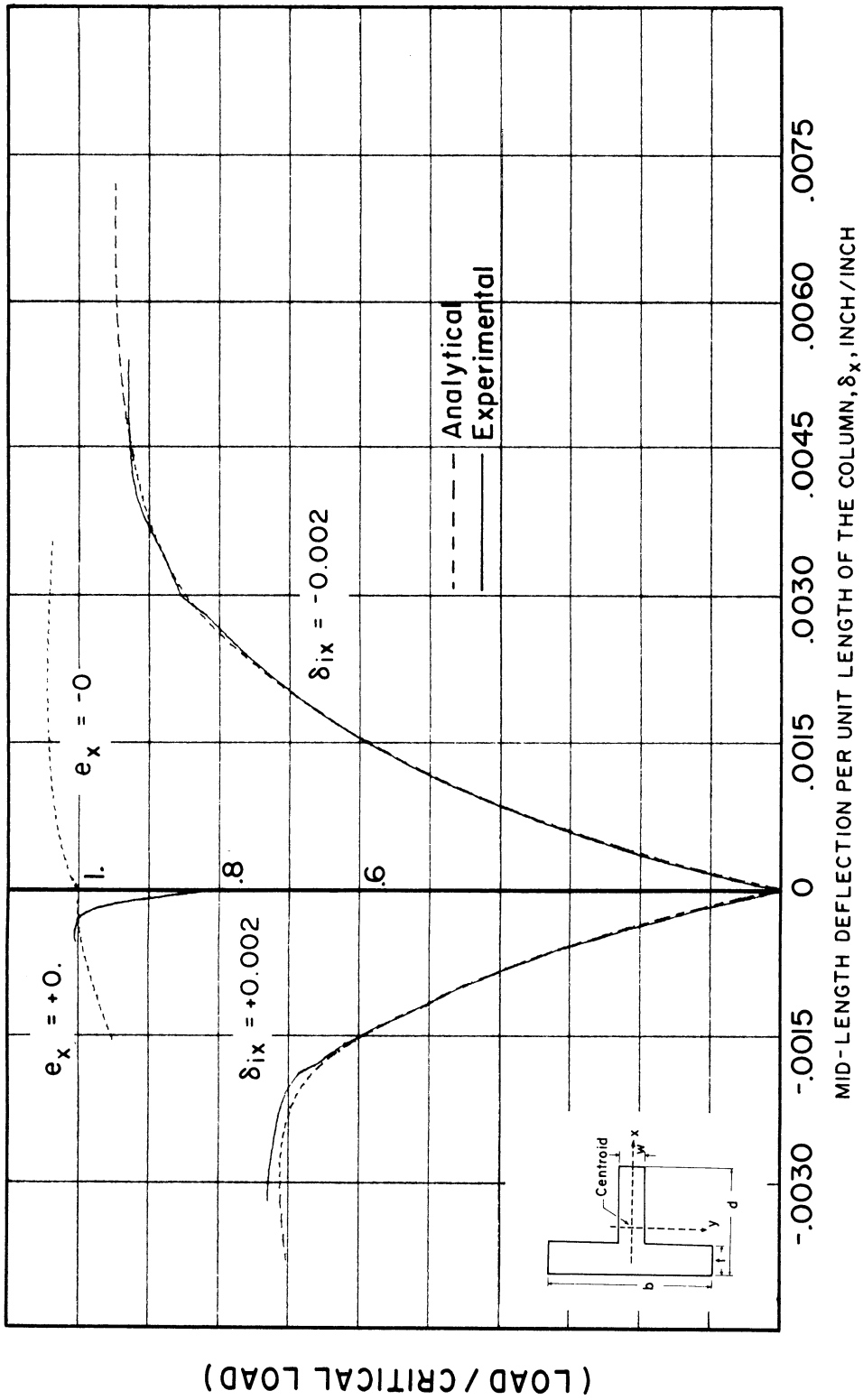
Fig. 6.14. Average Stress vs. Mid-length Deflection Curves
Test and Analytical Results (d = 1.5"; L/r = 40)
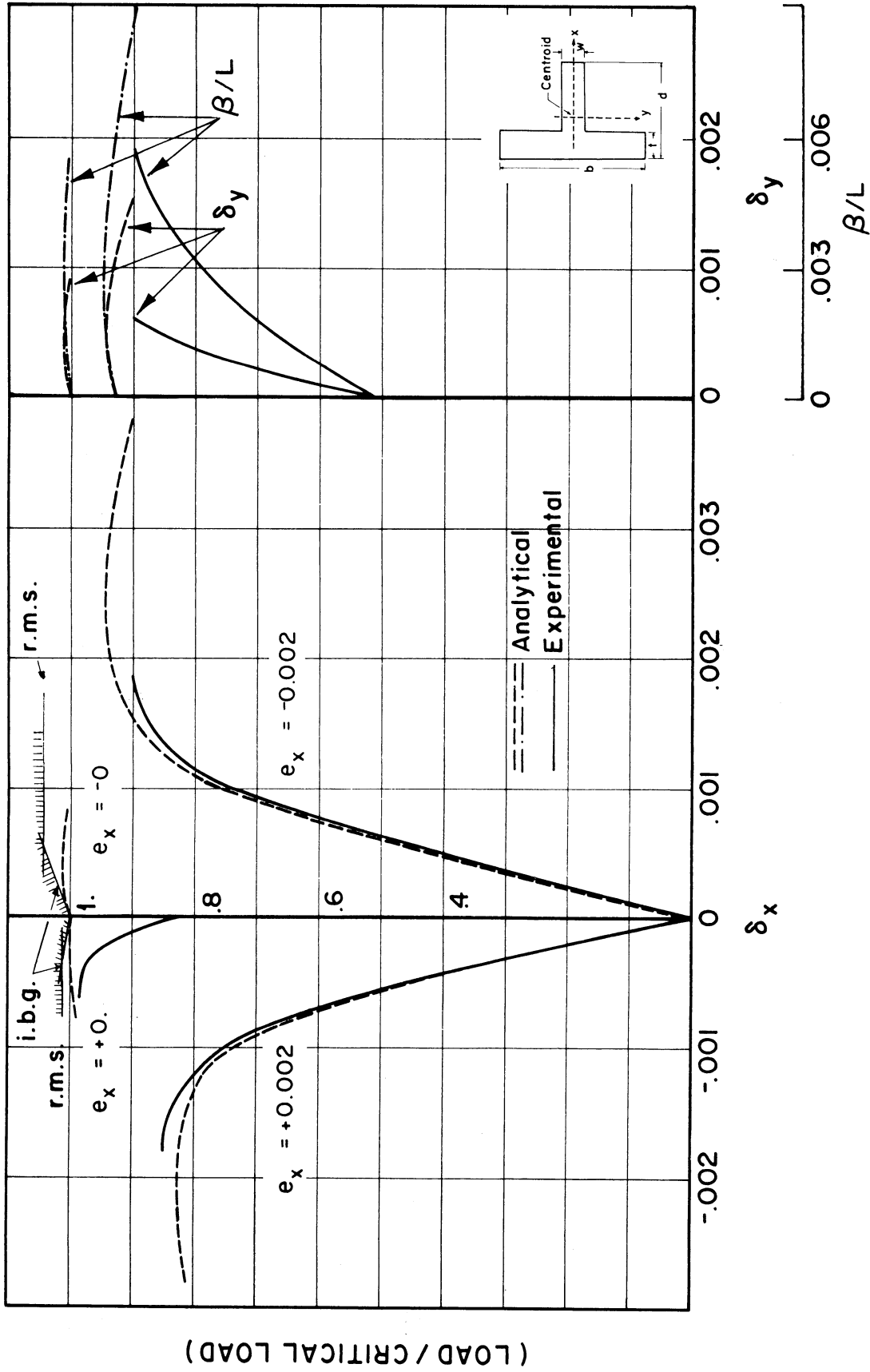
Fig. 6.15. Average Stress vs. Mid-length Deflection Curves
Test and Analytical Results (d = 2.5"; L/r = 30)

CHAPTER VII

SUMMARY AND CONCLUSIONS

The post buckling behavior of a tee shaped aluminum column has been studied. Attention has been focused on the cases where the buckling commences in the plane of symmetry. The effects of initial curvature and eccentricity of loading in the web or the flange directions have been considered. The problems discussed and the conclusions derived can be summarized as follows:

1. Bounds of behavior of a column, specifically a T column, have been discussed in Chapter II. The differing inelastic buckling gradients and the reduced moduli for buckling towards or away from the flange have been explained and illustrated graphically.

2. Equations of torsional flexural buckling and the choice of the coordinates have been discussed in Chapter III. The initial crookedness and the eccentricity of loading, in a general form, have been intorduced in these equations. The limiting point up to which the column will not buckle out of its plane of symmetry has been determined and simplifications of the equilibrium equations for the state of planar bending have been made.

3. In Chapter IV the problem of torsion of a cross section subjected to a varying strain in the inelastic range with possible presence of a strain regression region has been treated. This is the problem encountered in the evaluation of the torsional stiffness of the column cross section in the inelastic range of biplanar bending. At the conclusion of this chapter the relation (4.83) (which has been used in the column analysis) has been suggested to approximate the torsional stiffness of the column cross section under the above conditions.

4. An incremental procedure has been presented in Chapter V for the purpose of obtaining a quantitative evaluation of the ultimate load carrying capacity of the tee shaped columns and a comparison is made with the qualitative predictions that bound the behavior of the column. The 7090 digital computer was utilized to carry out the manipulation. Combinations studied were summarized in Table 5.1. A selected number of load-deflection history and the tables of the results were presented in Chapter V.

The following conclusions may be drawn from the incremental analysis:

    i. For $d = 1.5''$ ($\alpha = 9.248$), except for $L/r = 10$, the column did not buckle out of its plane of symmetry in the loading stage. For $L/r = 10$, biplanar bending accompanied with torsion

started almost at the ultimate load. In

Fig. 5.11, dashed lines show the case where

the column was prevented from deflection in

the y direction.

ii. For $d = 2.5''$ ($\alpha = 2.030$) and $d = 3.''$

($\alpha = 1.197$) the dimensionless graphs of the

load vs. the components of the deflection in

the x and the y directions as well as the twist

are shown on Figs. 5.14 through 5.17. In

these figures the behavior of the column is

indicated where prevented from buckling out

of the plane of symmetry. From these figures

it can be seen that as α ($= \dfrac{I_x}{I_y}$) becomes smaller

(d becomes larger) the difference between the

ultimate average stress when buckling

accompanies torsion and the ultimate average

stress, in buckling away from the flange (to

the right), when the column is prevented from

buckling in the y direction becomes larger.

iii. A noticeable difference exists between the

ultimate load carrying capacity of the T column

in buckling towards or away from the flange.

As α tends towards unity this difference

becomes smaller. The ultimate load for

different values of slenderness ratio and

initial crookedness in buckling towards or

away from the flange is given on Figs. 5.20

and 5.21.

iv. Figures 5.12, 5.18 and 5.19 and also Tables

5.6 and 5.7 show the difference between the

ultimate load evaluated on the basis of a

half-sine curve deflection shape assumption

and a more exact deflection shape. It can be

noticed that as initial crookedness becomes

larger the difference between the ultimate

load evaluated on the above two bases becomes

larger.

v. Figures 5.22 through 5.26 and also Tables

5.8 and 5.9 present a comparison between

the initial crookedness and the eccentric

loading.

vi. Three different stress-strain relations have

been used in the incremental analysis

(Figs. 5.18 and 5.19).

5. A series of tests was conducted to confirm the analytical

results. A procedure of deflection and twist measurement

for the pinned-end columns has been developed and

presented in Chapter III. Table 6.1 compares the

analytical and the experimental results.

APPENDIX A

Main Computer Program Flow Diagram

INPUT

Evaluate the Coordinates of the Mesh
Initiate the Curvature, Deflection, Twist,
Initial Deflection, Moment, Stress,
Strain, ..., Matrices

"Ideal" Column Concentric Loading

T

Execute FINTAN.
Set $P = P_t$
Set Stress and Strain Matrices

F

$\langle P \rangle = 0$

Execute RMATIX.

$P_{max} = P(0)$

α

Estimate $[\Delta\phi]$
Calculate $[\Delta\delta]$

$\langle \beta_l \rangle = $ New $\langle \beta_l \rangle$

$q = 1$ (x-axis)

$l = 0$
(if $\phi_{0q} = 0$, $l = 1$)

T

$|$New β_l - Old $\beta_l| < \epsilon$
(for all l)

F

Improve $\Delta\phi_{lq}$
Calculate $\Delta\delta_{lq}$
Normalize when
$q = 1$
(for all l)

$q = 2$
(y-axis)

T

Execute CALBET.

T

Convergence achieved with no change in estimated $[\Delta\phi]$

F

$q = 1$

F

$l = l + 1$

Estimate C_{lq}

Improve C_{lq}

Execute CALMAP.

When Planar Bending Execute CALALF.

Planar Bending?

T

$|P_l - P_{avg}| < \epsilon$
(for all l)

F

$l > m-1$
(if $\phi_{mq} = 0$,
$l > m-2$)

F

Moment equilibrium satisfied?

Calculate [SR]

T

$q = 1$

F

T

Calculate P_{avg}

T

Record P_l, ...

One cycle of increment is complete

Record and print:
    Curvature
    Deflection
    Axial Load
    Moment
    Stress and Strain
        Matrices
    ...

$P_{avg} > P_{max}$

T

$P_{max} = P_{avg}$

F

α

Increment enough?

F

T

Print
    Final
    Results

TERMINATE

T = True
F = False

-190-

RELATED PROGRAMS

CALALF. Calculates the vector $\{\alpha\}$ according to relation 5.45 and determines if biplanar bending has commenced.

CALBET. Calculates $\{\beta'\}$, then $\{\beta\}$ using relation 5.32d, when end section is deleted ($\phi = 0$), uses FINEPS. to find the strain at that section.

CALMAP. When planar bending:

    Calculates axial load (relation 5.42a).

    Also evaluates the moment equilibrium

        equation (5.42b).

  When biplanar bending:

    Calculates axial load (relation 5.32a).

    Also evaluates the moment equilibrium

        equation (relation 5.32b when $q = 2$ and

        relation 5.32c when $q = 1$).

ET. Calculates tangent modulus for a given strain (relation 5.1, Fig. 2.6).

FINEPS. Finds strain for a given stress (from relation 5.1).

FINTAN. Finds the stress and the strain at the tangent modulus load for a given slenderness ratio.

GS. Finds the secant shear modulus for a given strain (relation 4.68).

RMATIX. Generates the matrix $[R]$.

SIGMA. Finds the stress for a given strain (relation 5.1).

REFERENCES

1. Shanley, F. R., "Inelastic Column Theory," Journal of Aeronautical Science, Vol. 14, No. 5, May 1947, p. 261.

2. Duberg, J. E. and Wilder, T. W., "Column Behavior in the Plastic Strength Range," Journal of Aeronautical Science, Vol. 17, No. 6, June 1950, p. 323. Also NACA Report 1072, 1952.

3. Johnston, Bruce G., "Inelastic Buckling Gradient," Trans. ASCE, Vol. 131, 1966. Also Journal of Engineering Mechanics Division, ASCE, Vol. 90, No. EM6, Proc. Paper 4158, December 1964, pp. 31-47.

4. Musschenbroek, Petrus van, "Physicae Experimentales et Geometricae," 1729.

5. Considère, M., "Résistance des Pièces Comprimées," Congrès International des Precédés de Construction, Annexe, Librairie Polytechnique, Paris, 1891, p. 371.

6. Engesser, Friedrich, "Ueber die Knickfestigkeit gerader Stäbe," Zeitschrift des Architekten und Ingenieurvereins zu Hanover, Vol. 35, No. 4, 1889, p. 445.

7. Jasinski, F., "Noch ein Wort zu den 'Knickfragen'," Schweizerische Bauzeitung, Vol. 25, No. 25, June 22, 1895, p. 172.

8. Kármán, Theodor von, "Unter suchungen über Knickfestigkeit," Mitteilungen über Forschungsarbeiten auf dem Gebiete des Ingenieurwesens, p. 18, Verein Deutscher Ingenieure, Heft 81, Berlin, 1910.

9. Shanley, F. R., "The Column Paradox," Journal of Aeronautical Science, Vol. 13, No. 5, December 1946, p. 678.

10. Illyushin, A. A., "Some Fundamental Problems of the Theory of Plasticity," Izvestiya Akademii Nauk U.S.S.R. Otdelenia Tehniceskih Nauk 1949. Translated by W. Prager, Brown University, October 1950.

11. Shanley, F. R., "Strength of Materials," McGraw-Hill Book Co., Inc., New York, 1957.

12. Duberg, J. E. and Wilder, T. W., III, "Inelastic Column Theory," NACA TN2267, January 1951.

13. Lin, Tung-Hua, "Inelastic Column Buckling," Journal of Aeronautical Science, Vol. 17, No. 3, March 1950, p. 159.

14. Johnston, B. G., "Buckling Behavior above the Tangent Modulus Load," Journal of Engineering Mechanics Division, Proc. ASCE, Vol. 87, No. EM6, December 1961, p. 79.

15. Augusti, G., "Svergolamento e Collasso di Elementi Strutturali in Campo Inelastico" (Buckling and Collapse of Structural Elements in the Inelastic Range), Ingegneria Civile, No. 11, Rome, April-June 1964.

16. Batterman, Richard H. and Johnston, Bruce G., "Behavior and Maximum Strength of Metal Columns," Journal of Structural Division, ASCE, Vol. 93, No. ST2, Proc. Paper 5190, April 1967, pp. 205-230.

17. Wagner, H., "Verdrehung und Knickung von offenen Profilen, Festschrift," Funfundzwanzig Jahre Technische Hochschule Danzig, Danzig, 1929. Translated by S. Reiss, Torsion and Buckling of Open Sections, National Advisory Committee for Aeronautics, Tech. Memo. No. 807, 1936.

18. Kappus, R., "Drillknicken zentrisch gedruckter Stabe mit offenen Profilenim elastischen Bereich," Luftfahrtforschung Vol. 14, No. 9, September 20, 1937, pp. 444-457. Translated by J. Vanier, Twisting Failure of Centrally Loaded Open-Section Columns in the Elastic Range, National Advisory Committee for Aeronautics, Tech. Memo. No. 851, 1938.

19. Ostenfeld, A., "Exzentrisch beanspruchte Säulen, III, Beliebige Exzentrizität. Versuche mit Holz-und Stahlsäulen," Politecknisk Laereanstalts Laboratorium for Bygningsstatik, Meddelels No. 5, Kopenhagen, 1931.

20. Wagner, H. and Pretschner, W., "Verdrehung und Knickung von offenen Profilen," Luftfahrtforschung, Vol. 11, December 5, 1934, pp. 174-180. Translated by J. Vanier, Torsion and Buckling of Open Sections, National Advisory Committee for Aeronautics, Tech. Memo. No. 784, 1936.

21. Bleich, F. and Bleich, H., "Bending, Torsion and Buckling of Bars Composed of Thin Walls," Prelim. Pub. 2nd Congress International Association of Bridge and Structural Engineers, English edition, Berlin, 1936, p. 871.

22. Bleich, F., "Buckling Strength of Metal Structures," McGraw-Hill Book Co., Inc., New York, 1952.

23. Lundquist, E. E. and Fligg, C. M., "A Theory for Primary Failure of Straight Centrally Loaded Columns," National Advisory Committee for Aeronautics, Tech. Report No. 582, 1937.

24. Niles, A. S., "Experimental Study of Torsional Column Failure," National Advisory Committee for Aeronautics, Tech. Note No. 733, 1939.

25. Goodier, J. N., "Buckling of Compressed Bars by Torsion and Flexure," Cornell University Eng. Exp. Sta. Bull. No. 27, December 1941; "Flexural-Torsional Buckling of Bars of Open Torsional Loads," Cornell University Eng. Exp. Sta. Bull. No. 28, January 1942.

26. Timoshenko, S. P., "Theory of Bending, Torsion and Buckling of Thin-Walled Members of Open Cross Section," Journal of the Franklin Institute, Vol. 239, No. 3, p. 201, No. 4, p. 249, No. 5, p. 343, 1945.

27. Timoshenko, S. P. and Gere, J. M., "Theory of Elastic Stability," McGraw-Hill Book Co., Inc., New York, 1961.

28. Zickel, J., "General Theory of Pretwisted Beams and Columns," Graduate Division of Applied Mathematics, Brown University, Tech. Report No. 73, June 1952.

29. Hill, N. H. and Clark, J. W., "Lateral Buckling of Eccentrically Loaded I-section Columns," Trans. ASCE, Vol. 116, 1951, p. 1179.

30. Salvadori, M., "Lateral Buckling of I-Beams," Trans. ASCE, Vol. 121, 1956, p. 1163.

31. Thurlimann, B., "Deformations of, and Stresses in, Initially Twisted and Eccentrically Loaded Columns of Thin-Walled Open Cross Section," Report No. 3 to the Column Research Council and the Rhode Island Department of Public Works, Graduate Division of Applied Mathematics, Brown University, June 1953.

32. Culver, Charles G., "Initial Imperfections in Biaxial Bending," Journal of Structural Division, Proc. ASCE, June 1966.

33. Neal, B. G., "The Lateral Instability of Yielded Mild Steel Beams of Rectangular Cross Section," Philosophical Transactions of the Royal Society of London, Series A, Mathematical and Physical Sciences, No. 846, Vol. 242, January 24, 1950, pp. 197-242.

34. Galambos, T. V., "Inelastic Lateral-Torsional Buckling of Eccentrically Loaded Wide Flange Steel Columns," Ph.D. Dissertation, Lehigh University, 1959.

35. Galambos, T. V. and Keller, R. L., "Column Under Combined Bending and Thrust," Journal of Engineering Mechanics Division, ASCE, Vol. 85, No. EM2, Proc. Paper 1990, April 1959.

36. Birnstiel, C., "Ultimate Load of H-Columns under Biaxial Loading," Proc. ASCE, Vol. 89, No. ST2, April 1963.

37. Birnstiel, Charles, Leu, Keh-Chun, Tesoro, J. A., and Tomasetti, R. L., "Experiments on H-Columns under Biaxial Bending," Research Division, New York University, January 1967.

38. Ringo, Boyd C., "Equilibrium Approach to the Ultimate Load on a Biaxially Loaded Beam Column," Ph.D. Dissertation, The University of Michigan, 1964.

39. Rossow, Edwin C., Barney, George B. and Lee, Sing-Lip, "Buckling of Steel Columns with Initial Curvature," 1966, publication pending.

40. Lee, G. C., Fine, D. S. and Hastreiter, W. R., "Inelastic Torsional Buckling of H-Columns," Civil Engineering Research Report No. 8, State University of New York at Buffalo, August 1966.

41. Hoff, N. J., "Buckling and Stability," Journal of the Royal Aeronautics Society, Vol. 58, Aero Reprint No. 123, January 1954.

42. Johnston, Bruce G., "The Structual Metal Column: A Chronology," publication pending in "ASTM Symposium on Test Methods for Compression Members," 1966.

43. Timoshenko, S. P. and Goodier, J. N., "Theory of Elasticity," McGraw-Hill Book Co., Inc., New York, 1951.

44. Gerard, George and Becker, H., "Handbook of Structural Stability," National Advisory Committee for Aeronautics, Tech. Notes 3781-3786, July-August 1957, July 1958.

45. Gerard, George, "Introduction to Structural Stability Theory," McGraw-Hill Book Co., Inc., New York, 1962.

46. Ramberg, W. and Osgood, W. R., "Description of Stress-Strain Curves by Three Parameters," NACA TN No. 902, July 1943.

47. Augusti, Giuliano, Discussion: "Inelastic Buckling Gradient," Journal of Engineering Mechanics Division, Proc. ASCE, No. EM4, August 1965. Closure: No. EM1, February 1966.

48. Augusti, Giuliano, "In Tema di Svergolamento delle Structure in Campo Inelastico" (Considerations on Buckling of Structures in the Inelastic Range), Ingegneria Civile, Vol. 3, No. 10, January-March 1964, p. 575.

49. Osgood, W. R., "Column Curves and Stress-Strain Diagrams," U.S. Bureau of Standards Journal of Research, Vol. 9, Research Paper No. 492, October 1932.

50. Wagner, H., "Torsional Buckling of Compressed Thin-Walled Sections," Festschrift Funfundzwanzig Jahre Technische Hochschule Danzig, 1929, p. 329. See also Goodier's paper in Journal of Applied Mechanics, Vol. 17, 1950, p. 383.

51. Bryan, G. H., "On the Stability of a Plane Plate under Thrusts in its own Plane, with applications to the 'buckling' of the sides of a ship," Proc. London Math. Soc., Vol. 22, 1891, p. 54.

52. Stowell, Elbridge Z., "A Unified Theory of Plastic Buckling of Columns and Plates," NACA TN No. 1556, April 1948.

53. Haaijer, G., "Plate Buckling in the Strain-Hardening Range," Trans. ASCE, Vol. 124, 1951.

54. Haaijer, G. and Thurlimann, B., "On Inelastic Buckling in Steel," Trans. ASCE, Vol. 125, 1960.

55. Johnston, Bruce G., "Column Research Council Guide to Design Criteria for Metal Compression Members," 2nd ed., John Wiley and Sons, Inc., New York, 1966.

56. "Specification for the Design of Light Gage Cold-Formed Steel Structural Members," Light Gage Cold-Formed Steel Design Manual, American Iron and Steel Institute, 1962.

57. Timoshenko, Stephen P., "Strength of Materials," D. Van Nostrand Company, Inc., Princeton, 1957.

58. Timoshenko, Stephen P., "Non-uniform Torsion of Thin-Walled Bars of Open Cross Section," Bull. Polytechnic Institute S. Petersburg, 1905.

59. Timoshenko, Stephen P., "Collected Papers," McGraw-Hill Book Co., Inc., New York, 1953.

60. Kaplan, Wilfred, "Advanced Calculus," Addison-Wesley Publishing Co., Inc., Reading, 1957.

61. Muskhelishvilli, N. I., "Some Basic Problems of the Mathematical Theory of Elasticity," Noordhoff, Graningen, 1953.

62. Cowan, H. J., Appl. Sci. Res., Hauge (A)3, 1952, p. 344.

63. Mitra, D. N., Bull. Calcutta Math. Soc. 27, 1955, p. 191.

64. Gorgidze, A. Ya., Trudy Tbilios Math. Inst. Razmadze 17, 1949, p. 95.

65. Sherman, D. I. and Narodetskii, M. Z., Inzh. sborn. Akad. Nauk U.S.S.R. 6, 1950, p. 17.

66. Craven, A. H., Mathematika 1, 1954, p. 96.

67. Takayama, Hisao, J. Soc. Appl. Mech., Japan 2, 1949, p. 88.

68. Suhareviki, I. V., Inzh. sborn. Akad. Nauk U.S.S.R. 19, 1954, p. 107.

69. Christopherson, D. C. and Southwell, R. V., "Relaxation Methods Applied to Engineering Problems," Proc. Royal Society of London, Series A, No. 934. Vol. 168, 1938.

70. Southwell, R. V., "Relaxation Method in Engineering Science," Clarendon Press, Osford, 1946.

71. Shaw, F. S., "The Torsion of Solid and Hollow Prisms in the Elastic and Plastic Range by Relaxation Methods," Australian Council for Aeronautics, Report ACA-11, 1944, p. 38.

72. Shaw, F. S., "Relaxation Methods," Dover Publications Inc., New York, 1953.

73. Allen, D. N. De G., "Relaxation Methods," McGraw-Hill Book Co., Inc., London, 1955.

74. Dobie, W. B. and Gent, A. R., Struct. Engr. 30, 1952, p. 203.

75. Ely, J. F. and Zienkiewicz, O. C., "Torsion of Compound Bars - A Relaxation Solution," Int. J. Mech. Sci., Pergamon Press Ltd., Vol. 1, 1960, p. 356.

76. Sokolnikoff, I. S., "Mathematical Theory of Elasticity," McGraw-Hill Book Co., Inc., New York, 1956.

77. Love, A. E. H., "Mathematical Theory of Elasticity," Dover Publications Inc., New York, 1956.

78. Todd, John, "Survey of Numerical Analysis," McGraw-Hill Book Co., Inc., New York, 1962, pp. 384, 393.

79. Liebmann, H., "Die angenaherte Ermittlung harmonischer Funktionen und konformer Abbildung (nach Ideen von Boltzmann und Jacobi)," Sitzungsberichte der Bayer, Akad. Wiss., Math.-Phys. Kl, Vol. 47, 1918, pp. 385-416.

80. Richardson, L. F., Trans. Royal Society A 240, 1938, p. 307; Math Gazette 12, 1925, p. 415.

81. Householder, Alston, "Principles of Numerical Analysis," McGraw-Hill Book Co., Inc., New York, 1953.

82. Bodewig, E., "Matrix Calculus," Interscience Publishers, Inc., New York, 1956.

83. Forsythe, G. E. and Wasow, W. R., "Finite-Difference Methods for Partial Differential Equations," John Wiley and Sons, Inc., Princeton, 1965, pp. 181, 208, 236.

84. Young, David M., "Iteration Methods for Solving Partial Difference Equations of Elliptic Type," Trans. Amer. Math. Soc., Vol. 76, 1954, pp. 92-111.

85. Frankel, Stanley P., "Convergence Rates of Iterative Treatments of Partial Differential Equations," Math. Tables Aids Comput., Vol. 4, 1950.

86. Friedman, Bernard, "The Iterative Solution of Elliptic Difference Equations," Report NYO-7698, Institute of Mathematical Science, New York University, 1956.

87. Householder, Alston, "The Approximate Solution of Matrix Problems," J. Assoc. Comput. Mach., Vol. 5, 1958.

88. Arms, R. J., Gates, L. D. and Zondek, B., "A Method of Block Iteration," J. Soc. Indust. Appl. Math., Vol. 4, 1956.

89. Keller, H. B., "On Some Iterative Methods for Solving Elliptic Difference Equations," Quart. Appl. Math., Vol. 16, 1958.

90. Sortley, George H., Weller, R. and Fried, B., "Numerical Solution of Laplace's and Poisson's Equations with Application to Photoelasticity and Torsion," Bull. 107, Vol. IX, No. 5, Ohio State University Studies Engineering Series, September 1940.

91. Eldarwish, I. A. and Johnston, Bruce G., "Torsion of Structural Shapes," Trans. ASCE, Vol. 131, 1966. Also Journal of Structural Division, Proc. ASCE, Vol. 91, No. ST1, February 1965.

92. Newmark, N. M., "Numerical Procedure for Computing Deflections, Moments and Buckling Loads," Trans. ASCE, Vol. 108, 1943.

93. The MAD (Michigan Algorithm Decoder) Manual, Computing Center, The University of Michigan, Ann Arbor, August 1966.

94. Deming, William E., "Statical Adjustment of Data," John Wiley and Sons, Inc., Princeton, 1943.

95. Berg, G. V., "Computer Analysis of Structures," College of Engineering, The University of Michigan, Ann Arbor, 1963.

96. Bellman, Richard E., "Introduction to Matrix Analysis," McGraw-Hill Book Co., Inc., New York, 1960.

97. ASCE Second Progress Report of the Special Committee on Steel Columns, Paper 1789, Trans. ASCE, Vol. 95, 1931.

98. Massonnet, C. and Campus, F., "Recherches sur le Flambment de Colonnes en Acier, A-37, A profil en Double Te, Sollicatees Obliquement," I.R.S.I.A. Bulletin No. 17, 1956.

99.   Baker, J. F., Horne, M. R. and Heyman, J., "The Steel Skeleton - Plastic Behavior and Design," Vol. 2, Cambridge University Press, Cambridge, England, 1956.

100. Mason, R. E., Fisher, G. P. and Winter, G., "Eccentrically Loaded, Hinged Steel Columns," Proc. ASCE, Paper 1792, Vol. 84, No. EM4, October 1958.

101. Estuar, Fiorello R. and Tall, Lambert, "The Testing of Pinned-end Columns," Report No. 249.22, Fritz Engineering Lab., Lehigh University, January 1964.

102. Lay, Maxwell G., Aglietti, Richard A. and Galambos, Teodore V., "Testing Techniques for Restrained Beam Columns," Fritz Engineering Lab. Reprint No. 285, reprinted from Experimental Mechanics, Vol. 6, No. 1, January 1966.

103. Yarimci, Erol, Yura, Joseph A. and Lu, Le-Wu, "Techniques for Testing Structures Permitted to Sway," Fritz Engineering Lab. Report No. 273.40, Lehigh University.

104. ALCOA Structural Handbook, Aluminum Company of America, Pittsburgh, Pennsylvania, 1960, p. 224.

105. Timoshenko, Stephen P., "History of Strength of Materials," McGraw-Hill Book Co., Inc., New York, 1953.

106. Timoshenko, S. and Lessells, J. M., "Applied Elasticity," Westinghouse Technical Night School Press, East Pittsburgh, Pennsylvania, 1925.

107. Paris, Paul C., "Limit Design of Columns," Journal of Aeronautical Science, Vol. 21, No. 1, January 1954.